Theoretical simulation studies for 3D and 2D systems

Dissertation
zur Erlangung des Grades
des Doktors der Naturwissenschaften
der Naturwissenschaftlich-Technischen Fakultät
der Universität des Saarlandes

von

M.Sc. Meijuan Zhou

Saarbrücken
2020

Tag des Kolloquiums: 12. Februar 2021

Dekan:	Prof. Dr. Jörn Walter
Berichterstatter:	Prof. Dr. Dominik Munz
	Dr. Hilke Bahmann
Vorsitz:	Prof. Dr. Uli Kazmaier
Akad. Mitarbeiter:	Dr. Anle Wang

Declaration of original authorship

I declare that this dissertation has been composed solely by myself except where states otherwise by reference or acknowledgment. This dissertation has not been submitted for any other degree or professional qualification.

Saarbrücken, November 2020 — Meijuan Zhou Meijuan Zhou

(Place, Date) (Signature)

The thesis has been partially/entirely reproduced from the following publications:

1. **Meijuan Zhou*** and Michael Springborg, Theoretical study of the mechanism behind the site- and enantio-selectivity of C–H functionalization catalysed by chiral dirhodium catalyst. Phys. Chem. Chem. Phys., 22:9561−9572, **2020**. (Reproduced by permission from Royal Society of Chemistry) https://doi.org/10.1039/D0CP00249F

2. Michael Springborg*, **Meijuan Zhou**, Mohammad Molayem and Bernard Kirtman, Surfaces, Shapes, and Bulk Properties of Crystals. J. Phys. Chem. C, 122:11926−11932, **2018**. (With permission from Copyright (2018) American Chemical Society) https://doi.org/10.1021/acs.jpcc.8b03041

3. **Meijuan Zhou***, Michael Springborg and Bernard Kirtman, Theoretical Treatment for Properties of Surfaces and Their Interplay with Bulk Properties of Crystals. Adv. Theory Simul., 2:1800117, **2019**. (Copyright Wiley-VCH GmbH. Reproduced with permission) https://doi.org/10.1002/adts.201800117

Contents

1. Acknowledgement

I want to thank various people who supported and helped me during the whole period of my PhD study at Saarland University.

First of all, I would like to express my deepest gratitude to my supervisor, Prof. Dr. Michael Springborg for giving me the chance, help and support during my PhD study, for his patient guidance, constant encouragement and nice advice of my research works, and for his patient revision and nice assistance in publishing my work.

I would also like to thank my office roommate Kai Huwig for his nice help, company and teaching me about some lab-course work. Prof. Dr. Michael Springborg and Kai Huwig both helped me a lot in improving my oral English and teaching me about programming. Also many thanks to my other office roommate Hao Xu for his nice help and support.

I would also like to thank Prof. Dr. Bernard Kirtman, University of California, Santa Barbara. He and Prof. Dr. Michael Springborg gave me a lot of guidance and help for my studies on the effects of shape.

I would also like to thank my colleague Nicolas Louis for his much help and support in dealing with the problems of software and server patiently. I also want to thank my colleague Silvia Nagel for her kind help with office issues and my accommodation and some office problems.

I would also like to thank my nice friend Dr. Zhen Liu for her great help and support in company over more than three years.

I would also like to thank Dr. Mohammad Molayem for his advice, help and discussions. I am very grateful to my colleagues Prof. Dr. Hilke Bahmann, Dr. Valeri G. Grigorian, Dr. Jihène Jerbi, Philipp Thiel and Chencheng Fan for their nice help and company. I would also like to thank Prof. Dr. Gregor Jung for his nice help.

At last I want to thank my parents, my husband and my family members for their love, continued support and encouragement.

2. Kurzzusammenfassung

Die theoretische Simulation ist für das Verständnis und die Vorhersage der Eigenschaften für die Experimente zunehmend nützlich geworden. In einem ersten Teil verwendeten wir die theoretischen Simulationen, um ein detailliertes Verständnis des Reaktionsmechanismus hinter der hohen Regio- und Enantioselektivität für die tertiäre CH-Bindungsfunktionalisierung durch Carbenen zu erhalten, die durch eines chiralen Dirhodiumkomplex katalysiert wird. In einem zweiten Teil werden realistische Modelle dazu benutzt, um zu demonstrieren, dass die sogenannten polaren Oberflächen durch eine Ladungsumverteilung zwischen dem kompletten Satz von Oberflächen stabilisiert werden können, die von der Gesamtform der Probe und der Art des Materials abhängt. Es wird dabei auch gezeigt, dass diese Ladungsumverteilung zu Änderungen in sowohl Volumen- als auch Oberflächeneigenschaften führt.

3. Abstract

Theoretical simulation has become increasingly useful for the understanding and prediction of the properties of materials. In a first part, we used theoretical simulations to obtain a detailed understanding of the reaction mechanism behind the highly site- and enantio-selectivity for the tertiary C–H bond functionalization involving carbenes and catalyzed by a chiral dirhodium complex. In a second part, realistic models were used to demonstrate that so-called polar surfaces may be stabilized through a charge redistribution between the complete set of surfaces that depends upon the overall shape of the sample and on the nature of the material. Moreover, it is demonstrated that this charge re-distribution affects both bulk and surface properties.

4. Preface

The work presented in this thesis was published in three articles. The three articles are placed after section 8.

For the first publication, all calculations were performed using the Gaussian 09 program package [1]. Hirshfeld surfaces analysis is studied with the Multiwfn software [2] based on the Gaussian calculation results. Space-filling models were drawn using CYLVIEW [3]. The ONIOM layer structures were constructed with the GaussView 5.0.9 software [1].

The studies of the second part were carried through using Fortran 77 programs written by Prof. Dr. Michael Springborg. Density functional theory (DFT) calculations were carried out for ZnO slabs systems with the Vienna *ab initio* simulation package (VASP) [4-7] in the third publication. The 3D visualization of these structures is constructed using the VESTA 3 software [8] in the third publication.

5. Introduction

Theoretical simulation builds a bridge between chemistry, physics, physical chemistry, mathematics, molecular physics, biochemistry, materials, solid state physics, and computational science [9-13]. The theoretical simulations not only play an important role in the explanation and discovery of new phenomena, and in addressing problems and results which appear in the experiments, but also in the prediction and deduction of the structures and properties of materials [9-13]. In many different subject areas, the theoretical simulation can be used as a guide for the experiment, and save time and resources, whereas, the experiment can provide practical possibilities for the theoretical prediction and deduction. The theoretical simulation and experiment complement each other. For the further development of science and technology, theoretical simulation plays a more and more important role.

In the first part of the present work, theoretical calculations have been performed to explain in detail the catalytic reaction mechanism for the high site- and enantio-selectivity of C–H functionalization at the tertiary sites when being catalyzed by a chiral dirhodium complex, and it is demonstrated that the *S*-configuration ligand of the dirhodium(II) complex plays an important role in the configurations of the product. These results are discussed further in sec. 6. In the following two parts, theoretical simulations have been carried out to demonstrate that polar surfaces may be stabilized through a charge redistribution between the complete set of surfaces and that this depends upon the overall shape of the sample and the nature of the material (presented in sec. 7), and thereby, an interconnection between bulk and surface properties results (discussed in sec. 8). Our theoretical simulation analysis is important for understanding how polar surfaces are stabilized and how the surface and bulk properties of macroscopic crystalline materials interact with each other.

6. Theoretical study of the mechanism behind the site- and enantio-selectivity of C–H functionalization catalyzed by a chiral dirhodium complex

6.1 Introduction to the tertiary C–H bond functionalization reaction

The C–H functionalization involving carbenes and catalyzed by dirhodium complexes is very important for the synthesis of pharmaceuticals and complex natural products [14-25]. Different types of dirhodium catalysts were studied by Davies and co-workers [22-24]. They demonstrated that the non-activated primary C–H bonds can be functionalized by the D_2-symmetric dirhodium catalyst Rh_2[*R*-tris(*p*-^{t}BuC_6H_4)TPCP]$_4$ (TPCP: 1,2,2-triarylcyclopropanecarboxylates) (Figure 1(a)) with a high site- and enantio-selectivity [24]. Moreover, the sterically most accessible secondary C-H bonds are highly selectively functionalized by the dirhodium catalyst Rh_2[*R*-3,5-di(*p*-^{t}BuC_6H_4)TPCP]$_4$ (Figure 1(b)) that also has D_2-symmetry [22]. In addition, they synthesized a sterically less selective dirhodium catalyst with a structure close to C_4 symmetry, Rh_2(*S*-TCPTAD)$_4$ [23] (TCP: tetrachlorophthalimido TAD: adamantyl) (Figure 1(c)).

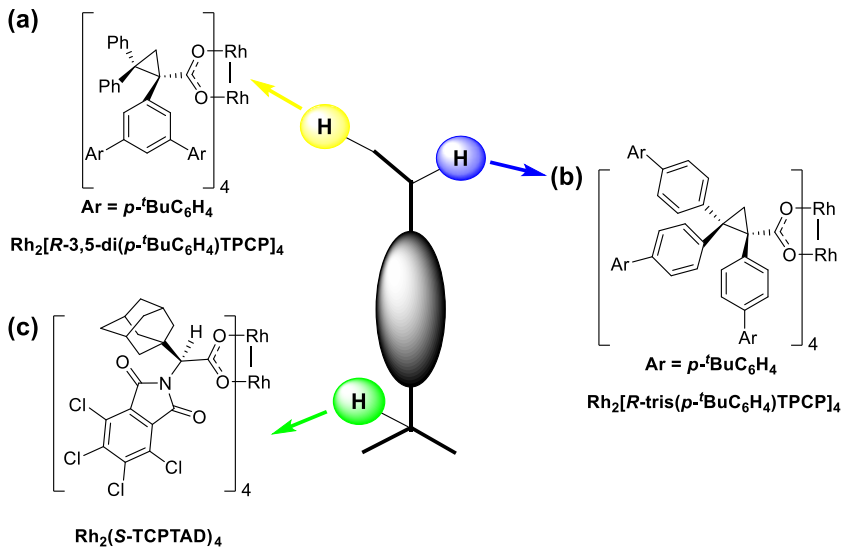

Figure 1: The structures of dirhodium catalysts: (a) Rh_2[*R*-tris(*p*-^{t}BuC_6H_4)TPCP]$_4$ [24], (b) Rh_2[*R*-3,5-di(*p*-^{t}BuC_6H_4)TPCP]$_4$ [22], and (c) Rh_2(*S*-TCPTAD)$_4$ [23].

We shall here study the dirhodium catalyst Rh_2(*S*-TCPTAD)$_4$ (Figure 1(c)), which has two shallow pockets that form one chiral crown on the top and another smaller crown on the bottom (Figure 2). This dirhodium catalyst, Rh_2(*S*-TCPTAD)$_4$, exhibits a high site- and enantio-selectivity for the tertiary C–H bond functionalization reaction. The diameter (roughly 16.20 Å) of the chiral crown made of the phthalimido groups is much larger than that of the small crown made of adamantyl groups (roughly 7.80 Å) as shown through X-ray and computational studies [23].

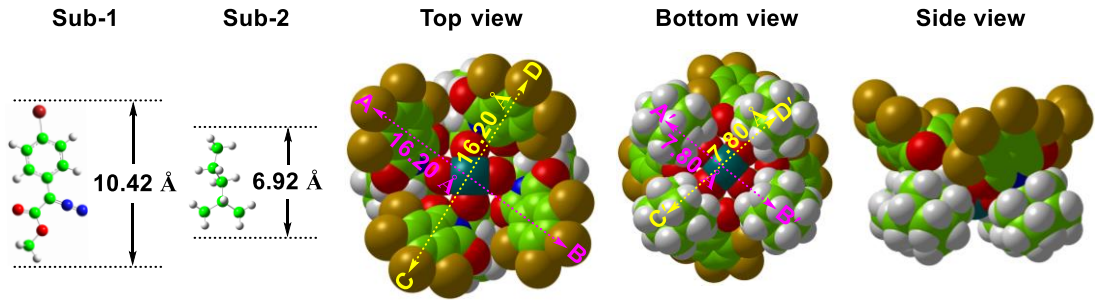

Figure 2: The structure of the experimentally studied catalyst [Rh_2(*S*-TCPTAD)$_4$] [23] is shown with space-filling models. Ball-and-stick model structures for the experimentally studied the reactant 1 [(*p*-Br-C_6H_4)CN=N($COOCH_3$)] (Sub-1) and 2 [$(CH_3)_2CHCH_2CH_2CH_3$] (Sub-2). The dimensions of the top chiral crown made of the phthalimido groups are almost 16.20 Å, and those of the bottom chiral crown made of adamantyl groups are almost 7.80 Å. The AB and CD distances are defined as the ones between the two top chlorine atoms of the two opposite ligands of the dirhodium catalysts along the directions of AB and CD, respectively. The A'B' and C'D' distances are defined as the ones between the two bottom hydrogen atoms of the two opposite ligands of the dirhodium catalysts along the directions of A'B' and C'D', respectively. The lengths of Sub-1 and Sub-2 are respectively 10.42 and 6.92 Å. C: green, O: red, Cl: brown, H: white, Br: deep red, N: blue, Rh: dark cyan.

Experiment results [23] considered as reactants the donor/acceptor carbene [(*p*-BrC_6H_4)CN=N($COOCH_3$)] (Sub-1) and 2-methylpentane [$(CH_3)_2CHCH_2CH_2CH_3$] (Sub-2). There may be two possibilities for the reactants to approach the catalyst, i.e., at the top and bottom crowns. After comparing the lengths of the reactants Sub-1 and Sub-2 with the diameters of the two crowns (Figure 2), respectively, the top crown made of the phthalimido groups is found to be the only possible reactive site for the tertiary C–H bond functionalization reaction.

In these functionalization reactions of non-activated C–H bonds, the dirhodium

catalysts with diazo compounds lead to dirhodium carbenoids that play an important part in controlling the site-, stereo-, and enantio-selectivity [21–24]. According to some reports [19-32], the presence of electron donating groups (EDG) or electron withdrawing groups (EWG) affects the carbene electrophilicity and selectivity for the carbenes. The intermediate donor/acceptor carbenoids are more stable than conventional acceptor carbenoids according to theoretical and experimental studies [26,27]. The donor/acceptor dirhodium carbenoids have unequal regioselectivity, and that site is favored that has the highest ability to stabilize the resulting positive charge [26,27]. A theoretical study [27] on the reaction of different diazoacetates for a model dirhodium catalyst has revealed that the activation energy obtained for vinyldiazoacetate is 3.8 kcal/mol lower than the one for methyldiazoacetate. Similarly, according to another theoretical study [26], the activation energy for a dirhodium catalyst for the reaction of a diazoacetate containing both donor and acceptor groups is 10.9 kcal/mol lower than what is found for a diazoacetate containing only an acceptor group. If there are only acceptor groups in the diazo compounds, the highly electrophilic carbene center cannot be well stabilized through the acceptor groups [19,26,27]. Furthermore, in their work [23] Davies et al. identified the most stable structure of the donor/acceptor dirhodium carbenoids Rh_2(*S*-TCPTAD)$_4$[(*p*-Br-C_6H_4)C(COOMe)] inside the top shallow crown through theoretical electronic-structure calculations using the DFT/M06-L method. However, their study did not provide a complete understanding of the reaction mechanism. The purpose of the present work was to obtain this complete understanding of the reaction mechanism.

6.2 Choices of computational methods and catalyst model

All calculations were performed using the Gaussian 09 program package [1]. Experimental studies [23] have shown that the chiral dirhodium catalyst Rh_2(*S*-TCPTAD)$_4$ can be highly selective in functionalizing the tertiary C–H bond in a dichloromethane (CH_2Cl_2) solvent at room temperature [23]. The donor/acceptor

dirhodium carbenoids Rh_2(*S*-TCPTAD)$_4$[(*p*-Br-C_6H_4)C(COOR)], which are obtained after N_2 elimination when the donor/acceptor carbene [(*p*-Br-C_6H_4)-CN=N(COOR)] has reacted with the chiral dirhodium catalyst [Rh_2(*S*-TCPTAD)$_4$], play a very

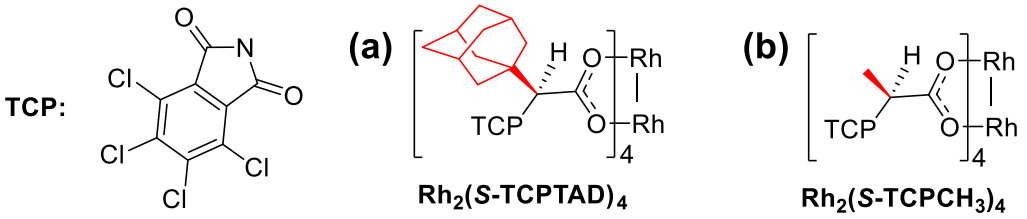

Figure 3: The structures of (a) the experimentally studied dirhodium catalyst [Rh-$_2$(*S*-TCPTAD)$_4$] [23] and (b) the simplified structure of the dirhodium catalyst Rh_2(*S*-$TCPCH_3$)$_4$ used in this work.

important role in the tertiary C-H bond functionalization reactions according to theoretical and experimental studies [23,26,27]. Based on these results, we designed a more detailed study aimed at identifying the most probable mechanism. Because Sub-1 [(*p*-Br-C_6H_4)-CN=N($COOCH_3$)] cannot enter the small crown of Rh_2(*S*-TCPTAD)$_4$ in Figure 2, the small crown of the catalyst Rh_2(*S*-TCPTAD)$_4$ cannot be the active site in the process of the C–H functionalization. Accordingly, we simplified the structure of the chiral dirhodium catalyst [Rh_2(*S*-TCPTAD)$_4$] (Figure 3a) to the structure [Rh_2(*S*-$TCPCH_3$)$_4$] (Figure 3b). Further arguments for our choice of computational methods and catalyst model are given below.

For the optimization of the structures of the donor/acceptor dirhodium carbenoids, we did test calculations using the B3LYP [33], B3LYP-D3 [34,35] (with empirical dispersion corrections), B3LYP-D3BJ [34,35] (with Becke and Johnson damping), WB97XD [36], and M06-2X [37], which could be relevant for the present systems. This method B3LYP [33] was the only one of those we considered that was able to provide a realistic structure for the donor/acceptor chlorine carbenoids (see Figures. 4 and 5). The other methods, i.e., B3LYP-D3 [34,35] (with empirical dispersion corrections), B3LYP-D3BJ [34,35] (with Becke and Johnson damping), WB97XD

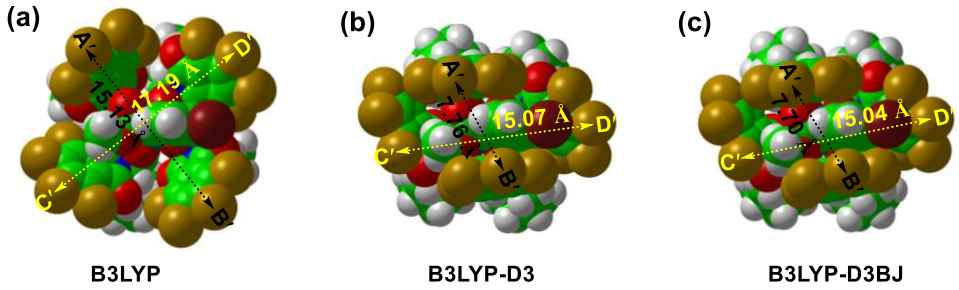

Figure 4: Space-filling models for the structures of the donor/acceptor dirhodium carbenoids {Rh_2(*S*-TCPTAD)$_4$[(*p*-Br-C_6H_4)C($COOCH_3$)]}. They are respectively optimized using (a) B3LYP [33], (b) B3LYP-D3 [34,35], and (c) B3LYP-D3BJ [34,35]. The A'B' and C'D' distances are defined as the ones between the two top chlorine atoms of the two opposite ligands of the dirhodium catalysts along the A'B' and C'D' directions, respectively. C: green, O: red, Cl: brown, H: white, Br: deep red, N: blue, Rh: dark cyan.

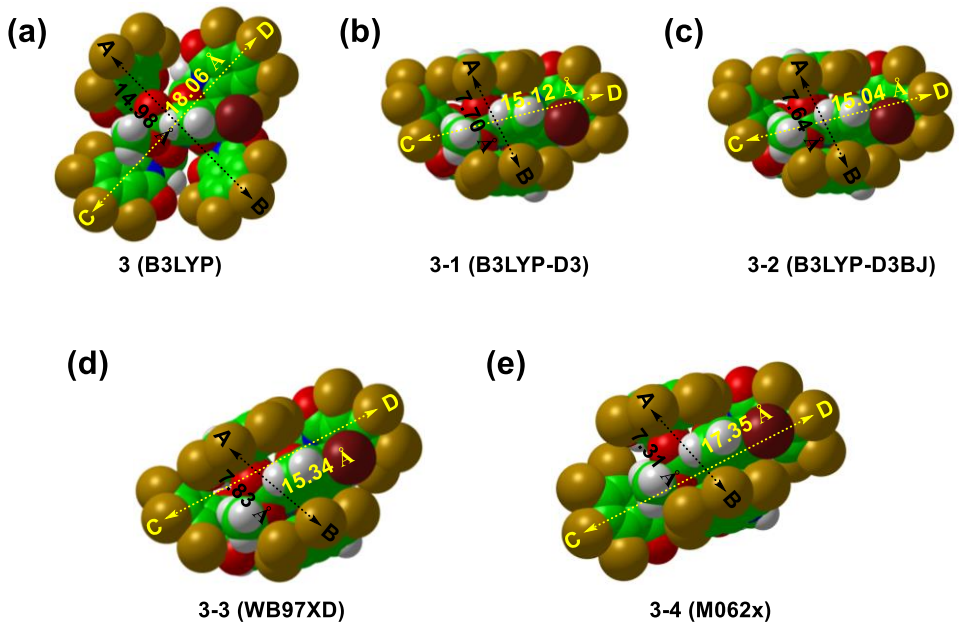

Figure 5: Space-filling models for the structures of the donor/acceptor dirhodium carbenoids {Rh_2(*S*-TCPCH_3)$_4$[(*p*-Br-C_6H_4)C($COOCH_3$)]} (3, 3-1, 3-2, 3-3, and 3-4). They are respectively optimized using (3) B3LYP [33], (3-1) B3LYP-D3 [34,35], (3-2) B3LYP-D3BJ [34,35], (3-3) WB97XD [36], and (3-4) M06-2X [37] methods. The AB, and CD distances are defined as the ones between the two top chlorine atoms of the two opposite ligands of the dirhodium catalysts along the AB and CD directions, respectively. C: green, O: red, Cl: brown, H: white, Br: deep red, N: blue, Rh: dark cyan.

[36], and M06-2X [37], have all been designed to include dispersion interactions but failed in our studies in describing the structures of the donor/acceptor dirhodium

carbenoids and the chiral crowns of the dirhodium catalysts become very distorted (see Figure 4 and 5). This would imply that it becomes impossible for Sub-2 to enter the chiral crowns of the dirhodium catalysts and to react with Sub-1. Only with the B3LYP method, the structures of {Rh_2(*S*-TCPTAD)$_4$[(*p*-Br-C_6H_4)C($COOCH_3$)]} (Figure 4(a)) and {Rh_2(*S*-TCPCH_3)$_4$[(*p*-Br-C_6H_4)C($COOCH_3$)]} (Figure 5(a)) become realistic. It is seen that with the B3LYP method, the distances AB and CD for structure {Rh_2(*S*-TCPCH_3)$_4$[(*p*-Br-C_6H_4)C($COOCH_3$)]} (Figure 5(a)) are 14.98 and 18.06 Å, respectively, whereas for structure of Figure 4(a) {Rh_2(*S*-TCPTAD)$_4$[(*p*-Br-C_6H_4)C($COOCH_3$)]}, the A'B' and C'D' distances are 0.15 Å longer and 0.87 Å shorter respectively.

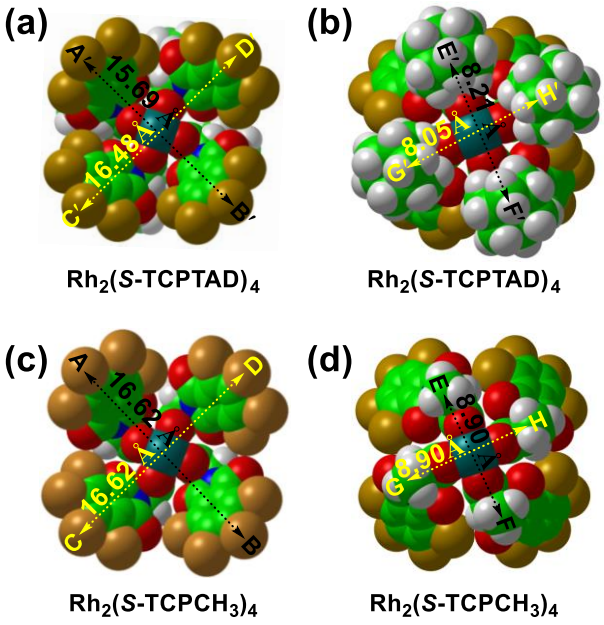

Figure 6: Space-filling models for the structures of the donor/acceptor dirhodium catalysts Rh_2(*S*-TCPTAD)$_4$ (top panels) and Rh_2(*S*-TCPCH_3)$_4$ (bottom panels). (The top view: (a) and (c). The bottom view: (b) and (d)) The A'B', C'D', AB, and CD distances are defined as the ones between the two top chlorine atoms of the two opposite ligands of the dirhodium catalysts along the A'B', C'D', AB and CD directions, respectively. The E'F', G'H', EF and GH distances are defined as the ones between the two bottom hydrogen atoms of the two opposite ligands of the dirhodium catalysts along the E'F', G'H', EF and GH directions, respectively. C: green, O: red, Cl: brown, H: white, Br: deep red, N: blue, Rh: dark cyan.

For the two Rh_2(*S*-TCPCH_3)$_4$ and Rh_2(*S*-TCPTAD)$_4$ species optimized with the B3LYP [33] method, shown in Figure 6, the average diameter of the wider crown for

[Rh_2(*S*-TCPCH$_3$)$_4$] is 16.62 Å, which is just 0.53 Å larger than that for [Rh_2(*S*-TCPTAD)$_4$]. The average diameter of the smaller crown for [Rh_2(*S*-TCPCH$_3$)$_4$] is 8.90 Å, which is just 0.77 Å larger than that for [Rh_2(*S*-TCPTAD)$_4$]. In addition, it is seen that the structures {Rh_2(*S*-TCPCH$_3$)$_4$[(*p*-Br-C$_6$H$_4$)C(COOCH$_3$)]} (Figure 5(a)) and {Rh_2(*S*-TCPTAD)$_4$[(*p*-Br-C$_6$H$_4$)C(COOCH$_3$)]} (Figure 4(a)) are very similar. Therefore, we are convinced that it is justified to use the simplified chiral dirhodium catalyst Rh_2(*S*-TCPCH$_3$)$_4$ instead of the experimentally studied catalyst Rh_2(*S*-TCPTAD)$_4$ in our theoretical studies. This choice will lead to a significant reduction in the computational costs. Most of the results to be reported below were obtained using the B3LYP [33] method.

We used the B3LYP [33] hybrid functional (for a discussion of this choice, see the beginning of the next section) and a mixed basis set (LANL2DZ [38] with ECP for Rh and Br, LANL2DZ [38] for Cl, and 6-31G(d) [39] for the other atoms) in gas phase (T = 298.15 K) without any symmetry constraint. We verified that the reactants and products had no imaginary vibrational frequency, and that the structures of transition states (TS) have only a single imaginary vibrational frequency. Intrinsic reaction coordinate (IRC) [40] calculations were also invoked to confirm that we have located saddle points as transition states that connect two intermediates or total-energy-minima structures. In addition, we considered intermediate structures roughly halfway along the reaction coordinate connecting structures of local total-energy-minima and transition states. To get further information on the effects of a solvent and of changing the computational approach, single-point calculations were performed using the M06 functional [37, 41] in combination with the basis sets LANL2DZ [38] with ECP for Rh and Br, LANL2DZ [38] for Cl, and 6-31+G(d,p) for the other atoms and including SMD [42] solvation effects from dichloromethane. Natural Bond Orbital (NBO) charge analysis was used to provide a measure of charge transfer [43]. Hirshfeld surfaces analysis [44], which is based on partitioning the electron density into molecular fragments, was used to identify interactions between such fragments. This was done with the help of the Multiwfn software [2].

Space-filling models were drawn using CYLVIEW [3]. The ONIOM layer structures were constructed using the GaussView 5.0.9 software [1].

6.3 A schematic representation of the considered process

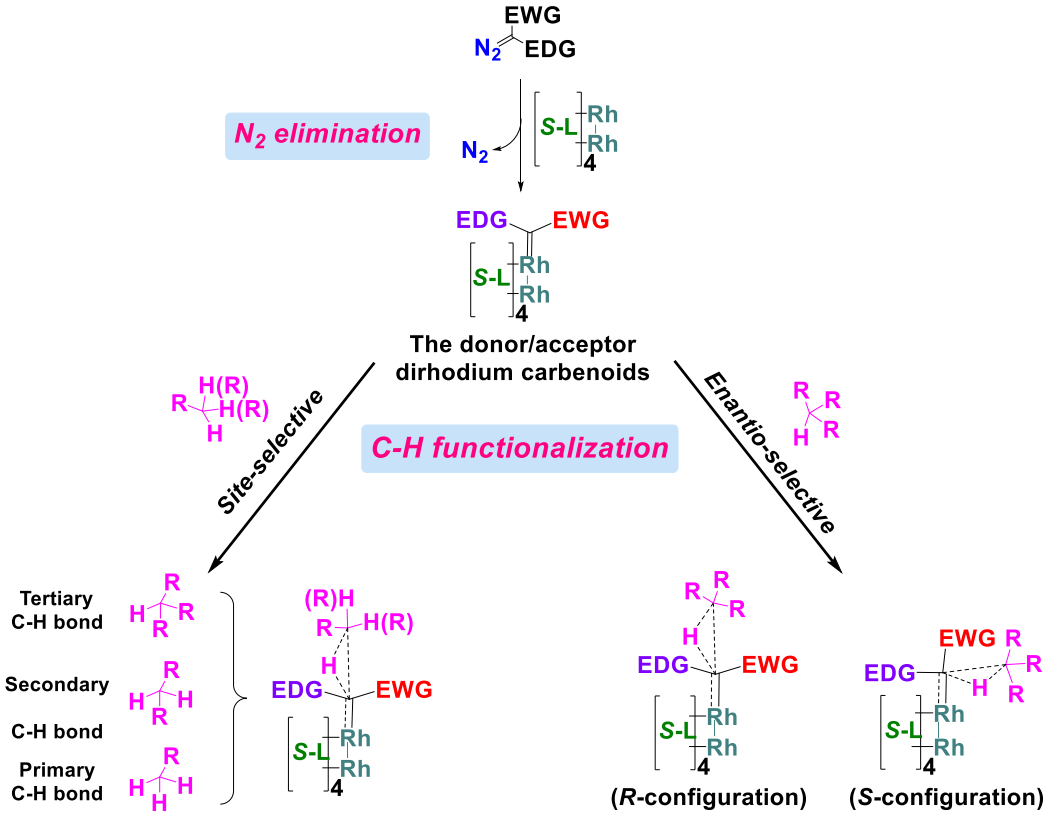

Figure 7: A schematic representation of the C–H functionalization processes for the reactions of donor/acceptor carbene catalyzed by a chiral dirhodium catalyst with *S*-configuration ligands (*S*-L). It mainly includes two processes, N_2 elimination and the site- and enantio-selective functionalization of C-H bonds.

In the present work, the C–H bond functionalization mechanisms are studied using the reaction of 2-methylpentane with aryl diazoacetate derivatives catalyzed by a simplified chiral dirhodium complex Rh_2(*S*-TCPCH$_3$)$_4$. DFT calculations are carried through to study the site-selectivity of the C–H bond functionalization at the tertiary site compared with the secondary and primary sites although these latter contain less steric hindrance (see Figure 7). Moreover, we studied the higher enantio-selectivity for these reactions by comparing the *R*- and *S*-configuration product formation for the tertiary C–H bond functionalization catalyzed by the dirhodium complex with *S*-ligands (Figure 7). We also demonstrated the importance of the *S*-ligands in the

reaction of the tertiary C–H bond functionalization by comparing the catalytic properties of Rh_2(*S*-TCPCH$_3$)$_4$ and Rh_2–(O$_2$CH)$_4$. In this work, we obtained a detailed understanding of the mechanisms for the high site- and enantio-selectivity for the tertiary C–H bond functionalization when the reactions are catalyzed by a chiral dirhodium complex. Even though we have studied a specific reaction in great detail we are convinced that our conclusions are generally valid also for other catalytic reactions involving chiral catalysts and for which limited space is available for the catalytic reaction.

This work was published in the journal of Physical Chemistry Chemical Physics. (Meijuan Zhou* and Michael Springborg, Theoretical study of the mechanism behind the site- and enantio-selectivity of C–H functionalization catalysed by chiral dirhodium catalyst. Phys. Chem. Chem. Phys., 22:9561-9572, **2020**.)

7. Surfaces, Shapes, and Bulk Properties of Crystals

7.1 Introduction

For macroscopic, crystalline materials, the properties of the surfaces as well as of the bulk are interesting and of technological importance. Heterogeneous catalysis, for instance, depends crucially on the local properties at the surfaces of the catalyst. On the other hand, the responses to mechanical, magnetic, and electric perturbations are determined primarily by the bulk properties of the system.

Most often, it is indirectly assumed that the bulk and surface properties are essentially independent of one another. Thus, limited attention has been paid to the coupling between the two. An exception can be found within the treatment of the so-called polar surfaces. In a seminal paper, Tasker [45] presented a classification of

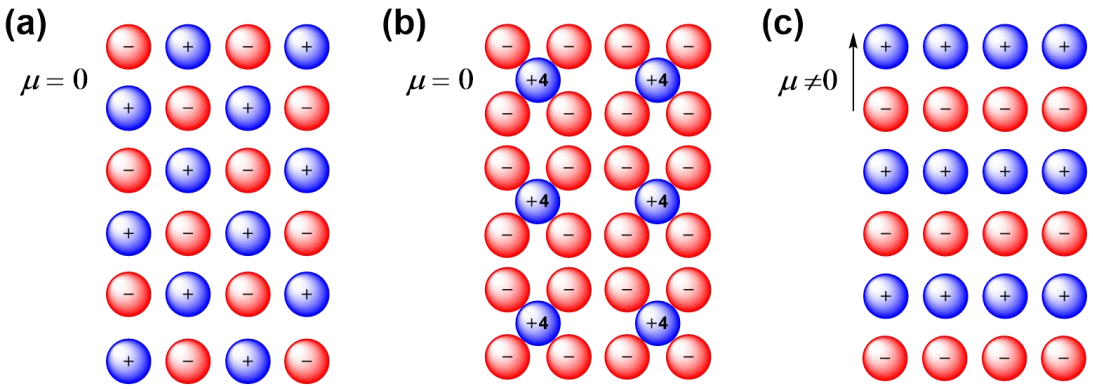

Figure 8. The conditions of polar surface [45]: 1. Charged atomic layers 2. Non-zero dipole moment normal to surface. Type (a) and (b) are non-polar surface, and type (c) is polar surface.

different types of surfaces. In Figure 8, the surfaces of type (a) and (b) both belong to non-polar surfaces. Because the system has equal anions and cations in each atomic layer, the dipole moment is zero for type (a). On the other hand, type (b) has charged atomic layers but still zero-dipole moment. For the polar surface of type (c), we have charged atomic layers and a non-zero dipole moment along the normal to the surface. This leads to a nonvanishing electric field acting on the ions in the bulk and according to Tasker such arrangements should not be realizable. This is an example of a

coupling between the surface and the bulk.

It turns out that oxides represent an especially challenging case as far as the understanding of polar surfaces is concerned (see, e.g., the review papers by Noguera et al. [46,47]). The polar surfaces of crystalline ZnO have attracted particular attention (see, e.g., the theoretical studies of Wander et al. [48], Meyer and Marx [49], Mora-Fonz et al. [50] and Setvin et al. [51]). Tasker's criterion indicates that these surfaces should not exist, but they are nevertheless observed in the experiment. Several studies have been devoted to rationalizing this discrepancy, including the three theoretical papers mentioned above. In these papers, a number of different scenarios have been proposed, including a charge transfer between the opposite, parallel sides of a slab [48,49] as well as the existence of lower symmetry surfaces [50] and the rearrangement of the surface layers with the formation of isolated oxygen vacancies [51]. The first suggestion is noteworthy with regard to our present work as it implies that it is not sufficient to study an individual polar surface without taking into consideration the other surfaces of the system.

Surfaces can also influence bulk properties. We shall explore this issue in detail in this work. In the present work, we shall generalize the conditions set up by Tasker and thereby demonstrate that (almost) all surfaces, whether polar or not, can be stabilized through a charge transfer that causes the electric field acting on the ions in the inner part of the sample to vanish. Subsequently, we demonstrate that such a charge transfer between surfaces affects the dipole moment per unit indicating that typical bulk properties can be affected. In addition, the same surface for samples of different shapes may have different charge densities. Subsequently, we illustrate these theoretical findings through the results from model calculations on finite quasi-two-dimensional systems with up to almost 10 000 atoms that are designed as models for certain three-dimensional systems.

7.2 Theory

7.2.1 The discussion by Tasker [45]

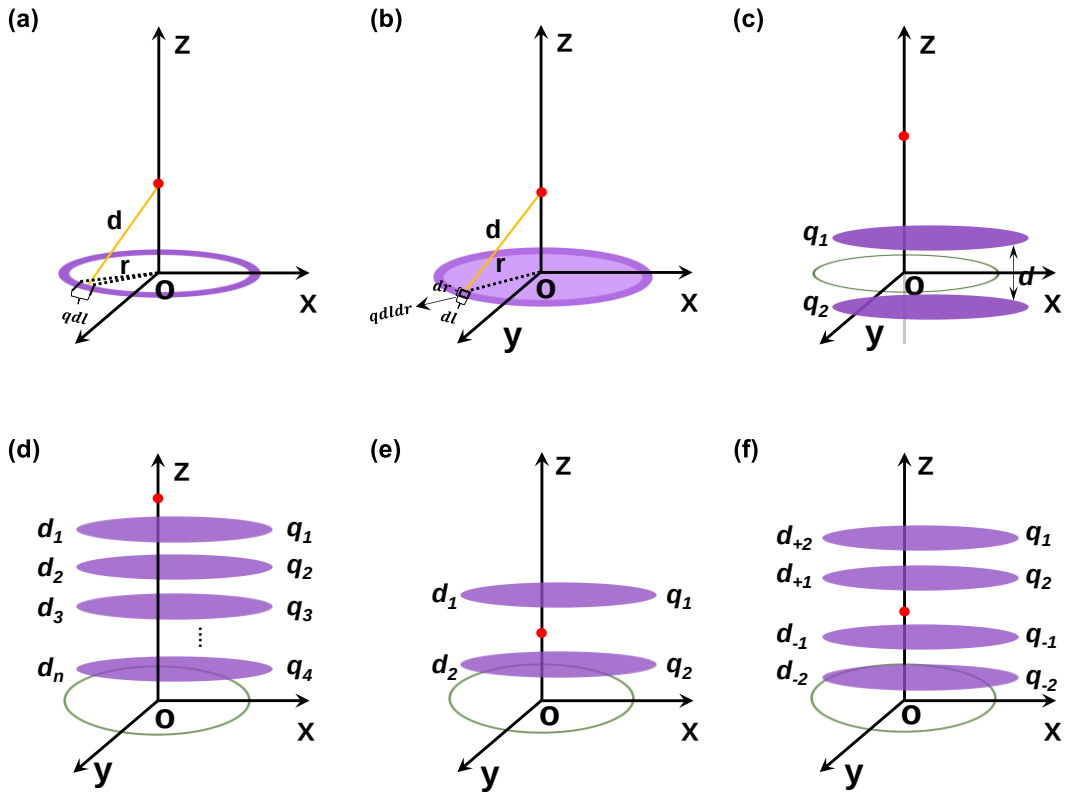

Figure 9. Six cases for the potential at the red reference point generated by the infinitely thin and uniformly charged ring or more charged planes.

Based on the seminal paper of Tasker [45], we shall discuss the scenarios that are shown in Figure 9. The electric potential at a distance r generated by a point charge Q,

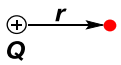

is:

$$V = \frac{1}{4\pi\epsilon}\frac{Q}{r} \tag{1}$$

Here, we set $4\pi\epsilon = 1$, so that Eq. (1) changes into $V = \frac{Q}{r}$ (2)

A. In the case of Figure 9(a), we consider a constant charge density q on an infinitely thin and uniformly charged ring. The radius of this ring is r. The potential at the red reference point (0, 0, z), can be expressed as:

$$V = \int_0^{2\pi r} \frac{qdl}{d} = \frac{2\pi qr}{(r^2+z^2)^{1/2}} \tag{3}$$

B. In the case of Figure 9(b), the infinitely thin and uniformly charged ring is changed into an infinite plane with uniformly charge. The potential at the red reference point (0, 0, z) is:

$$V = \int_0^\infty \int_0^{2\pi r} \frac{qdl}{d} dr = \int_0^\infty \frac{2\pi qr}{(r^2+z^2)^{1/2}} dr = 2\pi q \int_z^\infty dt \to \infty \qquad (4)$$

by substituting

$$t = (r^2 + z^2)^{1/2}$$

$$dt = \frac{r}{(r^2 + z^2)^{1/2}} dr \qquad (5)$$

The force / electric field (along the z direction) acting on a test charge (we set the charge of the charged particle to be 1) is equal to the z component of the gradient of the potential. Of symmetry reasons, the electric field is parallel to the z direction.

At first, we calculate the electric field E_z' for Figure 9(a),

$$E_z' = -\frac{dV}{dz} = -\frac{d}{dz}\frac{2\pi qr}{(r^2+z^2)^{1/2}} = \frac{2\pi qrz}{(r^2+z^2)^{3/2}}$$

Based on the equation E_z' for Figure 9(a), we get E_z for Figure 9(b) through integration,

$$E_z = -\frac{dV}{dz} = \int_0^\infty \frac{2\pi qrz}{(r^2+z^2)^{3/2}} dr = -2\pi qz \int_{z^{-1}}^0 d\left(\frac{1}{(r^2+z^2)^{1/2}}\right) = 2\pi q \qquad (6)$$

C. In the case of Figure 9(c), the potential at the red reference point is:

$$V = 2\pi q_1 \int_{z-d/2}^\infty dt + 2\pi q_2 \int_{z+d/2}^\infty dt \qquad (7)$$

If $q_2 = -q_1$ (charge neutrality),

the potential becomes finite,

$$V = 2\pi q_1 \int_{z-d/2}^\infty dt - 2\pi q_1 \int_{z+d/2}^\infty dt = 2\pi q_1 \int_{z-d/2}^{z+d/2} dt = 2\pi q_1 d \qquad (8)$$

Because $\mu = q_1 d$, with μ being the density of dipoles perpendicular to the planes we have,

$$V = 2\pi\mu \qquad (9)$$

Because the system of Figure 9(c) has charge neutrality, the electric field will vanish at the reference point.

D. If the system of Figure 9(c) has many (n) layers, it will change into the system of Figure 9(d), and the potential at the red reference point becomes,

$$V = \sum_{i=1}^{n} 2\pi q_i \int_{|z-d_i|}^{\infty} dt \tag{10}$$

If this system is also electric neutral,

$$\sum_{i=1}^{n} q_i = 0$$

and $z > d_i, i = 1, 2, 3, \cdots, n.$ (d_i is the z coordinate of the i'th charged layer)

Eq. (10) will change into:

$$V = 2\pi \sum_{i=1}^{n} q_i \, d_i \tag{11}$$

For the system of Figure 9(d), the electric field vanishes.

E. In the case of Figure 9(e), the red reference point is located between the two charged layers. According to Eq. (10), the potential equals to:

$$V = 2\pi q_1 \int_{|z-d_1|}^{\infty} dt + 2\pi q_2 \int_{|z-d_2|}^{\infty} dt = 2\pi q_1 \int_{d_1-z}^{\infty} dt + 2\pi q_2 \int_{z-d_2}^{\infty} dt \to \infty \tag{12}$$

According to Eq. (6), the z component of the gradient of the potential becomes:

$$E_z = -\frac{dV}{dz} = 2\pi(q_1 - q_2) \tag{13}$$

If $q_1 = q_2$, the force / electric field (along the z direction) acting on the test charge (we set the charge of the charged particle to be 1) will vanish.

F. In the case of Figure 9(f), the red reference point is located between more ($n_+ + n_-$) layers (in the example of the figure $n_+ = n_- = 2$). The potential equals:

$$V = 2\pi \left[\sum_{i=1}^{n_+} q_{+i} \int_{d_{+i}-z}^{\infty} dt + \sum_{i=1}^{n_-} q_{-i} \int_{z-d_{-i}}^{\infty} dt \right]$$

$$= 2\pi \left[q_{+2} \int_{d_{+2}-z}^{\infty} dt + q_{+1} \int_{d_{+1}-z}^{\infty} dt + q_{-1} \int_{z-d_{-1}}^{\infty} dt + q_{-2} \int_{z-d_{-2}}^{\infty} dt \right] \to \infty \tag{14}$$

According to Eq. (13), the z component of the gradient of the potential becomes:

$$E_z = -\frac{dV}{dz} = 2\pi\left(\sum_{i=1}^{n_+} q_{+i} - \sum_{i=1}^{n_-} q_{-i}\right) \tag{15}$$

If $\sum_{i=1}^{n_+} q_{+i} = \sum_{i=1}^{n_-} q_{-i}$

the electric field/force (along the z-direction) acting on the test charge (we set the charge of the charged particle to be 1) will vanish. The case of Figure 9(f) is similar to Tasker type 3 (Figure 8(c)). The red reference point is then the position of an atom located in some atomic layer, and the atomic layers 'above' and 'below' this red reference point may have different charge densities. Therefore, the electric field or force for this system may not vanish. In this case, charge has to be transferred from one side to another side, so that the electric field or force will vanish according to Eqs. (13) and (15). This was the instability discussed by Tasker.

From the above discussion, as long as the total charge above the red reference point equals that below the red reference point, the electric field/force generated at the red reference point will vanish.

7.2.2 2D systems

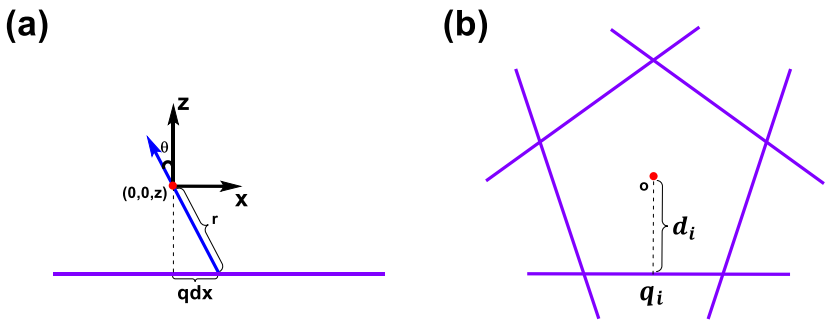

Figure 10. (a) A case for a straight line with a uniform charge density q. (b) A case for more straight lines with uniform linear charge densities q_i in different directions.

According to Eq. (1), and by setting $4\pi\epsilon = 1$, the potential that is produced by the straight line with a uniform linear charge at the red reference point in Figure 10(a) equals:

$$V = \int_{-\infty}^{+\infty} \frac{qdx}{r} = \int_{-\infty}^{+\infty} \frac{qdx}{(x^2 + z^2)^{1/2}} \tag{16}$$

Here, $\epsilon = \epsilon_0 \epsilon_r$, so that we have taken into account that the field of a given charge may be screened. The force / field (along the z-direction) acting on the test charge (the red reference point) becomes:

$$E_z = -\frac{dV}{dz} = \int_{-\infty}^{+\infty} \frac{qz}{(x^2+z^2)^{3/2}}\,dx \tag{17}$$

$$x = z\tan\theta$$

$$\mathrm{d}x = dz\tan\theta = \frac{z}{(\cos\theta)^2}\,d\theta \tag{18}$$

$$r^3 = (x^2+z^2)^{3/2} = \frac{z^3}{(\cos\theta)^3} \tag{19}$$

Inserting Eqs. (18) and (19) into Eq. (17), the force / field (along the z-direction) will change into:

$$E_z = \int_{-\pi/2}^{+\pi/2} \frac{q\cos\theta}{z}\,d\theta = \frac{1}{z}\int_{-\pi/2}^{\pi/2} q\cos\theta\,d\theta = \frac{1}{z}\int_{-\pi/2}^{\pi/2} q\,d\sin\theta = \frac{2q}{z} \tag{20}$$

For the case of Figure 10(b), according to Eq. (20), the force/field will then become,

$$\vec{E} = \sum_{i=1}^{n} \frac{2q_i}{d_i}\,\vec{1}_i \tag{21}$$

by adding the contributions from each line separately. d_i: the distance from the red reference point to the straight line with uniform linear charge density q_i. Moreover, $\vec{1}_i$ is a unit vector parallel to the inward pointing normal to the i'th side.

From Eq. (21) we see that the force/field acting on the test charge (we set the charge of the charged particle to be 1) depends on the position of the point of interest. Alternatively, Eq. (21) shows that the force/field generated by surface charges gets increasingly smaller when the size of the system gets bigger. Thus, in the middle of a large system, the force/field from surface charges (below, we shall discuss why only these charges are of relevance) can essentially be ignored, whereas the lattice will experience some distortions when approaching some surface. These distortions will not get arbitrarily large since the forces of Eq. (21) will be partially compensated by the force/field from the neighboring atoms. In total, our analysis implies that the problem of polar surfaces is irrelevant for 2D systems (and for 1D systems as well).

7.2.3 3D systems

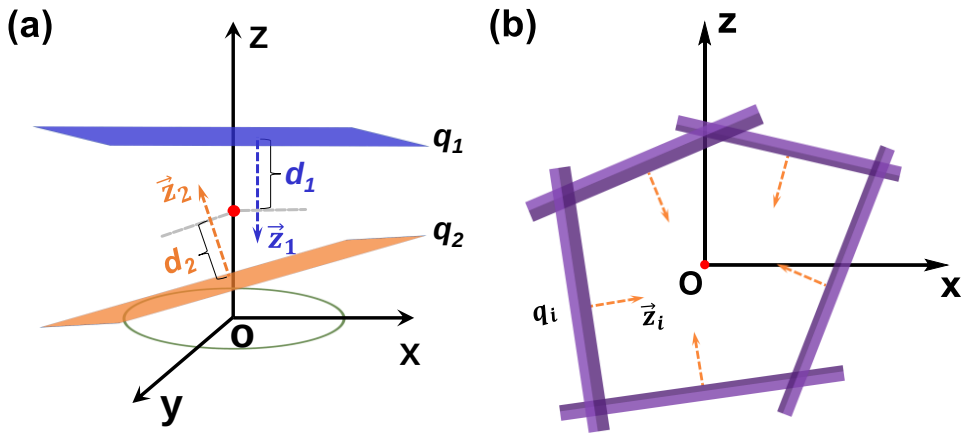

Figure 11. (a) A case for the potential at the red reference point generated by the two non-parallel charged planes. (b) A generalization of the case of (a).

For the case of Figure 11(a), we consider a point between two non-parallel planes. The red reference point is the position of an atom located between two non-parallel atomic layers, and the atomic layers 'above' and 'below' this red reference point have different charge densities. Therefore, we set $\vec{z}_i$ as the inwards pointing normal to the corresponding plane. According to Eqs. (13) and (15) requiring that atoms far away from the charges of the planes form a stable structure can be formulated as, the condition of vanishing electric field/force acting on the red reference charge, i.e.,

$$\vec{E} = -\vec{\nabla}V = 2\pi(q_1 \vec{z}_1 + q_2 \vec{z}_2) = 0 \tag{22}$$

For the case of Figure 11(b), the condition of vanishing electric field/force acting on the red reference point will be:

$$\vec{E} = -\vec{\nabla}V = 2\pi \sum_{i=1}^{n} q_i \vec{z}_i = 0 \tag{23}$$

Below we shall study some 2D systems as model systems for certain 3D systems. Thereby, we shall impose the condition of Eq. (23), although for 2D systems, rather Eq. (21) should be satisfied.

7.2.4 Generalizing the discussion by Tasker [45]

We consider a neutral, large, finite, regular system that consists of very many mostly identical units. Only at the boundaries, deviations from this regularity may occur. The system is assumed to be so large that the thermodynamic limit has been reached. In that limit, we can define a central region and various boundary regions as shown in Figure 12(a). Inside each region, the units are assumed to be identical. The central region consists of units whose properties are independent of the size and the shape of the system, whereas this is not the case for the boundary regions. For a three-dimensional (3D) system, the boundary regions can be separated into a set of two-dimensional (2D) side regions, a set of one-dimensional (1D) edge regions, and a set of zero-dimensional (0D) corner regions. In each of the boundary regions, the repeated units may be larger than those of the central region (because of structural relaxations at the boundaries and/or to adsorbents).

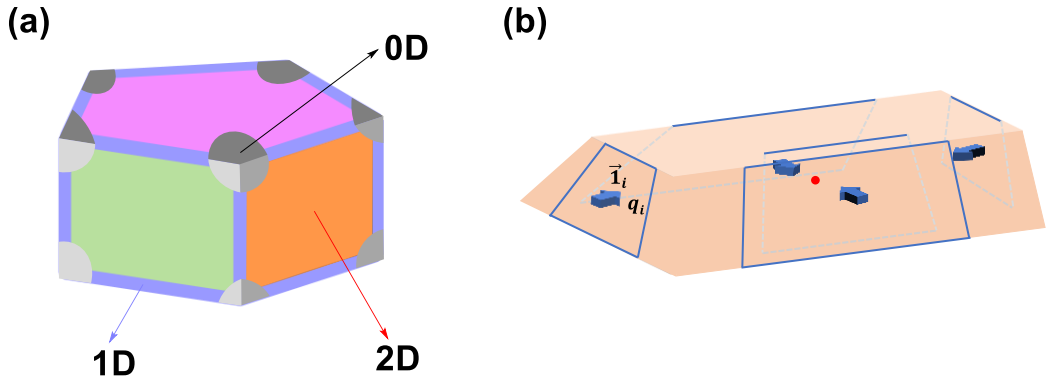

Figure 12. (a) Schematic representation of a 3D system with several different sides. (b) In the 3D system, the red circle marks the position of an atom in the middle of the central region. q_i is the charge density of the i'th layer of atoms, and $\vec{1}_i$ is normal to this layer. For the sake of simplicity, the top and bottom surfaces are ignored. Moreover, the system of the figure has just one layer of charges at each surface, except for the front surface that has two such layers.

Often, such systems are treated as being infinite and periodic. Here, we will explicitly consider instead the large, finite system. In passing, we add that even when treating the system as being infinite and periodic (i.e., without surfaces), it is possible to include effects that can be ascribed to the surfaces of the finite system as we have

demonstrated elsewhere for the calculations of the dipole moment per unit [52]. The units of the central region are equivalent to the unit cells of the infinite, periodic system and are, accordingly, nonunique. Consequently, as the complete system is separated into non-overlapping units, the units of the boundary regions are also nonunique. Ultimately, this implies that the separation of any extensive quantity, Z, into contributions from the individual units is nonunique,

$$Z = \sum_n Z_n = \sum_n \int_{\vec{r}\in\boldsymbol{\Omega}_n} Z(\vec{r})d\vec{r} \tag{24}$$

although the total value Z is unique. In this expression, Ω_n is the volume associated with the nth unit. For different regions, Ω_n may have different sizes and even different compositions (corresponding, i.e., to surface reconstructions and/or adsorbents).

By construction, all units in each region will be identical and, initially, independent of the presence or properties of the other regions, that is, Z_n will take the same value for all units *n* of the same region. If we now imagine scaling the size of the system by some factor f, the properties of each unit in the different regions will, per construction, remain unchanged. As the number of units in the central region scales as f^3 and the number in each of the other regions scales as f^P with $P < 3$, the units of the central region must be neutral (otherwise, the charge distribution in the sample will depend on its size, f, which is in conflict with the assumption of having reached the thermodynamic limit). Thus, charge will accumulate only in the boundary regions. This fact will become important below and was also indirectly used above when we considered the field at a reference point generated by charges that we assumed were confined to the boundary regions. We add that similar arguments apply to extended 2D or 1D systems. A 2D system will separate into a central region, various side regions, and corner regions. A 1D system will separate into a central region and two termination regions. Again, only the boundary regions can accumulate charge.

As a generalization of Tasker's discussion, we consider a system like that of Figure 12(b) in which each surface may be composed of several atomic layers. Then, the

field at the reference point in the middle of the central region becomes:

$$\vec{E} = 2\pi \sum_i q_i' \vec{1}_i = 2\pi \sum_k \left[\sum_{i \in k} q_i' \right] \vec{1}_k = 2\pi \sum_k q_k \vec{1}_k \tag{25}$$

Here, $\vec{1}_i$ is an inward-pointing normal for the i'th atomic layer, q_i' is the charge density of that layer, which is assumed to be constant, and the layer is assumed to be infinitely large. These two assumptions will be retained throughout our discussion. Moreover, q_k is the sum of the charge densities of all atomic layers associated with the kth surface.

Based on the discussion above on 3D system and on Eq. (25), we find that even in the case of more parallel atomic layers (as illustrated in Figure 12(b)), only the sum of the charge densities q_k is relevant. Since, as demonstrated above, the units of the central region are neutral, only the total charge densities associated with the surfaces contribute to the field $\vec{E}$. Accordingly, it is straightforward to separate the total charge density into contributions from individual surfaces.

In deriving Eq. (25), we have made the approximation that the true charge density of each surface can be approximated through a model charge density, i.e., a plane of a constant charge density,

$$\rho_{\text{true}}(\vec{r}) \approx \rho_{\text{model}}(\vec{r})$$

We have then calculated the true field according to

$$\vec{E}_{\text{true}}(\vec{r}) = [\vec{E}_{\text{true}}(\vec{r}) - \vec{E}_{\text{model}}(\vec{r})] + \vec{E}_{\text{model}}(\vec{r})$$

and included only the last term. This is possible if the total charges of $\rho_{\text{true}}(r)$ and $\rho_{\text{model}}(r)$ per, for instance, surface unit cell are identical. In that case

$$\vec{E}_{\text{true}}(\vec{r}) - \vec{E}_{\text{model}}(\vec{r}) = \mathrm{O}(1/d)$$

with *d* being the distance between the point of interest and the charge density whose field we are interested in. Thus, for very large values of *d*, this term can be ignored.

The stability (i.e., the generalized condition of Tasker) requires that the electrostatic

field vanishes at the positions of ions of the central region:

$$\vec{E} = 2\pi \sum_k q_k \vec{1}_k \equiv \vec{0} \tag{26}$$

If the charge densities at the surfaces are such that this condition is not satisfied, then a charge redistribution at the surfaces must occur to achieve structural stability. This simple generalization of the result obtained by Tasker is of central importance for the present work and its consequences will be developed in the following. For 2D and 1D systems, the contribution from the individual boundary regions decays with the distance to the reference point, so that the treatment leading to Eq. (26) must be modified. Moreover, for 3D systems, only the side regions (2D systems) contribute to $\vec{E}$ in the thermodynamic limit, and the edge (1D systems) and corner regions (0D systems) provide contributions that become negligible for sufficiently large systems.

7.3 Stabilizing Polar surfaces

Figure 12(b) shows a large 3D sample of the material of interest with a given shape that has been obtained by cutting parts of a larger sample without changing the charge distribution of the latter. In general, this will lead to an unstable situation if the surfaces are polar, as the stability condition of Eq. (26) will not be fulfilled. Thus far, structural and electronic relaxation effects have been ignored. However, electronic relaxation effects (including the possible occurrence of surface states) will modify the original surface charge densities q'_{k0},

$$q'_{k0} \rightarrow q_{k0} \tag{27}$$

so that the charge neutrality constraint remains being satisfied:

$$\sum_k q_{k0} L_k = 0 \tag{28}$$

(L_k is the size (area) of the kth surface). This will make the individual q_{k0} dependent on the overall shape.

Based on the generalized condition of Tasker [45], when determining the effect of the overall shape, we have to take into account a possible charge transfer between the

surfaces.

If we ignore, at first, the charge transfer between surfaces, then the field defined in Eq. (25) will be:

$$\vec{E} = 2\pi \sum_k q_{k0}\, \vec{1}_k \equiv \vec{E}_0 \tag{29}$$

Subsequently, assuming that $\vec{E}_0$ does not vanish, there must be a charge flow between the different surfaces to satisfy the generalized condition of Tasker, Eq. (26), that is:

$$q_{k0} \rightarrow q_{k0} + \Delta q_k \equiv q_k \tag{30}$$

with the additional charges Δq_k determined by the facts that $\vec{E}$ must vanish and that the complete system remains being neutral. This is a nonlocal charge redistribution that differs from a local redistribution related to structural relaxation.

Charge neutrality requires that,

$$\sum_k \Delta q_k\, L_k = 0 \tag{31}$$

Moreover, the condition of Eq. (26) becomes:

$$2\pi \sum_k \Delta q_k\, \vec{1}_k \equiv -\vec{E}_0 \tag{32}$$

because of Eq. (29). For a 3D system, Eqs. (31) and (32) provide four conditions on the charge transfers $\{\Delta q_k\}$. Often, however, there will be more than four surfaces so that many different solutions to these equations can be found. This means that the general solution can be written as:

$$\Delta q_k = \Delta q_{k0} + \Delta q_{k1} \tag{33}$$

where $\{\Delta q_{k0}\}$ is a particular solution and $\{\Delta q_{k1}\}$ is the general solution with $-\vec{E}_0$ in Eq. (32) replaced by $\vec{0}$. The set of solutions $\{\Delta q_{k1}\}$ forms a $\mathrm{P}-4$ dimensional subspace of the P-dimensional space of $\{\Delta q_k\}$ (with P being the number of sides of the sample of interest), and it is interesting to notice that these solutions depend solely on the overall shape of the system and not on the size of the units or on the number or types of atoms in the system. Moreover, the resulting set $\{\Delta q_k\}$ does not depend on

the choice of $\{\Delta q_{k0}\}$. We see that, in general, it is always possible in principle to stabilize any surface through appropriate charge transfers between the different surfaces. This can occur with or without simultaneous structural relaxation and/or the addition of adsorbates. Typically, there will be a number of possible solutions for $\{\Delta q_{k1}\}$. What actually occurs in practice depends upon the energetics and is well beyond the scope of the present study.

7.4 The dipole Moment Per Cell

7.4.1 An intensive nonlocal property

An intensive nonlocal property that explicitly depends on the surfaces of the system is the dipole moment per cell [52]. In considering a set of systems of the same material and shape but increasing size, this property can be calculated either as the dipole moment per unit or as the change in the dipole moment per added unit, both evaluated in the limit of infinitely large systems. Thus, for the extensive property Z (in our case, one of the components of the total dipole moment), we can define the corresponding intensive quantity in the thermodynamic limit as:

$$\bar{Z} = \lim_{N\to\infty} \frac{Z(N)}{N} = \lim_{N\to\infty} \frac{Z(N+\Delta N) - Z(N)}{\Delta N} \tag{34}$$

with $Z(N)$ being the value of Z for the system with N cells.

In the results to be reported below, we shall use the second equality of Eq. (34). The size of the system will be increased, while preserving the shape, by displacing the surfaces along their outward pointing normal (i.e., along $-\vec{1}_i$ in Figure 12(b)). For discussion purposes, it is more revealing to use the second relation of Eq. (34). Thus, one contribution to the dipole moment per cell due to the increase in size arises because the number of (neutral) units in the central region grows. As the units in the surface regions in general contain charge, a second contribution to the dipole moment per cell comes from the displaced surface charges along the outward pointing normals, as discussed in detail earlier [52]. In the case of 1D systems, the so-called charge

quantization [53,54] reduces the number of possible values for the dipole moment per cell, but this effect does not occur in 2D or 3D systems.

In the present work, we shall generalize the conditions set up by Tasker and thereby use that we have demonstrated that (almost) all surfaces, whether polar or not, can be stabilized through a charge transfer that causes the electric field acting on the ions in the inner part of the sample to vanish. We, then, demonstrate that such a charge transfer between surfaces affects the dipole moment per unit indicating that bulk properties can thereby be affected.

In calculating the surface contributions to the dipole moment per cell, according to Eq. (30), it will be used that the extra charge density Δq_k is placed along the kth side of the sample. We emphasize that the surface charge densities will provide a field in the middle of the sample only for 3D systems. When scaling the size of a 3D system by the factor f mentioned above, the numbers of cells in the central region and in the complete system both scale as f^3. On the other hand, the distances of the boundary regions to the origin of coordinates (which conveniently is chosen as the center of the system) will scale as f, so that, of the boundary regions, only the surface (as opposed to the edge and corner) regions will give a finite contribution to the dipole moment per unit in the infinite system limit. In total, the dipole moment per unit can therefore be written as,

$$\vec{\mu} = \vec{\mu}_C + \sum_k \Delta\mu_k \vec{1}_k \tag{35}$$

where $\vec{\mu}_C$ is the dipole moment of a single (neutral) unit cell in the central region, which is independent of the surfaces and/or shape of the sample. $\Delta\mu_k$ is the contribution to the dipole moment per bulk unit cell that originates from the charge associated with the kth surface and is accordingly related to q_{k0}. $\vec{\mu}_C$ is equivalent to Z_n of Eq. (24) for n representing a unit of the central region and is, accordingly, nonunique, which must also be the case for the contributions due to the charges associated with the surface regions. As discussed in detail in our previous work [52], the individual contributions to the second term in Eq. (35) can be interpreted as originating from the displacement of this charge along the outward pointing normal to

the kth surface when increasing the size of the system. It will be confirmed by our numerical results below that $\Delta\mu_k$ depends on the overall shape of the sample. We also find that, for some shapes, the occurrence of (occupied or empty) surface states gives a contribution to the charges of the individual surfaces, whereas for other shapes the same surfaces may not possess such surface states.

7.4.2 2D system with four sides

With the modification of Eq. (30) we have an additional charge distribution that gives an additional contribution to the total dipole moment of the system. At first, we shall consider a 2D system. We have an extra charge density Δq_k that is constant along a finite, straight line that we will ascribe the kth side. This line will be parallel to the kth side and may even be identical to it. We shall below discuss it in more detail.

This charge density gives an extra contribution to the total dipole moment equal to (taking the kth line in Figure 13 as an example):

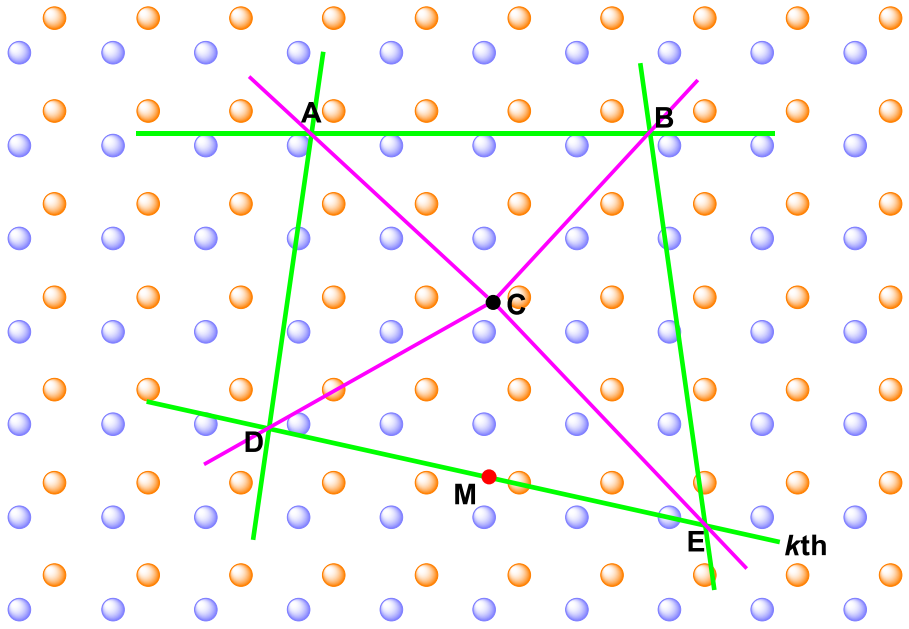

Figure 13. A schematic representation of a two-dimensional system with four sides (green lines). The magenta lines separate the system into four regions, given the numbers 1, 2, 3, and 4. A, B, D, and E mark the corners of the system, and C the center of the coordinate system, and M the midpoint of the line DE (the kth side, and the area (length) of the kth side is L_k). Each unit cell consists of two atoms (blue and orange).

$$\Delta\vec{\mu}_k = \int_{\vec{r}_{kD}}^{\vec{r}_{kE}} \left(\vec{r} - \vec{R}_C\right) \Delta q_k d\vec{r}$$

$$= \int_{\vec{r}_{kD}}^{\vec{r}_{kE}} \left(\vec{r} - \vec{r}_{Mk}\right) \Delta q_k d\vec{r} + \int_{\vec{r}_{kD}}^{\vec{r}_{kE}} \left(\vec{r}_{Mk} - \vec{R}_C\right) \Delta q_k d\vec{r} \qquad (36)$$

where the line integral runs along the line and where we have included the special choice for the origin of the coordinate system, $\vec{R}_C$, and $\vec{r}_{Mk} = \frac{1}{2}(\vec{r}_{kD} + \vec{r}_{kE})$ is the midpoint of the kth line for which the two end-points are $\vec{r}_{kD}$ and $\vec{r}_{kE}$ (see Figure 13), respectively. Then, using that Δq_k is constant, and that the first integral of Eq. (36) vanishes of symmetry reason, Eq. (36) will change into:

$$\Delta\vec{\mu}_k = 0 + \int_{\vec{r}_{kD}}^{\vec{r}_{kE}} \left(\vec{r}_{Mk} - \vec{R}_C\right) \Delta q_k d\vec{r} = \left(\vec{r}_{Mk} - \vec{R}_C\right)\Delta q_k \int_{\vec{r}_{kD}}^{\vec{r}_{kE}} d\vec{r} = \left(\vec{r}_{Mk} - \vec{R}_C\right)\Delta q_k L_k$$

Therefore:

$$\Delta\vec{\mu}_k = \left(\vec{r}_{Mk} - \vec{R}_C\right)\Delta q_k L_k \qquad (37)$$

Ultimately, such contributions from all sides have to be added up and added to the total dipole moment of the system.

Then, the total dipole moment can be written as:

$$\vec{\mu} = \vec{\mu}_0 + \sum_k \Delta\vec{\mu}_k = \vec{\mu}_0 + \sum_k \left(\vec{r}_{Mk} - \vec{R}_C\right)\Delta q_k L_k \qquad (38)$$

We introduce the generalized Tasker constraints mentioned in the parts of 7.2 and 7.3, that is, Eqs. (25) and (26). In addition, the charge neutrality constraint of Eq. (31) gives a third constraint for Δq_k. We shall here consider a special case, i.e., those that were considered in our model calculations, where we have 2D systems with four sides. This means that Eq. (33) can be written as

$$\Delta q_k = \Delta q_{k0} + t\Delta q_{k1} \qquad (39)$$

where Δq_{k0} and Δq_{k1} are constants, whereas $-\infty \leq t \leq +\infty$ is a parameter.

With $\vec{\mu}_0$ being the value of the dipole moment before the modifications of the present section, we may write

$$\vec{\mu} = \vec{\mu}_0 + \sum_k \left(\vec{r}_{Mk} - \vec{R}_C\right)(\Delta q_{k0} + t\Delta q_{k1})L_k$$

$$= \left[\vec{\mu}_0 + \sum_k \Delta q_{k0}\left(\vec{r}_{Mk} - \vec{R}_C\right)L_k\right] + t\left[\sum_k \Delta q_{k1}\left(\vec{r}_{Mk} - \vec{R}_C\right)L_k\right]$$

$$\equiv \vec{\mu}_1 + t\Delta\vec{\mu} \tag{40}$$

Let us discuss this in some detail and thereby consider some of our two-dimensional systems for illustration. An example is shown in Figure 14. In this case, of reasons to be discussed below, $\Delta\vec{\mu} = \vec{0}$. For the more general case of a 2D system with four sides, we may consider different shapes and for each of those calculate $\vec{\mu}_1$ and $\Delta\vec{\mu}$.

By setting: $\vec{\mu} = \vec{\mu}_1 + t\Delta\vec{\mu}$, we have

$$\mu_x = \mu_{x1} + t\Delta\mu_x \tag{41}$$

$$\mu_y = \mu_{y1} + t\Delta\mu_y \tag{42}$$

Combining Eq. (41) with Eq. (42) gives,

$$\mu_y = \mu_{y1} + t\Delta\mu_y = \mu_{y1} + \frac{\mu_x - \mu_{x1}}{\Delta\mu_x}\Delta\mu_y = \left(\mu_{y1} - \mu_{x1}\frac{\Delta\mu_y}{\Delta\mu_x}\right) + \frac{\Delta\mu_y}{\Delta\mu_x}\mu_x \tag{43}$$

or, by dividing with the number of atoms, N,

$$\frac{\mu_y}{N} = \left(\frac{\mu_{y1}}{N} - \frac{\mu_{x1}}{N}\frac{\Delta\mu_y}{\Delta\mu_x}\right) + \frac{\Delta\mu_y}{\Delta\mu_x}\frac{\mu_x}{N} \tag{44}$$

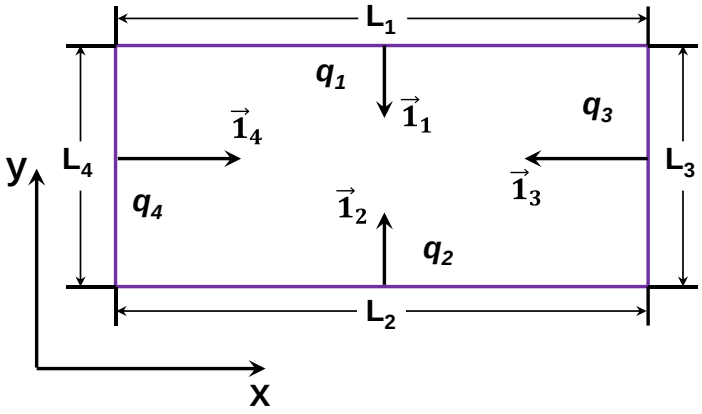

Figure 14. An example of a system for which $\Delta\vec{\mu} = \vec{0}$.

Ultimately, this means that, in general, the possible values for $(\vec{\mu}_x, \vec{\mu}_y)$ will form a

straight line where different points correspond to different values of t according to Eq. (39). Thus, we may for instance plot the straight lines of Eq. (43) in the limit $N \to \infty$ and then see if there are common values for all shapes or, alternatively, how they differ. In some few cases (see below) the straight lines may reduce to single points (i.e., when $\Delta\vec{\mu} = \vec{0}$ in Eq. (40)). We notice that because of charge neutrality, the dipole moment will be independent of $\vec{R}_C$.

That, the lines can reduce to single points, is illustrated in Figure 14. In this case, we have a rectangular shape. The conditions that we have charge neutrality and that $\vec{E} = \vec{0}$ are in this case

$$L_1 q_1 + L_2 q_2 + L_3 q_3 + L_4 q_4 = 0 \qquad (44)$$

$$q_2 - q_1 = 0$$

$$q_4 - q_3 = 0 \qquad (45)$$

Moreover, we have that:

$$L_1 = L_2 \text{ and } L_3 = L_4$$

$$q_1 = q_2 \text{ and } q_3 = q_4$$

From Eq. (37) and Figure 14 we then see that $\vec{\mu}$ is independent of the precise charge distribution on the surfaces as long as the conditions of Eq. (44) and (45) are satisfied. We add that these arguments can be generalized to any parallelogram, and that equivalent arguments may apply to other shapes, too.

Finally, from Eqs. (31), (32) and (35) we see that the equations that determine Δq_k do not depend on the precise charge distribution of the system but only on its shape. Therefore, keeping the same shape but varying the size will leave Δq_k (in Eq. (39)) unchanged. For a rectangle, the generalized Tasker criterion requires that the charge densities associated with opposite sides have to be identical so that there is no contribution to the dipole moment from these surfaces. Once this is established, changing the charge densities will not change the total dipole moment. For a parallelogram, the same arguments apply as one can see by using a coordinate system with axes that are parallel to the opposite sides.

7.5 The purpose of the present work

For the identification of polar surfaces, Tasker [45] presented two conditions: 1. Charged atomic layers; 2. Non-zero dipole moment perpendicular to the surface. According to Tasker, a polar surface leads to a nonvanishing electric field acting on the ions in the bulk. Therefore Tasker concluded that these surfaces should not exist, but nevertheless such arrangements (e.g. the polar surfaces of ZnO) are realized in the experiment. Many studies [48-50] have been devoted to the understanding of the existence of the polar surfaces of crystalline ZnO. In these papers, some explanations have been proposed. For the present purpose, an explanation that focuses on a charge transfer between the opposite and parallel sides of a slab [48,49] is relevant because it implies that it is not sufficient to study an individual polar surface without taking into consideration the other surfaces. In a recent work [52], we have also found that surfaces can influence bulk properties.

In this work, we presented the two stability requirements, including that the electrostatic field vanishes at the positions of the ions of the central region (i.e., the generalized condition of Tasker) and the charge neutrality. We have shown how the values for this property (the bulk dipole moment per unit) can be calculated subject to the generalized Tasker constraints. From the results of calculations for very large systems, using a sufficiently simple model, we were able to show that applying these constraints leads to a change in the dipole moment per atom or per unit in the thermodynamic limit. We demonstrated that the so-called polar surfaces may be stabilized through a charge redistribution between the complete set of surfaces that depends upon the overall shape of the sample and the nature of the material. This charge redistribution, in turn, is governed by the generalized Tasker conditions. The purpose of the present work was to study the interplay between the surface and bulk properties of macroscopic crystalline materials with an emphasis on polar surfaces. To that end, we generalized the scheme, originally proposed by Tasker [45], to identify stable polar surfaces. We could show that it is always possible to stabilize a given surface through a charge redistribution involving the entire set of surfaces. On the

other hand, our study suggests that consideration of other shapes (particularly containing more surfaces) would provide many more possibilities to realize this same surface (Figure 15).

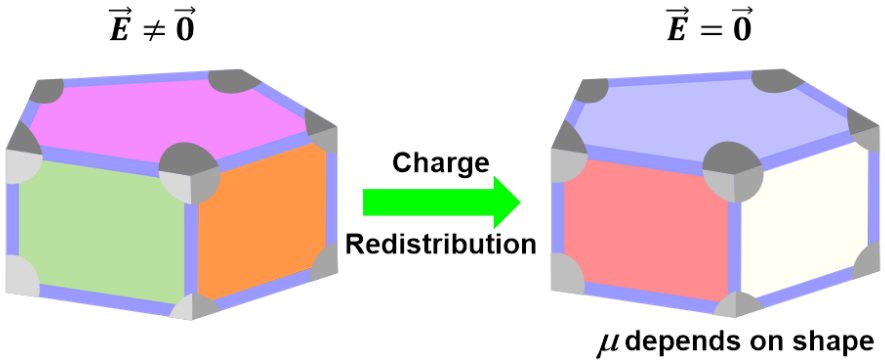

Figure 15. Schematic representation of a 3D system with several different sides. The entire set of surfaces are involved through a charge redistribution to stabilize a given surface.

This work is published in the Journal of Physical Chemistry C. (Michael Springborg*, Meijuan Zhou, Mohammad Molayem and Bernard Kirtman, Surfaces, Shapes, and Bulk Properties of Crystals. J. Phys. Chem. C, 122:11926–11932, **2018**.)

8. Theoretical Treatment of Properties of Surfaces and Their Interplay with Bulk Properties of Crystals

8.1 Introduction

The properties of crystalline materials continue to be exploited for a very large range of applications. In many cases, it is the bulk properties that are of interest. In the thermodynamic limit, that is, for sufficiently large systems, these properties are either intensive or extensive depending upon whether they are independent of the system size or proportional to it. In either case, since the boundary regions make up a very small part of the complete system, it may be suggested that the boundary regions are of no importance. On the other hand, the properties of the boundaries themselves can also be of interest for applications. An example is heterogeneous catalysis, in which case the bulk part of the sample is often assumed to be irrelevant.

These considerations suggest that bulk properties and surface properties are essentially independent of each other and can be treated separately. Theoretical studies of the properties of crystals often utilize this approach. For bulk properties, one typically treats the system as being infinite and periodic, thus completely ignoring the boundary regions. For the study of surface properties, one often constructs a simple model system that contains the surface of interest while ignoring other surfaces as well as the bulk region with the exception that the latter defines the structure of the surface.

Recently, we have demonstrated that for any real material, there is a delicate interplay whereby the concerted interactions between all surfaces and the bulk region will influence the properties of the individual surfaces [55]. Moreover, in some cases, these interactions will also affect the bulk properties. As an example of the latter, we considered the dipole moment per atom, an intensive property closely related to the polarization (i.e., the dipole moment per unit volume) and that has relevance for

piezoelectricity and other responses to electric fields. The purpose of the present work is to provide further details about this interplay and its consequences. As in the previous study we use simple model calculations that allow for application to very large, finite systems and thereby examine and illustrate concepts without attempting to provide accurate results for any real system.

8.2 The surface and bulk

Our goal is to consider neutral, macroscopic, 3D crystalline samples, cf. Figure 16(a). For the sake of simplicity, however, we shall illustrate the concepts through 2D systems. Both 2D and 3D systems, cf. Figure 16, can be separated into a central region and a number of boundary regions. Each region is assumed to consist of units that are identical, although the units of different regions will usually be different. In the central region, the units are chosen to be the same as the unit cells of the corresponding infinite, periodic system. Note that this choice is not unique. In the boundary regions, the units will often be larger than those of the central region due to the effects of structural and electronic relaxations near the surfaces. Since the sample is completely divided into units, those of the boundary regions will depend, in part, upon how the units of the central region are chosen and, in part, they may be constructed according to convenience. In the thermodynamic limit, the size of the central region will be much larger than that of any other region, which is why most bulk properties are independent of the boundary regions. We add that the units of the central region may be chosen independently of the boundary regions and the overall shape of the sample.

The units of the central region are neutral as can easily be seen as follows. Consider, for example, a 2D system like that of Figure 16(b). If the units of the central region carried charges, the fact that the complete system is neutral implies that a compensating charge must be accumulated at the boundaries. If you double the linear dimension of the system, then the total charge of the central region will be four times larger. On the other hand, per construction, each boundary region does not change

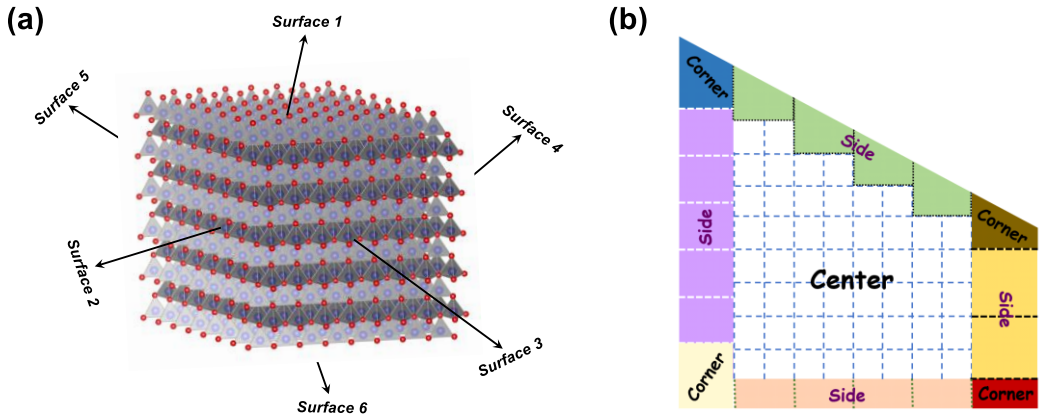

Figure 16. Schematic representation of (a) 3D and (b) 2D systems. They both consist of a central region as well as various boundary regions.

extension in the direction(s) perpendicular to the surface(s) at which it is placed. Therefore, the charge per cell in the boundary regions would have to increase on average in order to maintain neutrality. This is in conflict with the assumption that the thermodynamic limit has been reached. Thus, only the units of the boundary regions may be charged. Thereby, we have established that charge is concentrated in the boundary regions.

We may continue by studying the effects of this charge distribution on the atoms in the central region. To that end we consider an approach originally proposed by Tasker [45]. Tasker studied the electrostatic field created by a set of parallel layers of ions at a point far away from those layers, which represents the position of an atom in the bulk. In order to ensure that the crystal structure is stable, the electrostatic field at the atom would have to vanish. Since the details of the charge distribution were not relevant for his argument, he approximated each infinite layer of ions using a 2D plane with a constant charge density. Thereby, he was able to identify certain arrangements of the layers of ions for which the electrostatic field at the bulk atom does not vanish and concluded that such so-called polar surfaces either could not exist or would experience substantial reconstruction.

8.2.1 The electrostatic field for an arbitrary shape

According to the discussion in part 7.2.1, we generalized Tasker's analysis by

considering an arbitrary shape for the sample and the corresponding charged layers with different orientations as shown schematically in Figure 17. Then, the electrostatic

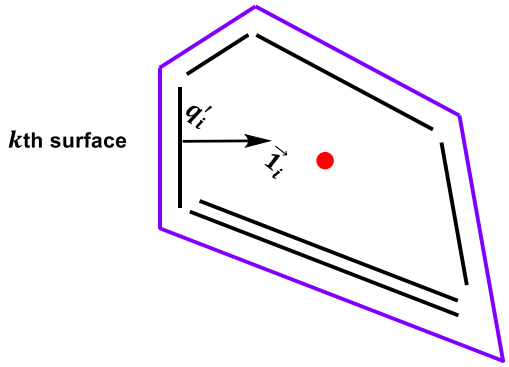

Figure 17. A schematic representation of a 2D system. It shows the layers with the charge densities q_i' as well as an inward-pointing normal to a given layer, $\vec{1}_i$. The boundary of the system is shown through purple lines. The red dot represents a point in the central part of the system.

field at an atom in the central region, generated by the charges localized in the surface regions, becomes:

$$\vec{E}_{\text{charge}} = \frac{1}{4\pi\epsilon} 2\pi \sum_i q_i' \vec{1}_i = \frac{1}{4\pi\epsilon} 2\pi \sum_k \left[\sum_{i\in k} q_i' \right] \vec{1}_k = \frac{1}{4\pi\epsilon} 2\pi \sum_k q_k \vec{1}_k \qquad (46)$$

where $\vec{1}_i$ is an inward-pointing normal to the i'th layer of ions and q_i' is the charge density of that layer and

$$\epsilon = \epsilon_0 \epsilon_r \qquad (47)$$

is the dielectric constant of the material. Finally, q_k is the sum of the charge densities of all layers associated with the kth surface.

8.2.2 Dipole surfaces with a periodic stacking sequences

Another contribution to the electric field that occurs in certain cases has been analyzed by Meyer and Vanderbilt and by Meyer and Marx [49,56]. Thus, for crystals with a periodic stacking sequence as in Figure 18, which results in a dipole moment perpendicular to the surface, there is a field from the dipole layers, $\vec{E}_{\text{dipole}}$. We shall now analyze this in detail and thereby generalize the earlier treatments.

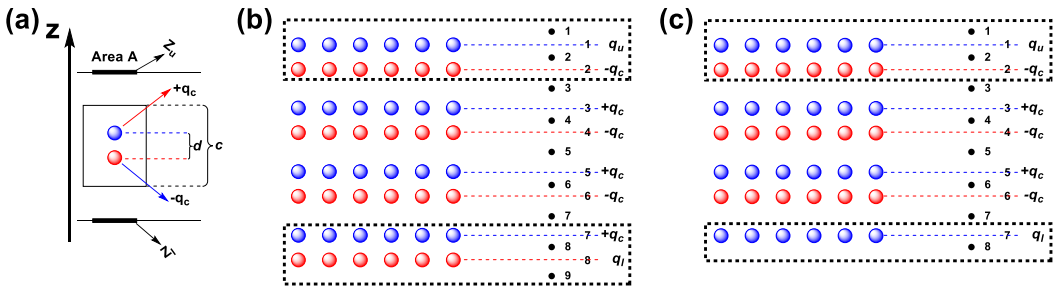

Figure 18. (a) An example of a slab geometry for a system with two atoms per unit cell. Z_u and Z_l are the charge densities associated with the upper and lower surface region, respectively. (b) and (c) are two examples of the slab geometry structures. The black dotted boxes on the top and the bottom places represent the uppermost and bottommost surface regions, respectively.

A. The dipole moment per cell for the unit cell in Figure 18(a)

In Figure 18(a), the slab geometry has two atoms per unit cell. For atoms in the central region, the charges of those are $+q_c$ and $-q_c$. At the surfaces, the charge densities of the uppermost and bottommost layers are, respectively, Z_u and Z_l, and they may be different from those of the bulk atoms. d is the distance between the two atoms inside one unit cell, and the contribution from the bulk unit cell to the dipole moment per cell equals,

$$\vec{\mu}_c = dq_c\vec{1}_z \tag{48}$$

where $\vec{1}_z$ is a unit vector along the z direction.

With c being the lattice vector along the z direction, the surface contribution to the dipole moment per cell becomes,

$$\vec{\mu}_s = \frac{1}{2}c(Z_u - Z_l)\vec{1}_z \tag{49}$$

This result follows from considering the case that one extra layer of unit cells is added to each of the top and bottom regions. Thereby in effect, two layers of unit cells are added (resulting in the factor 1/2 above), whereas the top and the bottom charges are displaced in the positive and the negative z direction, respectively.

The total dipole moment per unit cell is accordingly,

$$\vec{\mu} = \vec{\mu}_c + \vec{\mu}_s = \left[dq_c + \frac{1}{2}c(Z_u - Z_l)\right]\vec{1}_z \tag{50}$$

In passing, we add that this is a clear example of how the surfaces give a finite

contribution to the dipole moment per cell, i.e., to a bulk property.

B. The dipole moment per cell for both cases in Figures 18(b) and (c)

For the case in Figure 18(b), $Z_u = q_u - q_c$ and $Z_l = q_c + q_l$

whereas for the case in Figure 18(c), $Z_u = q_u - q_c$ and $Z_l = q_l$

From Figure 18(b) and (c), Z_u and Z_l represent respectively the charge densities of the uppermost and bottommost surface regions which are marked by the black dotted boxes.

We have the dipole moment per cell for the case in Figure 18(b),

$$\vec{\bar{\mu}} = \vec{\bar{\mu}}_c + \vec{\bar{\mu}}_s = \vec{\bar{\mu}}_c + \frac{1}{2}c(Z_u - Z_l)\vec{1}_z = \vec{\bar{\mu}}_c + \frac{1}{2}c(q_u - q_c - q_c - q_l)\vec{1}_z \qquad (51)$$

and for the case in Figure 18(c),

$$\vec{\bar{\mu}} = \vec{\bar{\mu}}_c + \vec{\bar{\mu}}_s = \vec{\bar{\mu}}_c + \frac{1}{2}c(Z_u - Z_l)\vec{1}_z = \vec{\bar{\mu}}_c + \frac{1}{2}c(q_u - q_c - q_l)\vec{1}_z \qquad (52)$$

Because the system is neutral,

For the case in Figure 18(b), $(q_u - q_c) + (q_c + q_l) = q_u + q_l = 0$ (53)

For the case in for Figure 18(c), $(q_u - q_c) + q_l = q_u - q_c + q_l = 0$ (54)

The dipole moment per cell for the case in Figures 18(b) and (c), when inserting Eq. (53) into Eq. (51) and Eq. (54) into Eq. (52), becomes:

$$\vec{\bar{\mu}} = \vec{\bar{\mu}}_c + (q_u - q_c)c\vec{1}_z \qquad (55)$$

The same results are obtained in both cases, so that using Eq. (48), $\vec{\bar{\mu}}$ can be written as,

$$\vec{\bar{\mu}} = \vec{\bar{\mu}}_c + (q_u - q_c)c\vec{1}_z = dq_c\vec{1}_z + (q_u - q_c)c\vec{1}_z = [q_u c - q_c(c - d)]\vec{1}_z \qquad (56)$$

C. The electric field for both cases in Figure 18 (b) and (c)

We shall study the field created at various points inside the system. We have given these (marked by the black dots) numbers in Figures 18 (b) and (c) as also is the case for the atomic layers. In the point n, the field is given by (using the Tasker approach of approximating the charge density through a constant density on a two-dimensional plane)

$$\vec{E}_n = \frac{1}{4\pi\epsilon} 2\pi \left[\sum_{i\geq n} q_i - \sum_{i<n} q_i\right]\vec{1}_z \tag{57}$$

where q_i is the density associated with the i'th atomic layer.

For the systems of Figures 18 (b) and (c), the electric field $\vec{E}_n$ at the nth point is,

$$\vec{E}_1 = \frac{1}{4\pi\epsilon} 2\pi\,[q_u - q_c + q_c - q_c + q_c - q_c + q_c - q_l]\vec{1}_z = \vec{0} \tag{58}$$

$$\begin{aligned}\vec{E}_2 &= \frac{1}{4\pi\epsilon} 2\pi\,[-q_u - q_c + q_c - q_c + q_c - q_c + q_c - q_l]\vec{1}_z \\ &= \frac{1}{4\pi\epsilon} 2\pi\,[-2q_u + (q_u - q_c + q_c - q_c + q_c - q_c + q_c - q_l)]\vec{1}_z \\ &= \frac{1}{4\pi\epsilon}(-4\pi q_u)\vec{1}_z\end{aligned} \tag{59}$$

$$\begin{aligned}\vec{E}_3 &= \frac{1}{4\pi\epsilon} 2\pi\,[-q_u + q_c + q_c - q_c + q_c - q_c + q_c - q_l]\vec{1}_z \\ &= \frac{1}{4\pi\epsilon} 2\pi\,[-2q_u + 2q_c + (q_u - q_c + q_c - q_c + q_c - q_c + q_c - q_l)]\vec{1}_z \\ &= \frac{1}{4\pi\epsilon}[-4\pi(q_u - q_c)]\vec{1}_z\end{aligned} \tag{60}$$

$$\begin{aligned}\vec{E}_4 &= \frac{1}{4\pi\epsilon} 2\pi\,[-q_u + q_c - q_c - q_c + q_c - q_c + q_c - q_l]\vec{1}_z \\ &= \frac{1}{4\pi\epsilon} 2\pi\,[-2q_u + 2q_c - 2q_c + (q_u - q_c + q_c - q_c + q_c - q_c + q_c - q_l)]\vec{1}_z \\ &= \frac{1}{4\pi\epsilon}(-4\pi q_u)\vec{1}_z\end{aligned} \tag{61}$$

$$\begin{aligned}\vec{E}_5 &= \frac{1}{4\pi\epsilon} 2\pi\,[-q_u + q_c - q_c + q_c + q_c - q_c + q_c - q_l]\vec{1}_z \\ &= \frac{1}{4\pi\epsilon}[-4\pi(q_u - q_c)]\vec{1}_z\end{aligned} \tag{62}$$

$$\vdots$$

It is clear that far away from the surface the field oscillates between $\frac{1}{4\pi\epsilon}(-4\pi q_u)\vec{1}_z$ and $\frac{1}{4\pi\epsilon}[-4\pi(q_u - q_c)]\vec{1}_z$, i.e., between two constant values. The field is the derivative of the potential that moreover is a continuous function. Thus, from position $2k-1$ to position $2k$ in Figure 18 (b) and (c) (k being an integer) the field has the value $\frac{1}{4\pi\epsilon}(-4\pi q_u)\vec{1}_z$ and the potential drops accordingly with this constant value times the distance between the layers $2k-1$ and $2k$, d. On the other hand, from position $2k$ to position $2k+1$ the field has the value $\frac{1}{4\pi\epsilon}[-4\pi(q_u - q_c)]\vec{1}_z$ and the potential drops accordingly with this constant value times the

distance between the layers $2k$ and $2k-1$, $c-d$. In order to assure that we have a potential that is periodic far away from the surfaces, these two potential drops will have to add to 0,

$$\frac{1}{4\pi\epsilon}(-4\pi q_u)d + \frac{1}{4\pi\epsilon}[-4\pi(q_u - q_c)](c-d) = 0 \tag{63}$$

giving,

$$q_u = \frac{c-d}{c} q_c \tag{64}$$

If we consider the high-symmetry case for this system,

$$d = \tfrac{1}{2}c \tag{65}$$

and

$$q_u = q_l \tag{66}$$

then from Eqs. (64), (65) and (66),

$$q_u = q_l = \frac{1}{2} q_c \tag{67}$$

Then from Eqs. (56), (65), (66) and (67),

$$\vec{\mu} = [q_u c - q_c(c-d)]\vec{1}_z = \vec{0} \tag{68}$$

as should be due to the symmetry $z \to -z$

Thus, from Eq. (68) we see that the surface charge densities compensate the bulk dipole moment.

D. The general expression for the electric field from dipole layers, $\vec{E}_{\text{dipole}}$

Usually, one or more individual surfaces of a 3D system are like the ones shown schematically in Figure 19(a). Each surface of interest is then often being modeled using a slab geometry as shown in Figure 19(b). In this case, the inward-pointing normals from the surfaces are both parallel to the z axis. Thus, if $\vec{1}_z$ is a unit vector along the z axis, then

$$\vec{1}_1 = -\vec{1}_2 = \vec{1}_z \tag{69}$$

and, putting $\vec{E}_{\text{dipole}}$ aside for the moment, the generalized Tasker condition of Eq.

(46) reduces to

$$(q_1 - q_2)\vec{1}_z = \vec{0} \tag{70}$$

Combining this condition with the charge-neutrality requirement given by

$$q_1 + q_2 = 0 \tag{71}$$

leads to the unique solution

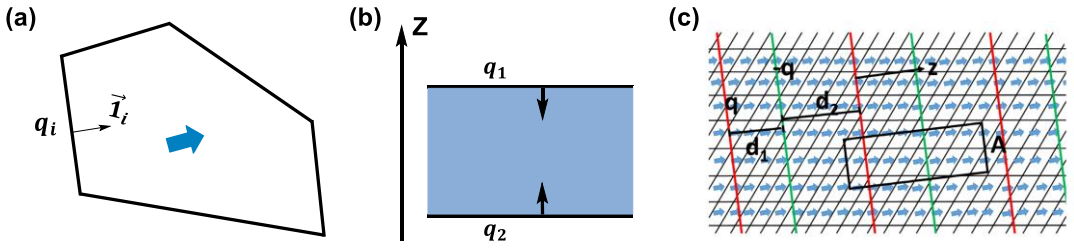

Figure 19. (a) A general shape of some material plus its dipole moment per cell (the thick blue arrow). (b) A schematic representation of a slab is commonly used for treating a single surface. (c) A schematic representation of how the effects of a non-vanishing dipole per cell can be interpreted as being created by a sequence of alternatingly charged 2D layers. The thin black lines show the separation into different unit cells, and the thick blue arrows the dipole moment contribution from the individual unit cells. The red and green lines show the model system of planes that are used to describe the effects of the non-vanishing dipole moment per cell. They are separated by distances of d_1 and d_2 and have charge densities of $\pm q$. The rectangle marks the region that is used to identify the relation between q and the dipole moment per cell.

$$q_1 = q_2 = 0 \tag{72}$$

However, it is not realistic in general to ignore $\vec{E}_{\text{dipole}}$ and, therefore,

$$q_1 = -q_2 \neq 0 \tag{73}$$

corresponds to a more correct description as we now shall discuss.

We will interpret the presence of a non-vanishing dipole moment per cell as being equivalent to having a set of alternatingly charged 2D planes as in Figure 19(c). They are separated by distances of d_1 and d_2 and have charge densities of $\pm q$. Ultimately, our result shall be formulated without having to determine these charge densities and distances. The volume element marked with the box that is shown in Figure 19(c) has a volume equal to $A \cdot (d_1 + d_2)$ with A being the area of the cross-section of the volume element. Moreover, we place the z axis as shown in the figure, i.e., parallel to the normals of the 2D planes. We shall denote the

volume of one unit cell V_{uc}.

Then, the total dipole moment inside this volume element from the system of our interest equals $\frac{A(d_1+d_2)}{V_{uc}}\vec{\mu}$. On the other hand, the dipole moment from the same volume element but caused by the 2D planes equals $-Aqd_1\vec{1}_z$. The two expressions shall be identical,

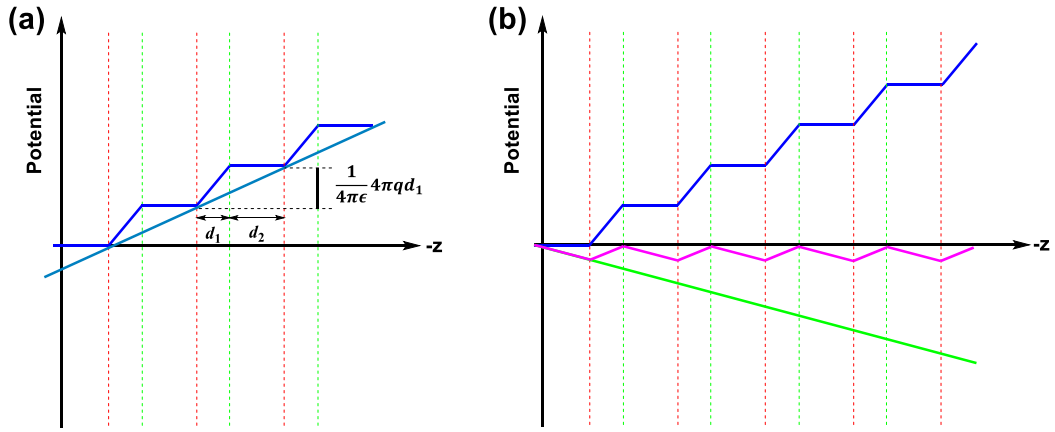

Figure 20. The potential along the z direction inside the slab. The charge density layers are shown through the vertical red and green dotted lines. (a) The potential profile for the system of alternatingly positively and negatively charged 2D planes of Figure 19(c). (b) The blue curve shows the potential due to the alternating positively and negatively charged layers, and the green curve the potential due to the extra surface charge. The sum of the potential is given as the magenta curve.

$$\frac{A(d_1+d_2)}{V_{uc}}\vec{\mu} = -Aqd_1\vec{1}_z \tag{74}$$

or

$$q = -\frac{d_1+d_2}{d_1 V_{uc}}|\vec{\mu}| \tag{75}$$

According to the discussion above, the potential from the set of 2D planes in Figure 19(c) is piecewise linear. It will have a slope of $\frac{1}{4\pi\epsilon}4\pi q$ over a distance of d_1 and be constant over the distance of d_2. Thus, it increases by $\frac{1}{4\pi\epsilon}4\pi q d_1$ (shown in Figure 20(a)) over the total distance of d_1+d_2. Therefore, the average slope (using Eq. (75)) of the curve in Figure 20 is equal to,

$$\frac{1}{4\pi\epsilon}\frac{4\pi q d_1}{d_1+d_2} = \frac{1}{4\pi\epsilon}\frac{4\pi d_1}{d_1+d_2}\left[-\frac{d_1+d_2}{d_1 V_{uc}}|\vec{\mu}|\right] = -\frac{1}{4\pi\epsilon}\frac{4\pi}{V_{uc}}|\vec{\mu}| \tag{76}$$

which indeed is independent of the (arbitrary) distances d_1 and d_2 and of the charge density q as should be.

In order to compensate this potential that is non-periodic in the bulk, we will add charges to the surfaces (but still keep the charge-neutrality constraint). With the system of Figure 19(a) as one example, we get immediately a modified, generalized Tasker condition,

$$\frac{1}{4\pi\epsilon}2\pi\sum_i q_i\,\vec{1}_i = -\frac{1}{4\pi\epsilon}\frac{4\pi}{V_{uc}}\vec{\mu} \tag{77}$$

where q_i is the charge density associated with the i'th surface and $\vec{1}_i$ is an inward-pointing normal to this surface as shown in Figure 19(a).

For facilitating the understanding, it may be useful to split the total potential into two parts, one from the sequence of two-dimensional layers of charge with densities alternating between positively and negatively charged 2D planes of Figure 19(c) and one from the additional surface charge density. This separation is shown in Figure 20 (b), where it is seen that the additional surface charge density has to be exactly so large that the potential becomes periodic.

In reality, the charge distribution inside the slab is not that of a superposition of two dimensional layers with a constant density but has much more structure due to the spatial distribution of the nuclei and, in particular, the electrons. However, on the average, the potential will show a profile like that of the blue curve and the surface charge density has then to compensate the overall change in this potential so that it becomes periodic (shown with the magenta curve in Figure 20 (b)). This means that in reality, the blue curve will not be piecewise linear but show some other structure (most likely, more smooth), but its change from one unit cell to the next will be a constant. In fact, in order to avoid forces acting on the electrons or nuclei, the total potential (the magenta curve) has to be identical to a constant.

Below, we shall use polar ZnO to obtain a quantitative description of the effects of the surface charges on the bulk structures. In this case [56],

$$\vec{E}_{\text{dipole}} = \frac{1}{4\pi\epsilon}\frac{4\pi}{V_{uc}}\vec{\mu} = \frac{1}{4\pi\epsilon}\frac{4\pi}{Aa}\vec{\mu} = \frac{1}{4\pi\epsilon}\frac{4\pi}{a}m\vec{1}_z \tag{78}$$

where $m = \vec{\mu}/A$ is the dipole density per area, A is the area of the cross-section of the volume element, $V_{uc} = Aa$ and a is the distance between repeating layers.

E. Density functional theory (DFT) calculations for stoichiometric slabs of ZnO

To determine the surface charges discussed above and their effects, density functional theory (DFT) calculations were carried out for stoichiometric slabs of ZnO containing both O- and Zn-terminated surfaces using the Vienna *ab initio* simulation package (VASP) [4-7]. Exchange and correlation effects were described using the generalized gradient approximation (GGA) [57] of Perdew, Burke, and Ernzerhof (PBE) [58] with the energy cutoff for the plane-wave expansion set to 400 eV [59]. Two structures, shown in Figure 21, were constructed using the ZnO bulk crystal geometry [60]. Both structures contain the $(000\bar{1})$ Zn-terminated surface to the left and the (0001) O-terminated surface to the right. For structure I, we considered 15 atomic bilayers with a (1 × 1) surface unit cell whereas for structure II, eight bilayers and a (2 × 2) surface unit cell were used. A vacuum region of 20 Å was included in all calculations. In each case, we examined both the fixed geometry and a relaxed geometry (see later) with lattice parameters fixed at the experimental bulk values.

A Bader analysis [61] was used to decompose the total charge density into atomic contributions. Each structure contains alternating layers of Zn and O atoms. Denoting the Bader charges of the Zn and O atoms of the mth bilayer by $\tilde{Q}_{Zn,m}$ and $\tilde{Q}_{O,m}$, respectively, we constructed the accumulated charges as

$$Q_n = \sum_{m=1}^{n} \tilde{Q}_m = \sum_{m=1}^{n} \left[\tilde{Q}_{Zn,m} + \tilde{Q}_{O,m}\right] \tag{79}$$

where the atomic bilayers are enumerated starting from the left in Figure 21 and $\tilde{Q}_m$ is the total charge of the mth bilayer. For structure II, we used the averaged values of the atomic charges per bilayer. These accumulated charges are shown in the panels at the bottom of Figure 21.

We note that Q_n converges rapidly to a roughly constant value when starting

from either side of the slab (i.e., for n close to 1 or 15 for structure I and close to 1 or 8 for structure II). That the converged value in all cases is markedly different from zero is in conflict with the condition of Eq. (72), i.e., $q_1 = q_2 = 0$. Instead, the fact that we have a regular charge distribution in the middle of the slab implies that the field due to the surface charges compensates the field due to the repeated sequence of dipoles, that is, $\vec{E}_{\text{dipole}} = -\vec{E}_{\text{charge}}$ for this structure. However, our results do not imply that the results of slab calculations will be found for an arbitrary shape containing the same individual surface(s) as the slab. For other shapes, the generalized Tasker condition will most often lead to different results.

It is of interest to estimate how much a surface charge density of the magnitude found in our ZnO calculations will affect the bulk structure. For this purpose, we see from Figure 21 that a realistic value for the magnitude of the charge per surface unit cell is slightly less than 0.3 $|e|$. In order to obtain the charge density q, one must divide by the area of the surface unit cell, which is calculated to be 9.14 Å^2 from the experimental crystal structure [60]. We also use for the relative dielectric constant of Eq. (47), the value ϵ_r = 8.5 [62]. Finally, a Bader analysis of the atoms in bulk ZnO gives atomic charges of roughly ±1, which allows us to estimate a typical value for the force acting on an ion in the central part of the slab.

Furthermore, based on ZnO VASP calculations on the crystalline ZnO with four atoms per unit cell, the resulting total energy and force curves were obtained and associated with typical nuclear displacements. The nuclear displacement $|u|\approx$ 0.03 Å can be roughly estimated according to the force on the atoms. Hence, these calculations demonstrate that the bulk properties can be affected by the surface charge. This is just a crude estimate. Although non-negligible, such a displacement is small enough that bulk structural distortions due to surface charges will likely be difficult to calculate with reliability. On the other hand, geometric distortions at the surface may be substantially larger.

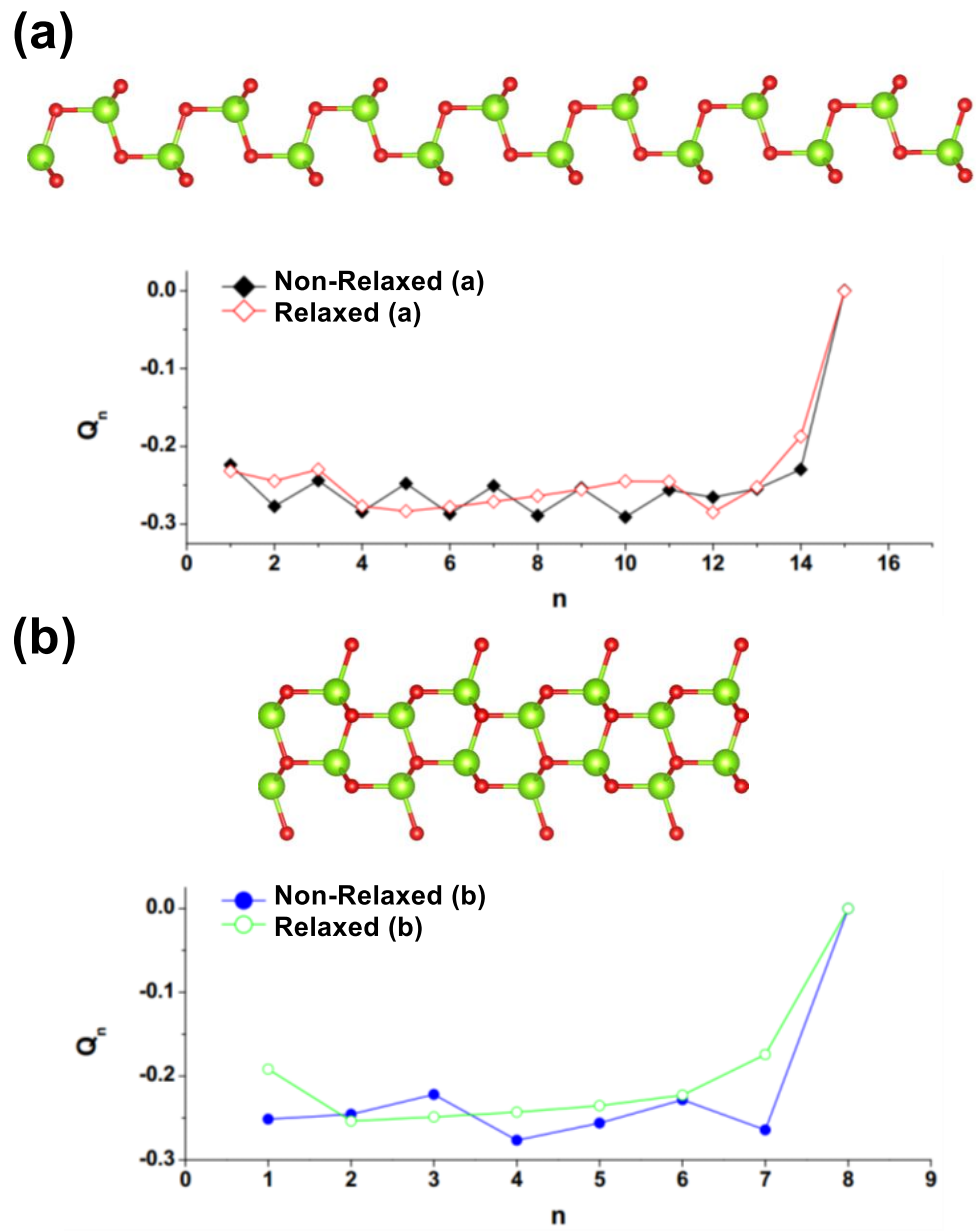

Figure 21. Accumulated layer charges per 1 × 1 surface unit cell from VASP calculations on polar slabs of ZnO. Atomic charges were obtained using a Bader analysis [60] and accumulated charges Q_n are defined in Eq. (79) where the layers are enumerated starting from the right. The structures correspond to the (0001) O-terminated surface to the left and the $(000\bar{1})$ Zn-terminated surface to the left. For structure (a), we considered 15 atomic bilayers and for structure (b), eight bilayers. The 3D visualization of these structures were constructed using the VESTA 3 software [8]. Here, the smaller red and the larger green spheres represent oxygen and zinc atoms, respectively.

8.2.3 The interplay between all the surfaces of the system

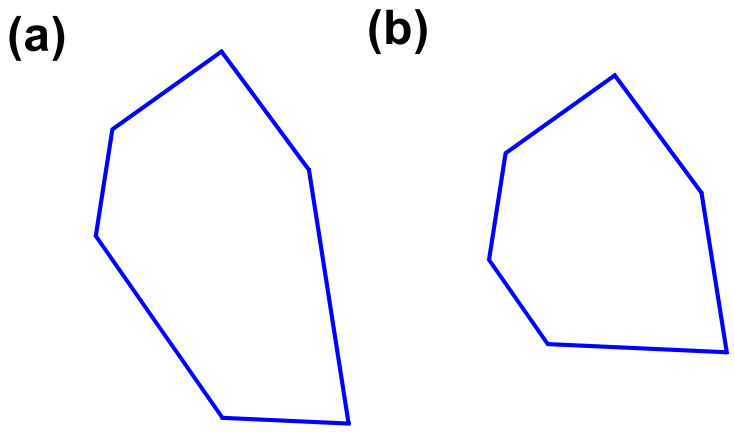

Figure 22. A schematic representation of two different samples (a) and (b) with the same types of surfaces but different shapes. In this case, the sample (b) can be created from the sample (a) by cutting one surface.

We may consider two different samples with different shapes. A simple example is shown in Figure 22 where the two samples contain the same types of surfaces but their relative sizes are different. In this case, the sample (b) can actually be obtained by making a parallel cut on one side of the original sample (a). Because the surfaces have changed relative size, the charge-neutrality condition ($\Delta q_k L_k = 0$ with L_k being the size of the kth surface and Δq_k being defined below) will, in general, not be satisfied for the second sample if the original charge densities are retained. Thus, the two samples will differ not only in shape but also in their electronic charge distribution and/or their minimum energy structure. Of course, this is just one possible example. In other constructions, the shape may be altered in a way that initially preserves charge neutrality, but instead violates the generalized Tasker condition.

In general, the change from one sample to the other may be described, at least partly, as a flow of electronic charge between the different surfaces

$$q_{k0} \rightarrow q_{k0} + \Delta q_k \equiv q_k \tag{80}$$

in such a way that charge neutrality, that is

$$\sum_k q_k L_k = \sum_k (q_{k0} + \Delta q_k) L_k = 0 \tag{81}$$

is maintained. Through this charge flow, the generalized Tasker condition shall still be

satisfied

$$\frac{1}{4\pi\varepsilon} 2\pi \sum_k (q_{k0} + \Delta q_k)\, \vec{1}_k = \vec{0} \tag{82}$$

Because the sample on the left in Figure 22 satisfies the generalized Tasker condition,

$$\frac{1}{4\pi\varepsilon} 2\pi \sum_k q_{k0}\, \vec{1}_k = \vec{0} \tag{83}$$

Eq. (82) can be written as,

$$\frac{1}{4\pi\varepsilon} 2\pi \sum_k \Delta q_k\, \vec{1}_k \equiv \vec{0} \tag{84}$$

For a 3D system, Eq. (81) provides one condition and Eq. (84) another three scalar conditions that the charge-density shifts $\{\Delta q_k\}$ must satisfy. Thus, for samples with more than four surfaces, there is, at first, a whole continuum of possible solutions.

As already noted, in order to accomplish the charge transfer implied by any particular solution of Equations (81) and (84), an electronic relaxation is required. It may be that the particular solution corresponds to a charge redistribution that can be closely simulated by transferring electrons between localized orbitals on different surfaces. In that event, based on the orbital occupancies shown schematically in Figure 23(I), an initial guess for a charge distribution could be obtained by occupying orbitals as shown in Figure 23(II). Then, an additional structural relaxation will normally be needed, in order to arrive at the stable ground state with the occupied orbitals of Figure 23(III).

These arguments demonstrate that the surface properties are determined partly by the bulk in the sense that the generalized Tasker condition for the electrostatic field at a bulk atom puts limits on the charge distribution at the surfaces. Moreover, since this condition involves all surfaces simultaneously, there is a coupling between the individual surfaces, which ultimately implies that the same surface for samples of different shapes may have different properties. Moreover, even for the same shape, there are many possibilities for the charge distribution and structure of a given surface

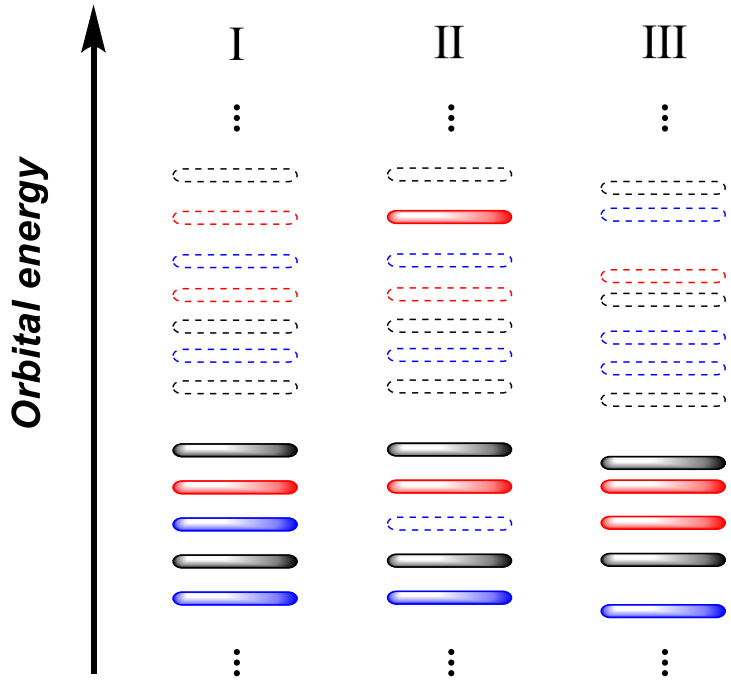

Figure 23. Schematic presentation of the orbitals closest to the Fermi level of a large, finite system. The full and dashed sticks represent occupied and empty orbitals, respectively. Moreover, the black sticks represent orbitals localized to the bulk region, whereas the blue and red sticks represent orbitals that are localized to electron-donating and electron-accepting surfaces, respectively.

with a relative stability that depends upon the system. This is a relevant issue, in particular, for oxide surfaces. It has often been argued that the latter belongs to the class of polar surfaces and, accordingly, should not be stable, although they are observed in experiment. Several studies have been devoted to this conundrum [49,46-48,50,51] that often reach different conclusions. This may be due, at least in some degree, to the fact that the generalized Tasker condition, by itself, does not provide a unique solution for a given surface, since the charge density depends upon an interplay between all the surfaces of the system of interest.

8.3 The effects of the surfaces on a bulk property

8.3.1 The dipole moment per atom

How can an allowed set of surface charges affect bulk properties? Although this is not the case for all properties, one property that does contain a finite contribution

from the surfaces regardless of the size of the system is the dipole moment per atom [52]. Formally, any intensive property, which corresponds to an extensive property Z can be calculated as Eq. (34). In the present case, Z is one of the vector components of the total dipole moment,

$$\vec{\mu} = \int \rho(\vec{r})\vec{r}\, d\vec{r} \tag{85}$$

Since the system is neutral, $\vec{\mu}$ is independent of our choice of the origin for the coordinate system and, for convenience, we place this origin at the middle of the bulk region. Then, from the last expression in Eq. (34), it follows that the dipole moment per atom can be written as,

$$\vec{\bar{\mu}} = \vec{\mu}_C + \sum_k \Delta\vec{\mu}_k \tag{86}$$

where $\vec{\mu}_C$ is the dipole moment per atom of a single (neutral) unit cell in the central region whereas $\Delta\vec{\mu}_k$ is the contribution from the kth side. In general, $\vec{\bar{\mu}}$ will have a nonvanishing contribution from the surface regions. We emphasize, however, that the separation in Eq. (86) is not unique since it depends critically on the definition of the bulk unit cell. In fact, one may construct bulk unit cells so that one of the two terms in Eq. (86) vanishes, although how to do this in practice is non-trivial.

8.3.2 A 3D-like model systems with different shapes

In order to explore the surface contribution to the dipole moment per atom further, we performed calculations for a simple finite 2D model system lying in the (*x, y*) plane. This model is completely equivalent to a 3D system that has two neutral, oppositely placed surfaces parallel to the (*x, y*) plane with identical properties for the atomic layers parallel to the (x,y) plane. The advantage of using the simpler 2D model is that we can study many cases having large spatial extensions without requiring excessive computer resources. Accordingly, we shall treat the system as if it were 3D.

Our model has been described in detail elsewhere [55] and will, therefore, be described here only briefly. In the current application, the bulk unit cell contains two atoms, each having one electron and a nuclear charge of unity. A single atomic orbital

is placed on each atom and all atoms are fixed at the positions they occupy in the bulk. More details may be found in refs. [55,63]. Initially, we construct a very large system and, then, cut out a finite segment with four sides. In each set of calculations, the shape of the segment is retained but the sample is made gradually larger up to around 8000 atoms in total. Due to this (automatic) approach it may happen that some of the systems become non-stoichiometric when only one of the two atoms per unit cell is included. Therefore, we shall study the dipole moment per atom and not per cell. We emphasize that for sufficiently large systems, the deviations from stoichiometry become increasingly small and, therefore, can be ignored. For every size, we calculate the (2D) dipole moment per atom and afterward extrapolate the entire set of values to the infinite-system-size limit in the spirit of Eq. (34).

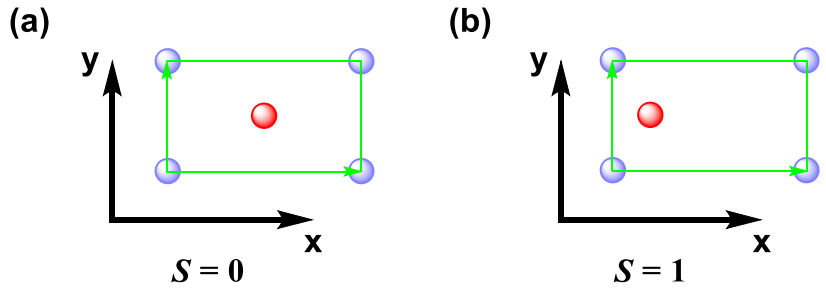

Figure 24. Schematic presentation (a) and (b) of how the bulk unit cell changes when passing from the high-symmetry structure (a) with $s = 0$ to the structure (b) with a lower symmetry for $s = 1$. The green lines show the unit cell boundaries while the black and red dots mark the positions of the two different types of atom. By moving the latter atom with respect to the former, whose position is fixed, one passes from the most symmetric structure at $s = 0$ to a maximum displacement at $s = 1$.

Two systems were studied, one of them more covalent and the other more ionic. Moreover, eight different parallelogram shapes were studied in this work. Finally, we considered the variation from a high-symmetry structure to displaced structures with reduced symmetry. The displacements were generated by moving one type of atom, with the other type fixed, as shown in Figure 24. These displacements are quantified by a parameter s that goes from $s = 0$ at the configuration where the bulk unit cell can be constructed as being centro-symmetric to a maximum at $s = 1$ in six equidistant steps. Here, however, it is worthwhile to mention that when choosing the bulk unit

cell as in Figure 24, $\vec{\mu}_C$ vanishes for $s = 0$ so that any nonzero value for the dipole moment per atom then can be ascribed solely to surface contributions. When $s = 0$, it may happen that not only the bulk unit cell has inversion symmetry but also that the complete sample has inversion symmetry. In that case, the total dipole moment will vanish for obvious reasons.

We calculated the dipole moment per atom for the 8 parallelogram shapes including both the covalent and ionic models before and after satisfying the generalized Tasker conditions. Through these calculations, we can illustrate the consequences of this interplay by studying the effects of the surfaces on a bulk property (the dipole moment per atom). The generalized Tasker conditions are shown to have a profound impact on the dipole moment per atom.

8.4 Heterogeneous Catalysis

As we have seen, the interplay between all surfaces and the bulk may affect the charge distribution on each surface. In other words, the properties associated with any surface will depend on the overall shape of the system of interest. This includes, for example, the catalytic properties. Accordingly, in order to study the catalytic properties of a given surface, it is, in principle, necessary to study the complete, essentially macroscopic system with a given shape. When using theoretical modeling for such a study, one has to ensure that the generalized Tasker condition is satisfied. Moreover for an arbitrary shape, one must use the particular charge distribution that corresponds to the ground-state structure for that system. Determining this structure can be an overwhelming challenge, but it may be possible to obtain the most important information regarding catalytic properties through simpler studies. In this section, we shall discuss briefly some ideas behind this suggestion.

A simple model description of a heterogeneous catalytic process, that does not necessarily duplicate what occurs mechanistically, includes the following steps.

1. The reactants approach the surface of the catalyst and feel its presence through electrostatic fields.

2. One or more of the reactants forms a chemical bond with the catalytic surface.

3. The reaction takes place on the surface and the product(s) are formed.

4. The products leave the catalytic surface.

In theoretical studies, one usually starts by specifying the catalytic surface under consideration and, then, constructs a convenient geometry (very often a slab) with such a surface. An electronic structure calculation will, then, give an orbital energy diagram like that of Figure 23(I). Subsequently, the steps 1–4 above are studied for the chemical reaction of interest. Our present analysis suggests that in the case of a charged surface, there will be effects on the electronic structure that can be related to the shape of the catalytic substrate. In fact, one can expect that there will be an initial charge transfer between the surfaces leading to a reordering/relaxation of the orbitals in order to arrive at a situation like that of Figure 23(III). This will necessarily have consequences for steps 2 and 3 above, which will depend critically on the chemical reaction and on the atomic composition and structure of the substrate. The nature and importance of these consequences have, to our knowledge, not been addressed as yet.

As we have shown in Figure 17 and Eq. (46), the electrostatic field at an atom in the central region (the black dot in Figure 25(a)), contributed from surface charges localized in the side regions, vanishes,

$$\vec{E}_{\text{charge}} = \frac{1}{4\pi\epsilon} 2\pi \sum_k q_k \vec{1}_k \equiv \vec{0} \tag{87}$$

Moreover, the system is neutral,

$$\sum_k q_k L_k = 0 \tag{88}$$

where $\vec{1}_k$ is an inward-pointing normal to the kth layer of ions, q_k is the sum of the charge densities of all layers associated with the kth surface, and L_k is the area of the kth layer of ions in the system of Figure 25(a).

We begin by determining the electrostatic field that acts on the molecules just outside one of the surfaces (cf. Figure 25(b)). In the simplest approximation, that field may be obtained using the same approach as in deriving the generalized Tasker condition, that is, by assuming that we have layers of constant charge density parallel

to the various surfaces and, then, calculating the resultant potential. For the situation in Figure 25(a), the reference point (red dot) is in the direction of all inward-pointing normal to the surfaces with the single exception of the i'th surface.

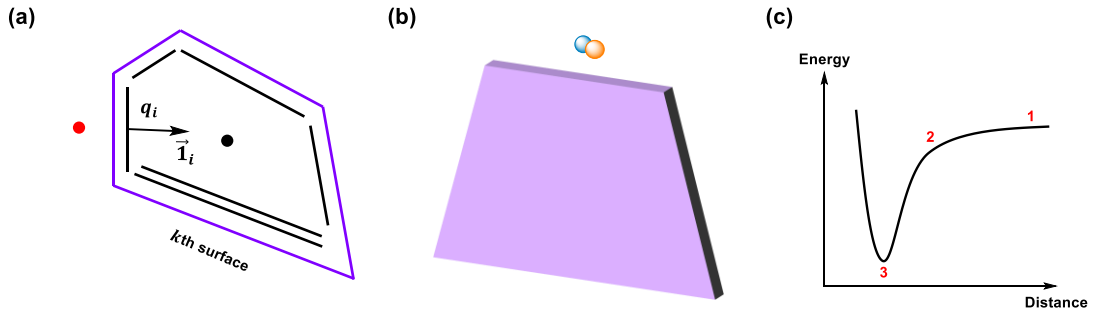

Figure 25. (a) A schematic representation of a 2D system. It shows the layers with the charge densities q_i as well as an inward-pointing normal to a given layer, $\vec{1}_i$. The boundary of the system is shown through purple lines. The black and red dots represent a point in the central part of the system and a point just outside one of the sides, respectively. (b) A schematic representation of a molecule approaching a surface ultimately being chemisorbed on this surface. (c) A schematic representation of the energy of a molecule approaching a surface ultimately being chemisorbed on this catalyst.

Thus, from Eq. (87), the electrostatic field at the red reference point in Figure 25(a) is

$$\vec{E} = \frac{1}{4\pi\epsilon} 2\pi \left[\sum_{k \neq i} q_k \vec{1}_k + q_i(-\vec{1}_i) \right] = \frac{1}{4\pi\epsilon} 2\pi \left[\sum_{k} q_k \vec{1}_k - 2q_i \vec{1}_i \right]$$

$$= -\frac{1}{4\pi\epsilon} 4\pi q_i \vec{1}_i \qquad (89)$$

This field will be felt by the molecule(s) when they approach the surface in step 1 above. It will modify their properties and thereby affect the catalytic performance of the surface. In passing we add that a more correct description will correspond to take the full charge density of the i'th surface into account and not just approximating the field through that of a 2D layer of constant charge density. This is necessary because we can no longer assume that the point of our interest lies very far from the i'th surface. This will modify the expression in eq. (89) that then becomes

$$\vec{E}(\vec{r}) = \frac{1}{4\pi\epsilon} 2\pi \sum_{k \neq i} q_k \vec{1}_k + \frac{1}{4\pi\epsilon} \sum_{n \in i} \frac{Q_n}{|\vec{r} - \vec{R}_n|^3} (\vec{r} - \vec{R}_n)$$

$$= \frac{1}{4\pi\epsilon} 2\pi \sum_k q_k \vec{1}_k + \frac{1}{4\pi\epsilon} \sum_{n\in i} \frac{Q_n}{\left|\vec{r} - \vec{R}_n\right|^3} \left(\vec{r} - \vec{R}_n\right) - \frac{1}{4\pi\epsilon} 2\pi q_i \vec{1}_i$$

$$= \frac{1}{4\pi\epsilon} \sum_{n\in i} \frac{Q_n}{\left|\vec{r} - \vec{R}_n\right|^3} \left(\vec{r} - \vec{R}_n\right) - \frac{1}{4\pi\epsilon} 2\pi q_i \vec{1}_i \qquad (90)$$

where the n summation runs over the atoms at the i'th surface, Q_n and $\vec{R}_n$ are the charge and position of the nth atom, and $\vec{r}$ is the point of interest. However, results of model calculations indicate that the changes compared to Eq. (89) are indeed only very small. This conclusion can be proven by the potential profiles shown in Figure 26.

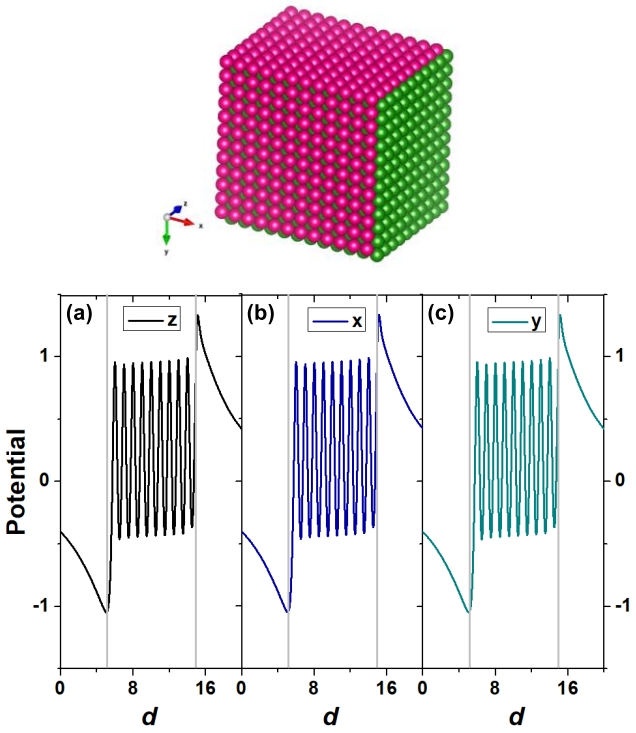

Figure 26. The potential (the bottom panels) across the finite system (the top panel). The gray vertical lines mark the boundaries of the samples. The left-most panel (a) is for the potential along the z direction, i.e., along a direction perpendicular to the surface of our interest. The other two panels (b) and (c) in each row are the potential along the two other directions, i.e., the x and y direction.

For the results in Figure 26, we calculated the potential using Eq. (91) with the n summation running over all atoms of the system.

$$\vec{E}(\vec{r}) = \frac{1}{4\pi\epsilon} \sum_n \frac{Q_n}{\left|\vec{r} - \vec{R}_n\right|^3} \left(\vec{r} - \vec{R}_n\right) \qquad (91)$$

We see that the true potential indeed is regular in the inner part so that the system really shows the existence of a central region. Moreover, we also see that the potential resembles very well what would be generated by a sequence of 2D layers each having a constant charge density. Thus, the approximate charge distribution considered by Tasker does indeed lead to a realistic description of the potential, not only far away from the surface regions.

For an initial study of the effects created by the surface of some sample, we consider a model system (Figure 25(b)) consisting of a diatomic AB molecule placed parallel to the field of Eq. (89) with an A–B interatomic distance equal to R. It should be noted at the outset that the effect of a given electrostatic field on a diatomic molecule is minimal compared to the effect on a larger molecule containing delocalized orbitals. Thus, our model will provide a minimal estimate of the electric field effect. We will assume that there is one valence electron per atom and that the nuclear charges were set equal to +1.

For simplicity, the structure of the catalyst shall be kept fixed, whereas that of the molecule shall be optimized in the presence of the catalyst. We shall discuss the consequences of having different surface charges for the same type of surface but for catalysts of the same material with the different shapes. Different surface charges will result when taking the generalized Tasker conditions into account.

Thus, we imagine that the smaller molecule will approach a specific surface of some samples of the same catalyst that have some shapes. At first, the molecule will feel the presence of the surface through the electrostatic potential that the charge distribution inside the sample creates. The molecule may respond to this, both by changing structure (most likely only slightly) and by a redistribution of the electrons within the molecule. The scenario is sketched in Figure 25(c) which shows schematically the total energy for a molecule that is approaching a surface as a function of the distance between the molecule and the surface. At position 3, the molecule is chemisorbed on the surface, implying that chemical bonds between the substrate and the molecule have been formed. However, initially, at 1, the molecule starts feeling the presence of the substrate first of all through the electrostatic field due

to the charge at the surface, i.e., the electrostatic field we quantify through $\vec{E}$ above in Eq. (89). This field will lead to a reorganization of the electrons (and eventually also the nuclei) inside the molecule which also will affect the spatial distribution of the molecular orbitals and their energies. Thus, at 2, when the molecule is getting so close to the surface that chemical bonds between the molecule and the surface can be created, the energies and spatial distribution of the orbitals both of the molecules and of the substrate will ultimately determine the chemical bonds between the two.

The key properties of the molecule and their dependance on the electrostatic field, include the structure (here, the bond length), the total and orbital energies, and the electronic charge distribution, for instance, as quantified through the Mulliken gross population on one of the two atoms. Since we are not able to determine uniquely the charge that the surface of interest will receive in order to satisfy the generalized Tasker condition (many different charges are possible) and the frontier orbitals of the surface it is not possible to study in detail the covalent substrate-molecule interactions. However, some information on the possible covalent substrate-molecule interactions can be obtained by studying the changes in the frontier orbitals of the molecule as a function of the field that this feels due to the charge of the surface. Thus, modifying the orbital energies of the molecule and/or the electronic distribution within the molecule will enhance or reduce its ability to form chemical bonds with the substrate. Therefore, these changes will also be of relevance when being interested in the chemical interactions between substrate and molecule.

When repeating this analysis for the same molecule and the same surface but for samples with different shapes, the difference between the two cases will at first be related to the initial differences in the charges associated with the surface. Accordingly, we discussed differences in the properties of some small molecules in an external electrostatic field when changing this field. This corresponds to having different charge densities of the same surface for samples with different shapes. These differences may ultimately modify the way the molecule will create chemical bonds with the surfaces of the samples.

8.5 A simple model for the shape effects on heterogeneous catalysis

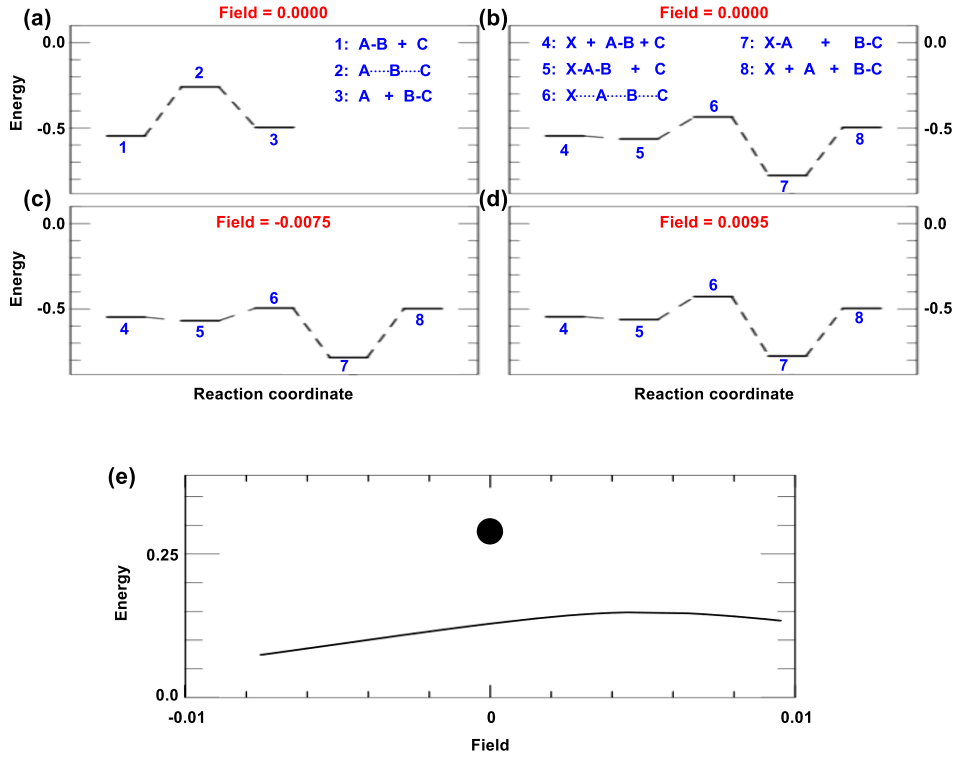

Figure 27. The energy profile (a) for the reaction A-B + C → A + B-C without the catalyst and the field (2: transition state). The energy profiles (b), (c) and (d) for the reaction X + A-B + C → X + A + B-C in the presence of catalyst and with the different field strength (X: the catalyst modelled through a single atom; 6: transition state). (e) The energy barrier for the same reactions as in figures (a-d), i.e., E_2-E_1 in the absence of the catalyst and E_6-E_5 in the presence of the catalyst. The black curve shows the results with the catalyst, whereas the dot marks those without the catalyst (in which case there is no field).

We shall perform calculations for a model that shall take the shape effects of a heterogenous catalysis into account. Thereby, we shall consider a simplified chemical model reaction. Thus, the effects due to the heterogeneous catalyst are modelled through a combination of an electrostatic field and a single atom, X. We shall consider different values of the electrostatic field. For the case of Figure 27, we shall calculate the total energy for the following systems. we may consider the two situations described below. The first case describes the reaction in the absence of the catalyst and the second to the reaction in the presence of the catalyst.

The reaction without catalyst changes the structures according to: 1→2→3

with the structures being

1: A-B + C (the stable structure A-B with the isolated C)

2: A· · ·B· · ·C (the transition state)

3: A + B-C (the stable structure B-C with the isolated A)

The reaction in the presence of the catalyst X changes the structures according to: 4→5→6→7→8, with

4: X + A-B + C (the isolated catalyst X and A atoms together with the stable structure A-B)

5: X-A-B + C (the isolated catalyst X and A atoms together with the stable structure A-B)

6: X· · ·A· · ·B· · ·C (the transition state)

7: X-A + B-C (the intermediate structure X-A and the stable structure B-C)

8: X + A + B-C (the isolated catalyst X and A atoms together with stable B-C molecule)

In Figure 27(e), the two corresponding activation energies for the two types of reactions are

$$E_{a,1} = E_2 - E_1 \tag{92}$$

$$E_{a,2} = E_6 - E_5 \tag{93}$$

In the presence of the catalyst, the last step, $7 \rightarrow 8$, may require substantial input of energy. This reaction is important in order to avoid that the catalyst gets poisoned, but is not relevant for the present discussion.

From Figure 27 we see that the activation energies for the reaction with catalyst are lower than that without catalyst. For two different samples of the same material, the same surface may have different charges as a consequence of the generalized Tasker condition. As consequences of this difference, there will be different fields outside the surface of interest. Moreover, because of the different charges, the occupation of the orbitals of the two surfaces will differ. Thus, a molecule approaching the surface will feel a potential that depends on the overall shape of the sample and, moreover, will

interact with different frontier orbitals of the two surfaces. Both effects can affect the catalytic properties of the surfaces.

8.6 The purpose of the present work

Almost 40 years ago, Tasker analyzed a possible instability of the bulk structure as caused by an electric field, which was generated by certain sequences of parallel layers of charged atoms in the surface regions. It was concluded that such polar surfaces could not exist without major structural relaxations. Although for many years the bulk properties of crystalline materials and the properties of individual surfaces have been studied individually, the interplay between a set of surfaces as determined by the bulk for a given system has not yet been studied. For the stabilization of a given system, it has to be required that no atom in the bulk experiences a force from charges associated with the surfaces, a condition that we have formulated in terms of a generalized Tasker condition. This requirement implies a charge transfer between different surfaces for a given sample. Also an overall charge neutrality has to be satisfied. These requirements determine the charge redistribution that may occur and that depend upon the whole set of the surfaces. In other words, it depends on the shape of the material. For different samples, the same individual surface may possess different properties when the samples have different shapes. There is an interplay between all the surfaces of a given sample through the bulk part of the system. The purpose of the present work is to provide further details about this interplay between all surfaces and the bulk region and about its consequences.

This work was published in Advanced Theory and Simulations (Meijuan Zhou*, Michael Springborg and Bernard Kirtman, Theoretical Treatment for Properties of Surfaces and Their Interplay with Bulk Properties of Crystals. Adv. Theory Simul., 2:1800117, **2019**.)

References

[1] M. J. Frisch, G. W. Trucks, H. B. Schlegel, G. E. Scuseria, M. A. Robb, J. R. Cheeseman, G. Scalmani, V. Barone, B. Mennucci, G. A. Petersson, H. Nakatsuji, M. Caricato, X. Li, H. P. Hratchian, A. F. Izmaylov, J. Bloino, G. Zheng, J. L. Sonnenberg, M. Hada, M. Ehara, K. Toyota, R. Fukuda, J. Hasegawa, M. Ishida, T. Nakajima, Y. Honda, O. Kitao, H. Nakai, T. Vreven, J. A. Montgomery Jr., J. E. Peralta, F. Ogliaro, M. Bearpark, J. J. Heyd, E. Brothers, K. N. Kudin, V. N. Staroverov, T. Keith, R. Kobayashi, J. Normand, K. Raghavachari, A. Rendell, J. C. Burant, S. S. Iyengar, J. Tomasi, M. Cossi, N. Rega, J. M. Millam, M. Klene, J. E. Knox, J. B. Cross, V. Bakken, C. Adamo, J. Jaramillo, R. Gomperts, R. E. Stratmann, O. Yazyev, A. J. Austin, R. Cammi, C. Pomelli, J. W. Ochterski, R. L. Martin, K. Morokuma, V. G. Zakrzewski, G. A. Voth, P. Salvador, J. J. Dannenberg, S. Dapprich, A. D. Daniels, O. Farkas, J. B. Foresman, J. V. Ortiz, J. Cioslowski and D. J. Fox, Gaussian 09, Rev. D.01, Gaussian, Inc., Wallingford, CT, **2010**.

[2] T. Lu and F. Chen, Multiwfn: a multifunctional wavefunction analyzer. J. Comput. Chem., 33(5):580–592, **2012**.

[3] C. Y. Legault, CYLView, 1.0b, Université de Sherbrooke, Canada, 2009, http://www.cylview.org.

[4] G. Kresse and J. Hafner, Ab. initio molecular dynamics for liquid metals. Phys. Rev. B, 47:558−561, **1993**.

[5] G. Kresse and J. Hafner, *ab initio* molecular-dynamics simulation of the liquid-metal—amorphous-semiconductor transition in germanium. Phys. Rev. B, 49: 14251−14269, **1994**.

[6] G. Kresse and J. Furthmüller, Efficient iterative schemes for *ab initio* total-energy calculations using a plane-wave basis set. Phys. Rev. B, 54: 11169−11185, **1996**.

[7] G. Kresse and J. Furthmüller, Efficiency of ab-initio total energy calculations for metals and semiconductors using a plane-wave basis set. Com. Mat. Sci., 6(1):15−50, **1996**.

[8] K. Momma and F. Izumi, VESTA 3 for three-dimensional visualization of crystal, volumetric and morphology data. J. Appl. Crystallogr., 44:1272–1276, **2011**.

[9] G. H. Grant and W. G. Richards, Computational Chemistry. Oxford, **1995**.

[10] F. Jensen, Introduction to Computational Chemistry. John Wiley & Sons,**1999**.

[11] S. E. Koonin, Computational Physics. Addison-Wesley, **1986**.

[12] J. Thijssen, Computational physics. Cambridge university press, **2007**.

[13] T. Schlick, Molecular Modeling and Simulation - An Interdisciplinary Guide. Springer, New York, **2002**.

[14] H. M. L. Davies and A. M. Walji, Direct synthesis of (+)-erogorgiaene through a kinetic enantiodifferentiating step. Angew. Chem., Int. Ed., 44:1733–1735, **2005**.

[15] H. M. L. Davies, X. Dai and M. S. Long, Combined C−H activation/cope rearrangement as a strategic reaction in organic synthesis: total synthesis of (−)-Colombiasin A and (−)-Elisapterosin B. J. Am. Chem. Soc., 128(7):2485–2490, **2006**.

[16] H. M. L. Davies and J. R. Manning, Catalytic C–H functionalization by metal carbenoid and nitrenoid insertion. Nature, 451:417–424, **2008**.

[17] H. M. L. Davies and J. R. Denton, Application of donor/acceptor-carbenoids to the synthesis of natural products. Chem. Soc. Rev., 38:3061–3071, **2009**.

[18] Y. Lian and H. M. L. Davies, Rhodium-catalyzed [3+2] annulation of indoles. J. Am. Chem. Soc., 132(2):440–441, **2010**.

[19] H. M. L. Davies and D. Morton, Guiding principles for site selective and stereoselective intermolecular C–H functionalization by donor/acceptor rhodium carbenes. Chem. Soc. Rev., 40:1857–1869, **2011**.

[20] M. P. Doyle, L. J. Westrum, W. N. E. Wolthuis, M. M. See, W. P. Boone, V. Bagheri and M. M. Pearson, Electronic and steric control in carbon-hydrogen insertion reactions of diazoacetoacetates catalyzed by dirhodium(II) carboxylates and carboxamides. J. Am. Chem. Soc., 115(3): 958–964, **1993**.

[21] K. Liao, W. Liu, Z. L. Niemeyer, Z. Ren, J. Bacsa, D. G. Musaev, M. S. Sigman and H. M. L. Davies, Site-selective carbene-induced C–H functionalization catalyzed by dirhodium tetrakis(triarylcyclopropanecarboxylate) complexes. ACS Catal.,

8(1):678–682, **2018**.

[22] K. Liao, S. Negretti, D. G. Musaev, J. Bacsa and H. M. L. Davies, Site-selective and stereoselective functionalization of unactivated C–H bonds. Nature, 533(7602):230–234, **2016**.

[23] K. Liao, T. C. Pickel, V. Boyarskikh, J. Bacsa, D. G. Musaev and H. M. L. Davies, Site-selective and stereoselective functionalization of non-activated tertiary C–H bonds. Nature, 551(7682):609–613, **2017**.

[24] K. Liao, Y.-F. Yang, Y. Li, J. N. Sanders, K. N. Houk, D. G. Musaev and H. M. L. Davies, Design of catalysts for site-selective and enantioselective functionalization of non-activated primary C–H bonds. Nat. Chem., 10:1048–1055, **2018**.

[25] L. Fu, D. M. Guptill and H. M. L. Davies, Rhodium(II)-catalyzed C–H functionalization of electron-deficient methyl groups. J. Am. Chem. Soc., 138(18):5761–5764, **2016**.

[26] J. Hansen, J. Autschbach and H. M. L. Davies, Computational study on the selectivity of donor/acceptor-substituted rhodium carbenoids. J. Org. Chem., 74(17):6555–6563, **2009**.

[27] D. T. Nowlan, T. M. Gregg, H. M. L. Davies and D. A. Singleton, Isotope Effects and the Nature of Selectivity in Rhodium-Catalyzed Cyclopropanations. J. Am. Chem. Soc., 125(51):15902–15911, **2003**.

[28] H. M. L. Davies, T. J. Clark and L. A. Church, Stereoselective cyclopropanations with vinylcarbenoids. Tetrahedron Lett., 30(38):5057–5060, **1989**.

[29] H. M. L. Davies, P. R. Bruzinski and M. J. Fall, Effect of diazoalkane structure on the stereoselectivity of rhodium(II) (*S*)-N-(arylsulfonyl)prolinate catalyzed cyclopropanations. Tetrahedron Lett., 37(24):4133–4136, **1996**.

[30] H. M. L. Davies and L. Rusiniak, Effect of catalyst on the diastereoselectivity of methyl phenyldiazoacetate cyclopropanations. Tetrahedron Lett., 39(48):8811–8812, **1998**.

[31] M. P. Doyle, Q.-L. Zhou, C. Charnsangavej, M. A. Longoria, M. A. McKervey and C. F. García, Chiral catalysts for enantioselective intermolecular cyclopropanation reactions with methyl phenyldiazoacetate. Origin of the solvent effect in reactions

catalyzed by homochiral dirhodium(II) prolinates. Tetrahedron Lett., 37(24):4129–4132, **1996**.

[32] H. M. L. Davies and S. A. Panaro, Effect of rhodium carbenoid structure on cyclopropanation chemoselectivity. Tetrahedron, 56(28):4871–4880, **2000**.

[33] (a) C. Lee, W. Yang and R. G. Parr, Development of the Colic-Salvetti correlation-energy formula into a functional of the electron density. Phys. Rev. B: Condens. Matter Mater. Phys., 37(2):785–789, **1988**; (b) A. D. Becke, A new mixing of Hartree-Fock and local density-functional theories. J. Chem. Phys., 98:1372, **1993**; (c) A. D. Becke, Density-functional thermochemistry. III. The role of exact exchange. J. Chem. Phys., 98:5648, **1993**; (d) P. J. Stephens, F. J. Devlin, C. F. Chabalowski and M. J. Frisch, *ab initio* calculation of vibrational absorption and circular dichroism spectra using density functional force fields. J. Phys. Chem., 98(45):11623–11627, **1994**; (e) A. S. Novikov, M. L. Kuznetsov, B. G. M. Rocha, A.J. L. Pombeiro and G. B. Shul'pin, Oxidation of olefins with H_2O_2 catalysed by salts of group III metals (Ga, In, Sc, Y and La): epoxidation versus hydroperoxidation. Catal. Sci. Technol., 6:1343–1356, **2016**.

[34] (a) S. Grimme, J. Antony, S. Ehrlich and H. Krieg, A consistent and accurate *ab initio* parametrization of density functional dispersion correction (DFT-D) for the 94 elements H-Pu. J. Chem. Phys., 132:154104, **2010**; (b) S. Grimme, S. Ehrlich and L. Goerigk, Effect of the damping function in dispersion corrected density functional theory. J. Comput. Chem., 32(7), 1456–1465, **2011**.

[35] (a) A. D. Becke and E. R. Johnson, Exchange-hole dipole moment and the dispersion interaction. J. Chem. Phys., 122:154104, **2005**; (b) E. R. Johnson and A. D. Becke, A post-Hartree–Fock model of intermolecular interactions. J. Chem. Phys., 123:024101, **2005**; (c) E. R. Johnson and A. D. Becke, A post-Hartree-Fock model of intermolecular interactions: Inclusion of higher-order corrections. J. Chem. Phys., 124:174104, **2006**.

[36] (a) S. Grimme, Semiempirical GGA-type density functional constructed with a long-range dispersion correction. J. Comput. Chem., 27(15):1787–1799, **2006**; (b) A. D. Becke, Density-functional thermochemistry. V. Systematic optimization of

exchange-correlation functionals. J. Chem. Phys., 107:8554–8560, **1997**; (c) J.-D. Chai and M. Head-Gordon, Long-range corrected hybrid density functionals with damped atom–atom dispersion corrections. Phys. Chem. Chem. Phys., 10:6615–6620, **2008**; (d) Q. Wu and W. Yang, Empirical correction to density functional theory for van der Waals interactions. J. Chem. Phys., 116:515–524, **2002**.

[37] (a) Y. Zhao and D. G. Truhlar, The M06 suite of density functionals for main group thermochemistry, thermochemical kinetics, noncovalent interactions, excited states, and transition elements: two new functionals and systematic testing of four M06-class functionals and 12 other functionals. Theor. Chem. Acc., 120:215–241, **2008**; (b) Y. Zhao and D. G. Truhlar, Density functionals with broad applicability in chemistry. Acc. Chem. Res., 41(2):157–167, **2008**.

[38] (a) P. J. Hay and W. R. Wadt, *ab initio* effective core potentials for molecular calculations. Potentials for K to Au including the outermost core orbitals. J. Chem. Phys., 82:299, **1985**; (b) A. W. Ehlers, M. Böhme, S. Dapprich, A. Gobbi, A. Höllwarth, V. Jonas, K. F. Köhler, R. Stegmann, A. Veldkamp and G. Frenking, A set of f-polarization functions for pseudo-potential basis sets of the transition metals Sc□Cu, Y□Ag and La□Au. Chem. Phys. Lett., 208(1–2), 111–114, **1993**; (c) L. E. Roy, P. J. Hay and R. L. Martin, Revised basis sets for the LANL effective core potentials. J. Chem. Theory Comput., 4(7):1029–1031, **2008**.

[39] (a) R. Ditchfield, W. J. Hehre and J. A. Pople, Self-consistent molecular-orbital methods. IX. An extended gaussian-type basis for molecular-orbital studies of organic molecules. J. Chem. Phys., 54:724, **1971**; (b) W. J. Hehre, R. Ditchfield and J. A. Pople, Self-consistent molecular orbital methods. XII. further extensions of gaussian-type basis sets for use in molecular orbital studies of organic molecules. J. Chem. Phys., 56:2257, **1972**.

[40] (a) C. Gonzalez and H. B. Schlegel, An improved algorithm for reaction path following. J. Chem. Phys., 90:2154–2161, **1989**; (b) C. Gonzalez and H. Bernhard, Schlegel Reaction path following in mass-weighted internal coordinates. J. Phys. Chem., 94(14):5523–5527, **1990**.

[41] M. Walker, A. J. A. Harvey, A. Sen and C. E. H. Dessent, Performance of M06,

M06-2X, and M06-HF Density Functionals for conformationally flexible anionic clusters: M06 functionals perform better than B3LYP for a model system with dispersion and ionic hydrogen-bonding interactions. J. Phys. Chem. A, 117:12590−12600, **2013**.

[42] A. V. Marenich, C. J. Cramer and D. G. Truhlar, Universal solvation model based on solute electron density and on a continuum model of the solvent defined by the bulk dielectric constant and atomic surface tensions. J. Phys. Chem. B, 113(18):6378–6396, **2009**.

[43] (a) A. E. Reed, L. A. Curtiss and F. Weinhold, Intermolecular interactions from a natural bond orbital, donor-acceptor viewpoint. Chem. Rev., 88(6):899–926, **1988**; (b) F. Weinhold and C. R. Landis, Valency and Bonding: A Natural Bond Orbital Donor–Acceptor Perspective, Cambridge University Press, Cambridge, UK, **2005**; (c) J.-W. Zou, M. Huang, G.-X. Hu and Y.-J. Jiang, Toward a uniform description of hydrogen bonds and halogen bonds: correlations of interaction energies with various geometric, electronic and topological parameters. RSC Adv., 7:10295–10305, **2017**.

[44] (a) M. A. Spackman and P. G. Byrom, A novel definition of a molecule in a crystal. Chem. Phys. Lett., 267(3-4):215–220, 1997; (b) M. A. Spackman and D. Jayatilaka, Hirshfeld surface analysis. CrystEngComm, 11:19–32, **2009**.

[45] P. W. Tasker, The Stability of Ionic Crystal Surfaces. J. Phys. C: Solid State Phys. 12:4977−4984, **1979**.

[46] C. Noguera, Polar oxide surfaces. J. Phys.: Condens. Matter, 12:R367−R410, **2000**.

[47] J. Goniakowski, F. Finocchi and C. Noguera, Polarity of oxide surfaces and nanostructures. Rep. Prog. Phys., 71:016501, **2008**.

[48] A. Wander, F. Schedin, P. Steadman, A. Norris, R. McGrath, T. S. Turner, G. Thornton and N. M. Harrison, Stability of polar oxide surfaces. Phys. Rev. Lett., 86, 3811−3814, **2001**.

[49] B. Meyer and D. Marx, Density-functional study of the structure and stability of ZnO surfaces. Phys. Rev. B, 67:035403(1−11), **2003**.

[50] D. Mora-Fonz, T. Lazauskas, M. R. Farrow, C. R. A. Catlow, S. M. Woodley and

A. A. Sokol, Why are polar surfaces of ZnO stable? Chem. Mater., 29:5306−5320, **2017**.

[51] M. Setvin, M. Reticcioli, F. Poelzleitner, J. Hulva, M. Schmid, L. A. Boatner, C. Franchini and U. Diebold, Polarity compensation mechanisms on the perovskite surface $KTaO_3$ (001). Science, 359:572−575, **2018**.

[52] M. Molayem, M. Springborg and B. Kirtman, Surface effects on converse piezoelectricity of crystals. Phys. Chem. Chem. Phys., 19:24724−24734, **2017**.

[53] K. N. Kudin, R. Car and R. Resta, Quantization of the dipole moment and of the end charges in push-pull polymers. J. Chem. Phys., 127:194902, **2007**.

[54] M. Springborg and B. Kirtman, How much can donor/acceptor-substitution change the responses of long push-pull systems to DC fields? Chem. Phys. Lett., 454(1-3): 105−113, **2008**.

[55] M. Springborg, M. J. Zhou, M. Molayem and B. Kirtman, Surfaces, Shapes, and Bulk Properties of Crystals. J. Phys. Chem. C, 122:11926−11932, **2018**.

[56] B. Meyer and D. Vanderbilt, *ab initio* study of $BaTiO_3$ and $PbTiO_3$ surfaces in external electric fields. Phys. Rev. B, 63:205426(1−10), **2001**.

[57] J. P. Perdew, J. A. Chevary, S. H. Vosko, K. A. Jackson, M. R. Pederson and D. J. Singh and C. Fiolhais, Atoms, molecules, solids, and surfaces: Applications of the generalized gradient approximation for exchange and correlation. Phys. Rev. B, 46(11):6671−6687, **1992**.

[58] J. P. Perdew, K. Burke and M. Ernzerhof, Generalized Gradient Approximation Made Simple. Phys. Rev. Lett., 77(18):3865−3868, **1996**.

[59] Y. Liu, W. Xu, Y. Shan and H. Xu, High Reactivity of the ZnO(0001) Polar Surface: The Role of Oxygen Adatoms. J. Phys. Chem. C, 121:15711−15718, **2017**.

[60] H. Sawada, R. Wang and A. W. Sleight, An Electron Density Residual Study of Zinc Oxide. J. Solid State Chem., 122(1):148−150, **1996**.

[61] R. F. W. Bader, Atoms in Molecules: A Quantum Theory, Oxford University Press, New York, **1990**.

[62] T. Hanada, in Oxide and Nitride Semiconductors: Processing, Properties, and Applications, (Eds: T. Yao, S.-K. Hong), Springer, Heidelberg, Germany, **2009**.

[63] For s = 0 both systems have $\vec{a}$ = (5, 0), $\vec{b}$ = (0, 3), $\vec{u}_1$= (1, 1), $\vec{u}_2$ = (3.5, 2.5), $d_{11} = d_{12} = d_{22}$ = 4. For s = 1, the only change is $\vec{u}_2$ = (2.0, 2.5). For the covalent system, we have ϵ_1 = −6, ϵ_2 = −8, $t_{0,11}$ = 8, $t_{0,12}$ = 24, $t_{0,11}$ = 6, whereas for the ionic system we have ϵ_1 = −2, ϵ_2 = −8, $t_{0,11}$ = 2, $t_{0,12}$ = 9, $t_{0,11}$ = 4.

[64] R. I. Eglitis and D. Vanderbilt, *ab initio* calculations of $BaTiO_3$ and $PbTiO_3$ (001) and (011) surface structures. Phys. Rev. B, 76:155439, **2007**.

[65] R. I. Eglitis and M. Rohlfing, First-principles calculations of the atomic and electronic structure of $SrZrO_3$ and $PbZrO_3$ (001) and (011) surfaces. J. Phys. Condens. Matter, 22:415901, **2010**.

[66] R. I. Eglitis, *ab initio* hybrid DFT calculations of $BaTiO_3$, $PbTiO_3$, $SrZrO_3$ and $PbZrO_3$ (111) surfaces. Appl. Surf. Sci., 358:556−562, **2015**.

[67] N. A. Spaldin, A beginner's guide to the modern theory of polarization. J. Solid State Chem., 195:2−10, **2012**.

9. Publications

Large parts of our studies are published in the following articles and are in the order:

1. **Meijuan Zhou*** and Michael Springborg, Theoretical study of the mechanism behind the site- and enantio-selectivity of C–H functionalization catalysed by chiral dirhodium catalyst. Phys. Chem. Chem. Phys., 22:9561-9572, **2020**. (Reproduced by permission from Royal Society of Chemistry)

2. Michael Springborg*, **Meijuan Zhou**, Mohammad Molayem and Bernard Kirtman, Surfaces, Shapes, and Bulk Properties of Crystals. J. Phys. Chem. C, 122:11926−11932, **2018**. (With permission from Copyright (2018) American Chemical Society)

3. **Meijuan Zhou***, Michael Springborg and Bernard Kirtman, Theoretical Treatment for Properties of Surfaces and Their Interplay with Bulk Properties of Crystals. Adv. Theory Simul., 2:1800117, **2019**. (Copyright Wiley-VCH GmbH. Reproduced with permission.)

PCCP

ROYAL SOCIETY OF CHEMISTRY

PAPER

Cite this: *Phys. Chem. Chem. Phys.*, 2020, **22**, 9561

Theoretical study of the mechanism behind the site- and enantio-selectivity of C–H functionalization catalysed by chiral dirhodium catalyst†

Meijuan Zhou *[a] and Michael Springborg [ab]

Received 15th January 2020,
Accepted 7th April 2020

DOI: 10.1039/d0cp00249f

rsc.li/pccp

The C–H functionalization is very important for the synthesis of pharmaceuticals and complex natural products. Rhodium carbenoids, obtained when a dirhodium(II) catalyst containing a crown formed by chiral ligands reacts with diazo compounds with both an electron donating group and an electron withdrawing group, play an important part in controlling site- and enantio-selectivity for functionalization of non-activated C–H bonds. It has earlier been demonstrated that the tertiary C–H bond is more favored to be functionalized inside the crown of the dirhodium catalyst with *S*-configuration ligands compared with the secondary and primary C–H bonds although the latter possess weaker steric effects. We argue that the higher site- and enantio-selectivity for some types of C–H bond functionalization can be related to intermolecular hydrogen bonding, steric hindrance, and weak interactions when the dirhodium catalyst is interacting with the chiral ligands.

1. Introduction

The C–H functionalization involving carbenes and catalysed by dirhodium catalysts is very important for the synthesis of pharmaceuticals and complex natural products.[1–12] According to some reports,[6–19] the presence of electron donating groups (EDG) or of electron withdrawing groups (EWG) affects the carbene electrophilicity and selectivity for the carbenes. The reactions of the dirhodium(II) catalysts with diazo compounds lead to dirhodium carbenoids that play an important part in controlling the site-, stereo-, and enantio-selectivity for functionalization of non-activated C–H bonds.[8–11] Moreover, intermediate donor/acceptor carbenoids are more stable than conventional acceptor carbenoids according to theoretical and experimental studies.[13,14]

For example, theoretical studies[14] on the reaction of different diazoacetates for a model dirhodium catalyst have revealed that the activation energy obtained for vinyldiazoacetate is 3.8 kcal mol^{-1} lower than the one for methyldiazoacetate. Similarly, according to another theoretical study,[13] the activation energy for a dirhodium catalyst for the reaction of a diazoacetate containing both donor and acceptor groups is 10.9 kcal mol^{-1} lower than what is found for a diazoacetate containing only an acceptor group. If there are only acceptor groups in the diazo compounds, the highly electrophilic carbene centre cannot be well stabilized through the acceptor groups.[6,13,14]

These reactions lead to the elimination of N_2. Subsequently, donor/acceptor dirhodium carbenoids will be formed and afterwards an intermolecular C–C bond results from a hydride transfer.[8–11,13,14] In this process, the C–H bonds are inserted into the carbene centre of the donor/acceptor dirhodium carbenoids with unequal regioselectivity probability, and that site is favoured that has the highest ability to stabilize the resulting positive charge.[13,14] According to some reports,[6,13,14] the donor/acceptor carbenoids have higher selectivity than conventional acceptor carbenoids. From an electronic point of view, the reactivity of the substrate 2-methylpentanes is expected to follow the trend: tertiary C–H bonds > secondary C–H bonds > primary C–H bonds, whereas from the point of view of steric hindrance, the primary C–H bond is most likely to be inserted into the carbene centre, followed by the secondary C–H bond, whereas for the tertiary C–H bond steric hindrance makes the insertion most unlikely.[6,9,13,14]

Different types of dirhodium catalysts were studied by Davies and co-workers.[9–11] They demonstrated that the non-activated primary C–H bonds can be functionalized by the D_2-symmetric dirhodium catalyst Rh_2[*R*-tris(*p*-^{t}BuC$_6$H$_4$)TPCP]$_4$ (Fig. 1(a)) with high site- and enantio-selectivity.[11] Moreover,

[a] *Physical and Theoretical Chemistry Department, University of Saarland, 66123 Saarbrücken, Germany. E-mail: meijuan.zhou@uni-saarland.de, m.springborg@mx.uni-saarland.de*

[b] *Materials Science, Tianjin University, Tianjin 300072, China*

† Electronic supplementary information (ESI) available. See DOI: 10.1039/d0cp00249f

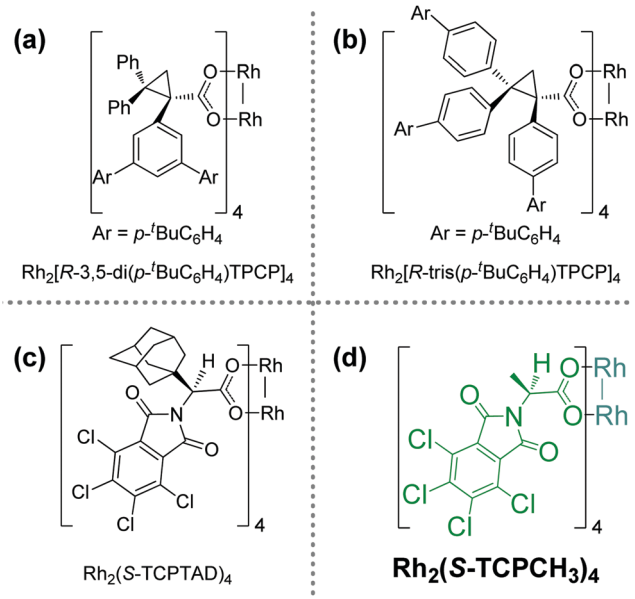

Fig. 1 The structures of dirhodium catalysts: Rh_2[*R*-tris(*p*-^{t}BuC$_6$H$_4$)TPCP]$_4$,[11] Rh_2[*R*-3,5-di(*p*-^{t}BuC$_6$H$_4$)TPCP]$_4$,[9] Rh_2(*S*-TCPTAD)$_4$[10] and the simplified structure of the dirhodium catalyst Rh_2(*S*-TCPCH$_3$)$_4$ used in this work.

the sterically most accessible secondary C–H bonds are highly selectively functionalized by the dirhodium catalyst Rh_2[*R*-3,5-di(*p*-^{t}BuC$_6$H$_4$)TPCP]$_4$ (Fig. 1(b)) that also has D_2-symmetry.[9] In addition, they synthesized a sterically less selective dirhodium catalyst with a structure close to C_4 symmetry, Rh_2(*S*-TCPTAD)$_4$[10] (Fig. 1(c)). This has two shallow pockets that form a chiral crown. The diameter (roughly 16.2–17.5 Å) of the pocket made of the phthalimido groups is much larger than that of the pocket made of adamantyl groups (roughly 7.8–8.1 Å) as shown through X-ray and computational studies.[10] Thus, the reactants can easier approach the catalyst by entering the shallow, wider pocket made of the phthalimido groups.

Through theoretical electronic-structure calculations using the DFT/M06-L method, Davies *et al.* identified the most stable structure of the donor/acceptor dirhodium carbenoids Rh_2(*S*-TCPTAD)$_4$[(*p*-Br-C$_6$H$_4$)C(COOMe)] inside the shallow and wider pocket. They speculated that the substrate with tertiary C–H bonds had to enter the shallow, wider pocket to react with the carbene.[10] However, their study did not provide a complete understanding of the reaction mechanism.

The purpose of the present work is to use theoretical studies in obtaining a detailed understanding of the reaction mechanism. As an extension of the earlier studies,[10,13,14] we shall here present a detailed understanding of the mechanism behind the highly site- and enantio-selectivity for the tertiary C–H bond functionalization.

In the present paper, the C–H bond functionalization mechanisms are studied using the reaction of 2-methylpentane with aryl diazoacetate derivatives catalysed by a simplified chiral dirhodium catalyst Rh_2(*S*-TCPCH$_3$)$_4$ (Fig. 1(d)). The justification for this simplification will be given below. DFT calculations are carried through to study the site-selectivity for these reactions by the C–H bond functionalization at the tertiary site compared with the secondary and primary sites although these latter contain less steric hindrance (Fig. 2). Moreover, we shall study the higher enantio-selectivity for these reactions by comparing the *R*- and *S*-configuration product formation for the tertiary C–H bond functionalization catalysed by the dirhodium catalyst with *S*-ligands (Fig. 2). We also demonstrate the importance of the *S*-ligands in the reaction of the tertiary C–H bond functionalization by comparing the catalytic properties of Rh_2(*S*-TCPCH$_3$)$_4$ and Rh_2–(O$_2$CH)$_4$.

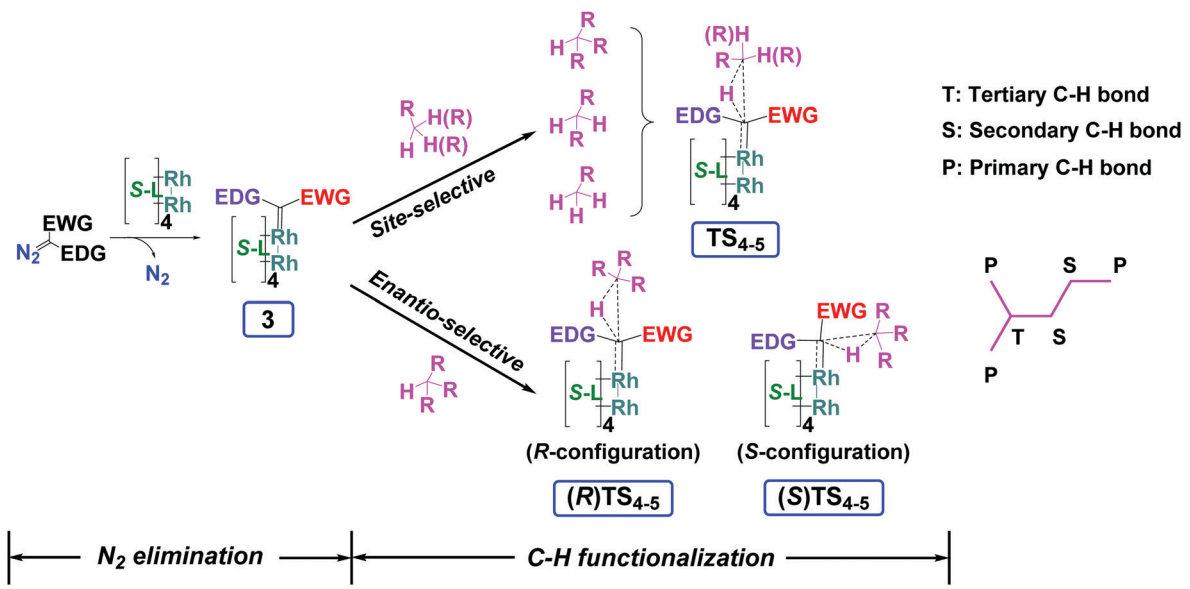

Fig. 2 A schematic representation of the site- and enantio-selective functionalization of C–H for the reactions of donor/acceptor carbene catalysed by a chiral dirhodium catalyst with *S*-configuration ligands (*S*-L). The three different types of C–H bonds in the structure of 2-methylpentane are shown to the right. Some of the structures that are discussed further in the manuscript are explicitly marked.

2. Computational methods

All calculations were performed using the Gaussian 09 program package.[20] We used the B3LYP[21] hybrid functional (for a discussion of this choice, see beginning of the next section) and a mixed basis set (Lanl2dz[22] with ECP for Rh and Br, Lanl2dz[22] for Cl, and 6-31G(d)[23] for the other atoms) in the gas phase (T = 298.15 K) without any symmetry constraint. We verified that the reactants and products had no imaginary vibrational frequency, and that all the structures of transition states (TS) have only a single imaginary vibrational frequency. Intrinsic reaction coordinate (IRC)[24] calculations were also invoked to confirm that we have located saddle points as transition states that connect two intermediates or total-energy-minima structures. In addition, we considered intermediate structures roughly halfway along the reaction coordinate connecting structures of local total-energy-minima and transition states.

To get further information on the effects of a solvent and of changing the computational approach, single-point calculations were performed using the M06 functional[25] in combination with the basis sets Lanl2dz[22] with ECP for Rh and Br, Lanl2dz[22] for Cl, and 6-31+G(d,p) for the other atoms and including SMD[26] solvation effects from dichloromethane. Natural Bond Orbital (NBO) charge analysis was used to provide a measure of charge transfer.[27] Hirshfeld surfaces analysis,[28] which is based on partitioning the electron density into molecular fragments, was used to identify interactions between such fragments. This was done with the help of the Multiwfn software.[29] Space-filling models were drawn using CYLVIEW.[30] The ONIOM layers structures were constructed using the GaussView 5.0.9 software.[20]

3. Results and discussion

Choice of theoretical approach

Experimental studies on the tertiary C–H bond functionalization have suggested that the chiral dirhodium catalyst Rh_2(*S*-TCPTAD)$_4$ can be highly selective in functionalizing the tertiary C–H bond in a dichloromethane (CH_2Cl_2) solvent at room temperature.[10] The donor/acceptor dirhodium carbenoids Rh_2(*S*-TCPTAD)$_4$[(*p*-Br-C_6H_4)C(COOR)], which are obtained after N_2 elimination when the donor/acceptor carbene [(*p*-Br-C_6H_4)-CN═N(COOR)] has reacted with the chiral dirhodium catalyst [Rh_2(*S*-TCPTAD)$_4$], play a very important role in these reactions.[10]

Based on these results, we designed a more detailed study aimed at identifying the most probable mechanism. The ball-and-stick model structures for the two substrates and the space-filling models of [Rh_2(*S*-TCPTAD)$_4$] and [Rh_2(*S*-TCPCH$_3$)$_4$] are shown in Fig. 3, which are both optimized with the B3LYP method.[21] For the two optimized structures, the average diameter of the wider crown for [Rh_2(*S*-TCPCH$_3$)$_4$] is 16.62 Å, which is just 0.53 Å larger than that for [Rh_2(*S*-TCPTAD)$_4$]. The average diameter of the smaller crown for [Rh_2(*S*-TCPCH$_3$)$_4$] is 8.90 Å, which is just 0.77 Å larger than that for [Rh_2(*S*-TCPTAD)$_4$]. Comparing the length of the two substrate molecules with these

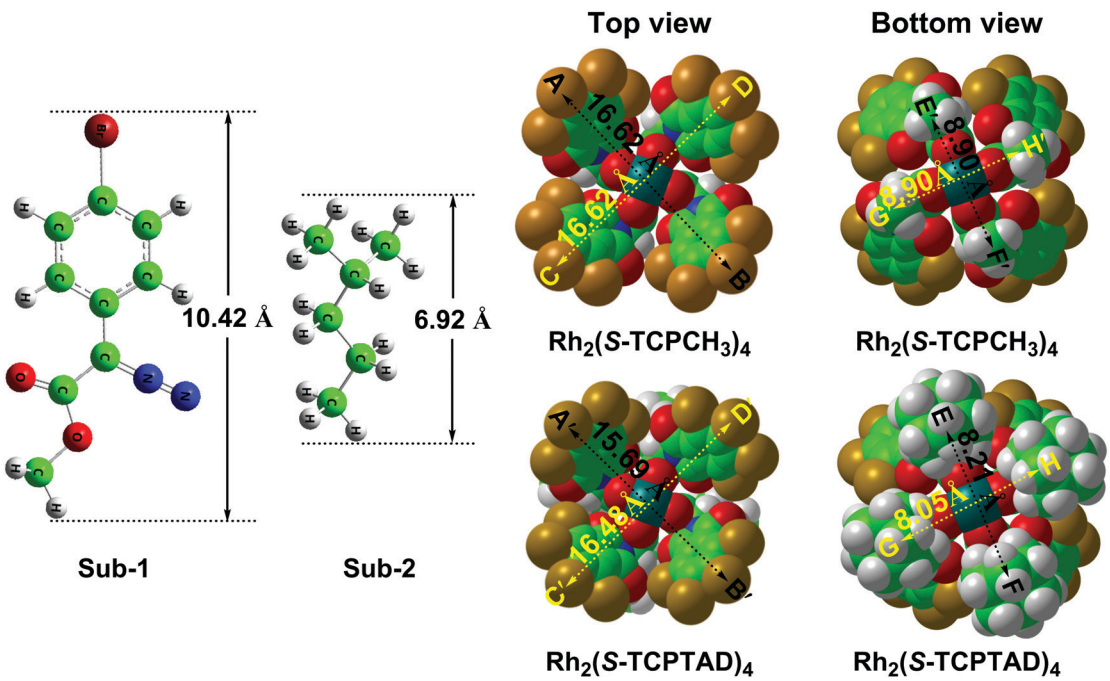

Fig. 3 Left: Ball-and-stick model structures for the two substrates. 10.42 and 6.92 Å are the lengths of the substrate 1 [(*p*-Br-C_6H_4)CN═N(COOCH$_3$)] and substrate 2 [$(CH_3)_2CHCH_2CH_2CH_3$], respectively. Right: Space-filling models for Rh_2(*S*-TCPTAD)$_4$ and Rh_2(*S*-TCPCH$_3$)$_4$. It shows the top and bottom views of the optimized structure of the experimentally studied catalyst [Rh_2(*S*-TCPTAD)$_4$] and the simplified catalyst [Rh_2(*S*-TCPCH$_3$)$_4$], respectively. The AB, CD, E′F′, G′H′, A′B′, C′D′, EF and GH distances are defined as the ones between the two top chlorine atoms of the two opposite ligands of Rh_2(*S*-TCPCH$_3$)$_4$ and Rh_2(*S*-TCPTAD)$_4$ along the AB, CD, E′F′, G′H′, A′B′, C′D′, EF and GH, directions, respectively. C: green, O: red, Cl: brown, H: white, Br: deep red, N: blue.

crown diameters, the substrate [(*p*-Br-C_6H_4)CN═N($COOCH_3$)] cannot enter the small crowns of Rh_2(*S*-TCPTAD)$_4$ or Rh_2(*S*-$TCPCH_3$)$_4$. Thus, the small crown of the catalyst Rh_2(*S*-TCPTAD)$_4$ cannot be the active site in the process of C–H functionalization. Accordingly, we simplified the structure of the chiral dirhodium catalyst [Rh_2(*S*-TCPTAD)$_4$] to the structure [Rh_2(*S*-$TCPCH_3$)$_4$] shown in Fig. 3 in order to reduce the computational costs. We considered as reactants the donor/acceptor carbene [(*p*-Br-C_6H_4)CN═N($COOCH_3$)] (here called Sub-1) and 2-methylpentane [$(CH_3)_2CHCH_2CH_2CH_3$] (Sub-2), respectively.

As a result of several test calculations we chose to use the B3LYP[21] method although it does not include any explicit description of dispersion interactions, which could be relevant for the present systems. This method was the only one of those we have considered that was able to provide a realistic structure for the donor/acceptor chlorine carbenoids (see Fig. S1, ESI†). The other methods, B3LYP-D3[31,32] (with empirical dispersion corrections), B3LYP-D3BJ[31,32] (with Becke and Johnson damping), WB97XD[33] and M062x,[34] have all been designed to include dispersion interactions but failed in describing the structures of the donor/acceptor dirhodium carbenoids.

Further arguments for this choice are given below when discussing the N_2 elimination. Therefore, most of the results to be reported below were obtained with the B3LYP[21] method.

N_2 elimination

According to the work of Davies and coworkers,[10] the donor/acceptor dirhodium carbenoids Rh_2(*S*-TCPTAD)$_4$[(*p*-Br-C_6H_4)-C(COOR)] play a very important role in the reactions for the C–H bond functionalization. An N_2 elimination is considered as the first step (Fig. 4). Therefore, we shall start by discussing this N_2 elimination.

In Fig. 4, it is seen that for the first step optimized with B3LYP method, the donor/acceptor carbene at first is located at the top of the Rh1 atom inside the chiral crown of the dirhodium catalyst. This step is exothermic by 5.98 kcal mol^{-1}. Moreover, the C9 atom of Sub-1 coordinates to the upper Rh

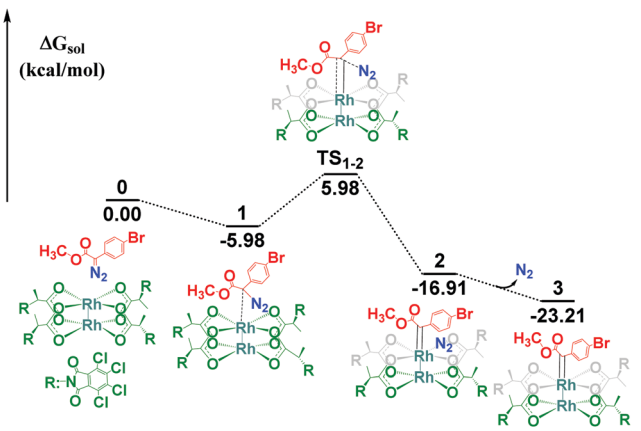

Fig. 4 Energy profile for the N_2 elimination in the first step. The relative free energies in dichloromethane (CH_2Cl_2) as solvent are given in kcal mol^{-1}.

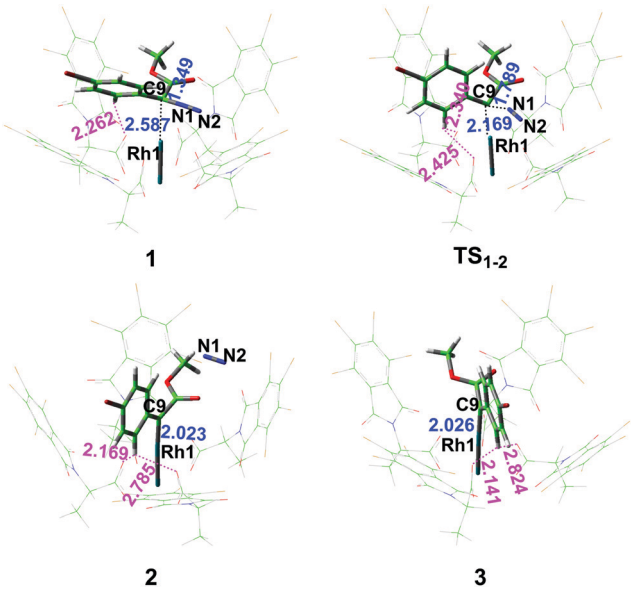

Fig. 5 Optimized structures and geometric parameters for the N_2 elimination of Fig. 4. Numbers in blue and pink give intra- and intermolecular distances in Å, respectively. C: green, O: red, Cl: brown, H: white, Br: deep red, N: blue. Pink numbers represent the distances between C–H and O for the weak hydrogen bonds.

atom (Rh1) of Rh_2(*S*-$TCPCH_3$)$_4$. Subsequently, Sub-1 will have to overcome an energy barrier of 11.96 kcal mol^{-1} for the nitrogen elimination that leads to the stable donor/acceptor dirhodium carbenoid intermediate 3 and the formation of a C9═Rh1 bond. As seen in Fig. 5, the Rh1–C9 bond length changes from 2.587 Å for structure 1 to 2.169 Å for structure TS_{1-2}. After N_2 has left the crown, the Rh1–C9 bond length becomes 2.026 Å for structure 3.

According to our theoretical approach, the carbenoid intermediate 3 possesses two weak hydrogen bonds C–H$\cdots$O formed between [(*p*-Br-C_6H_4)CN═N($COOCH_3$)] and the ligand oxygen atoms of the catalyst. In this step, according to the O$\cdots$H distances, these bonds can be regarded as weak hydrogen bonds.[35] Such weak hydrogen bonds play an important role in stabilizing structures of intermediates and transition states.

In Fig. S1(a) (ESI†) we show the resulting structure as found with six different computational approaches. In this figure, the structures of the donor/acceptor dirhodium carbenoids Rh_2(*S*-$TCPCH_3$)$_4$[(*p*-Br-C_6H_4)C(COOR)] (3, 3-1 and 3-2) and of the of the donor/acceptor dirhodium carbenoids Rh_2(*S*-TCPTAD)$_4$[(*p*-Br-C_6H_4)C(COOR)] (3′, 3-1′ and 3-2′) obtained at the B3LYP,[21] B3LYP-D3,[31,32] and B3LYP-D3BJ[31,32] level are shown.

It is seen that with the B3LYP method, the distances AB and CD for structure 3 are 14.98 and 18.06 Å, respectively, whereas for structure 3′, the A′B′ and C′D′ distances are 0.15 Å longer and 0.87 Å shorter, respectively. On the other hand, the B3LYP-D3[31,32] and D3BJ[31,32] methods for which Grimme's empirical dispersion corrections are included, the chiral crowns of the dirhodium catalysts become very distorted (*cf.* Fig. S1(a), ESI†). This would imply that it becomes impossible for Sub-2 to enter the chiral crowns of the dirhodium catalysts and to react

with Sub-1. This is an unrealistic finding that also was found using the WB97XD[33] and M06-2X[34] methods (see Fig. S1(b), ESI†). Only for the B3LYP method, the structures of 3 and 3′ become realistic. In that case, there is enough space for Sub-2 to react with Sub-1 inside the chiral crowns. In addition, it is seen that the structures 3′ and 3 are very similar, justifying using the simplified chiral dirhodium catalyst [Rh_2(*S*-TCPCH$_3$)$_4$] instead of the experimentally studied catalyst Rh_2(*S*-TCPTAD)$_4$ in our theoretical studies.

As a consequence of the N_2 elimination the net charge of C9 in TS_{1-2} is less negative than for the intermediate 1 and the charges of the Rh1 and N1 atoms become more negative as can be seen from the Natural Bond Orbital (NBO) analysis (Table S1, ESI†). The breaking of the C9═N1 double bond and the formation of the C9═Rh1 double bond and of the N≡N triple bond are all involved in this process.

In the process 1 → 2 → 3 *via* TS_{1-2}, the stable donor/acceptor dirhodium carbenoid intermediate 3 is formed with the creation of the C9═Rh1 double bond and with an electron transfer from Sub-1 to Rh_2(*S*-TCPCH$_3$)$_4$ (Fig. 4 and Table S1, ESI†). Thus, the first step for the tertiary C–H functionalization involves the formation of a carbenoid accompanied by the elimination of molecular nitrogen.[5,10,13]

Next, we shall discuss why the C–H bond functionalization has a high site- and enantio-selectivity at the tertiary site, and how the chiral crown formed by the *S*-ligands in the catalyst plays an important role in this C–H functionalization by comparing with the catalytic properties of a simplified dirhodium formate Rh_2–$(O_2CH)_4$ catalyst.

C–H functionalization: site-selectivity

Following the first step, *i.e.*, the N_2 elimination, there are more different possible reaction steps as shown in Fig. 6 and Fig. S2 (ESI†). In all cases, the second reactant, 2-methylpentane (Sub-2), will approach the chiral crown of the dirhodium catalyst after having formed the carbenoid intermediate 3.

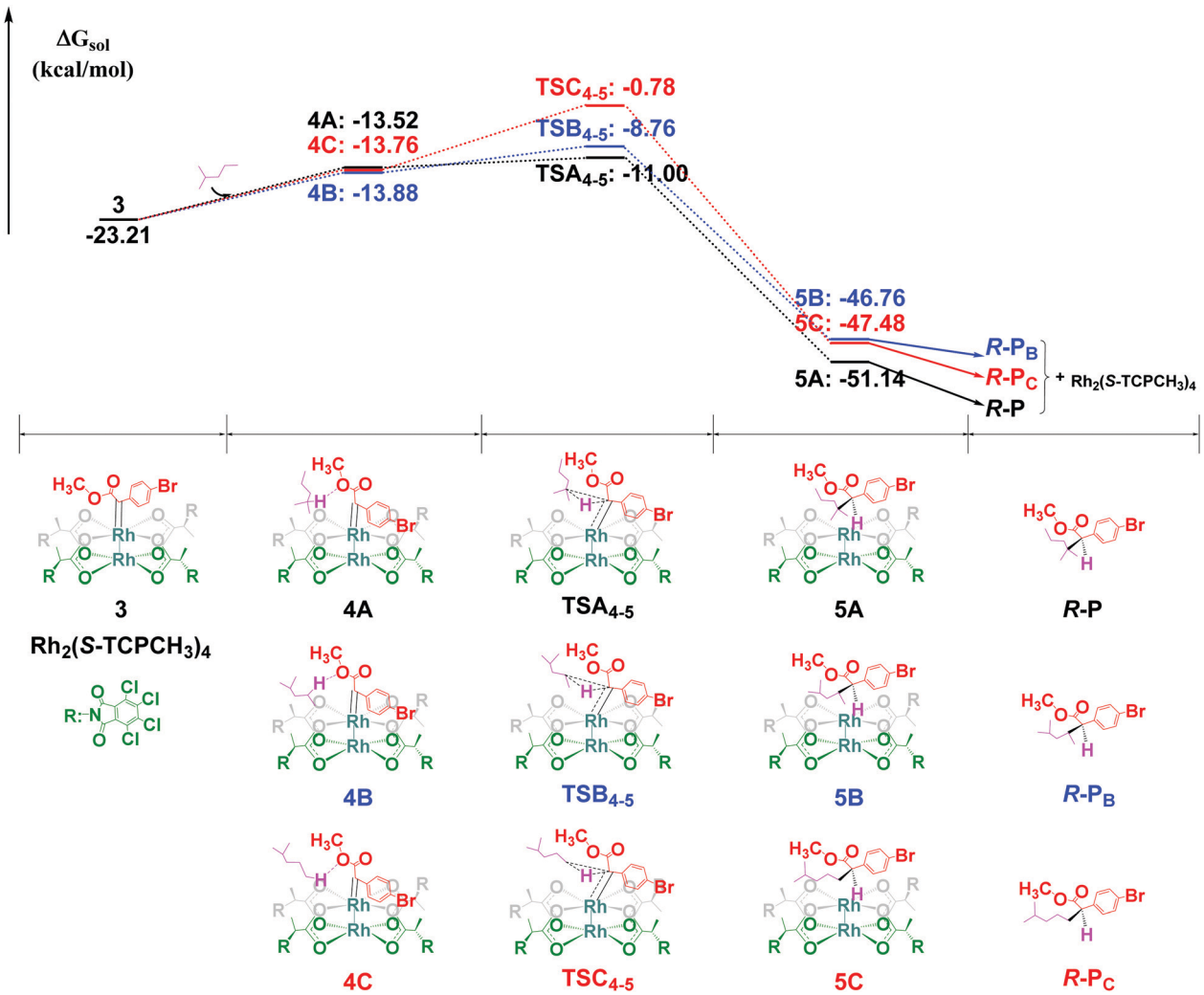

Fig. 6 Energy profiles for the three different pathways for the C–H functionalization of 2-methylpentane. Pathway A for the tertiary C–H functionalization (black pathway). Pathway B for the secondary C–H functionalization where the secondary carbon atom is bonded to the primary carbon (blue pathway). Pathway C for the primary C–H functionalization where the primary carbon atom is bonded to the secondary carbon (red pathway). The relative free energies in dichloromethane (CH_2Cl_2) as solvent are given in kcal mol^{-1}.

Thereby, one may imagine functionalization of the primary, secondary, or tertiary C–H bond (Fig. 2). What exactly will happen shall be addressed next.

Fig. 6 and Fig. S2 (ESI†) show that the carbon atom of the donor/acceptor carbene can be inserted into five different C–H bonds. The case that Sub-2 approaches the chiral crown of $Rh_2(S\text{-TCPCH}_3)_4$ and the subsequent formation of the intermediate 4A (the black pathway for the tertiary C–H functionalization in Fig. 6) is an endothermic reaction with an energy of 13.52 kcal mol^{-1}. The intermediates 4B and 4C have very similar, although slightly higher energies as 4A. The formation of the intermediates 4D (pathway D for the secondary C–H functionalization in Fig. S2, ESI†) and 4E (pathway E for the primary C–H functionalization in Fig. S2, ESI†) are connected with reaction energies of 11.32 and 14.11 kcal mol^{-1}, respectively.

When C9 of Sub-1 is inserted into the tertiary C–H bond there is an energy barrier of 12.21 kcal mol^{-1}. This may be compared with the very similar energy barrier for the N_2 elimination in Fig. 4, *i.e.*, 11.96 kcal mol^{-1}. Thus, both steps for the tertiary C–H bond functionalization can be considered as being rate-determining. However, it should be added that the N_2 elimination is irreversible and not decisive for the selectivity. As with the $Rh_2(S\text{-TCPCH}_3)_4$ recovery, the more stable structure 5A is formed at the end of the functionalization process. Subsequently, the *R*-product (*R*-P) is formed inside the crown of $Rh_2(S\text{-TCPCH}_3)_4$, and two weak hydrogen bonds are created between the *R*-P and the chiral dirhodium catalyst (Fig. 7). The energy barriers related to the C–H bond functionalization are 14.45 kcal mol^{-1} for the secondary C–H and 22.43 kcal mol^{-1} for the primary C–H, *i.e.*, 2.24 and 10.22 kcal mol^{-1} higher than that for the tertiary C–H bond functionalization, respectively.

For the other secondary C–H bond functionalization, *i.e.*, the process in which the secondary carbon atom is bonded to the tertiary carbon atom (see Fig. S2(a), ESI†), an energy barrier of 24.20 kcal mol^{-1} has to be overcome. Also this barrier is higher than that of pathway B. The other primary C–H bond functionalization in which the primary carbon atom becomes bonded to the tertiary carbon atom takes place with a barrier (26.28 kcal mol^{-1}) that is higher than that of pathway C in Fig. 6 (see Fig. S2(b), ESI†).

Next, we use information on the structure, the NBO charges, and the Hirshfeld surfaces analysis to explain why the C–H bond functionalization has a high site-selectivity at the tertiary site.

According to previous theoretical studies,[13,36] the C–H insertion can be considered as a concerted nonsynchronous process, so that for the transition state the C*n*–H*n*–C9 plane (*n* = 1, 2, 3, 4, or 5 for the tertiary, secondary, and primary C–H

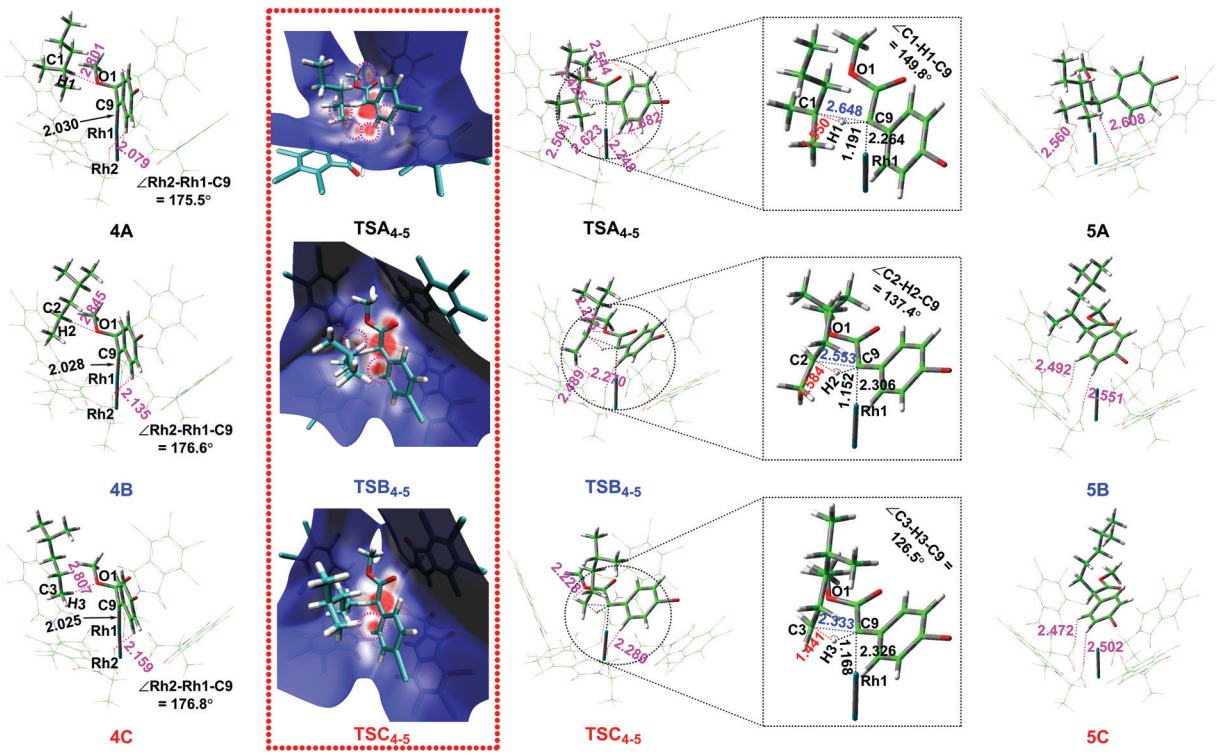

Fig. 7 Optimized structures and geometric parameters for the pathways for the C–H bond insertion reactions of Fig. 6. The red dotted bordered rectangles represent the Hirshfeld surfaces of the complex [(*p*-Br-C_6H_4)C(COOR)–$(CH_3)_2CHCH_2CH_2CH_3$]. For these surfaces, the red region implies interactions with higher electron density, which mainly originates from weak hydrogen bonding interactions; blue marks regions with very little interaction and very low electron density; white shows weaker interactions with some electron density. Pink circles represent the intermolecular interaction regions that are mainly due to the weak hydrogen bonding interactions. Numbers in blue and pink give intra- and intermolecular distances in Å, respectively. Pink numbers represent the distances between C–H and O for weak hydrogen bonds. C: green, O: red, Cl: brown, H: white, Br: deep red, N: blue.

functionalization) becomes almost orthogonal to the carbenoid plane (see Fig. S4, ESI†).

Thus, when X–C–H reacts with C′–Y (with X any Y being some groups of atoms), C′–Y is inserted into the C–H bond, whereby the C–H–C′ angle becomes (much) smaller than 180°. For the case of C–H functionalization of 1,4-cyclohexadiene, the C–H–C angle becomes 165° whereas in the case of C–H functionalization of cyclopentane, the C–H–C angle becomes 127°.[13] These values compare well with those for the C–H insertion reactions between simple alkanes and diazomethane and methyl diazoacetate, for which the C–H–C angles lie in the range 117–128°.[36]

As can be seen in Fig. 7 and Fig. S3 (ESI†), each of the transition structures TSA_{4-5}, TSB_{4-5}, TSC_{4-5}, TSD_{4-5}, and TSE_{4-5} contains a central triangular region (formed by the C*n*, H*n*, and C9 atoms) with a C*n*–H*n*–C9 angle that varies strongly (149.8°, 137.4°, 126.5°, 143.3°, and 126.5°, respectively, for $n = 1$–5). These values, significantly below 180°, suggest that the transition states involve the three-centred interactions mentioned above.

The substituents around the activated carbon atoms of 2-methylpentane will preferably approach the insertion site so that steric hindrance is kept at a minimum.[13] As shown in Fig. S4 (ESI†), the triangle links three groups of atoms of different sizes. Of those, the larger group prefers to be above the plane of the dirhodium carbenoid, whereas the other groups prefer positions near the carbenoid plane, which leads to the smallest steric hindrance compared to other arrangements of the three groups. Nevertheless, for the tertiary C–H bond the steric hindrance is present making the C1–H1–C9 angle of TSA_{4-5} larger than for the other cases and the C1–C9 distance of TSA_{4-5} larger than those of C*n*–C9 for the other transition states (Fig. 7 and Fig. S3, ESI†). Of the same reason, the Rh1–C9 distance of TSA_{4-5} is smaller than those in the other transition states, and the Rh1–C9 distances of the five TS structures are all longer than those in the structures of 4A, 4B, 4C, 4D and 4E, respectively (Fig. 7 and Fig. S3, ESI†). Thereby, Rh1–C9 can be characterized as being between double and single bond.

It can be seen from the above analyses that for the tertiary C–H functionalization the steric hindrance forces Sub-2 away from the carbenoid plane compared to the other C–H functionalizations, whereby Sub-2 comes closer to the ligands of the catalyst. This explains why there are more intermolecular hydrogen bonds formed between the complex [(*p*-Br-C_6H_4)-C(COOR)–$(CH_3)_2CHCH_2CH_2CH_3$] and the ligands of the catalyst in the structure of TSA_{4-5} than is the case for TSB_{4-5}, TSC_{4-5}, TSD_{4-5}, and TSE_{4-5} (Fig. 7 and Fig. S3, Table S2, ESI†). Accordingly, for the tertiary C–H functionalization the larger number of weak hydrogen bonds leads to a better compensation of the steric hindrance than what is the case for the primary and secondary C–H functionalization.

The existence of weak interactions for this system can also be interfered by the Hirshfeld surface analysis.[28] The results of this analysis[28] are shown in Fig. 7 and Fig. S5 (ESI†), where the existence of weak hydrogen bonds for all structures 4A, 4B, 4C, 4D and 4E can be recognized. In addition, from an energetic point of view, 4A, 4B, 4C, 4D and 4E are very similar; *cf.* Fig. 6 and Fig. S2 (ESI†).

When C*n*–H*n* ($n = 1$–5) of Sub-2 approaches the carbene carbon atom C9 of Sub-1 in the intermediate structure, one intermolecular hydrogen bond is formed between Sub-2 and Sub-1, as shown in Fig. 7 and Fig. S3 (ESI†). Also this can be demonstrated through the Hirshfeld surfaces of Sub-2 [$(CH_3)_2CHCH_2CH_2CH_3$] for the five intermediates, *cf.* Fig. 7 and Fig. S5 (ESI†). For the structures 4A, 4B, 4C, 4D and 4E, the attractive interaction is mainly due to weak hydrogen bonding but also steric hindrance affects the stability of the system. In particular, when the tertiary C1–H1 approaches the carbene carbon atom C9 in the structure 4A, the angle (175.5°) of Rh2–Rh1–C9 becomes slightly smaller than those (176.6°, 176.8°, 176.6° and 176.2°) of the structures 4B, 4C, 4D and 4E, (Fig. 7 and Fig. S3, Table S2, ESI†) since the tertiary carbon atom C1 experiences a larger steric hindrance than the other carbon atoms.

Through this structural change, Sub-2 has more space inside the crown of the catalyst for the structure 4A than for the other cases. The slight deformation of the structure makes it easier for the tertiary C1–H1 to approach the carbene carbon C9.

Fig. 7 and Fig. S5 (ESI†) show also the Hirshfeld surfaces of the complex [(*p*-Br-C_6H_4)C(COOR)–$(CH_3)_2CHCH_2CH_2CH_3$] for the TS structures. The weaker hydrogen bonds are shown as red circles in Fig. 7 and Fig. S5 (ESI†) and are formed between the C–H of the complex [(*p*-Br-C_6H_4)C(COOR)–$(CH_3)_2CHCH_2CH_2CH_3$] and the oxygen atoms of the catalyst. This interpretation is consistent with the ONIOM layers structures for the TS structures shown in Fig. S5 (ESI†). We also identify regions (shown in white for the Hirshfeld surfaces) between the complex [(*p*-Br-C_6H_4)C(COOR)–$(CH_3)_2CHCH_2CH_2CH_3$] and the catalyst that represent weaker interactions (mainly π–π stacking, and C═O···π and σ···π interactions) and which have a low electron density. Also this has an influence on the stability of the system.

According to the NBO charges of Table S3 (ESI†), the net charges of Rh1, C8, C9, C10, C11, C12 and O1 in the five intermediate structures change very little compared with those of structure 3. From Fig. 8 and Fig. S6 (ESI†) (generated by Multiwfn[29] and VMD[37] softwares based on the NBO calculations), the net charges change mostly for C*n* (*n*: 1–5, *i.e.*, the activated carbon atom) and for C9 in the five TS structures. Compared with the atomic charge distributions of 4A, 4B, 4C, 4D and 4E, Cn loses electrons and C9 atom obtains electrons in the TS structures. This suggests that charge is transferred from Sub-2 to Sub-1. When the three-centred triangles of C*n*–H*n*–C9 ($n = 1$–5) are formed in the TS structures (Fig. 7 and Fig. S3, ESI†), C9 gets electrons from C*n* and H*n*, which leads to a weakening of the double bonds between C9 and Rh1 and of the single bond between C*n* and H*n*. The main difference for the different TS structures is that the bonding environment for the five activated carbon atoms is different. The net charge of the C1 atom in TSA_{4-5} is more positive than those in the other TS structures. In addition, H1 of TSA_{4-5} becomes more positively charged. Thereby the negatively charged C9 atom becomes bonded to the positively charged C1 and H1. Thus, even if

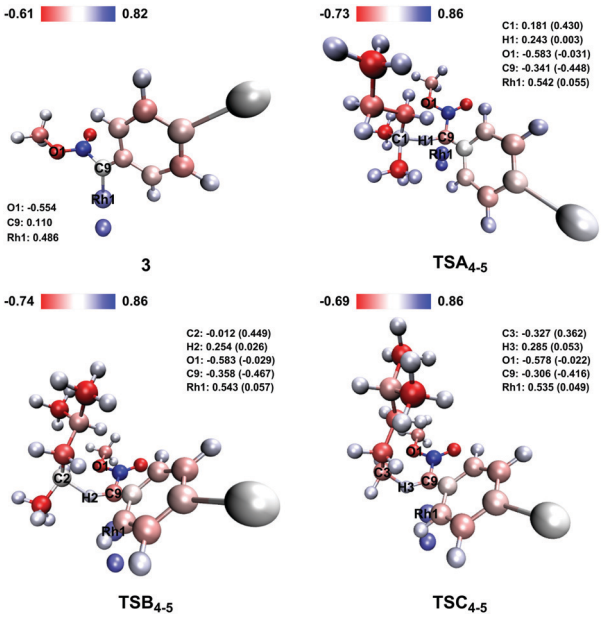

Fig. 8 The Natural Bond Orbital (NBO) charges (in |e|) for selected atoms for the structures shown in Fig. 7 (generated by Multiwfn[29] and VMD[37] softwares based on the NBO calculations). In brackets, the charge differences for TSA_{4-5}, TSB_{4-5}, and TSC_{4-5} compared with 4A, 4B, and 4C, respectively, are listed. Blue and red colours represent positive and negative charge, respectively.

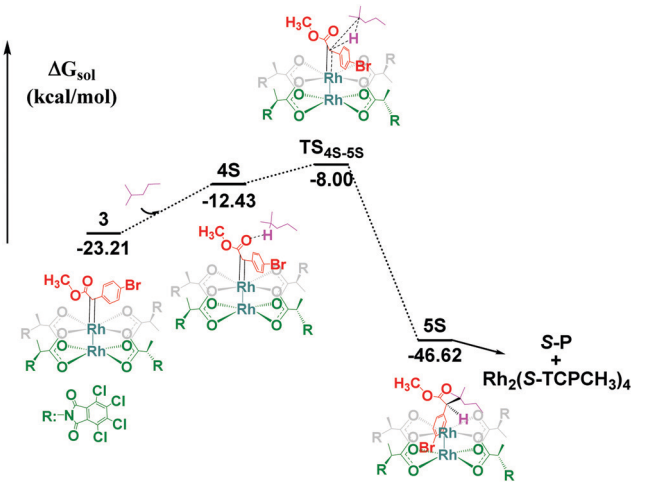

Fig. 9 Energy profile for the pathway of the *S*-configuration product for the C–H functionalization of 2-methylpentane. The relative free energies in dichloromethane (CH_2Cl_2) as solvent are given in kcal mol^{-1}.

the functionalization by the tertiary carbocation is also influenced by steric effects, also electrostatic interactions play a role in explaining why the tertiary C–H functionalization is more favourable.

In total, we arrive at the following conclusion. When Sub-1 is reacting with Sub-2 catalysed by the chiral dirhodium catalyst Rh_2(*S*-TCPCH$_3$)$_4$, the energy barrier for this step is significantly lower than those for the primary and secondary C–H bond functionalizations, which can be explained by the analysis of the structures, NBO charges, and Hirshfeld surfaces. Thereby intermolecular hydrogen bonding and other weak interactions together with steric hindrance can explain why the dirhodium catalyst Rh_2(*S*-TCPTAD)$_4$ has a higher site-selectivity for the functionalization of the non-activated tertiary C–H bond. This selectivity was already observed but only marginally explained in the earlier experimental study by Davies and co-workers.[10]

C–H functionalization: enantio-selectivity

According to experiment, the functionalization of the tertiary C–H bonds of 2-methylpentane with the aryldiazoacetate derivatives have good yields and high enantioselectivity (77–86% e.e.) when catalysed by the dirhodium catalyst Rh_2(*S*-ligands)$_4$ at lower temperatures. After the reaction of 2-methylpentane with the aryldiazoacetate derivatives, the products are mainly the *R*-configuration according to the work of Davies and co-workers.[10]

Here, we find (see Fig. 4) that the donor/acceptor dirhodium carbenoid 3 is very stable after the N_2 elimination. Subsequently, 2-methylpentane attacks the donor/acceptor dirhodium carbenoid at the position of the methoxy group, and the *R*-configuration product is obtained *via* an energy barrier of 12.21 kcal mol^{-1}.

On the other hand, when the 2-methylpentane attacks the donor/acceptor dirhodium carbenoid at the position of the carbonyl group, as shown in Fig. 9, the intermediate 4S is formed. The *S*-configuration 5S is obtained *via* an energy barrier of 15.21 kcal mol^{-1}. This energy barrier is accordingly higher than that for the *R*-configuration product (*R*-P).

The changes in NBO charges of the atoms for TS_{4S-5S} are shown in Table S4 (ESI†) and are similar to those for the structure of TSA_{4-5} (Table S3, ESI†). Only C9 of TS_{4S-5S} has 0.014 |*e*| less electrons than in TSA_{4-5}. According to experiment,[10] the e.e. value for the *R*-configuration products catalysed by the Rh_2(*S*-TCPTAD)$_4$ is in good agreement with our results.

The AB and CD distances for the structure of TSA_{4-5} are both longer (by 0.52 and 1.57 Å, respectively) than those for the structure of the intermediate 3 (Fig. S7, ESI†). For the structure of TSA_{4-5}, the chiral crown is nearly intact but for the structure of TS_{4S-5S} it is deformed. Then, the AB and CD distances of the structure of TS_{4S-5S} become, respectively, 2.23 Å shorter and 2.60 Å longer compared to the intermediate 3. For the structure TS_{4S-5S} (Fig. S7, ESI†), the chiral crown of the catalyst is even stronger deformed since the orientation of the ligand 2 (L2) is changed. When Sub-2 approaches C9 of Sub-1 at the position of the carbonyl group, the phenylene ring of Sub-1 requires more space due to the repulsions with L2 of the catalyst. Thus, the shape of the crown is strongly affected by steric hindrance.

On the other hand, hydrogen bonding plays an important role in the stability for both systems TS_{4S-5S} and TSA_{4-5} as they both have six weak intermolecular hydrogen bonds (Fig. 7 and 10). Therefore, steric hindrance is the reason that the structure of TS_{4S-5S} is less stable, and the formation of the *S*-configuration products will have to overcome a higher energy barrier (by about 3.00 kcal mol^{-1}) than that of the *R*-configuration products when catalysed by the chiral dirhodium catalyst Rh_2(*S*-TCPCH$_3$)$_4$.

C–H functionalization: Rh_2–$(O_2CH)_4$ as catalyst

To get further understanding of the selectivity of the catalyst we have also studied a simplified, achiral dirhodium formate

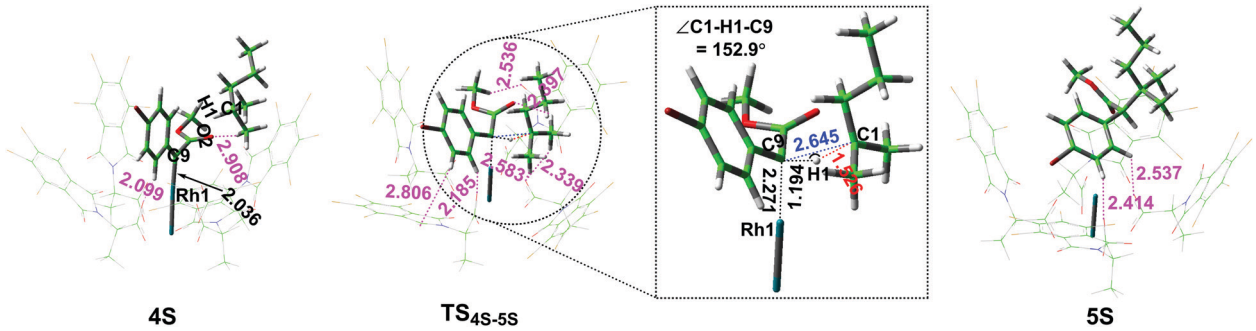

Fig. 10 Optimized structures and geometric parameters for the pathway for the C–H bond insertion reactions of Fig. 9. Numbers in blue and pink give intra- and intermolecular distances in Å, respectively. C: green, O: red, Cl: brown, H: white, Br: deep red, N: blue. Pink numbers represent the distances between C–H and O for the weak hydrogen bonds.

catalyst, Rh_2–$(O_2CH)_4$.[13] For this, we studied the reactions of $(p$-Br-$C_6H_4)$CN═N$(COOCH_3)$ with 2-methylpentane leading to the tertiary C–H bond functionalization. The mechanisms of N_2 elimination and C–H bond insertion of carbene carbon are similar to those of the reactions catalysed by $Rh_2(S$-TCPCH$_3)_4$. The optimized structures and geometric parameters of pathways HA for the whole C–H bond functionalization reactions are shown in Fig. S8 (ESI†). For the N_2 elimination process in Fig. S8 (ESI†), the formation of the intermediate 1H is accompanied by an energy increase of 3.69 kcal mol^{-1}, which is markedly different from the case of the intermediate 1 (Fig. 4), for which the energy is reduced by about 5.98 kcal mol^{-1}. Moreover, for this catalyst, the formation of the dirhodium carbenoid 3H needs to overcome an energy barrier of 12.96 kcal mol^{-1}, which is about 1.00 kcal mol^{-1} larger than that for the formation of dirhodium carbenoid 3 in Fig. 4.

For the same Rh_2–$(O_2CH)_4$ catalyst, the next reaction step, *i.e.*, the tertiary C–H functionalization has to overcome an energy barrier of 18.35 kcal mol^{-1} which is 6.14 kcal mol^{-1} higher than that of pathway A for the tertiary C–H functionalization in Fig. 6 for the 'true' catalyst. This demonstrates that the chiral structure of the ligands is important for processes of the tertiary C–H bond functionalization.

From these results it is seen that the higher site-selectivity for the tertiary C–H bond functionalization depends on the stability of the tertiary carbocation and the chiral structure of the dirhodium catalyst. In order to obtain even further understanding of the vital role of the *S*-ligand in the dirhodium catalyst $Rh_2(S$-TCPCH$_3)_4$, 2D scatter graphs and RDG (Reduced Density Gradient) isosurfaces can be employed. These have been suggested as useful for the visualization of weak interactions and were here generated using the Multiwfn[29] and VMD software,[37] respectively. The RDG method is a very popular method for studying weak interactions, and is based on the noncovalent interaction (NCI) method.[38] From the 2D scatter graphs (Fig. 11(a and b)) we can see that there are weakly attractive interactions (mainly hydrogen bonding interactions), steric hindrance, and some other weaker interactions for the structure of TSA_{4-5}. On the contrary, for the structure of $TS_{4HA-5HA}$, only the first two types of interactions are found, which can be related to the absence of the *S*-ligands. From the

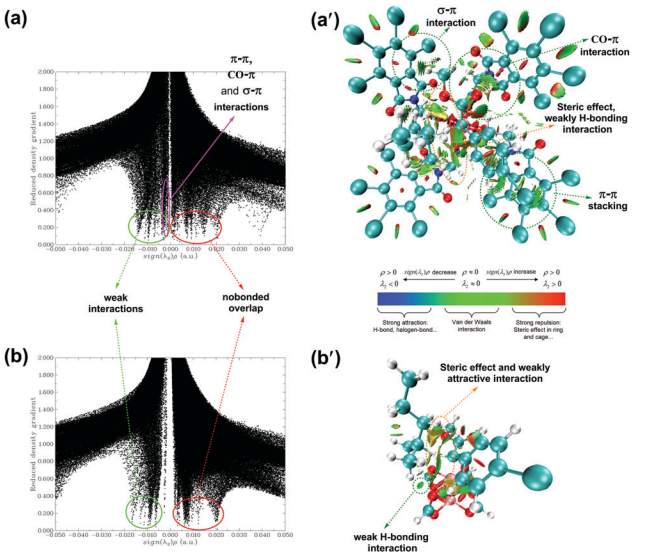

Fig. 11 The 2D scatter graphs for TSA_{4-5} (a) and $TS_{4HA-5HA}$ (b). The reduced density gradient is given as $\mathrm{RDG}(r) = \frac{1}{2(3\pi^2)^{1/3}} \frac{|\nabla\rho(r)|}{\rho(r)^{4/3}}$; λ_2 is the second eigenvalue of the electron-density Hessian matrix; ρ is the quantum-mechanical electron density. For the range of ρ shown in the figure, spikes for higher ρ and lower RDG for negative values represent non-covalent interactions, *e.g.*, dipole–dipole or strong hydrogen bonding interactions. Spikes for even lower ρ and for values closer to zero represent weak attractive interactions. Spikes for positive values of the abscissa represent weak nonbonding interactions, *e.g.*, steric clashes.[36] To the right are shown RDG (Reduced Density Gradient) isosurfaces (s = 0.5 a.u.) for TSA_{4-5} (a′) and $TS_{4HA-5HA}$ (b′). For the isosurfaces, blue implies attractive interactions, green represents weak non-covalent interactions, and red shows nonbonding interactions.[29,38]

RDG isosurfaces (Fig. 11(a′ and b′)), we can identify the weaker interactions for structure TSA_{4-5} as originating from π–π stacking, C═O···π and σ···π interactions.

Thus, all parts of the structure of the dirhodium catalyst are decisive for the reaction. Compared with the reactions of Fig. S8 (ESI†), the chiral ligands of the dirhodium catalyst can decrease the energy barriers of the insertion by providing intermolecular bonding, weak interactions, and increased steric hindrance as illustrated in Fig. 6 (black pathway).

4. Conclusions

In this work, we have studied the catalytic properties of a dirhodium complex, Rh_2(*S*-TCPCH$_3$)$_4$ containing *S*-ligands, for the C–H functionalization of 2-methylpentane when reacting with a donor/acceptor carbene. In the process of the tertiary C–H functionalization, shown in the top row of Fig. 12, the donor/acceptor carbene (*p*-Br-C$_6$H$_4$)CN=N(COOCH$_3$) initially enters the chiral crown of Rh_2(*S*-TCPCH$_3$)$_4$ after which an N_2 elimination reaction takes place. After N_2 has left the crown, the dirhodium carbenoid is formed. Subsequently, the 2-methylpentane approaches the crown of the catalyst along the direction towards the methoxy group. The insertion reaction of the carbene carbon atom into the tertiary C–H bond involves an energy barrier of 12.21 kcal mol^{-1}. Finally, the *R*-configuration product (*R*-P) is formed.

By analysing the structures, NBO charges, and Hirshfeld surfaces, the site-selectivity of the catalyst could be ascribed to intermolecular hydrogen bonding, steric hindrance, and weak interactions. For the tertiary C–H bond functionalization the larger number of weak hydrogen bonds gives a better compensation of the steric hindrance than what is the case for the primary and secondary C–H bond functionalization. As a consequence, the tertiary site is best suited for the C–H functionalization compared with the secondary and primary sites. The whole energy barrier of the C–H functionalization at

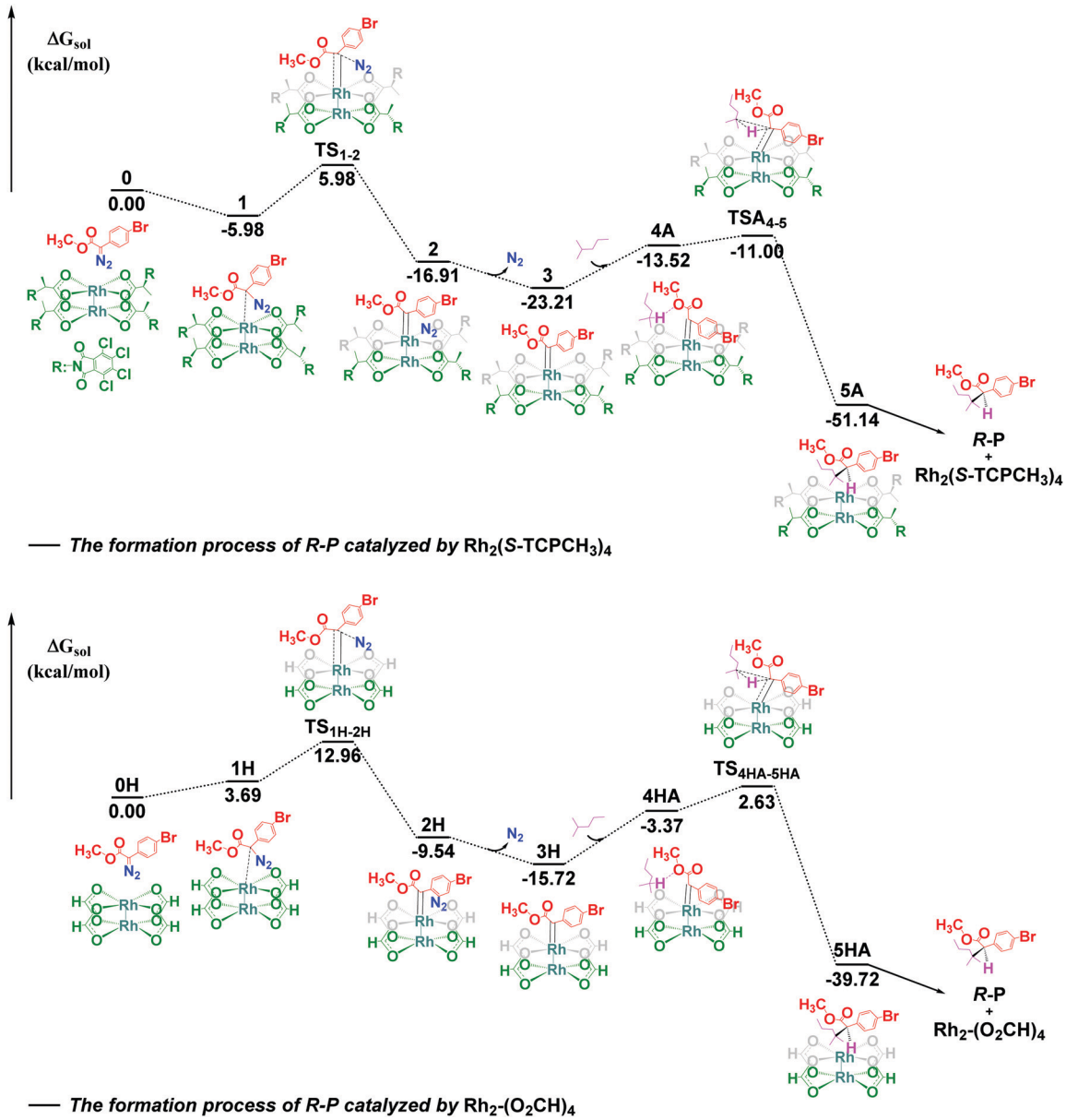

Fig. 12 Energy profiles for the whole processes for the formation of *R*-P (the tertiary C–H functionalization of 2-methylpentane with (*p*-Br-C$_6$H$_4$)CN=N(COOCH$_3$)) catalysed by the dirhodium catalysts Rh_2(*S*-TCPCH$_3$)$_4$ and Rh_2–(O$_2$CH)$_4$. The relative free energies in dichloromethane (CH_2Cl_2) as solvent are given in kcal mol^{-1}.

the tertiary site is 2.24, 11.99, 10.22, and 14.07 kcal mol^{-1} lower than those at the two secondary and the two primary sites, respectively.

For the chiral dirhodium catalyst Rh_2(*S*-TCPCH$_3$)$_4$ with *S*-ligands, the enantioselective C–H functionalization at the tertiary site of 2-methylpentane resulted mainly in the *R*-configuration product for the reaction of the donor/acceptor carbene (*p*-Br-C$_6$H$_4$)-CN=N(COOCH$_3$). Since the *R*- and *S*-configuration products involve similar hydrogen bonding the difference in the yield is mainly due to steric hindrance, because of differences in the deformation of the chiral crown of the catalyst. Therefore, when 2-methylpentane reacts with (*p*-Br-C$_6$H$_4$)CN=N(COOCH$_3$) for the chiral dirhodium catalyst Rh_2(*S*-TCPCH$_3$)$_4$, the energy barrier for the formation of the *R*-configuration product is 3.00 kcal mol^{-1} lower than that of the *S*-configuration product.

We also considered a simplified, achiral dirhodium formate catalyst Rh_2–(O$_2$CH)$_4$ as illustrated in the bottom of Fig. 12. Here, the mechanism for the tertiary C–H functionalization is similar to that catalysed by Rh_2(*S*-TCPCH$_3$)$_4$. However, due to the lack of the *S*-configuration phthalimido ligands for this catalyst, the formation of the *R*-P has to overcome an energy barrier that is 6.14 kcal mol^{-1} higher than that found for the Rh_2(*S*-TCPCH$_3$)$_4$ catalyst. Hence, the chiral arrangement of the ligands of the dirhodium catalyst plays an important role in the excellent site-selectivity. The chiral ligands can provide intermolecular bonding, steric hindrance, and weak interactions with the reactants.

In summary, we have arrived at a detailed understanding of the mechanisms for the high site- and enantio-selectivity when the reactions are catalysed by a chiral dirhodium complex. It demonstrates that the dirhodium carbenoids, derived from the reactions of the dirhodium(II) catalysts (*S*-configuration ligands) with the donor/acceptor diazo compounds, preferably leads to a C–H functionalization at the tertiary sites resulting in a *R*-configuration product. The excellent site- and enantio-selectivity for some C–H bond functionalization could be rationalized through energy barriers, intermolecular hydrogen bonding, steric hindrance, and weak interactions.

Even though we have studied a specific reaction in great detail we are convinced that our conclusions are generally valid also for other catalytic reactions involving chiral catalysts and for which limited space is available for the catalytic reaction.

Conflicts of interest

The authors declare no competing financial interests.

References

1 H. M. L. Davies and A. M. Walji, *Angew. Chem.*, 2005, **117**, 1761–1763 (*Angew. Chem., Int. Ed.*, 2005, **44**, 1733–1735).
2 H. M. L. Davies, X. Dai and M. S. Long, *J. Am. Chem. Soc.*, 2006, **128**(7), 2485–2490.
3 H. M. L. Davies and J. R. Manning, *Nature*, 2008, **451**, 417–424.
4 H. M. L. Davies and J. R. Denton, *Chem. Soc. Rev.*, 2009, **38**, 3061–3071.
5 Y. Lian and H. M. L. Davies, *J. Am. Chem. Soc.*, 2010, **132**, 440–441.
6 H. M. L. Davies and D. Morton, *Chem. Soc. Rev.*, 2011, **40**, 1857–1869.
7 M. P. Doyle, L. J. Westrum, W. N. E. Wolthuis, M. M. See, W. P. Boone, V. Bagheri and M. M. Pearson, *J. Am. Chem. Soc.*, 1993, **115**(3), 958–964.
8 K. Liao, W. Liu, Z. L. Niemeyer, Z. Ren, J. Bacsa, D. G. Musaev, M. S. Sigman and H. M. L. Davies, *ACS Catal.*, 2018, **8**(1), 678–682.
9 K. Liao, S. Negretti, D. G. Musaev, J. Bacsa and H. M. L. Davies, *Nature*, 2016, **533**(7602), 230–234.
10 K. Liao, T. C. Pickel, V. Boyarskikh, J. Bacsa, D. G. Musaev and H. M. L. Davies, *Nature*, 2017, **551**(7682), 609–613.
11 K. Liao, Yun-F. Yang, Y. Li, J. N. Sanders, K. N. Houk, D. G. Musaev and H. M. L. Davies, *Nat. Chem.*, 2018, **10**, 1048–1055.
12 L. Fu, D. M. Guptill and H. M. L. Davies, *J. Am. Chem. Soc.*, 2016, **138**(18), 5761–5764.
13 J. Hansen, J. Autschbach and H. M. L. Davies, *J. Org. Chem.*, 2009, **74**(17), 6555–6563.
14 D. T. Nowlan, T. M. Gregg, H. M. L. Davies and D. A. Singleton, *J. Am. Chem. Soc.*, 2003, **125**(51), 15902–15911.
15 H. M. L. Davies, T. J. Clark and L. A. Church, *Tetrahedron Lett.*, 1989, **30**(38), 5057–5060.
16 H. M. L. Davies, P. R. Bruzinski and M. J. Fall, *Tetrahedron Lett.*, 1996, **37**(24), 4133–4136.
17 H. M. L. Davies and L. Rusiniak, *Tetrahedron Lett.*, 1998, **39**(48), 8811–8812.
18 M. P. Doyle, Q.-L. Zhou, C. Charnsangavej, M. A. Longoria, M. A. McKervey and C. F. García, *Tetrahedron Lett.*, 1996, **37**(24), 4129–4132.
19 H. M. L. Davies and S. A. Panaro, *Tetrahedron*, 2000, **56**(28), 4871–4880.
20 M. J. Frisch, G. W. Trucks, H. B. Schlegel, G. E. Scuseria, M. A. Robb, J. R. Cheeseman, G. Scalmani, V. Barone, B. Mennucci, G. A. Petersson, H. Nakatsuji, M. Caricato, X. Li, H. P. Hratchian, A. F. Izmaylov, J. Bloino, G. Zheng, J. L. Sonnenberg, M. Hada, M. Ehara, K. Toyota, R. Fukuda, J. Hasegawa, M. Ishida, T. Nakajima, Y. Honda, O. Kitao, H. Nakai, T. Vreven, J. A. Montgomery Jr., J. E. Peralta, F. Ogliaro, M. Bearpark, J. J. Heyd, E. Brothers, K. N. Kudin, V. N. Staroverov, T. Keith, R. Kobayashi, J. Normand, K. Raghavachari, A. Rendell, J. C. Burant, S. S. Iyengar, J. Tomasi, M. Cossi, N. Rega, J. M. Millam, M. Klene, J. E. Knox, J. B. Cross, V. Bakken, C. Adamo, J. Jaramillo, R. Gomperts, R. E. Stratmann, O. Yazyev, A. J. Austin, R. Cammi, C. Pomelli, J. W. Ochterski, R. L. Martin, K. Morokuma, V. G. Zakrzewski, G. A. Voth, P. Salvador, J. J. Dannenberg, S. Dapprich, A. D. Daniels, O. Farkas, J. B. Foresman, J. V. Ortiz, J. Cioslowski and D. J. Fox, *Gaussian 09, Rev. D.01*, Gaussian, Inc., Wallingford, CT, 2010.
21 (*a*) C. Lee, W. Yang and R. G. Parr, *Phys. Rev. B: Condens. Matter Mater. Phys.*, 1988, **37**(2), 785–789; (*b*) A. D. Becke, *J. Chem. Phys.*, 1993, **98**, 1372; (*c*) A. D. Becke, *J. Chem. Phys.*, 1993, **98**, 5648; (*d*) P. J. Stephens, F. J. Devlin,

C. F. Chabalowski and M. J. Frisch, *J. Phys. Chem.*, 1994, **98**(45), 11623–11627; (*e*) S. N. Alexander, L. K. Maxim, G. M. R. Bruno, J. L. P. Armando and B. S. Georgiy, *Catal. Sci. Technol.*, 2016, **6**, 1343–1356.

22 (*a*) P. J. Hay and W. R. Wadt, *J. Chem. Phys.*, 1985, **82**, 299; (*b*) A. W. Ehlers, M. Böhme, S. Dapprich, A. Gobbi, A. Höllwarth, V. Jonas, K. F. Köhler, R. Stegmann, A. Veldkamp and G. Frenking, *Chem. Phys. Lett.*, 1993, **208**(1–2), 111–114; (*c*) L. E. Roy, P. J. Hay and R. L. Martin, *J. Chem. Theory Comput.*, 2008, **4**(7), 1029–1031.

23 (*a*) R. Ditchfield, W. J. Hehre and J. A. Pople, *J. Chem. Phys.*, 1971, **54**, 724; (*b*) W. J. Hehre, R. Ditchfield and J. A. Pople, *J. Chem. Phys.*, 1972, **56**, 2257.

24 (*a*) C. Gonzalez and H. B. Schlegel, *J. Chem. Phys.*, 1989, **90**, 2154–2161; (*b*) C. Gonzalez and H. B. Schlegel, *J. Phys. Chem.*, 1990, **94**(14), 5523–5527.

25 (*a*) Y. Zhao and D. G. Truhlar, *Theor. Chem. Acc.*, 2008, **120**(1–3), 215–241; (*b*) Y. Zhao and D. G. Truhlar, *Acc. Chem. Res.*, 2008, **41**(2), 157–167.

26 A. V. Marenich, C. J. Cramer and D. G. Truhlar, *J. Phys. Chem. B*, 2009, **113**(18), 6378–6396.

27 (*a*) A. E. Reed, L. A. Curtiss and F. Weinhold, *Chem. Rev.*, 1988, **88**(6), 899–926; (*b*) F. Weinhold and C. R. Landis, *Valency and Bonding: A Natural Bond Orbital Donor–Acceptor Perspective*, Cambridge University Press, Cambridge, UK, 2005; (*c*) J.-W. Zou, M. Huang, G.-X. Hua and Y.-J. Jiang, *RSC Adv.*, 2017, **7**, 10295–10305.

28 (*a*) M. A. Spackman and P. G. Byrom, *Chem. Phys. Lett.*, 1997, **267**, 215–220; (*b*) M. A. Spackman and D. Jayatilaka, *CrystEngComm*, 2009, **11**, 19–32.

29 T. Lu and F. Chen, *J. Comput. Chem.*, 2012, **33**, 580–592.

30 C. Y. Legault, *CYLView, 1.0b*, Université de Sherbrooke, Canada, 2009, http://www.cylview.org.

31 (*a*) S. Grimme, J. Antony, S. Ehrlich and H. Krieg, *J. Chem. Phys.*, 2010, **132**, 154104; (*b*) S. Grimme, S. Ehrlich and L. Goerigk, *J. Comput. Chem.*, 2011, **32**, 1456–1465.

32 (*a*) A. D. Becke and E. R. Johnson, *J. Chem. Phys.*, 2005, **122**, 154104; (*b*) E. R. Johnson and A. D. Becke, *J. Chem. Phys.*, 2005, **123**, 024101; (*c*) E. R. Johnson and A. D. Becke, *J. Chem. Phys.*, 2006, **124**, 174104.

33 (*a*) S. Grimme, *J. Comput. Chem.*, 2006, **27**, 1787–1799; (*b*) A. D. Becke, *J. Chem. Phys.*, 1997, **107**, 8554–8560; (*c*) J. D. Chai and M. Head-Gordon, *Phys. Chem. Chem. Phys.*, 2008, **10**, 6615–6620; (*d*) Q. Wu and W. T. Yang, *J. Chem. Phys.*, 2002, **116**, 515–524.

34 (*a*) Y. Zhao and D. G. Truhlar, *Theor. Chem. Acc.*, 2008, **120**, 215–241; (*b*) Y. Zhao and D. G. Truhlar, *Acc. Chem. Res.*, 2008, **41**, 157–167.

35 (*a*) G. A. Jeffrey, *An Introduction to Hydrogen Bonding*, Oxford University Press, Oxford, 1997; (*b*) T. Steiner, *Angew. Chem.*, 2002, **114**, 50–80 (*Angew. Chem., Int. Ed.*, 2002, **41**, 48–76); (*c*) T. Steiner, I. Majerz and C. C. Wilson, *Angew. Chem.*, 2001, **113**, 2728–2731 (*Angew. Chem., Int. Ed.*, 2001, **40**, 2651–2654); (*d*) M.-J. Zhou, Y. Li and L. Dang, *Asian J. Org. Chem.*, 2015, **4**, 904–911.

36 E. Nakamura, N. Yoshikai and M. Yamanaka, *J. Am. Chem. Soc.*, 2002, **124**(24), 7181–7192.

37 W. Humphrey, A. Dalke and K. Schulten, *J. Mol. Graphics*, 1996, **14**, 33–38.

38 E. R. Johnson, S. Keinan, P. Mori-Sánchez, J. Contreras-García, A. J. Cohen and W. Yang, *J. Am. Chem. Soc.*, 2010, **132**, 6498–6506.

Supporting information for:

Theoretical Study of the Mechanism Behind the Site- and Enantio-Selectivity of C-H Functionalization Catalysed by Chiral Dirhodium Catalyst

Meijuan Zhou*[a] and Michael Springborg [a,b]

[a] *Physical and Theoretical Chemistry Department, University of Saarland, 66123 Saarbrücken, Germany. E-mail: meijuan.zhou@uni-saarland.de.*
[b] *Materials Science, Tianjin University, Tianjin 300072, China. E-mail: m.springborg@mx.uni-saarland.de.*

Table of content

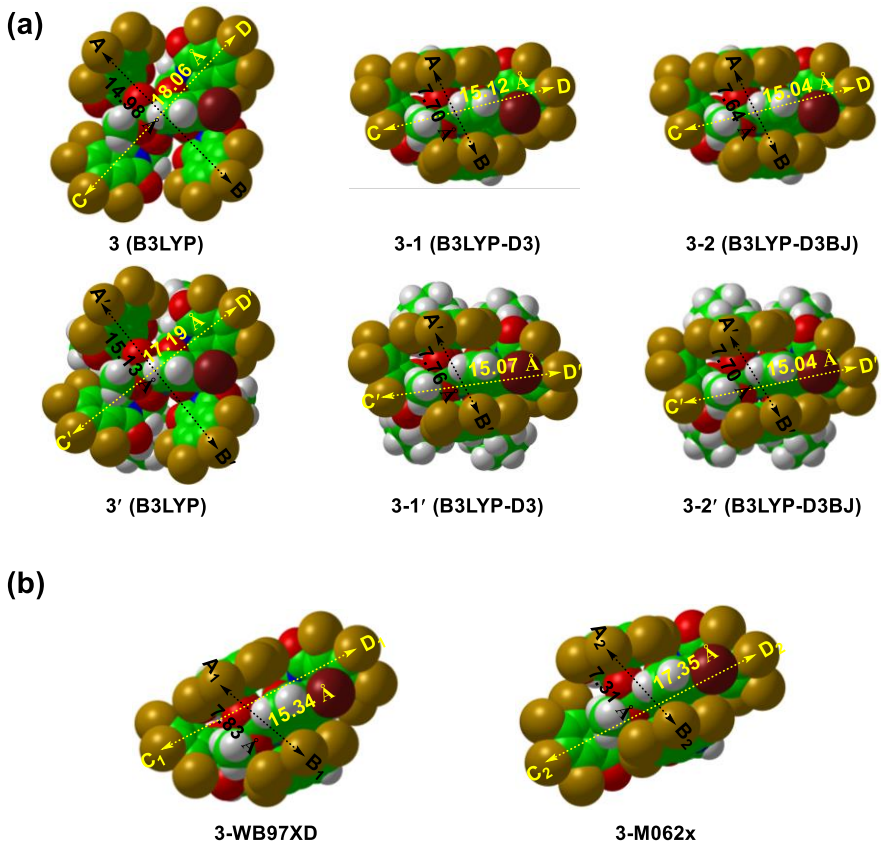

Fig. S1 (a) Space-filling models for the structures of the donor/acceptor dirhodium carbenoids {Rh_2(*S*-TCPCH$_3$)$_4$[(*p*-Br-C$_6$H$_4$)C(COOR)] (3, 3-1 and 3-2) and Rh_2(*S*-TCPTAD)$_4$[(*p*-Br-C$_6$H$_4$)C(COOR)] (3', 3-1' and 3-2')}. 3 and 3' are optimized using B3LYP[21], 3-1 and 3-1' using B3LYP-D3[31,32], and 3-2 and 3-2' using B3LYP-D3BJ[31,32]. The AB, CD, A'B' and C'D' distances are defined as the ones between the two top chlorine atoms of the two opposite ligands of the dirhodium catalysts along the AB, CD, A'B' and C'D' directions, respectively. (b) Space-filling models for the structures of the donor/acceptor dirhodium carbenoids {Rh_2(*S*-TCPCH$_3$)$_4$[(*p*-Br-C$_6$H$_4$)C(COOR)]. 3-WB97XD[33] and 3-M062X[34] are respectively optimized using WB97XD[33] and M062X[34] methods. The A_1B_1, C_1D_1, A_2B_2 and C_2D_2 distances are defined as the ones between the two top chlorine atoms of the two opposite ligands of the dirhodium catalysts along the A_1B_1, C_1D_1, A_2B_2 and C_2D_2 directions, respectively. C: green, O: red, Cl: brown, H: white, Br: deep red, N: blue.

Table S1 The Natural Bond Orbital (NBO) charges in $|e|$ for selected atoms for different structures of Fig. 5

Atom	1	TS_{1-2}	2	3
Rh1	0.557	0.490	0.486	0.486
C9	-0.158	-0.041	0.111	0.110
N1	0.121	0.079	-0.015	
N2	0.135	0.160	0.015	

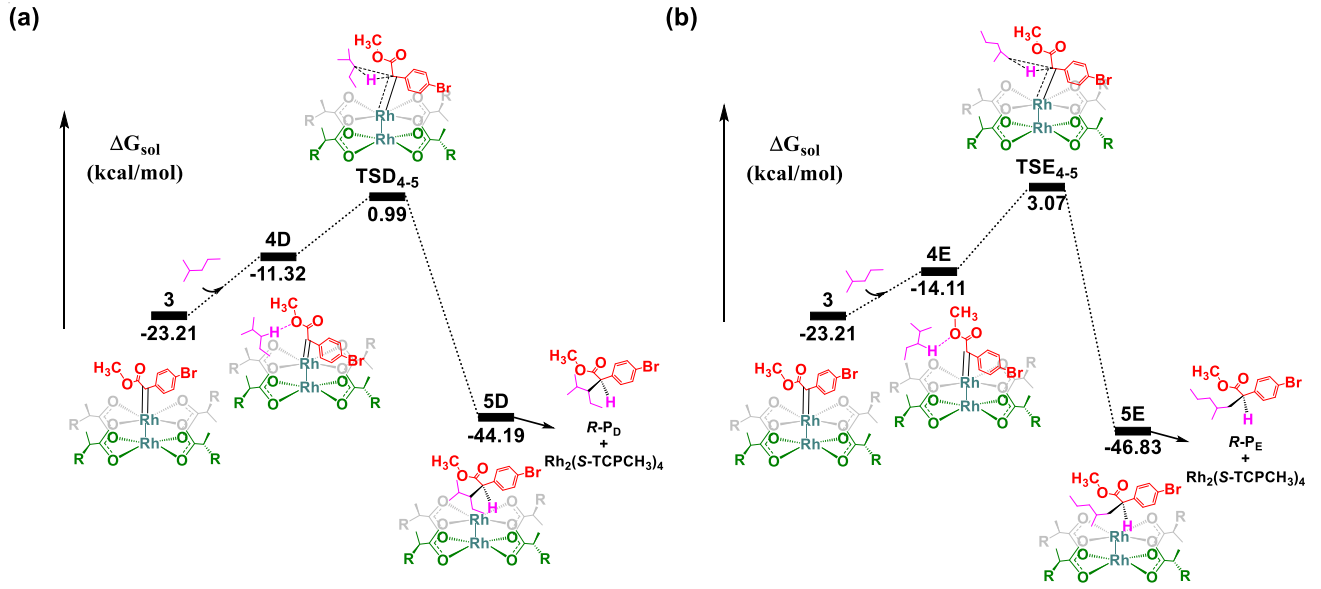

Fig. S2 Energy profiles for the two pathways for the C–H functionalization of 2-methylpentane. (a) Pathway D for the secondary C–H functionalization. In this case, the secondary carbon atom is bonded to the tertiary carbon. (b) Pathway E for the primary C–H functionalization. In this case, the primary carbon atom is bonded to the tertiary carbon. The relative free energies in dichloromethane (CH_2Cl_2) as solvent are given in kcal/mol.

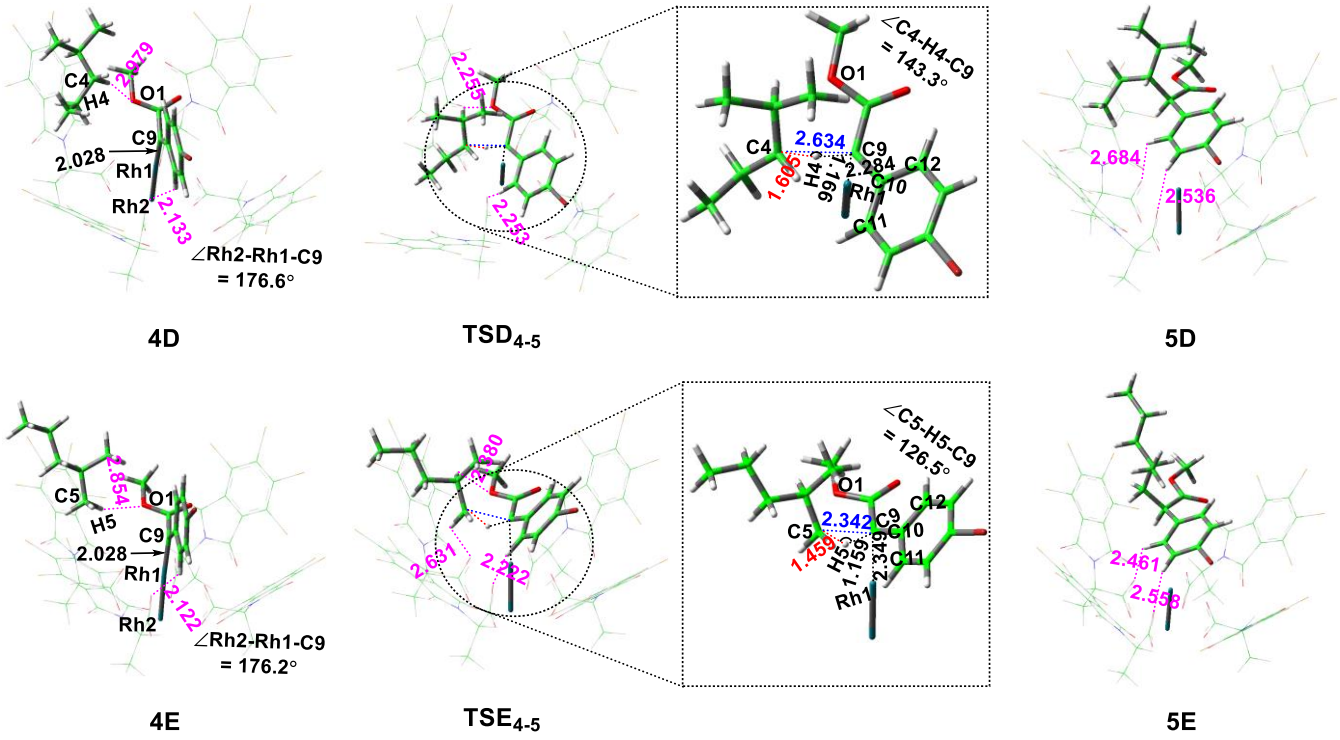

Fig. S3 Optimized structures and geometric parameters for the pathways for the C–H bond insertion reactions of Fig. S2. Blue, red, and black numbers give intramolecular distances, whereas pink numbers give intermolecular distances (Å). C: green, O: red, Cl: brown, H: white, Br: deep red, N: blue. Pink numbers represent the distances between C-H and oxygen atom for the weak hydrogen bonds.

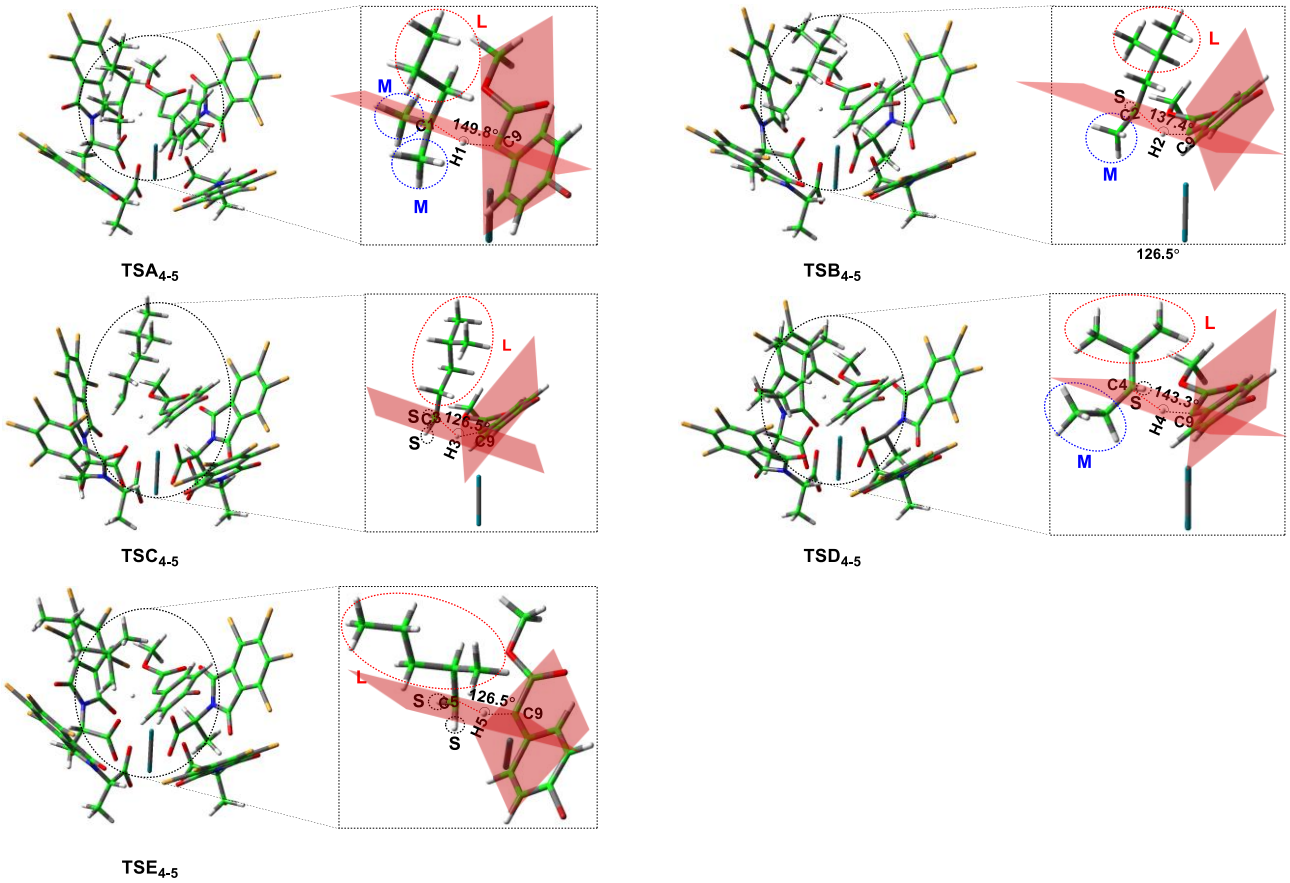

Fig. S4 The configurations for the structures of $TSA_{4\text{-}5}$, $TSB_{4\text{-}5}$, $TSC_{4\text{-}5}$, $TSD_{4\text{-}5}$ and $TSE_{4\text{-}5}$. L: the larger group; M: the medium-sized group; S: the smaller group. C: green, O: red, Cl: brown, H: white, Br: deep red, N: blue.

Table S2 A part of the geometric parameters for the structures shown in Figs. 7 and S3

Geometric parameter	∠Rh2-Rh1-C9	N (number of intermolecular hydrogen bonding)
4A	175.5°	2
4B	176.6°	2
4C	176.8°	2
4D	176.6°	2
4E	176.2°	2

Geometric parameter	∠Rh2-Rh1-C9	∠Cn-Hn-C9	N (number of intermolecular hydrogen bonding)
$TSA_{4\text{-}5}$	175.3°	∠C1-H1-C9 = 149.8°	6
$TSB_{4\text{-}5}$	176.7°	∠C2-H2-C9 = 137.4°	3
$TSC_{4\text{-}5}$	178.1°	∠C3-H3-C9 = 126.5°	2
$TSD_{4\text{-}5}$	175.8°	∠C4-H4-C9 = 143.3°	2
$TSE_{4\text{-}5}$	178.1°	∠C5-H5-C9 = 126.5°	3

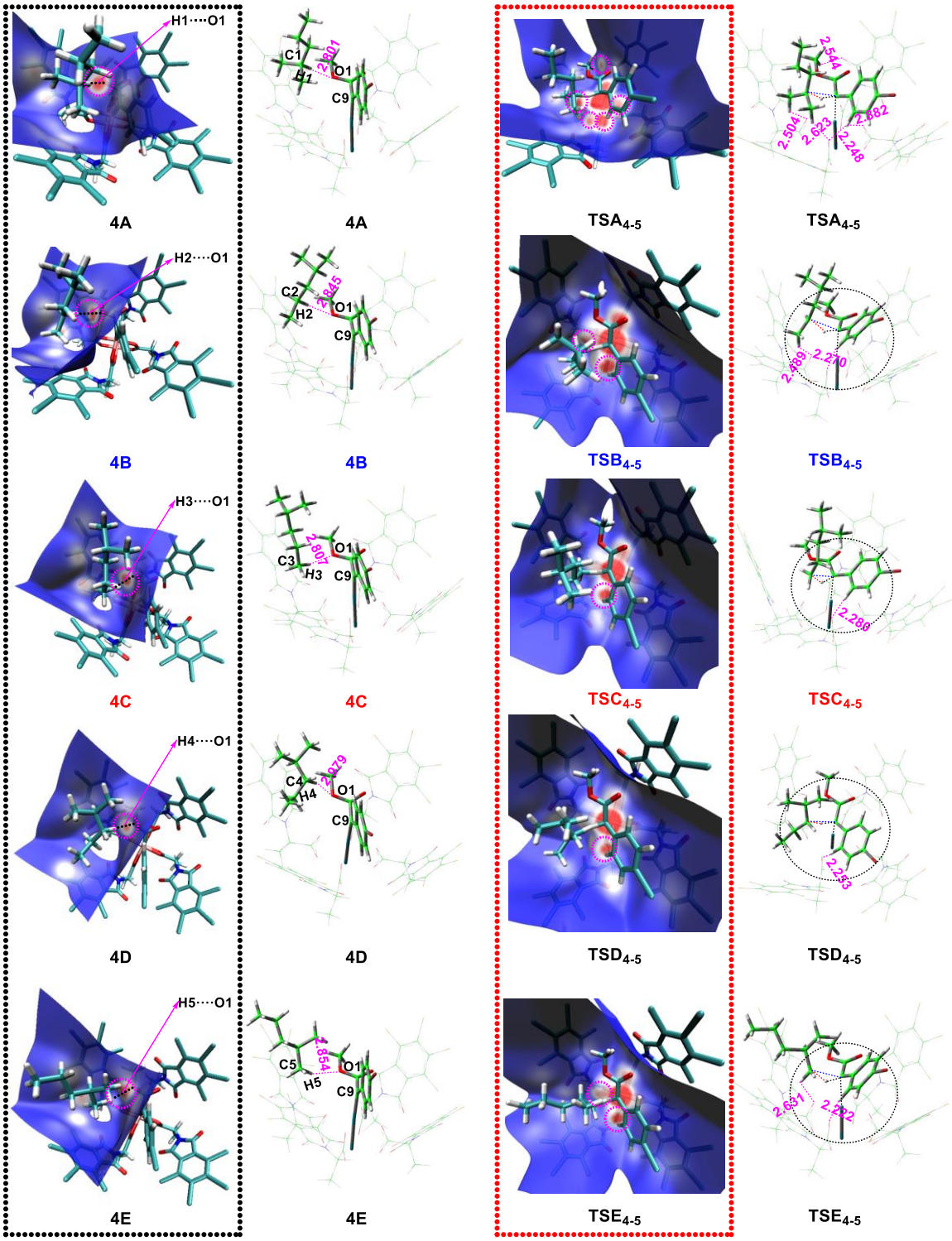

Fig. S5 The black dotted bordered rectangles represent the Hirshfeld surfaces of the second substrate [$(CH_3)_2CHCH_2CH_2CH_3$] for the intermediates structures. The second column: the ONIOM layers structures for the intermediates structures; The red dotted bordered rectangles represent the Hirshfeld surfaces of the complex [(*p*-Br-C_6H_4)C(COOR)-$(CH_3)_2CHCH_2CH_2CH_3$]. The fourth column: the ONIOM layers structures for the transition state structures. Pink numbers represent the distances between C-H and oxygen atom for the weak hydrogen bonds. For Hirshfeld surfaces, the red region implies the closer interactions with higher electron density, which mainly originate from the weak hydrogen bonding interaction; blue, no obvious interaction with very lower electron density; white, weaker interaction with less electron density. Pink circles represent the intermolecular interaction regions, and mainly due to the weak hydrogen bonding interactions.

Table S3 The Natural Bond Orbital (NBO) charges (in $|e|$) for selected atoms for the structures shown in Figs. 7 and S3

Atom	3	Atom	4A	TSA_{4-5}	Atom	4B	TSB_{4-5}
Rh1	0.486	Rh1	0.487	0.542	Rh1	0.486	0.543
C8	0.817	C8	0.819	0.859	C8	0.818	0.857
C9	0.110	C9	0.107	-0.341	C9	0.109	-0.358
C10	-0.165	C10	-0.165	-0.061	C10	-0.165	-0.062
C11	-0.106	C11	-0.105	-0.185	C11	-0.105	-0.199
C12	-0.131	C12	-0.130	-0.192	C12	-0.131	-0.195
O1	-0.554	O1	-0.552	-0.583	O1	-0.555	-0.583
O2	-0.611	C1	-0.250	0.181	C2	-0.460	-0.012
		H1	0.240	0.243	H2	0.227	0.254

Atom	4C	TSC_{4-5}	Atom	4D	TSD_{4-5}	Atom	4E	TSE_{4-5}
Rh1	0.486	0.535	Rh1	0.485	0.542	Rh1	0.487	0.536
C8	0.818	0.857	C8	0.817	0.855	C8	0.818	0.856
C9	0.110	-0.306	C9	0.110	-0.350	C9	0.108	-0.311
C10	-0.164	-0.076	C10	-0.165	-0.060	C10	-0.165	-0.070
C11	-0.105	-0.194	C11	-0.105	-0.204	C11	-0.104	-0.203
C12	-0.133	-0.193	C12	-0.130	-0.195	C12	-0.129	-0.195
O1	-0.556	-0.578	O1	-0.554	-0.578	O1	-0.556	-0.575
C3	-0.689	-0.327	C4	-0.460	0.013	C5	-0.690	-0.310
H3	0.231	0.285	H4	0.227	0.246	H5	0.239	0.285

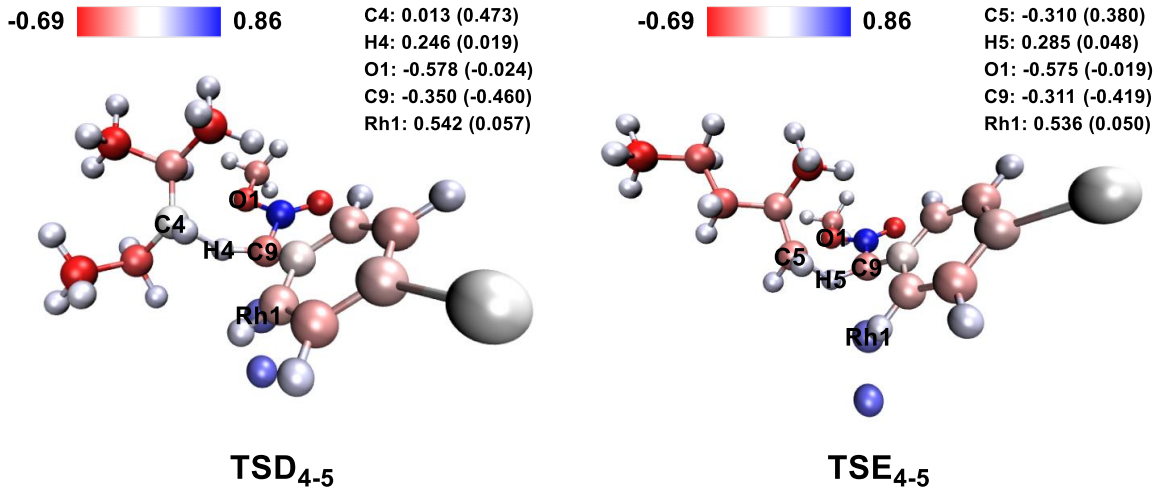

TSD_{4-5} TSE_{4-5}

Fig. S6 The Natural Bond Orbital (NBO) charges (in $|e|$) for selected atoms for the structures shown in Fig. S3 and Table S3. In bracket, the charge differences for TSD_{4-5} and TSE_{4-5} compared with 4D, and 4E, respectively. Blue and red colors represent positive and negative charge, respectively.

Table S4. The Natural Bond Orbital (NBO) charges (in $|e|$) for selected atoms for the structures shown in Fig. 9

Atom	4S	$TS_{4S\text{-}5S}$
Rh1	0.486	0.539
C8	0.817	0.861
C9	0.110	-0.327
C10	-0.168	-0.069
C11	-0.101	-0.192
C12	-0.133	-0.197
O2	-0.611	-0.666
C1	-0.246	0.186
H1	0.232	0.242

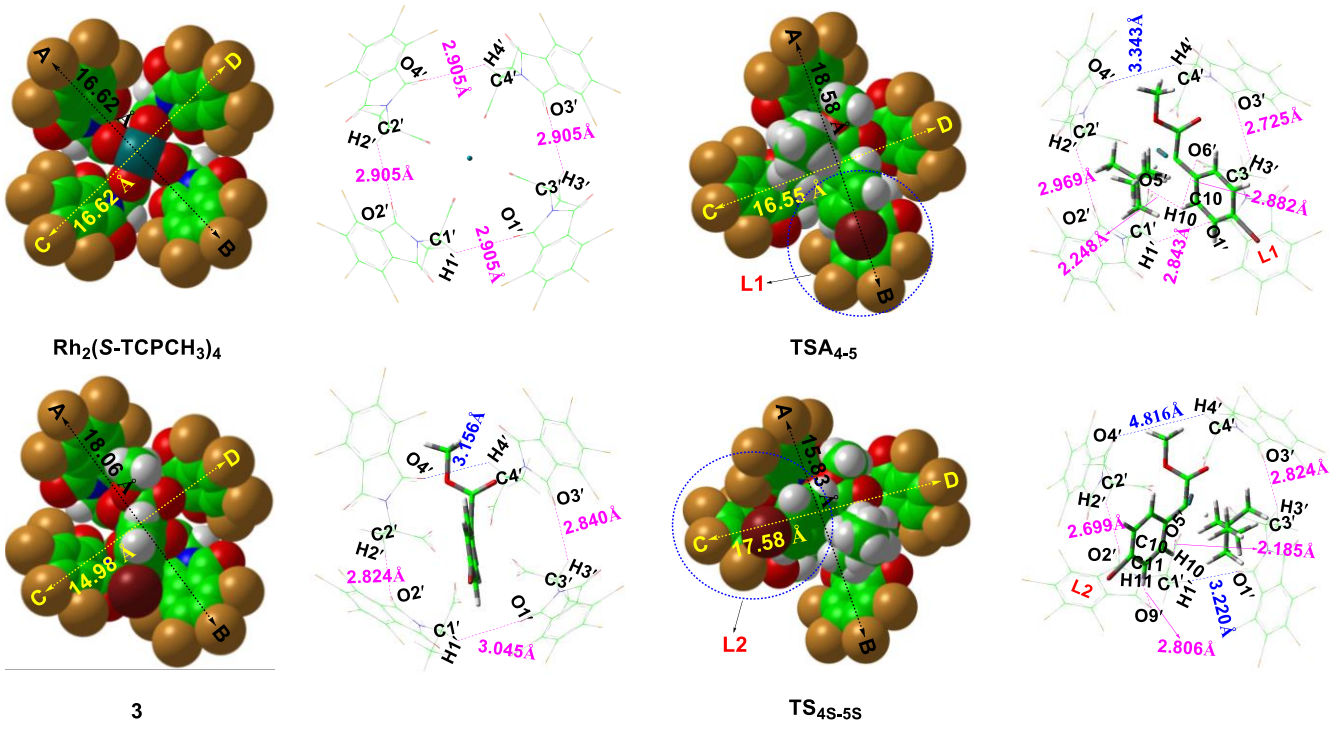

Fig. S7 Space-filling models and ONIOM layers structures. The AB and CD distances are defined as the ones between the two top chlorine atoms of the two opposite ligands of Rh_2(*S*-TCPCH$_3$)$_4$ along the AB and CD direction, respectively. C: green, O: red, Cl: brown, H: white, Br: deep red, N: blue. Also shown are the geometric parameters for the structures Rh_2(*S*-TCPCH$_3$)$_4$, 3, $TSA_{4\text{-}5}$ and $TS_{4S\text{-}5S}$ with blue numbers being intramolecular and pink numbers being intermolecular distances (in Å).

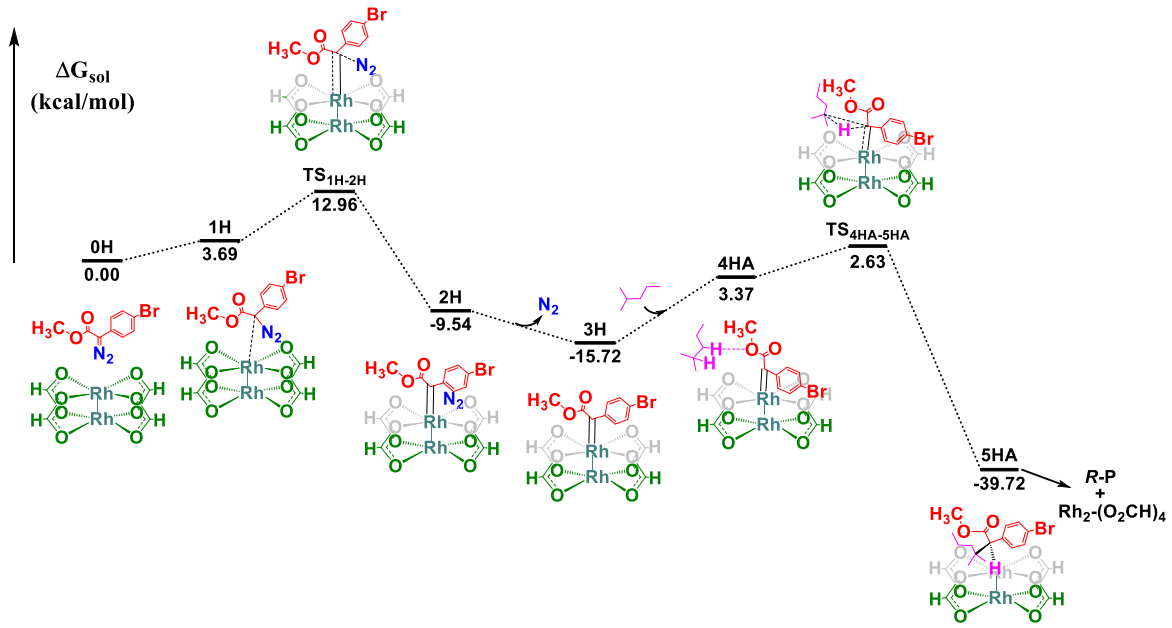

Fig. S8 Energy profiles for the pathway HA for the tertiary C–H functionalization reactions of (p-Br-C_6H_4)CN=N($COOCH_3$) with 2-methylpentane catalyzed by Rh_2-(O_2CH)$_4$. The relative free energies in dichloromethane (CH_2Cl_2) as solvent are given in kcal/mol.

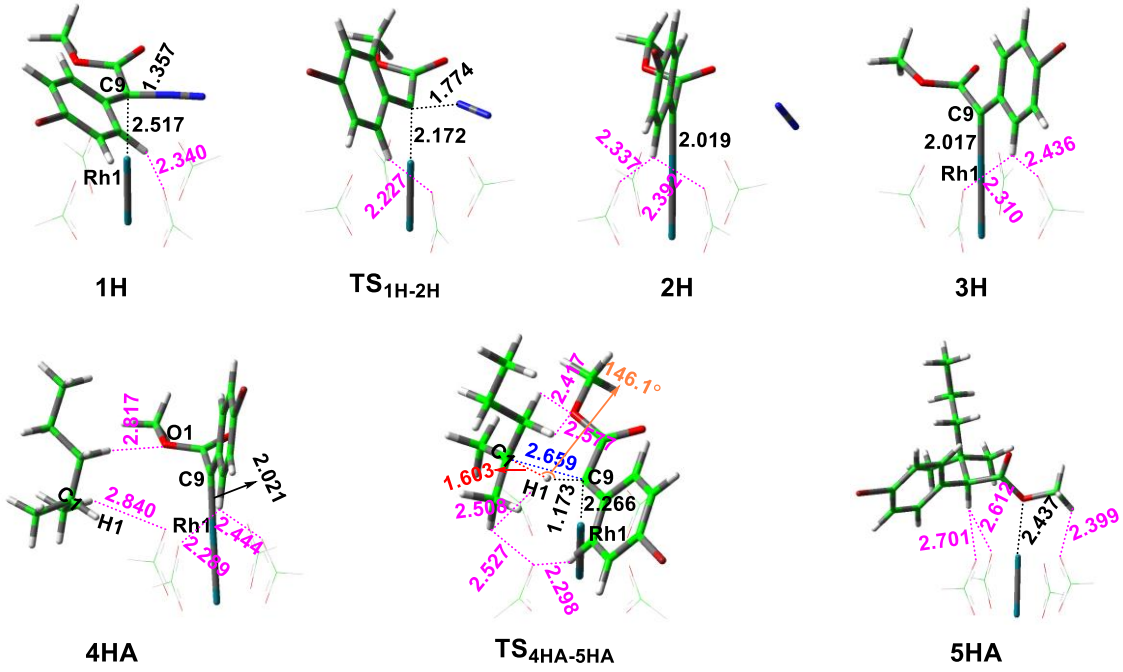

Fig. S9 Optimized structures and geometric parameters for the tertiary C–H bond functionalization reactions of (p-Br-C_6H_4)CN=N($COOCH_3$) with 2-methylpentane catalyzed by Rh_2-(O_2CH)$_4$ in Fig. S8. Blue, red, and black numbers give intramolecular bond lenths, pink numbers intermolecular bond lengths (in Å). C: green, O: red, H: white, Br: deep red, N: blue. Pink numbers represent the distances between C-H and O for the weak hydrogen bonds)

Cartesian coordinates (in Å) for optimized structures of this study

(Energies are gas-phase electronic energies in Hartree a.u.)

Rh_2(*S*-TCPCH$_3$)$_4$

-3567.243430

Rh	-0.00025400	-0.00001300	-3.56885500
O	-0.11279500	2.04951500	-3.51044900
O	0.11230200	-2.04956000	-3.51082400
O	-0.06339300	2.05249300	-1.24462700
O	0.06312900	-2.05293100	-1.24499400
O	2.04928400	0.11252300	-3.51073800
O	-2.04978600	-0.11255600	-3.51053600
O	-2.05284800	-0.06345000	-1.24470400
O	2.05258200	0.06301100	-1.24491800
C	-2.62181400	-0.08708600	-2.37984700
C	2.62143500	0.08683500	-2.38011200
C	-0.08715300	2.62150600	-2.37974300
C	0.08679200	-2.62174400	-2.38021100
Rh	-0.00013000	-0.00022900	-1.18616400
C	4.15636900	0.13518400	-2.37689300
C	4.23338600	-2.06157800	-1.13808600
C	5.62250800	-0.34539600	-0.38653900
O	3.43118600	-2.63946100	-1.84168100
C	4.97473200	-2.55843300	0.06982900
O	6.15574400	0.74088600	-0.35127400
C	5.82178300	-1.53502200	0.50972600
C	4.92323700	-3.77862100	0.72351200
C	6.64887200	-1.71194400	1.60602300
Cl	3.81698500	-5.04726400	0.19341100
C	5.75907800	-3.97159800	1.83846900
C	6.61671100	-2.94949700	2.27349800
Cl	7.71817400	-0.41739500	2.15554200
Cl	5.72418000	-5.51517400	2.69681700
Cl	7.66205600	-3.21349300	3.67330300
C	-0.13545800	4.15644000	-2.37631500
N	0.74570300	4.66345800	-1.32478400
C	2.06123100	4.23317200	-1.13736200
C	0.34511800	5.62239600	-0.38583600
O	2.63910200	3.43099600	-1.84099400
C	2.55807100	4.97440200	0.07063000
O	-0.74111300	6.15573900	-0.35062700
C	1.53471600	5.82153700	0.51049800
C	3.77820400	4.92273800	0.72440200
C	1.71164800	6.64855400	1.60684600
Cl	5.04674800	3.81634800	0.19435200
C	3.97119300	5.75851300	1.83940600
C	2.94915200	6.61623500	2.27440200
Cl	0.41717000	7.71796300	2.15632800
Cl	3.21316500	7.66149700	3.67426700
C	-4.15674300	-0.13539900	-2.37648300
N	-4.66380000	0.74557500	-1.32481700
C	-4.23348900	2.06106400	-1.13715200
C	-5.62245800	0.34470600	-0.38570700
O	-3.43140100	2.63909500	-1.84075200
C	-4.97451200	2.55760700	0.07108600
O	-6.15567200	-0.74159100	-0.35056600
C	-5.82149300	1.53410500	0.51091100
C	-4.92281000	3.77761100	0.72509100
C	-6.64831500	1.71075900	1.60745300
Cl	-3.81662500	5.04635000	0.19506800
C	-5.75837700	3.97031800	1.84030000
C	-6.61594700	2.94813000	2.27525600
Cl	-7.71754700	0.41610800	2.15686700
Cl	-5.72320400	5.51365300	2.69906900
Cl	-7.66095700	3.21178800	3.67537500
C	0.13514400	-4.15667300	-2.37704000
N	-0.74588900	-4.66389600	-1.32550200
C	-2.06141300	-4.23367200	-1.13786500
C	-0.34515500	-5.62291200	-0.38670400
O	-2.63938000	-3.43140400	-1.84131200
C	-2.55808300	-4.97506300	0.07009600
O	0.74111400	-6.15619000	-0.35165700
C	-1.53463800	-5.82219900	0.50975100
C	-3.77815100	-4.92353900	0.72400400
C	-1.71141000	-6.64935500	1.60602100
Cl	-5.04680100	-3.81714800	0.19422800
C	-3.97097300	-5.75945100	1.83893500
C	-2.94884300	-6.61717500	2.27371700
Cl	-0.41682000	-7.71876500	2.15523600
Cl	-5.51439500	-5.72452700	2.69756200
Cl	-3.21264800	-7.66260900	3.67349300
H	1.14909400	-4.42448400	-2.05745400
H	-4.42454600	-1.14936300	-2.05693500
H	-1.14936300	4.42423800	-2.05657700
H	4.42418300	1.14908200	-2.05714900
Cl	5.51470300	5.72340600	2.69786300
N	4.66357600	-0.74601200	-1.32547900
C	0.16873400	4.78589700	-3.73759300
H	-0.53776500	4.41734400	-4.48461500
H	0.07105800	5.87349700	-3.66682200
H	1.18071500	4.53482700	-4.06585900
C	-4.78614700	0.16904300	-3.73772900
H	-4.41757700	-0.53733000	-4.48486200
H	-5.87375100	0.07137200	-3.66700900
H	-4.53505200	1.18108000	-4.06580400
C	-0.16916700	-4.78592700	-3.73838600
H	0.53725000	-4.41725200	-4.48542400
H	-0.07147000	-5.87353700	-3.66778700
H	-1.18118600	-4.53482300	-4.06651100
C	4.78564600	-0.16892400	-3.73827500
H	4.41698100	0.53760600	-4.48521200
H	5.87325500	-0.07123700	-3.66764600
H	4.53454600	-1.18089200	-4.06655600

Sub-1: (*p*-Br-C$_6$H$_4$)CN=N(COOCH$_3$)

-620.239555

C	2.06826800	0.42786200	0.00020300
C	0.60011900	0.26669700	-0.00001800
C	-0.24466500	1.39260800	-0.00207100
C	0.00875900	-1.00979900	0.00191400
C	-1.62975300	1.25651400	-0.00213900
H	0.17206200	2.39584800	-0.00372200
C	-1.37806000	-1.15037000	0.00178200
H	0.63849100	-1.88928000	0.00340300
C	-2.19245500	-0.01954400	-0.00019900
H	-2.26236000	2.13730200	-0.00374900
H	-1.81755100	-2.14190900	0.00327400
Br	-4.10495400	-0.21653600	-0.00028600
C	3.07385000	-0.64696500	-0.00018400
O	2.82827500	-1.83837600	-0.00014400
O	4.33210000	-0.14298900	-0.00051500
N	2.55609300	1.65271100	0.00060700
N	2.95274700	2.71924400	0.00109200
C	5.38427600	-1.12115300	-0.00075700
H	5.32201900	-1.75210700	-0.89116900
H	6.31106500	-0.54710100	-0.00090400
H	5.32235000	-1.75221500	0.88959800

Sub-2: $(CH_3)_2CHCH_2CH_2CH_3$

-237.084754

C	-4.09003700	0.20687500	0.05269900
H	-3.67097900	0.83926300	-0.74589600
C	-5.61154500	0.13785500	-0.15138500
H	-6.06433000	1.13309500	-0.06785500
H	-5.87858800	-0.26321900	-1.13491300
H	-6.07786000	-0.50309600	0.60893200
C	-3.75783000	0.87076300	1.39742700
H	-4.14901400	0.27766400	2.23461300
H	-2.67479300	0.96983600	1.53792000
H	-4.19855600	1.87250200	1.46708900
C	-3.41674300	-1.17660800	-0.04886300
H	-2.35323400	-1.06687100	0.21093500
H	-3.84719900	-1.84064800	0.71710500
C	-3.51318000	-1.85651900	-1.42144300
H	-4.56427600	-2.04647200	-1.67427900
H	-3.13282300	-1.17016200	-2.19183200
C	-2.73586900	-3.17595400	-1.48636600
H	-2.82114200	-3.64385900	-2.47389800
H	-1.66929100	-3.01859300	-1.28295000
H	-3.10997300	-3.89294400	-0.74499400

1

-4187.493735

Rh	-0.14274300	-0.17019000	-3.85751200
O	0.16966100	1.84338300	-3.66050900
O	-0.50085000	-2.20102800	-3.92845600
O	0.14278400	1.73296800	-1.39402300
O	-0.69326500	-2.28988300	-1.67035400
O	1.88029900	-0.48443600	-3.71318400
O	-2.16925900	0.16414300	-3.89808800
O	-2.27931100	0.14899600	-1.63587000
O	1.75024500	-0.72910000	-1.46358200
C	-2.77681600	0.29313500	-2.79762700
C	2.37454100	-0.69889700	-2.57108900
C	0.26017000	2.34514900	-2.50188600
C	-0.75195500	-2.78899100	-2.83829400
Rh	-0.27269400	-0.29149600	-1.45143300
C	3.89687000	-0.89243500	-2.48616900
C	3.66947800	-3.25028200	-1.62161100
C	4.95532600	-1.76471600	-0.36893500
O	2.92475300	-3.64064500	-2.49472000
C	4.20988900	-3.99223500	-0.43184700
O	5.46065800	-0.71801000	-0.02630100
C	4.98230200	-3.10071400	0.32001600
C	4.04912400	-5.31030600	-0.03835500
C	5.61361000	-3.50542800	1.48434100
Cl	3.06339200	-6.42758400	-0.98639500
C	4.68797200	-5.73712300	1.14013200
C	5.46312800	-4.84247300	1.89497200
Cl	6.58526300	-2.37439000	2.43126500
Cl	4.51057200	-7.41261500	1.67087900
Cl	6.25704500	-5.39693900	3.37239400
C	0.47128400	3.86400100	-2.42907100
N	1.50778400	4.18296200	-1.44499900
C	2.75769500	3.56253300	-1.38791500
C	1.38591100	5.24748700	-0.54260200
O	3.11001300	2.63289200	-2.08418100
C	3.52437000	4.29931000	-0.32560200
O	0.40855300	5.95198900	-0.42011600
C	2.70211700	5.31356100	0.17759500
C	4.81737700	4.13057400	0.14085700
C	3.15254800	6.18126900	1.15792100
Cl	5.84770000	2.83739600	-0.48062400
C	5.29175000	5.01113800	1.12944200
C	4.46630900	6.02709100	1.63400500
Cl	2.10659800	7.45680100	1.79239800
Cl	5.07770300	7.12128600	2.87909400
C	-4.27897600	0.60907900	-2.86745000
N	-4.62757300	1.57723000	-1.82589100
C	-3.90796300	2.74443800	-1.56669300
C	-5.75524100	1.43820400	-1.00544400
O	-2.92280800	3.10941000	-2.17458200
C	-4.61990100	3.41171700	-0.42439800
O	-6.55151500	0.52853600	-1.05986800
C	-5.73997900	2.63817900	-0.10093300
C	-4.32895100	4.57712100	0.26569400
C	-6.60556600	3.01891600	0.91047800
Cl	-2.88516200	5.52175800	-0.11051200
C	-5.20106200	4.97630700	1.29472300
C	-6.33099200	4.20680500	1.61170300
Cl	-8.01912300	2.03920200	1.31368400
Cl	-4.86537900	6.45914600	2.19503300
Cl	-7.41660300	4.72810100	2.90483900
C	-1.14335100	-4.27477900	-2.90088200
N	-2.13366300	-4.54664200	-1.85881500
C	-3.32210600	-3.82358400	-1.71112400
C	-1.88512300	-5.39793700	-0.77801700
O	-3.71489400	-2.96782400	-2.47623800
C	-3.95007600	-4.33430800	-0.44710200
O	-0.88116300	-6.06200900	-0.62920500
C	-3.09041900	-5.28715200	0.10760200
C	-5.13992900	-3.99498400	0.17409100
C	-3.40278400	-5.92863900	1.29282100
Cl	-6.20106500	-2.75951900	-0.50671200
C	-5.47218200	-4.64349600	1.37698000
C	-4.61215300	-5.60382700	1.93068200
Cl	-2.30437700	-7.12491700	1.99629300
Cl	-6.98527500	-4.24115000	2.19696600
Cl	-5.04629100	-6.40952100	3.44323300
H	-0.25460300	-4.84082000	-2.59751100
H	-4.79619700	-0.31552500	-2.58628500

H	-0.45703000	4.27257600	-2.01541100
H	4.28587800	0.02343900	-2.02637700
Cl	6.94041000	4.83439800	1.73788500
N	4.19759000	-1.95898300	-1.52899600
C	0.76443600	4.51029100	-3.78527000
H	-0.05072500	4.30031900	-4.48115300
H	0.85042600	5.59442200	-3.66175600
H	1.69122400	4.11970300	-4.21379900
C	-4.74412000	1.06628300	-4.25218800
H	-4.51222300	0.29934200	-4.99431400
H	-5.82637000	1.22768100	-4.23871900
H	-4.24355300	1.99264900	-4.54602100
C	-1.60744200	-4.73200800	-4.28502400
H	-0.81892300	-4.54510300	-5.01737400
H	-1.82431400	-5.80443100	-4.26498500
H	-2.50323300	-4.18885900	-4.59488600
C	4.56854400	-1.12535200	-3.84055200
H	4.35826400	-0.28307900	-4.50322500
H	5.65169500	-1.20519300	-3.70522000
H	4.19467400	-2.03721900	-4.31189600
C	-0.47137600	-0.43814500	1.12394200
C	0.57268300	0.40293100	1.80029700
C	1.93107200	0.21547200	1.50568000
C	0.21771700	1.35346400	2.76950400
C	2.91403700	0.93843000	2.17911000
H	2.21783500	-0.48728400	0.73628000
C	1.19145400	2.09183900	3.44052400
H	-0.82449700	1.51838900	3.02963400
C	2.53610000	1.86891500	3.14794700
H	3.95943500	0.77583200	1.93898200
H	0.90374600	2.81665700	4.19394600
Br	3.88318100	2.85060600	4.10572400
C	-0.55885300	-1.93216800	1.27476800
O	-1.60074500	-2.55553200	1.21470600
O	0.64704800	-2.46434600	1.49927500
C	0.67446300	-3.89529600	1.68608500
H	0.48533200	-4.40593100	0.74048800
H	1.67841200	-4.11411800	2.04907200
H	-0.07409800	-4.19771700	2.42108600
N	-1.71262300	0.08832000	1.15632400
N	-2.74475000	0.53793200	1.14642600

$TS_{1\text{-}2}$

-4187.508343

Rh	0.68303800	-0.61039800	-2.89084700
O	1.03429900	1.40318700	-2.69273000
O	0.26936300	-2.63326800	-2.93486200
O	1.04774000	1.31339100	-0.42368100
O	0.16469000	-2.73277100	-0.66947300
O	2.70900400	-0.96923200	-2.80674200
O	-1.33656400	-0.23669800	-2.85002200
O	-1.38375900	-0.25251300	-0.58337600
O	2.65901600	-1.16095200	-0.54559000
C	-1.90910000	-0.10503200	-1.73493400
C	3.23903000	-1.15920000	-1.67990000
C	1.13083400	1.91523500	-1.54460100
C	0.03240100	-3.21314400	-1.84136300
Rh	0.63367000	-0.72907400	-0.44201800
C	4.76587600	-1.34472700	-1.64816000
C	4.60781900	-3.56709600	-0.47042300
C	5.94909000	-1.92409100	0.49661000
O	3.84076800	-4.08359300	-1.25363700
C	5.19770000	-4.13052800	0.79275200
O	6.48607100	-0.84959200	0.65028600
C	6.00359800	-3.14530400	1.37223900
C	5.05140100	-5.37407600	1.38376800
C	6.68315300	-3.38004600	2.55595700
Cl	4.02896800	-6.61547400	0.64811600
C	5.73262900	-5.62629400	2.58768200
C	6.54259000	-4.63809400	3.16834600
Cl	7.70152400	-2.13274000	3.28244600
Cl	5.56311300	-7.20039900	3.37457500
Cl	7.39260500	-4.97359400	4.68097200
C	1.28951000	3.44434500	-1.49833300
N	2.30083600	3.83594900	-0.51179600
C	3.56592600	3.25715600	-0.40740100
C	2.14755400	4.95792100	0.31432900
O	3.95397600	2.29680900	-1.04068500
C	4.29884300	4.06959200	0.62443900
O	1.16054900	5.65651700	0.37116700
C	3.44722900	5.09170900	1.05605300
C	5.58156800	3.94447800	1.13185100
C	3.85707800	6.01350500	2.00460600
Cl	6.64069400	2.63268100	0.60459500
C	6.01419000	4.87697800	2.09190200
C	5.15912400	5.90222300	2.52487400
Cl	2.77521900	7.29953800	2.54885500
Cl	5.71881400	7.06284400	3.73298600
C	-3.41431100	0.21016600	-1.76978200
N	-3.74657300	1.22144800	-0.76184800
C	-3.03415200	2.40573100	-0.56763700
C	-4.90364200	1.14932500	0.02565300
O	-2.03790300	2.73220700	-1.17915400
C	-3.77023100	3.14823000	0.51224600
O	-5.71463900	0.25102400	-0.00166700
C	-4.90228100	2.40169900	0.85547000
C	-3.49123100	4.35453300	1.13346300
C	-5.79088200	2.84886400	1.81858900
Cl	-2.03539100	5.26825000	0.73233200
C	-4.38671800	4.82144300	2.11276200
C	-5.52801300	4.07782100	2.44973300
Cl	-7.21966400	1.90196800	2.24718400
Cl	-4.06625800	6.35741300	2.92512100
Cl	-6.64341200	4.68417200	3.67895300
C	-0.43963100	-4.67771900	-1.91061200
N	-1.44645800	-4.91363500	-0.87403600
C	-2.58138500	-4.11832000	-0.68802500
C	-1.31402300	-5.90263000	0.10367900
O	-2.90208100	-3.18777100	-1.39667400
C	-3.27024800	-4.67598500	0.52451000
O	-0.39166600	-6.68635800	0.18466200
C	-2.51566300	-5.75704800	0.99035900
C	-4.43307500	-4.28491900	1.16634300
C	-2.90786600	-6.47717000	2.10528000
Cl	-5.35825500	-2.89290200	0.60242100
C	-4.84587400	-5.01167600	2.29774800
C	-4.09173900	-6.09979100	2.76216200
Cl	-1.94150900	-7.83682500	2.69550500
Cl	-6.32709100	-4.54550200	3.14119600
Cl	-4.62723700	-7.00199900	4.18496000
H	0.41496900	-5.29720500	-1.61490800
H	-3.91898600	-0.70407400	-1.43927400
H	0.33998300	3.82621200	-1.10815700
H	5.17426000	-0.37765600	-1.33046300
Cl	7.64617000	4.75225700	2.75536000
N	5.13016100	-2.27595100	-0.58139500
C	1.57495900	4.07011000	-2.86616600
H	0.77508100	3.81608800	-3.56456900
H	1.62260500	5.15908500	-2.76633800
H	2.51876800	3.70168500	-3.27733000
C	-3.91985400	0.61065400	-3.15808400
H	-3.70699600	-0.18555500	-3.87439900
H	-5.00188900	0.77080400	-3.12022000
H	-3.42947600	1.52424400	-3.50465200
C	-0.92938400	-5.09587600	-3.29871200
H	-0.13418600	-4.94372800	-4.03165800
H	-1.20371200	-6.15534100	-3.28862200
H	-1.79466900	-4.50128500	-3.60168000
C	5.36488000	-1.74502600	-2.99822100
H	5.10512500	-0.99771100	-3.75079200
H	6.45487200	-1.80013200	-2.91552200
H	4.97852400	-2.71329300	-3.32547700
C	0.65932200	-0.95330300	1.71486000
C	1.65940200	-0.32893800	2.62085000
C	2.73784700	0.40785100	2.10497800
C	1.57892400	-0.51786200	4.01715100
C	3.72560900	0.91050200	2.95313100
H	2.82736500	0.55352400	1.03791600
C	2.53114100	0.01652700	4.87464800
H	0.75163500	-1.08442600	4.43785000
C	3.60867700	0.72323600	4.32947600
H	4.58114500	1.43276200	2.54162800
H	2.45099900	-0.12269600	5.94693500
Br	4.94539900	1.44061900	5.50009700
C	0.22347900	-2.34980400	2.10149000
O	-0.91939600	-2.73448800	2.24307300
O	1.32327500	-3.10631700	2.22555800
C	1.13308300	-4.51774900	2.45578200
H	1.03472100	-5.03463300	1.50045500
H	2.03223300	-4.85477700	2.97162400
H	0.24729500	-4.68617000	3.07007100
N	-0.85655200	-0.10913300	2.15108900
N	-1.69211100	0.61485000	2.07173700

2

-4187.508343

Rh	-0.09730900	-0.22386900	-4.01971300
O	0.19748500	1.81486800	-3.95524300
O	-0.38016200	-2.25821700	-3.92830500
O	0.28970200	1.82649600	-1.68632300
O	-0.47683700	-2.24197200	-1.65810600
O	1.94328100	-0.53374500	-3.93556900
O	-2.13942100	0.09562300	-3.93768500
O	-2.11965300	0.16291600	-1.66811900
O	1.92584500	-0.62647000	-1.66663900
C	-2.67663100	0.25434300	-2.81136700
C	2.48371100	-0.69778400	-2.81208900
C	0.34318400	2.37395900	-2.83654600
C	-0.51475600	-2.80430300	-2.80088200
Rh	-0.10336700	-0.20563500	-1.55038000
C	3.99809200	-0.97157600	-2.79123800
C	3.67487000	-3.11998500	-1.50929000
C	5.18461400	-1.56655000	-0.65143900
O	2.85048300	-3.59981800	-2.25793600
C	4.23259100	-3.67225700	-0.22797300
O	5.80625900	-0.53098300	-0.55005100
C	5.15566000	-2.74920600	0.27518500
C	3.96715400	-4.85795800	0.43752300
C	5.84830900	-2.99639100	1.44835200
Cl	2.76546500	-5.99406100	-0.17577000
C	4.66425300	-5.12105300	1.63089900
C	5.59953900	-4.20121200	2.12931400
Cl	7.01904900	-1.83009600	2.07634400
Cl	4.35487900	-6.62336000	2.50780600
Cl	6.46960900	-4.55351400	3.62671100
C	0.54193700	3.89887900	-2.85295300
N	1.51833000	4.29871600	-1.83623600
C	2.74615900	3.67092100	-1.63033200
C	1.34211600	5.42942100	-1.02657300
O	3.15304600	2.69920200	-2.23367900
C	3.42174800	4.45398300	-0.53855500
O	0.38009000	6.16301300	-1.04853200
C	2.58388700	5.51598500	-0.18365000
C	4.64789400	4.27251200	0.07851300
C	2.95441300	6.42563900	0.79256200
Cl	5.68560900	2.90553800	-0.35012900
C	5.04020600	5.19029400	1.06880500
C	4.20101400	6.25833500	1.42228600
Cl	1.89140000	7.76367700	1.23817000
Cl	4.70995500	7.40125500	2.66961900
C	-4.18275800	0.56475300	-2.76584100
N	-4.44570600	1.47984400	-1.65390100
C	-3.77303500	2.69385600	-1.47768600
C	-5.21717400	1.12692900	-0.54314600
O	-2.98631500	3.17529100	-2.26549300
C	-4.23871200	3.22397400	-0.15249700
O	-5.81777400	0.08155600	-0.41098800
C	-5.12017500	2.29015700	0.40029400
C	-3.92597900	4.39676800	0.51395200
C	-5.72257800	2.51387600	1.62576600
Cl	-2.77386400	5.54840700	-0.16606900
C	-4.53348400	4.63758100	1.75911100
C	-5.42889600	3.70713100	2.30761200
Cl	-6.83658700	1.32764700	2.32209100
Cl	-4.16324200	6.12581000	2.63790200
Cl	-6.19354700	4.03320700	3.86827500
C	-0.67678300	-4.33397100	-2.79043900
N	-1.70270000	-4.72717800	-1.82233700
C	-2.97623200	-4.15871500	-1.75702300
C	-1.52271800	-5.77174600	-0.90899000
O	-3.37820900	-3.25108500	-2.45318400
C	-3.69818500	-4.91449300	-0.67470200
O	-0.51675900	-6.43430900	-0.78787400
C	-2.82546000	-5.88194400	-0.16573500

C	-4.98840000	-4.78607900	-0.18695300
C	-3.22009500	-6.74250500	0.84486100
Cl	-6.08273300	-3.55429600	-0.82325400
C	-5.40417700	-5.65550600	0.83788600
C	-4.52738700	-6.62449600	1.34987900
Cl	-2.11243000	-7.96085700	1.48612800
Cl	-7.04394800	-5.52319400	1.48366900
Cl	-5.06694400	-7.70591300	2.63935000
H	0.26272400	-4.73161400	-2.39031700
H	-4.67922600	-0.37126700	-2.48436800
H	-0.41101700	4.32702800	-2.52083700
H	4.47367800	-0.02395700	-2.51189100
Cl	6.60143100	4.99272800	1.87241600
N	4.31240000	-1.88942800	-1.69533800
C	0.90697300	4.45017300	-4.23356000
H	0.13379500	4.18163700	-4.95618000
H	0.98076700	5.54102300	-4.18414500
H	1.85859900	4.03781300	-4.58021300
C	-4.74283200	1.07884200	-4.09309300
H	-4.55217600	0.34528200	-4.87950100
H	-5.82301600	1.23075800	-4.00426600
H	-4.26813300	2.02081700	-4.37734600
C	-0.94812400	-4.92858900	-4.17432300
H	-0.13932400	-4.66152900	-4.85767600
H	-1.00159900	-6.01935900	-4.10002000
H	-1.88562700	-4.54673500	-4.58695000
C	4.55040100	-1.45896600	-4.13234900
H	4.32791200	-0.72472700	-4.90939200
H	5.63553200	-1.58291600	-4.06174500
H	4.09584200	-2.41074200	-4.41762600
C	-0.19080000	-0.13451800	0.46907400
C	0.84785600	0.14678400	1.41101200
C	2.12449000	0.61120400	0.98835600
C	0.64445400	-0.05490800	2.80760000
C	3.14231700	0.84359300	1.90267300
H	2.30020000	0.78631900	-0.06401300
C	1.65792300	0.16450600	3.72393200
H	-0.31860000	-0.40068700	3.16697300
C	2.90389700	0.61437600	3.26345300
H	4.11406300	1.18598300	1.56492200
H	1.49372100	-0.00250200	4.78238300
Br	4.29932400	0.92562900	4.52476100
C	-1.56407000	-0.28420700	1.02049400
O	-2.23509700	0.70355100	1.26288600
O	-1.96392400	-1.54781700	1.18589400
C	-3.32440500	-1.71528100	1.65044500
H	-3.42903600	-2.78280000	1.83993200
H	-3.48658200	-1.14524500	2.56802900
H	-4.02914500	-1.38676700	0.88414300
N	-2.28030300	1.31758100	4.41878700
N	-2.76989400	2.30350400	4.32315300

N_2

-109.524129

N	0.30404500	2.55968700	1.13193900
N	-0.79362100	2.61719700	1.01383000

3

-4077.985946

Rh	0.65066100	-0.55072900	-2.94888600
O	0.98714900	1.48202800	-2.90782900
O	0.32133200	-2.57628400	-2.83530800
O	1.02319500	1.52509400	-0.63774000
O	0.17049200	-2.52675700	-0.56858700
O	2.68117400	-0.90619700	-2.81001100
O	-1.38654600	-0.18772500	-2.92537200
O	-1.41925900	-0.08800600	-0.65725500
O	2.60580100	-0.96210800	-0.54127300
C	-1.94677400	-0.00016700	-1.81487400
C	3.18951300	-1.06678400	-1.67131900
C	1.11917500	2.05394500	-1.79377100
C	0.14632900	-3.10361200	-1.70442700
Rh	0.58394100	-0.49655600	-0.48123600
C	4.69443400	-1.38318900	-1.60574400
C	4.27696600	-3.49790600	-0.29534000
C	5.77883400	-1.95491400	0.59345200
O	3.47235400	-3.97617100	-1.06615900
C	4.76535200	-4.03043800	1.02212500
O	6.41446800	-0.92837300	0.70059800
C	5.68267200	-3.11309000	1.54570700
C	4.44553300	-5.19398200	1.70274200
C	6.31400500	-3.34341900	2.75630600
Cl	3.25094800	-6.32201800	1.06174500
C	5.08129700	-5.44056800	2.93334800
C	6.01022200	-4.52622000	3.45331500
Cl	7.47453700	-2.18224800	3.41243900
Cl	4.70213000	-6.91482700	3.83020800
Cl	6.80226400	-4.85713300	4.99810800
C	1.35772800	3.57284200	-1.82808500
N	2.31956900	3.96400200	-0.79427000
C	3.52564300	3.30865200	-0.54862600
C	2.15681300	5.11644300	-0.01298400
O	3.92060900	2.31579600	-1.12471800
C	4.19700800	4.09547600	0.54319200
O	1.21703500	5.87627400	-0.07380300
C	3.38051300	5.18656500	0.85733000
C	5.40380600	3.89460200	1.19154300
C	3.75367300	6.10628600	1.82308300
Cl	6.41401400	2.49279600	0.81376600
C	5.79838200	4.82187300	2.17205100
C	4.98088700	5.91907300	2.48448600
Cl	2.71778100	7.48137100	2.21678100
Cl	5.49304700	7.07429100	3.71920300
C	-3.44566700	0.34765500	-1.80788800
N	-3.70851500	1.28175700	-0.71160900
C	-3.00866100	2.48063500	-0.53677000
C	-4.48980800	0.94990600	0.39915000
O	-2.20512400	2.93890700	-1.32147600
C	-3.46646800	3.02614300	0.78470600
O	-5.11470400	-0.08086200	0.53269900
C	-4.36677600	2.11232400	1.34022800
C	-3.12511800	4.19146100	1.45003100
C	-4.95636900	2.34678400	2.56974300
Cl	-1.95286800	5.31949400	0.76471200
C	-3.71927000	4.44314200	2.69935000
C	-4.62967400	3.53051100	3.25298300
Cl	-6.09170300	1.18432500	3.27123800
Cl	-3.31173500	5.92228500	3.57809100
Cl	-5.36972800	3.86611700	4.82388100
C	-0.05268200	-4.62874200	-1.67851700
N	-1.11759800	-4.98438400	-0.73817300
C	-2.37878700	-4.38573600	-0.71986000
C	-0.99302500	-6.02516900	0.18870400
O	-2.73613600	-3.47510400	-1.43621600
C	-3.15378200	-5.11463500	0.34413200
O	-0.00841300	-6.71153800	0.34692800
C	-2.32123200	-6.09710100	0.89028400
C	-4.45614900	-4.95220300	0.78737000
C	-2.76878300	-6.93843400	1.89501600
Cl	-5.50046500	-3.70274600	0.10347400
C	-4.92560100	-5.80195200	1.80555400
C	-4.08892200	-6.78561200	2.35531100
Cl	-1.71113100	-8.17518200	2.58371600
Cl	-6.58235600	-5.62622800	2.39489800
Cl	-4.69540700	-7.84176100	3.63599200
H	0.86404900	-5.04288800	-1.24394900
H	-3.97130900	-0.57230000	-1.52637100
H	0.40868400	4.03097600	-1.52643000
H	5.18972600	-0.44430500	-1.33115000
Cl	7.33510100	4.59902800	3.01540500
N	4.95170600	-2.28740900	-0.48358800
C	1.77086100	4.09197300	-3.20780000
H	1.00817700	3.83322700	-3.94497800
H	1.87373000	5.18103100	-3.17320400
H	2.71863500	3.64791000	-3.52434900
C	-3.96303300	0.85904500	-3.15317800
H	-3.77366000	0.11103900	-3.92621600
H	-5.04073500	1.03885700	-3.09030800
H	-3.45881400	1.78531900	-3.43805100
C	-0.29541100	-5.23633400	-3.06209400
H	0.54030200	-4.99838700	-3.72346500
H	-0.37744200	-6.32436200	-2.97462900
H	-1.21022400	-4.83821100	-3.50878700
C	5.26746900	-1.91234100	-2.92193600
H	5.08687300	-1.18719000	-3.71820300
H	6.34632500	-2.06566700	-2.81994700
H	4.79347700	-2.85620700	-3.20156200
C	0.43955100	-0.37899100	1.53574600
C	1.44464000	-0.06787900	2.50475000
C	2.75630100	0.31817900	2.11137600
C	1.17358200	-0.16124300	3.90161800
C	3.74387800	0.57164900	3.05284900
H	2.98527700	0.40950500	1.05865200
C	2.15355300	0.08610900	4.84633700
H	0.18109600	-0.44089600	4.23865400
C	3.43719000	0.45043500	4.41362800
H	4.74348000	0.84787100	2.73656000
H	1.93695200	0.00389000	5.90532800
Br	4.78931600	0.79127400	5.71357600
C	-0.95195600	-0.50626200	2.04732200
O	-1.62143700	0.48921500	2.25915600
O	-1.36651700	-1.76496300	2.21558500
C	-2.74079000	-1.91700000	2.64282900
H	-2.85667200	-2.98026100	2.84915000
H	-2.92858900	-1.32858300	3.54396500
H	-3.42101000	-1.59874200	1.85060300

3-1

-4078.246099

Rh	0.77204800	-0.76423300	-3.09437700
O	0.98511900	1.28739400	-3.01372500
O	0.51976000	-2.81386000	-2.94663000
O	1.03038200	1.30474500	-0.73977400
O	0.50601800	-2.76419300	-0.67161200
O	2.82737800	-1.07189100	-3.04706800
O	-1.26410700	-0.43246700	-2.98350800
O	-1.23646800	-0.55589000	-0.71628100
O	2.82496100	-0.95751700	-0.78171800
C	-1.78925500	-0.33050400	-1.84659800
C	3.36783000	-1.17252700	-1.92037500
C	1.06181600	1.85229600	-1.89105300
C	0.35763100	-3.32464600	-1.80922200
Rh	0.80092000	-0.73609300	-0.61737400
C	4.84139700	-1.62031200	-1.82537100
C	4.07581400	-3.27913100	-0.13840300
C	5.41799600	-1.52492100	0.59059300
O	3.46603300	-3.98929500	-0.90672100
C	3.98526300	-3.21589200	1.35534100
O	6.08670300	-0.51690200	0.53788900
C	4.81421300	-2.18122300	1.79530300
C	3.19304500	-3.93033200	2.23873900
C	4.88999200	-1.84173800	3.13517200
Cl	2.16041900	-5.24143500	1.67210500
C	3.21580000	-3.55613300	3.59492500
C	4.05414800	-2.52000700	4.03938600
Cl	6.00702300	-0.58744000	3.69264400
Cl	2.17635100	-4.40024500	4.75298000
Cl	4.04777100	-2.04481400	5.74552500
C	1.14330400	3.38374100	-1.87949700
N	2.14417000	3.80795000	-0.90151000
C	3.42342800	3.25990400	-0.81434800
C	1.91523600	4.81673200	0.03966300
O	3.84605600	2.35021800	-1.49744600
C	4.10436100	4.00902200	0.29631600
O	0.89769900	5.46421400	0.14158900
C	3.18427000	4.91014500	0.83833200
C	5.38011500	3.88600900	0.81863100
C	3.50509700	5.69180900	1.93462800
Cl	6.51717500	2.71551500	0.14331100
C	5.72550100	4.67733200	1.92979400
C	4.79359100	5.56832000	2.48681300
Cl	2.31483000	6.79482200	2.63455300
Cl	5.23385500	6.53247600	3.90201400
C	-3.26109900	0.11231800	-1.75646300
N	-3.45209800	0.73160400	-0.44102200
C	-2.58621800	1.74358900	0.00693000
C	-4.00208800	0.00933200	0.62626600
O	-1.90372300	2.43973900	-0.71373800
C	-2.66282300	1.71545300	1.50364200
O	-4.66663800	-0.99769700	0.51992400
C	-3.54903700	0.70196000	1.87249100
C	-1.92702900	2.40338200	2.45305300
C	-3.74522300	0.36031900	3.19780700

Cl	-0.77349700	3.65136800	1.97006400
C	-2.10084600	2.05490700	3.80360900
C	-3.00571300	1.04693800	4.17472000
Cl	-4.82742400	-0.96982000	3.63793200
Cl	-1.14563900	2.88641300	5.04802500
Cl	-3.18294800	0.60460600	5.88140600
C	-0.12202200	-4.78244600	-1.71717500
N	-1.43377300	-4.76066300	-1.05348500
C	-2.52521100	-4.02045200	-1.52705100
C	-1.66080600	-5.29376100	0.22043500
O	-2.53965600	-3.36441200	-2.54611100
C	-3.59934600	-4.17527500	-0.49389700
O	-0.86752500	-5.94751100	0.86209100
C	-3.06246700	-4.88742000	0.58299500
C	-4.90472800	-3.71934900	-0.47791800
C	-3.80807800	-5.10834900	1.72810800
Cl	-5.61155600	-2.95673800	-1.90796700
C	-5.66118500	-3.90146300	0.69335100
C	-5.10953100	-4.57685700	1.79383800
Cl	-3.13566000	-6.03148400	3.08417300
Cl	-7.30569700	-3.26916200	0.77900500
Cl	-6.05661000	-4.76653900	3.27664000
H	0.54541000	-5.29249000	-1.01749300
H	-3.86544700	-0.79947100	-1.74672600
H	0.18216600	3.72709100	-1.48123800
H	5.44910900	-0.71059200	-1.76597900
Cl	7.33478000	4.52072900	2.64484100
N	4.99252400	-2.27687400	-0.51743100
C	1.41168400	3.99005300	-3.25606600
H	0.63148700	3.68244200	-3.95562700
H	1.41534200	5.08177400	-3.18113800
H	2.37452100	3.64706100	-3.64413400
C	-3.69122000	1.00963600	-2.91527300
H	-3.53632600	0.47954300	-3.85749300
H	-4.75144900	1.25893900	-2.81275500
H	-3.10336600	1.92964800	-2.92735500
C	-0.16934500	-5.49862600	-3.06300700
H	0.83063800	-5.50847200	-3.50482300
H	-0.50572700	-6.53051500	-2.92261000
H	-0.84274300	-4.98120300	-3.74873500
C	5.28807200	-2.48706400	-2.99938600
H	5.15568200	-1.93023900	-3.92992400
H	6.34394200	-2.74876200	-2.88425000
H	4.69261400	-3.40037700	-3.04943400
C	0.82088200	-0.65640300	1.37810400
C	1.62893100	0.17919200	2.20372300
C	2.82386300	0.76262600	1.69969700
C	1.28533800	0.42085200	3.56589200
C	3.65455800	1.49576400	2.52993300
H	3.11238300	0.59188700	0.67190400
C	2.07468100	1.21773500	4.37506100
H	0.36428900	0.01115100	3.96661500
C	3.26545100	1.74237400	3.85158400
H	4.60531800	1.85557900	2.16461600
H	1.78404800	1.42772200	5.39731900
Br	4.38295000	2.81668300	4.95856200
C	-0.21166100	-1.46091300	2.06621000
O	-1.32001200	-1.00876800	2.29505600
O	0.20705600	-2.68215800	2.39053900
C	-0.76880800	-3.53050000	3.04425700
H	-0.41093900	-4.54609100	2.90798200
H	-0.82453200	-3.27004100	4.10418800
H	-1.74655600	-3.39230000	2.58396700

3-2

-4078.444842

Rh	0.76816200	-0.75819000	-3.09505500
O	0.98730500	1.28891300	-3.01993800
O	0.51305100	-2.80535200	-2.95174900
O	1.03400300	1.30677000	-0.74798700
O	0.48717100	-2.75425300	-0.67920900
O	2.81876900	-1.07266800	-3.04840100
O	-1.26488000	-0.41891300	-2.99213600
O	-1.23963500	-0.54010000	-0.72698200
O	2.81585400	-0.95759300	-0.78489200
C	-1.79197200	-0.31617600	-1.85669700
C	3.35954900	-1.17306600	-1.92244500
C	1.06767000	1.85435300	-1.89852600
C	0.34588800	-3.31666200	-1.81606700
Rh	0.79322400	-0.73086600	-0.62576100
C	4.83089500	-1.62054900	-1.82787300
C	4.05938700	-3.25365900	-0.12065600
C	5.41365200	-1.49573900	0.57949900
O	3.44917800	-3.97605100	-0.87640600
C	3.96918700	-3.16390700	1.37141100
O	6.08998900	-0.49439900	0.50884000
C	4.80550400	-2.12686700	1.79408800
C	3.17936500	-3.86178100	2.26904300
C	4.88626500	-1.76981400	3.12817500
Cl	2.15016200	-5.18421300	1.73381300
C	3.20607500	-3.46539200	3.61725900
C	4.04745800	-2.42667100	4.04250800
Cl	6.01759400	-0.52733900	3.67147900
Cl	2.17426700	-4.28838400	4.79010400
Cl	4.04741100	-1.92608400	5.73673700
C	1.15791100	3.38352000	-1.88764600
N	2.16067600	3.79740200	-0.91054900
C	3.44054700	3.24909300	-0.83601900
C	1.92686200	4.77932400	0.05733900
O	3.86183700	2.35156200	-1.53529900
C	4.12112600	3.97718100	0.28791000
O	0.90650400	5.41859200	0.17714900
C	3.19548400	4.85744100	0.85652900
C	5.39861600	3.85200700	0.80385600
C	3.51478100	5.61045800	1.97214700
Cl	6.54732800	2.71638100	0.10001600
C	5.74106400	4.61795700	1.93174200
C	4.80564800	5.48516700	2.51386200
Cl	2.32323300	6.67932000	2.71296200
Cl	5.24400000	6.41691700	3.94547900
C	-3.26220900	0.12536200	-1.76627100
N	-3.44937900	0.74512800	-0.45254500
C	-2.57550500	1.74896800	-0.00114600
C	-4.00507900	0.02272000	0.61150100
O	-1.89369800	2.44776800	-0.71901300
C	-2.64942900	1.71259300	1.49505100
O	-4.67773800	-0.97782200	0.50045100
C	-3.54560000	0.70515700	1.85974200
C	-1.90361900	2.38276800	2.44839300
C	-3.73965800	0.35643900	3.18255900
Cl	-0.73198400	3.61434500	1.97946500
C	-2.08080900	2.02933600	3.79560700
C	-2.99344200	1.02960700	4.16124500
Cl	-4.82241000	-0.96998000	3.62038800
Cl	-1.12095500	2.84338600	5.04114200
Cl	-3.16986500	0.57797600	5.86094000
C	-0.12869200	-4.77418100	-1.72435400
N	-1.43781200	-4.75505400	-1.06001400
C	-2.52883600	-4.01067000	-1.52752700
C	-1.65738300	-5.28606300	0.21639400
O	-2.54822000	-3.35650800	-2.54733500
C	-3.59608300	-4.16068600	-0.48767800
O	-0.85933700	-5.93727300	0.85422900
C	-3.05657700	-4.87894000	0.58534500
C	-4.89910000	-3.70031600	-0.46313200
C	-3.80092900	-5.10259800	1.72999300
Cl	-5.61621800	-2.93582100	-1.88262000
C	-5.64947500	-3.88203400	0.71020300
C	-5.09731700	-4.56403000	1.80327100
Cl	-3.14208700	-6.04186000	3.07730600
Cl	-7.28608900	-3.24376600	0.80676300
Cl	-6.03733300	-4.75434100	3.28514000
H	0.53765100	-5.28324700	-1.02352000
H	-3.86817500	-0.78515900	-1.75015400
H	0.20152600	3.73612500	-1.48718200
H	5.44138400	-0.71251900	-1.77510100
Cl	7.34918100	4.45649500	2.63674700
N	4.98249100	-2.26316700	-0.51550400
C	1.42738700	3.98958500	-3.26242200
H	0.64132600	3.69245000	-3.95957800
H	1.44080000	5.08077500	-3.18440000
H	2.38505900	3.64079900	-3.65695800
C	-3.69702700	1.01748400	-2.92523400
H	-3.55202200	0.48252700	-3.86600800
H	-4.75564000	1.26966400	-2.81588800
H	-3.10825600	1.93639800	-2.94822000
C	-0.17282200	-5.49402800	-3.06672700
H	0.82860600	-5.50931300	-3.50462600
H	-0.51086500	-6.52456400	-2.92218300
H	-0.84261900	-4.98137600	-3.75899000
C	5.27632000	-2.49596100	-2.99400400
H	5.15227400	-1.94425000	-3.92843800
H	6.33020500	-2.76180600	-2.87264100
H	4.67793400	-3.40715500	-3.04279500
C	0.80439500	-0.66768100	1.36780300
C	1.62217600	0.15114600	2.19654400
C	2.79969300	0.75829400	1.68263600
C	1.30283400	0.35453200	3.56952500
C	3.63225500	1.49043100	2.51061800
H	3.06868500	0.60407100	0.64764800
C	2.09696300	1.14223400	4.38127100
H	0.39825100	-0.08156700	3.97877700
C	3.26486800	1.70057500	3.84411600
H	4.56881400	1.87621800	2.13719900
H	1.82909200	1.32014100	5.41530600
Br	4.38276800	2.76620700	4.95294600
C	-0.23596000	-1.46343400	2.05208100
O	-1.35209100	-1.01674300	2.24756200
O	0.18247600	-2.67313700	2.41775100
C	-0.80348400	-3.50483900	3.07352100
H	-0.46157500	-4.52589500	2.94025800
H	-0.85128300	-3.24062000	4.13253600
H	-1.77851700	-3.34881300	2.61507000

3'

-5478.773259

Rh	0.78141900	-0.68307800	-2.94469100
O	1.17936200	1.34005900	-2.94354100
O	0.38054500	-2.69687500	-2.79349000
O	1.17161400	1.43710700	-0.68207700
O	0.15843300	-2.58031200	-0.54180800
O	2.79707300	-1.09600500	-2.74671100
O	-1.24274600	-0.26045900	-2.99107700
O	-1.33636300	-0.10642900	-0.73372000
O	2.66100200	-1.09762500	-0.48746000
C	-1.84404600	-0.05664200	-1.90442300
C	3.28578900	-1.22396600	-1.59520300
C	1.29678600	1.94601900	-1.84576200
C	0.15612000	-3.19651200	-1.65916700
Rh	0.65008800	-0.56543900	-0.48847600
C	4.79999300	-1.49107700	-1.43152200
C	4.25921000	-3.64507600	-0.17992200
C	5.72448600	-2.13778400	0.81117100
O	3.46115400	-4.09353600	-0.97439600
C	4.68145400	-4.21039500	1.14718400
O	6.34724000	-1.11190300	0.98295100
C	5.56726200	-3.30575700	1.73932000
C	4.33313200	-5.39164100	1.78200100
C	6.12801600	-3.55723000	2.98024800
Cl	3.20168200	-6.52522800	1.04329100
C	4.89776500	-5.66195500	3.04204500
C	5.78797900	-4.75359800	3.63545100
Cl	7.24506100	-2.40688700	3.72485400
Cl	4.48036700	-7.15872700	3.88233500
Cl	6.48787700	-5.11160100	5.21820500
C	1.54275100	3.47285800	-1.86312100
N	2.52614900	3.80261800	-0.81906000
C	3.71345100	3.11124900	-0.57511000
C	2.29369900	4.81679800	0.12484400
O	4.11642000	2.14760400	-1.19403200
C	4.35362400	3.80242800	0.59878000
O	1.31239000	5.52221400	0.17290900
C	3.49990700	4.82637600	1.01759200
C	5.56163800	3.57536200	1.23735500
C	3.82862000	5.64680100	2.08398200
Cl	6.63131700	2.26572300	0.72328800
C	5.91347900	4.40371800	2.31796400
C	5.05402600	5.43021300	2.73850000
Cl	2.74144500	6.93547400	2.61047800
Cl	5.51183200	6.45936400	4.09990500
C	-3.36225700	0.22423700	-1.89882300
N	-3.62681700	1.23369400	-0.86202900

C	-2.91692500	2.43039600	-0.70093500
C	-4.43576100	0.95025100	0.24506800
O	-2.06091600	2.84799500	-1.45123300
C	-3.43526600	3.04242300	0.56942200
O	-5.05396500	-0.07955300	0.41560100
C	-4.35146200	2.15254200	1.13482900
C	-3.13691700	4.24794300	1.18234500
C	-4.99218900	2.44282800	2.32645300
Cl	-1.96029900	5.35901200	0.48102400
C	-3.78410700	4.55818200	2.39179500
C	-4.70441800	3.66394200	2.95880600
Cl	-6.14599000	1.30676800	3.04120700
Cl	-3.43238600	6.08940300	3.20290800
Cl	-5.50918600	4.07215500	4.48008900
C	-0.09085500	-4.71856100	-1.53742300
N	-1.28631500	-4.92732600	-0.70456500
C	-2.50795400	-4.26995000	-0.86465200
C	-1.26176300	-5.73887600	0.43981400
O	-2.75724000	-3.42900800	-1.70236900
C	-3.40533300	-4.80994500	0.21556000
O	-0.30304400	-6.35491200	0.84663400
C	-2.64947700	-5.67497500	1.01205900
C	-4.74643200	-4.58252100	0.47890000
C	-3.20848200	-6.31864800	2.10368700
Cl	-5.71089700	-3.51613900	-0.54584900
C	-5.32967300	-5.23233000	1.58199700
C	-4.56604900	-6.08906900	2.39010000
Cl	-2.24599300	-7.40535900	3.11147100
Cl	-7.03756900	-4.96784300	1.94939900
Cl	-5.31472500	-6.89280900	3.77489000
H	0.73210000	-5.07456200	-0.90649000
H	-3.80170800	-0.69163500	-1.48343400
H	0.60477000	3.89988000	-1.48577700
H	5.19355900	-0.55262100	-1.02021300
Cl	7.45083800	4.14654900	3.15097400
N	4.97537400	-2.45179900	-0.33009800
C	0.44980200	-0.37753200	1.51963800
C	1.42835200	-0.03981400	2.50742700
C	2.77695500	0.23258100	2.14514200
C	1.09663700	0.00365400	3.89403700
C	3.74251300	0.49888700	3.10538500
H	3.05248500	0.21654900	1.10006700
C	2.05170300	0.27447500	4.85768900
H	0.07463500	-0.17804000	4.20880100
C	3.37396200	0.51631100	4.45597300
H	4.77115600	0.67631400	2.81193300
H	1.78709200	0.30063700	5.90860500
Br	4.69302300	0.88088000	5.78270200
C	-0.95834200	-0.46239400	1.99598900
O	-1.62031400	0.54685400	2.16050600
O	-1.39378400	-1.70998500	2.19549100
C	-2.77216100	-1.82853600	2.61854600
H	-2.91026800	-2.88627300	2.83933900
H	-2.95095500	-1.22469100	3.51147100
H	-3.44402600	-1.50474900	1.82121100
C	1.95378400	4.14913200	-6.21400400
H	1.75262900	3.08869900	-6.41945000
H	2.09688600	4.64262600	-7.18554300
C	3.22772700	4.29066900	-5.35611200
H	4.07909200	3.84073800	-5.88393000
C	0.75944000	4.77996200	-5.46874000
H	-0.15124800	4.67309000	-6.07272700
C	0.55170000	4.05021600	-4.12577600
H	0.30773300	3.00085800	-4.30785400
H	-0.30059000	4.49094000	-3.58960100
C	3.03501800	3.55710700	-4.01032900
H	3.94828500	3.65157300	-3.40911900
H	2.87702200	2.48921300	-4.18398400
C	1.82740200	4.15464700	-3.24238300
C	2.10793600	5.66651800	-3.00919400
H	1.27935200	6.12080100	-2.45165400
H	3.01141900	5.79113200	-2.39745900
C	3.50806100	5.78416400	-5.09857500
H	3.67290600	6.31057300	-6.04891900
H	4.42664200	5.89944300	-4.50578200
C	1.04081800	6.27210700	-5.21085100
H	1.17218600	6.80667000	-6.16194200
H	0.18647300	6.73477000	-4.69768200
C	2.31149100	6.40328900	-4.34930700
H	2.51129700	7.46299500	-4.14161800
C	-3.49490700	1.64191400	-4.09398500
H	-2.43881500	1.44988200	-4.30647900
H	-3.54017600	2.57810500	-3.52543700
C	-4.08500400	0.47791800	-3.25783000
C	-4.28158600	1.80230100	-5.41363700
H	-3.83996800	2.62649000	-5.98942900
C	-4.20079800	0.49767300	-6.23164100
H	-3.15411500	0.26890500	-6.47522400
H	-4.73365800	0.61589700	-7.18563900
C	-4.03542400	-0.82935200	-4.09918700
H	-4.46139200	-1.65786800	-3.51629400
H	-2.99691000	-1.09310000	-4.31548400
C	-4.81857100	-0.65686500	-5.41678800
H	-4.75433700	-1.59074600	-5.99069800
C	-6.29355600	-0.33848400	-5.10536600
H	-6.86649500	-0.23075900	-6.03695000
H	-6.74821800	-1.16624400	-4.54343800
C	-5.57929000	0.79531900	-2.96983000
H	-5.65977000	1.71973600	-2.38291500
H	-6.02255800	-0.00698800	-2.36429700
C	-5.75750000	2.12104400	-5.10206700
H	-5.83005400	3.06165100	-4.53796500
H	-6.32170400	2.26304200	-6.03428300
C	-6.36742000	0.96404000	-4.28508800
H	-7.41430000	1.19182400	-4.04365300
C	-1.10352400	-5.16807500	-3.91046800
H	-0.95089900	-4.12340100	-4.19453100
H	-2.11882700	-5.24208200	-3.50172600
C	-0.06349900	-5.58330600	-2.83812500
C	-0.98580000	-6.08158100	-5.15063200
H	-1.72389000	-5.75903300	-5.89693100
C	0.43276900	-5.97367800	-5.74536900
H	0.63513200	-4.93857900	-6.05321500
H	0.51286100	-6.59825100	-6.64617300
C	1.36338200	-5.51356300	-3.45225100
H	2.10235400	-5.81960400	-2.69955800
H	1.59999400	-4.48293900	-3.72908900
C	1.46551300	-6.42419600	-4.69263200
H	2.47826400	-6.34125600	-5.10900200
C	1.18838800	-7.88477300	-4.28825400
H	1.27616700	-8.54649100	-5.16127300
H	1.93341600	-8.22180300	-3.55416800
C	-0.33501800	-7.06637900	-2.45457400
H	-1.34076300	-7.16371900	-2.02423400
H	0.37455900	-7.39079100	-1.68213400
C	-1.26248100	-7.54338600	-4.74666400
H	-2.28027800	-7.63760100	-4.34232600
H	-1.20571500	-8.19931500	-5.62638200
C	-0.22856200	-7.98295700	-3.69086700
H	-0.43017700	-9.01741000	-3.38189100
C	5.14685500	-3.01501200	-3.52793900
H	4.11177400	-2.85082800	-3.84166200
H	5.15256400	-3.92051200	-2.90952200
C	5.64864000	-1.80197400	-2.70428700
C	6.04890700	-3.22961900	-4.76378500
H	5.66794300	-4.08705800	-5.33415700
C	6.02769200	-1.96754300	-5.64906800
H	5.00417900	-1.76553100	-5.99353600
H	6.64315200	-2.12515900	-6.54569200
C	5.66328600	-0.53822200	-3.61017300
H	6.03053500	0.32200400	-3.03250400
H	4.64667000	-0.29796800	-3.93135600
C	6.56179300	-0.76571400	-4.84324500
H	6.53984800	0.13707900	-5.46785300
C	8.00612100	-1.04813800	-4.38836000
H	8.65881800	-1.19572800	-5.25998400
H	8.40339100	-0.18749300	-3.83241000
C	7.11449700	-2.08280600	-2.26927200
H	7.15040000	-2.97526600	-1.63033300
H	7.49498700	-1.24513600	-1.66907400
C	7.49450100	-3.51119200	-4.30820000
H	7.52775600	-4.42257100	-3.69471900
H	8.14003900	-3.68914400	-5.17943800
C	8.01856900	-2.30697900	-3.50024600
H	9.04156600	-2.50827700	-3.15533500

3-1'

-5479.205074

Rh	0.85156600	-0.72426700	-3.11399800
O	1.05333700	1.33090300	-3.05143800
O	0.59599400	-2.76955300	-2.94322600
O	0.99802200	1.36358600	-0.78362500
O	0.41844800	-2.67904400	-0.68139300
O	2.89254500	-1.03897400	-2.91861100
O	-1.17893100	-0.38900200	-3.15499400
O	-1.30549600	-0.48674200	-0.89454200
O	2.74169600	-0.86178800	-0.66799900
C	-1.79024000	-0.28854400	-2.06213500
C	3.36918600	-1.09386100	-1.76073900
C	1.10901800	1.90499000	-1.93423400
C	0.37931200	-3.27294700	-1.81126800
Rh	0.71475500	-0.65669400	-0.64613700
C	4.84807900	-1.45169600	-1.51273100
C	3.93218700	-3.13327300	0.12513000
C	5.22083500	-1.38438700	0.93937500
O	3.34841600	-3.83619500	-0.66843200
C	3.76242500	-3.08574900	1.61130900
O	5.86317900	-0.35692300	0.93769700
C	4.55939700	-2.05230700	2.10422300
C	2.92783600	-3.81345700	2.44350000
C	4.55913300	-1.72157600	3.44832400
Cl	1.94527000	-5.13411300	1.81311300
C	2.86983400	-3.44685800	3.80053900
C	3.67700900	-2.41007300	4.29910000
Cl	5.64046800	-0.46868100	4.07400300
Cl	1.76554400	-4.29989300	4.89024400
Cl	3.57587800	-1.95072600	6.00652200
C	1.32752300	3.42465800	-1.84421800
N	2.57209600	3.62793900	-1.08367400
C	3.74052000	2.88074400	-1.25685300
C	2.62859200	4.45138100	0.05025100
O	3.90595600	1.99386200	-2.06753300
C	4.69131200	3.36174100	-0.20118200
O	1.72622700	5.14371800	0.46315200
C	4.01247100	4.27592200	0.60842400
C	6.00612200	3.00969900	0.05193800
C	4.61909300	4.84025700	1.71735300
Cl	6.89404800	1.96313700	-1.06111800
C	6.62873800	3.54969000	1.19397900
C	5.94018000	4.45699000	2.01917800
Cl	3.74842500	5.99603200	2.73023000
Cl	6.74303200	5.13721600	3.44053000
C	-3.28616000	0.07294500	-2.04094700
N	-3.50724800	0.81859900	-0.78807200
C	-2.60948200	1.80333700	-0.33623500
C	-4.15642700	0.18654700	0.28439200
O	-1.85374400	2.43990300	-1.03819600
C	-2.75830700	1.84751400	1.15258100
O	-4.86524500	-0.79195500	0.19153700
C	-3.72719900	0.91268100	1.52009100
C	-2.02154800	2.53182400	2.10461400
C	-4.01148800	0.65248300	2.84792100
Cl	-0.73672000	3.65115300	1.63255800
C	-2.29130100	2.26916600	3.45925400
C	-3.28054000	1.34303300	3.82852400
Cl	-5.20449500	-0.57687100	3.29296800
Cl	-1.35444300	3.10574300	4.71356200
Cl	-3.58052000	1.00885300	5.54327200
C	-0.00278900	-4.75521200	-1.66702600
N	-1.38998500	-4.78236500	-1.16096300
C	-2.45018900	-4.01506000	-1.66795300
C	-1.69311000	-5.32941800	0.09455700
O	-2.41404800	-3.31628500	-2.65685600
C	-3.58183500	-4.18810700	-0.69766500
O	-0.93714500	-5.98873100	0.77449700
C	-3.10611400	-4.91965700	0.39308200
C	-4.88476200	-3.72189700	-0.73577800
C	-3.90395100	-5.14386000	1.50234000
Cl	-5.53611100	-2.97410400	-2.19884900
C	-5.69356300	-3.90168800	0.40052500
C	-5.19937500	-4.59525400	1.51801300
Cl	-3.29840300	-6.08257000	2.87828400
Cl	-7.33563100	-3.25814200	0.41669000

Cl	-6.21393400	-4.78957900	2.95410700
H	0.59276000	-5.10948600	-0.82087600
H	-3.79811200	-0.87980700	-1.87436500
H	0.53414200	3.77593100	-1.17646200
H	5.33835300	-0.49115500	-1.31638400
Cl	8.28900700	3.08724600	1.58246600
N	4.87458000	-2.13400900	-0.19905200
C	0.61712100	-0.55725500	1.34424800
C	1.39364800	0.26291300	2.21457800
C	2.58775300	0.89022000	1.76124100
C	1.01548000	0.45175100	3.57578100
C	3.37642000	1.62479700	2.62922900
H	2.90794800	0.74336900	0.74027200
C	1.76967400	1.23527300	4.43011800
H	0.09652300	0.00724400	3.94318900
C	2.95418300	1.81350900	3.95122400
H	4.32146000	2.03221200	2.29684500
H	1.45600700	1.39757800	5.45419000
Br	4.02077900	2.86930700	5.11970100
C	-0.45861900	-1.35470000	1.97420700
O	-1.57958200	-0.90361600	2.13005200
O	-0.05854700	-2.57447700	2.33351700
C	-1.06807500	-3.42400300	2.92987800
H	-0.70126000	-4.43974500	2.81643400
H	-1.18300000	-3.16553300	3.98556900
H	-2.01936100	-3.28761800	2.41594600
C	0.77221300	4.50473600	-6.06484900
H	0.66455100	3.44651000	-6.33935800
H	0.65570300	5.09298200	-6.98539900
C	2.16706300	4.75241300	-5.45412900
H	2.94184600	4.47474300	-6.18047000
C	-0.31513900	4.89657800	-5.04360600
H	-1.30909000	4.71481400	-5.47348900
C	-0.15479900	4.03207300	-3.77925400
H	-0.28442300	2.97911800	-4.03689700
H	-0.93223900	4.28103600	-3.04442100
C	2.33866800	3.88949300	-4.18640100
H	3.33305500	4.06574000	-3.75545100
H	2.28191400	2.82710800	-4.43501500
C	1.24644100	4.24916600	-3.15046800
C	1.38721100	5.75437600	-2.79780200
H	0.64059400	6.03289400	-2.04283300
H	2.37358700	5.94193100	-2.35270000
C	2.30802900	6.24351100	-5.08898900
H	2.20755600	6.86565900	-5.98891100
H	3.30659000	6.43706100	-4.67262100
C	-0.17044600	6.38511300	-4.67483700
H	-0.30049300	7.01325700	-5.56680600
H	-0.95279700	6.67341000	-3.95929900
C	1.22313100	6.62346700	-4.06098600
H	1.32974800	7.68003200	-3.78241100
C	-3.22046200	1.98725400	-3.79213600
H	-2.16920500	1.77533900	-4.00683300
H	-3.23710200	2.74088400	-2.99869800
C	-3.91918600	0.69536400	-3.31007600
C	-3.92586800	2.53641100	-5.04868000
H	-3.41018500	3.45009000	-5.37346300
C	-3.87940700	1.48520500	-6.17453600
H	-2.83603000	1.25583200	-6.43113800
H	-4.35768700	1.88099100	-7.08124600
C	-3.89089900	-0.35144100	-4.45874000
H	-4.38074100	-1.27585500	-4.12970100
H	-2.85750300	-0.60961100	-4.69988900
C	-4.60036900	0.20412500	-5.70809900
H	-4.56093300	-0.55178300	-6.50320800
C	-6.06867600	0.52729400	-5.37091600
H	-6.58987200	0.90615900	-6.26087900
H	-6.59110600	-0.38610900	-5.05383900
C	-5.40217700	1.02329500	-2.99349800
H	-5.45071300	1.76259300	-2.18389600
H	-5.91470500	0.12087100	-2.63323200
C	-5.39515300	2.86200000	-4.71179200
H	-5.43935800	3.62618900	-3.92331900
H	-5.90339900	3.27726400	-5.59298700
C	-6.11173600	1.57830400	-4.24432000
H	-7.15495700	1.80809000	-3.99056600
C	-0.53005500	-5.39231500	-4.13140600
H	-0.34529600	-4.36456800	-4.45248900
H	-1.60282500	-5.47174000	-3.91689800
C	0.28507300	-5.69982100	-2.85299400
C	-0.15190000	-6.38822600	-5.24791300
H	-0.73228400	-6.14907400	-6.14841000
C	1.35489400	-6.27290500	-5.55808500
H	1.59185800	-5.25531300	-5.89750000
H	1.62535900	-6.95834400	-6.37311800
C	1.80175400	-5.61268800	-3.17587600
H	2.38671900	-5.82209500	-2.27032500
H	2.05710100	-4.59680000	-3.48843400
C	2.16909000	-6.60758800	-4.29219900
H	3.24257900	-6.51864100	-4.50728300
C	1.84549300	-8.04253200	-3.83279000
H	2.11961400	-8.76313600	-4.61549900
H	2.43463800	-8.29435100	-2.94017600
C	-0.03037400	-7.15170500	-2.40647100
H	-1.09879300	-7.24248000	-2.16750800
H	0.52136600	-7.38731300	-1.48629100
C	-0.47265400	-7.82521500	-4.79039500
H	-1.54801300	-7.92413400	-4.58667800
H	-0.22809300	-8.54117700	-5.58709500
C	0.33903600	-8.15133100	-3.52079100
H	0.10406800	-9.16847800	-3.18085100
C	4.95590300	-3.39066800	-3.24361300
H	3.95974600	-3.13191000	-3.61469100
H	4.81715200	-4.14148100	-2.46127700
C	5.63884900	-2.13268900	-2.65553900
C	5.81412100	-3.97843100	-4.38105700
H	5.30598200	-4.86444600	-4.78525600
C	5.99313900	-2.92936400	-5.49544600
H	5.01395200	-2.64722300	-5.90578300
H	6.58249300	-3.35067700	-6.32140300
C	5.84325700	-1.08861300	-3.78916300
H	6.33299700	-0.19383400	-3.37878800
H	4.87292800	-0.77163700	-4.18062900
C	6.70190800	-1.68594800	-4.92035300
H	6.82581800	-0.93245500	-5.70892800
C	8.08161300	-2.08826600	-4.36390200
H	8.70860000	-2.50159100	-5.16578100
H	8.60210800	-1.20387300	-3.97070100
C	7.03527500	-2.53588600	-2.11601400
H	6.92034800	-3.27082300	-1.30917600
H	7.53332700	-1.65803600	-1.67955200
C	7.19415800	-4.38051300	-3.82346300
H	7.07660100	-5.14345700	-3.04145700
H	7.81076900	-4.82422300	-4.61716300
C	7.89707600	-3.13412800	-3.24678600
H	8.87600200	-3.41650400	-2.83770000

3-2'

-5479.501261

Rh	0.84391300	-0.71984800	-3.11549900
O	1.02448400	1.33494700	-3.06633000
O	0.61494800	-2.76580300	-2.94166400
O	0.98794700	1.37300000	-0.80042200
O	0.42316300	-2.66828000	-0.68365400
O	2.88684200	-1.00694500	-2.92809100
O	-1.18942500	-0.40893700	-3.15681300
O	-1.30608000	-0.48041900	-0.89730100
O	2.73801000	-0.84274100	-0.67828200
C	-1.79773400	-0.29820300	-2.06342700
C	3.36725200	-1.06118200	-1.77208200
C	1.08639300	1.91320600	-1.95197200
C	0.39689800	-3.26830300	-1.81012200
Rh	0.71214400	-0.64664500	-0.65561300
C	4.84927600	-1.39966800	-1.53104700
C	3.96042000	-3.06050500	0.13837900
C	5.23839900	-1.28370900	0.91077500
O	3.38889700	-3.79262600	-0.63663300
C	3.79175400	-2.97884700	1.62254200
O	5.87383000	-0.25268600	0.88333800
C	4.58563400	-1.93065800	2.09105900
C	2.96910200	-3.69583300	2.47445100
C	4.59136100	-1.57721600	3.42840700
Cl	1.99990100	-5.03979500	1.88282100
C	2.91548500	-3.30212300	3.82247100
C	3.71644000	-2.25134100	4.29496000
Cl	5.67682600	-0.32235000	4.03230400
Cl	1.83220400	-4.14277600	4.93488400
Cl	3.62189900	-1.76027300	5.98922000
C	1.29084100	3.43303100	-1.86974800
N	2.52257900	3.65389200	-1.09949800
C	3.70463000	2.92736900	-1.26629600
C	2.55269000	4.46972500	0.04095000
O	3.88833700	2.04102800	-2.07320100
C	4.64047800	3.42756000	-0.20701400
O	1.63169700	5.13633100	0.45422200
C	3.93666900	4.32267400	0.60446100
C	5.96195700	3.10803400	0.05057700
C	4.52660700	4.89532700	1.71709800
Cl	6.88420200	2.09238400	-1.05707700
C	6.56613300	3.65850200	1.19565300
C	5.85425400	4.54387600	2.02069400
Cl	3.63197600	6.02212300	2.73584300
Cl	6.63509000	5.23767300	3.44205200
C	-3.29295200	0.05830400	-2.04011400
N	-3.51667500	0.79513900	-0.78542800
C	-2.62337600	1.78055000	-0.32581100
C	-4.16110700	0.14944000	0.28133500
O	-1.87753900	2.43269600	-1.02301500
C	-2.76957300	1.80818900	1.16339200
O	-4.86416500	-0.83162200	0.17887400
C	-3.73478700	0.86501300	1.52266400
C	-2.03304700	2.48051600	2.12311300
C	-4.01246700	0.58740500	2.84743600
Cl	-0.74770200	3.60168400	1.67028700
C	-2.30231500	2.20388300	3.47348500
C	-3.28512200	1.27070900	3.83334200
Cl	-5.18615700	-0.65866400	3.28561200
Cl	-1.37387100	3.03184800	4.73318300
Cl	-3.57880500	0.91582800	5.54026200
C	0.03082300	-4.75217400	-1.66128300
N	-1.35037500	-4.79154800	-1.14795200
C	-2.41853400	-4.03418000	-1.65248100
C	-1.63688600	-5.32609000	0.11721700
O	-2.39433600	-3.34265600	-2.64636100
C	-3.54058900	-4.20775800	-0.67308300
O	-0.86628600	-5.96489100	0.79972500
C	-3.05255600	-4.93021300	0.41981700
C	-4.84689500	-3.75338000	-0.70651400
C	-3.84616800	-5.15719900	1.53076400
Cl	-5.51559200	-3.01923800	-2.16448500
C	-5.64760400	-3.93382900	0.43337600
C	-5.14354100	-4.61736600	1.54959100
Cl	-3.24299900	-6.09435900	2.90463100
Cl	-7.29059500	-3.30562100	0.45510000
Cl	-6.14796700	-4.81084100	2.98745900
H	0.63177500	-5.10270400	-0.81796700
H	-3.80915600	-0.89311500	-1.87850100
H	0.48964500	3.78563000	-1.21300400
H	5.33652800	-0.43416800	-1.35317200
Cl	8.23184600	3.23745100	1.58720500
N	4.89295700	-2.05946600	-0.20965600
C	0.61241400	-0.55401900	1.33232200
C	1.39177800	0.26553700	2.19663100
C	2.56636300	0.91439100	1.72690400
C	1.03451600	0.43417900	3.56473900
C	3.35361700	1.66012600	2.58531400
H	2.86797500	0.77380200	0.70011500
C	1.78795700	1.22501100	4.41154800
H	0.13335400	-0.03472800	3.94446200
C	2.94872400	1.83257100	3.91419000
H	4.28525100	2.08719200	2.24298600
H	1.49281200	1.37129800	5.44304300
Br	4.00852000	2.90438500	5.06889100
C	-0.45701000	-1.35360300	1.96767700
O	-1.59079100	-0.92667500	2.08949400
O	-0.03893600	-2.55170500	2.37628300
C	-1.04590900	-3.39820500	2.97669900
H	-0.67426300	-4.41306900	2.87699100
H	-1.16523800	-3.12704900	4.02833800
H	-1.99387100	-3.26789500	2.45689400
C	0.74260700	4.48123500	-6.09080800
H	0.63674100	3.42126500	-6.35744800
H	0.62564400	5.06249400	-7.01523500

C	2.13434400	4.73508300	-5.48204100
H	2.90970500	4.45388700	-6.20576800
C	-0.34374100	4.87784800	-5.07425900
H	-1.33699600	4.69199300	-5.50281900
C	-0.18238000	4.02420300	-3.80599300
H	-0.31099500	2.96911200	-4.05344400
H	-0.95813800	4.28059100	-3.07269800
C	2.30756400	3.88304600	-4.21022500
H	3.30087600	4.06754100	-3.78183600
H	2.25459300	2.81908800	-4.45109900
C	1.21549900	4.24672900	-3.17978500
C	1.35409900	5.75075500	-2.83659300
H	0.60646000	6.03239000	-2.08443500
H	2.34022900	5.94141600	-2.39330800
C	2.27286300	6.22639600	-5.12727900
H	2.17106100	6.84239000	-6.03076800
H	3.27083200	6.42391700	-4.71247200
C	-0.20150800	6.36666700	-4.71548300
H	-0.33141700	6.98873500	-5.61120300
H	-0.98453600	6.65827500	-4.00267800
C	1.18922000	6.61046600	-4.10322400
H	1.29412000	7.66848300	-3.83125800
C	-3.21473400	1.96608600	-3.79479300
H	-2.16690800	1.74464000	-4.01422900
H	-3.22147000	2.72327300	-3.00523900
C	-3.92227800	0.68504100	-3.30513100
C	-3.91926600	2.51379200	-5.04938000
H	-3.39715400	3.42078200	-5.38104400
C	-3.88642100	1.45792300	-6.16804700
H	-2.84653100	1.21799300	-6.42731600
H	-4.36465400	1.85296300	-7.07461900
C	-3.90771000	-0.36624800	-4.44508900
H	-4.40645500	-1.28239900	-4.10735600
H	-2.87744400	-0.63579200	-4.68622600
C	-4.61559200	0.18761300	-5.69286800
H	-4.58606900	-0.57243700	-6.48385200
C	-6.07730700	0.52499500	-5.35171700
H	-6.59866100	0.90381000	-6.24110000
H	-6.60617900	-0.38173400	-5.02775300
C	-5.39715700	1.02775100	-2.98353900
H	-5.43358900	1.77200100	-2.17858900
H	-5.91576300	0.13262900	-2.61548800
C	-5.38179500	2.85360500	-4.70901300
H	-5.41585100	3.62192600	-3.92467100
H	-5.88980000	3.26830600	-5.59010000
C	-6.10636600	1.58076000	-4.23232400
H	-7.14608200	1.82087600	-3.97556800
C	-0.49262000	-5.39729400	-4.12257700
H	-0.31426600	-4.36975800	-4.44683700
H	-1.56478900	-5.48518500	-3.91122700
C	0.32078700	-5.69525300	-2.84421900
C	-0.10605800	-6.39278000	-5.23325000
H	-0.68602700	-6.16028200	-6.13524000
C	1.39804500	-6.26934500	-5.54047600
H	1.62931300	-5.25178000	-5.88250600
H	1.67429700	-6.95561300	-6.35230000
C	1.83433300	-5.59985500	-3.16341300
H	2.41674800	-5.80495300	-2.25582800
H	2.08289000	-4.58307400	-3.47705600
C	2.21011700	-6.59414700	-4.27377000
H	3.28303800	-6.49970500	-4.48663900
C	1.89493700	-8.02717900	-3.81050700
H	2.17473300	-8.74860600	-4.58986400
H	2.48366900	-8.27203400	-2.91619700
C	0.01331700	-7.14404200	-2.39378500
H	-1.05485100	-7.23993300	-2.15815200
H	0.56422500	-7.37182500	-1.47171300
C	-0.41853600	-7.82787200	-4.77219900
H	-1.49331800	-7.93251700	-4.57058500
H	-0.16769800	-8.54485600	-5.56545000
C	0.39097000	-8.14385200	-3.50161800
H	0.16159800	-9.16080900	-3.15865000
C	4.94871700	-3.35026500	-3.24468000
H	3.95372500	-3.09243400	-3.61845600
H	4.80818600	-4.09427200	-2.45675600
C	5.63339700	-2.09126500	-2.66784700
C	5.80427600	-3.94559500	-4.37681100
H	5.29577700	-4.83378500	-4.77430300
C	5.98212300	-2.90614400	-5.49715900
H	5.00289500	-2.62665700	-5.90808900
H	6.57024300	-3.33334700	-6.32041500
C	5.83520600	-1.05699400	-3.80611000
H	6.32546400	-0.16073500	-3.40106100
H	4.86389400	-0.74294600	-4.19683200
C	6.69078100	-1.66086400	-4.93254800
H	6.81394400	-0.91321800	-5.72620200
C	8.06890300	-2.05940000	-4.37597800
H	8.69431800	-2.47837300	-5.17558000
H	8.59004300	-1.17290700	-3.98958900
C	7.02698400	-2.49052500	-2.12761800
H	6.91153400	-3.21903800	-1.31583600
H	7.52525600	-1.60989300	-1.69828100
C	7.18246500	-4.34397500	-3.81894700
H	7.06504400	-5.10055300	-3.03136700
H	7.79750500	-4.79381100	-4.60985200
C	7.88574000	-3.09589800	-3.25314500
H	8.86476900	-3.37571200	-2.84365600

3-WB97XD
-4077.043351

Rh	0.78188700	-0.72724900	-3.07623800
O	1.01299700	1.32118700	-2.98057400
O	0.51584500	-2.77380100	-2.94065800
O	1.07925200	1.31671100	-0.71979800
O	0.47289400	-2.72513400	-0.67836400
O	2.83389000	-1.06118600	-3.03192600
O	-1.25317500	-0.39324700	-2.94936400
O	-1.21032400	-0.49726500	-0.69247800
O	2.82272900	-0.97898800	-0.77693700
C	-1.77314100	-0.29829000	-1.81715500
C	3.36477800	-1.19003100	-1.91122700
C	1.10560000	1.87388100	-1.86114600
C	0.33453800	-3.28274300	-1.81276700
Rh	0.81120200	-0.71348600	-0.61492100
C	4.82490400	-1.66333200	-1.81302500
C	4.03107800	-3.28642200	-0.12155200
C	5.39364800	-1.55520000	0.58913200
O	3.42419200	-4.00268900	-0.87676000
C	3.92760900	-3.19871700	1.37054300
O	6.07279600	-0.56176300	0.52958700
C	4.77570600	-2.18602300	1.79997900
C	3.12535100	-3.88979200	2.25688700
C	4.86799500	-1.84491700	3.13417600
Cl	2.09600000	-5.19155900	1.71654600
C	3.15459200	-3.50369000	3.60371900
C	4.01735800	-2.49121600	4.03916200
Cl	6.02737800	-0.65318500	3.68493400
Cl	2.10906700	-4.30781100	4.75919400
Cl	4.03669200	-2.02234200	5.72829600
C	1.20010600	3.40019300	-1.83676200
N	2.20811000	3.80892700	-0.86934300
C	3.48602600	3.27005300	-0.81095800
C	1.99524100	4.81307100	0.07167500
O	3.90075700	2.37359900	-1.50529300
C	4.18517100	4.01532400	0.29115700
O	0.98883100	5.46467800	0.18480700
C	3.27496300	4.90360400	0.85275800
C	5.46981400	3.90185400	0.78238700
C	3.61171100	5.68310600	1.94042500
Cl	6.60562100	2.77809600	0.07197700
C	5.83030000	4.68830200	1.88545100
C	4.90691500	5.56595400	2.46353900
Cl	2.44837800	6.77344800	2.65991900
Cl	5.36630400	6.52071900	3.85718100
C	-3.25361800	0.08830600	-1.71753100
N	-3.45122000	0.71834200	-0.41688600
C	-2.60886100	1.75006200	0.00964800
C	-3.98979500	0.01071800	0.65716500
O	-1.94605700	2.44671200	-0.71855500
C	-2.68913800	1.75240000	1.50561700
O	-4.62057800	-1.01321900	0.57332100
C	-3.56496900	0.74582200	1.88988900
C	-1.97025200	2.46909300	2.44011200
C	-3.78054300	0.44778300	3.21822900
Cl	-0.83167200	3.70316600	1.94832800
C	-2.15478400	2.15727300	3.79228100
C	-3.06166200	1.16541000	4.18003200
Cl	-4.86859200	-0.84403700	3.68692300
Cl	-1.21881100	3.00990100	5.01056400
Cl	-3.27097900	0.78917000	5.88105400
C	-0.14418400	-4.73587500	-1.73149400
N	-1.44677900	-4.72686100	-1.06645400
C	-2.54216600	-3.99375400	-1.52155200
C	-1.67365500	-5.31410300	0.17568800
O	-2.56609900	-3.31252600	-2.51648500
C	-3.62110100	-4.20195600	-0.50238400
O	-0.88085500	-5.97999400	0.79358800
C	-3.08528100	-4.94899600	0.54131100
C	-4.93089300	-3.77108300	-0.48053600
C	-3.83613400	-5.24298700	1.66094200
Cl	-5.63369000	-2.95040700	-1.85765000
C	-5.69679500	-4.03691400	0.66187800
C	-5.14924800	-4.75706100	1.72869100
Cl	-3.16651700	-6.19589100	2.97392100
Cl	-7.34579800	-3.46428600	0.75005700
Cl	-6.11393600	-5.06630300	3.15751400
H	0.52725500	-5.25109400	-1.03896300
H	-3.81816100	-0.84913000	-1.68152800
H	0.24550500	3.74808700	-1.42559200
H	5.44773600	-0.76342200	-1.75944900
Cl	7.44108100	4.54844100	2.55629200
N	4.96298000	-2.30968400	-0.50653800
C	1.44984900	4.01804200	-3.20646400
H	0.65233000	3.73144700	-3.89430300
H	1.46708200	5.10796800	-3.11659500
H	2.39973300	3.67029500	-3.62047900
C	-3.74074800	0.93652000	-2.88408200
H	-3.58343500	0.39191300	-3.81691400
H	-4.80811500	1.14074900	-2.76511900
H	-3.19582800	1.88131800	-2.93281900
C	-0.18916300	-5.44572400	-3.07593400
H	0.81171100	-5.46191800	-3.51364300
H	-0.52940400	-6.47584400	-2.93691200
H	-0.85652400	-4.92799600	-3.76720600
C	5.26271600	-2.53640200	-2.98004600
H	5.14575600	-1.97939300	-3.91181500
H	6.31372200	-2.81081500	-2.85753200
H	4.65739800	-3.44269300	-3.03617100
C	0.83224100	-0.65096400	1.38151800
C	1.66971100	0.14840300	2.21093100
C	2.84388600	0.73928100	1.68287300
C	1.36526200	0.35996600	3.58161300
C	3.68973000	1.46901300	2.49614300
H	3.10074100	0.58284800	0.64292200
C	2.17321200	1.14389800	4.37876600
H	0.46092200	-0.06396200	4.00601800
C	3.33748900	1.68846300	3.82787700
H	4.62536600	1.84771800	2.10707700
H	1.91841400	1.32755700	5.41550300
Br	4.46796500	2.74470700	4.91712100
C	-0.23020100	-1.41632300	2.07579700
O	-1.29798900	-0.90698000	2.34103700
O	0.12034900	-2.65965200	2.35397800
C	-0.88550200	-3.46049900	2.99580500
H	-0.55986100	-4.49067900	2.87589800
H	-0.95096200	-3.19225000	4.05280500
H	-1.85278800	-3.29359100	2.51920700

3-M062x
-4075.763280

Rh	-0.23561600	0.01952200	-3.90290900
O	-0.61875300	2.06289000	-3.57332600
O	0.10818500	-2.03903100	-3.94772200
O	-0.66253700	1.78536300	-1.32886000
O	-0.08573500	-2.25739600	-1.70333200
O	1.85528700	0.26062800	-3.61682100
O	-2.31558000	-0.24178300	-3.95107600
O	-2.43856100	-0.53120500	-1.71271800
O	1.58042700	0.07163900	-1.38483300
C	-2.93269900	-0.33678900	-2.87116200
C	2.27746100	0.15496400	-2.45467300
C	-0.67456900	2.47528500	-2.39864300

C	0.06728800	-2.69669800	-2.88618200
Rh	-0.42624300	-0.24361100	-1.44824000
C	3.79015700	0.08719700	-2.17313300
C	3.21631100	-1.89571500	-0.83325900
C	3.88383400	0.00696200	0.29131400
O	2.96201200	-2.61822000	-1.76039200
C	2.80622500	-2.04116000	0.60233700
O	4.17642500	1.16275800	0.46382900
C	3.28670700	-0.93688000	1.29252800
C	2.04107600	-3.00459100	1.23166900
C	3.07292700	-0.78527600	2.64783000
Cl	1.49875000	-4.42570300	0.37509400
C	1.73523300	-2.81305500	2.58581800
C	2.25855100	-1.72331000	3.29248100
Cl	3.83977700	0.51164000	3.54081000
Cl	0.71278000	-3.97024300	3.41384500
Cl	1.89848400	-1.52808300	4.99671200
C	-0.76465100	3.98544800	-2.15491000
N	0.31696600	4.34900400	-1.24214000
C	1.62915100	3.92715500	-1.41983000
C	0.13747300	5.08570200	-0.07278500
O	2.01640500	3.19149100	-2.29377700
C	2.40456500	4.52166100	-0.27958600
O	-0.89981000	5.55692500	0.31151500
C	1.50110100	5.16491200	0.56003800
C	3.75089900	4.46406300	0.01774700
C	1.90807900	5.72838500	1.75132700
Cl	4.89601600	3.79849100	-1.12057400
C	4.17891100	5.01060700	1.23751700
C	3.26407000	5.63024000	2.09816400
Cl	0.76366500	6.52750100	2.80346700
Cl	3.81663900	6.31733500	3.60959500
C	-4.46476200	-0.18208200	-2.90371400
N	-4.86628700	0.36407100	-1.61184300
C	-4.15593200	1.42496300	-1.04393900
C	-5.49659100	-0.42527000	-0.64844400
O	-3.51289800	2.23578400	-1.66188300
C	-4.35022400	1.30157900	0.43732500
O	-6.11763500	-1.43086000	-0.87133700
C	-5.19696100	0.22520400	0.67101700
C	-3.74919200	1.98005800	1.47717000
C	-5.49571100	-0.18866600	1.95096300
Cl	-2.62472100	3.28718800	1.17303200
C	-4.04533900	1.57251600	2.78342400
C	-4.91149000	0.50057400	3.01934200
Cl	-6.52213600	-1.57826600	2.22964500
Cl	-3.32323300	2.42354500	4.13928000
Cl	-5.24595300	-0.00602800	4.66404800
C	0.26706900	-4.21014200	-3.00454300
N	-0.74440700	-4.88671000	-2.20227800
C	-2.07282300	-4.47902500	-2.11539400
C	-0.50324600	-6.10128900	-1.56962500
O	-2.54744500	-3.50897900	-2.64753900
C	-2.74890100	-5.51311800	-1.25552000
O	0.55250700	-6.67941200	-1.54284600
C	-1.81507000	-6.49712800	-0.94997000
C	-4.03743500	-5.56933800	-0.76570200
C	-2.14789800	-7.58215800	-0.16536600
Cl	-5.16143900	-4.26512200	-1.06212600
C	-4.39470600	-6.67028600	0.02634500
C	-3.46117100	-7.67094800	0.31807500
Cl	-0.96120000	-8.80835300	0.22164900
Cl	-6.02077000	-6.78193900	0.66055800
Cl	-3.92849100	-9.03956300	1.30245100
H	1.22768300	-4.42917000	-2.52329400
H	-4.89580100	-1.18965400	-2.94387500
H	-1.69438100	4.15658800	-1.60068400
H	4.11112900	1.10694200	-1.92989200
Cl	5.87008400	4.93195400	1.67202300
N	3.92675000	-0.68124800	-0.92625500
C	-0.71564900	4.80159500	-3.43644100
H	-1.54597100	4.51394400	-4.08403800
H	-0.79637500	5.86596100	-3.20156900
H	0.21687700	4.61030600	-3.97275900
C	-4.94006500	0.65874000	-4.07987200
H	-4.62351800	0.19218900	-5.01387600
H	-6.02983200	0.73230800	-4.06209500
H	-4.50724900	1.65994400	-4.02597300
C	0.25305600	-4.70478600	-4.44383700
H	1.04128900	-4.21032700	-5.01345900
H	0.42246500	-5.78464200	-4.46005400
H	-0.70600700	-4.47407000	-4.91466900
C	4.59711100	-0.46960200	-3.33350200
H	4.43665100	0.16160500	-4.20959200
H	5.65956800	-0.46966800	-3.07997600
H	4.28090900	-1.48593900	-3.57265600
C	-0.63635500	-0.37322000	0.51059900
C	-0.10033200	0.50375600	1.48398600
C	0.90797900	1.44421800	1.12954300
C	-0.53503600	0.45465800	2.84030400
C	1.47460400	2.25600400	2.09087700
H	1.26252400	1.48604500	0.10595100
C	-0.01185300	1.31038400	3.78738300
H	-1.31411700	-0.24405900	3.13240600
C	0.99147100	2.20729800	3.40142400
H	2.30961800	2.90246100	1.84822500
H	-0.36222700	1.29008700	4.81260100
Br	1.73810200	3.37622100	4.67794700
C	-1.60539000	-1.40013200	0.99047700
O	-2.73878100	-1.10823700	1.29603300
O	-1.09021700	-2.62029100	1.03168600
C	-2.01417600	-3.64152700	1.43486300
H	-1.48504800	-4.58358200	1.29349700
H	-2.28236400	-3.50877700	2.48565200
H	-2.91503200	-3.58600000	0.81989800

4A

-4315.039871

Rh	-0.17063300	-0.01962500	-4.19783300
O	0.13965300	2.01860700	-4.21614400
O	-0.47054600	-2.04627700	-4.02121900
O	0.23963000	2.11358200	-1.94918400
O	-0.59134200	-1.93675800	-1.75445500
O	1.86630500	-0.33640900	-4.09895700
O	-2.20926300	0.31977300	-4.14595900
O	-2.19849300	0.48827600	-1.88217500
O	1.83728600	-0.36401100	-1.82902800
C	-2.75007500	0.53443300	-3.03104100
C	2.40205300	-0.46611300	-2.96930900
C	0.29756700	2.61668700	-3.11918000
C	-0.62343000	-2.54423400	-2.87408900
Rh	-0.18874100	0.09582500	-1.73126300
C	3.91691000	-0.73265700	-2.93086000
C	3.61100600	-2.89596600	-1.66845600
C	5.06564500	-1.31571100	-0.76644300
O	2.79983100	-3.38088100	-2.42829200
C	4.17080700	-3.45514900	-0.39116700
O	5.65540000	-0.26427300	-0.63987200
C	5.05446900	-2.51135300	0.14334900
C	3.93958800	-4.66288600	0.24638500
C	5.73516300	-2.75593100	1.32397700
Cl	2.79381400	-5.83334100	-0.41084200
C	4.62741200	-4.92563100	1.44509800
C	5.51900600	-3.98192400	1.97769200
Cl	6.85104000	-1.56018100	1.99491100
Cl	4.36036500	-6.45574200	2.28648900
Cl	6.37473700	-4.33094400	3.48385800
C	0.52072300	4.13624700	-3.19356600
N	1.50420000	4.55870600	-2.19330300
C	2.72518100	3.92339400	-1.96813700
C	1.34442400	5.72036800	-1.42548600
O	3.11836400	2.92631500	-2.53784300
C	3.41420700	4.73870300	-0.90857700
O	0.39084100	6.46397000	-1.47103000
C	2.59055700	5.82348400	-0.59106900
C	4.64107500	4.56679600	-0.29012200
C	2.97629800	6.76570000	0.34765100
Cl	5.66112500	3.17295300	-0.66983900
C	5.04852700	5.51726200	0.66258600
C	4.22376300	6.60811200	0.97804300
Cl	1.93139400	8.13297200	0.74525800
Cl	4.75226900	7.79271800	2.17758200
C	-4.25288400	0.86355800	-3.00582600
N	-4.51001800	1.82078800	-1.92856000
C	-3.82444800	3.03309200	-1.79508300
C	-5.27041300	1.50726900	-0.79811700
O	-3.03868700	3.48166400	-2.60307800
C	-4.27094600	3.60661500	-0.48152400
O	-5.87800300	0.47143800	-0.62864500
C	-5.15081100	2.69570300	0.11028100
C	-3.93550000	4.79288400	0.14881700
C	-5.72597100	2.95393400	1.34181800
Cl	-2.78758000	5.91751300	-0.58185700
C	-4.51510200	5.06881500	1.39988800
C	-5.40535700	4.15898900	1.98981600
Cl	-6.83536500	1.79518000	2.08913400
Cl	-4.11459700	6.57504600	2.23482000
Cl	-6.12711600	4.52492700	3.56248600
C	-0.80566300	-4.07002200	-2.79891700
N	-1.88630600	-4.40477500	-1.86787600
C	-3.15412100	-3.82028800	-1.89785400
C	-1.76956000	-5.40559500	-0.89670200
O	-3.50171900	-2.93234400	-2.64683500
C	-3.94935500	-4.52969700	-0.83628000
O	-0.77093900	-6.05155700	-0.66875700
C	-3.12146100	-5.48830700	-0.24261200
C	-5.26723800	-4.37556000	-0.43833700
C	-3.59317200	-6.32104000	0.75841200
Cl	-6.30522600	-3.15535200	-1.18139000
C	-5.75878100	-5.21168500	0.58063500
C	-4.92943200	-6.17669000	1.17281000
Cl	-2.54944800	-7.54346100	1.49251900
Cl	-7.43489900	-5.04481600	1.11444400
Cl	-5.56598300	-7.22072500	2.44877100
H	0.10588500	-4.45993900	-2.33266300
H	-4.76177500	-0.05605200	-2.69400700
H	-0.42475700	4.59248800	-2.87799200
H	4.38333700	0.21758200	-2.64529500
Cl	6.61087300	5.33190900	1.46704500
N	4.22364500	-1.64954800	-1.83167400
C	0.89341300	4.62838100	-4.59452800
H	0.11461600	4.34643000	-5.30592900
H	0.98646500	5.71884800	-4.58661100
H	1.83711800	4.18639000	-4.92579800
C	-4.79935000	1.33498300	-4.35432900
H	-4.61276000	0.57057700	-5.11180100
H	-5.87819400	1.50216400	-4.27758500
H	-4.31242600	2.26049500	-4.67006300
C	-1.01559200	-4.72739100	-4.16487400
H	-0.16851800	-4.50430400	-4.81703000
H	-1.08967600	-5.81260900	-4.04197700
H	-1.92434100	-4.35318000	-4.64320800
C	4.48857400	-1.21624000	-4.26502200
H	4.27281100	-0.48180000	-5.04383600
H	5.57335600	-1.33482600	-4.18067200
H	4.04220700	-2.16947200	-4.55787400
C	-0.31319100	0.30551500	0.28409400
C	0.67662800	0.74747600	1.21710100
C	2.00747800	1.02289800	0.79619900
C	0.37671000	0.90529200	2.60300300
C	2.98747600	1.39999100	1.70326000
H	2.25854800	0.92107100	-0.25051900
C	1.34536500	1.29247200	3.51229600
H	-0.63306800	0.73147400	2.95798300
C	2.65029700	1.53262100	3.05543800
H	4.00218500	1.58244300	1.36749000
H	1.10359800	1.41098700	4.56237900
Br	3.98825000	2.06095400	4.30633600
C	-1.69750100	0.15454300	0.81252900
O	-2.39866100	1.13043900	1.01573200
O	-2.07378800	-1.11348900	1.00065200
C	-3.43669700	-1.29975400	1.44943300
H	-3.52287200	-2.36576200	1.65563400
H	-3.62384500	-0.71783500	2.35491500
H	-4.13679000	-0.99539200	0.66908200
C	-0.01090100	-3.21528900	3.55814700
H	-0.56587700	-2.60988200	2.82618000
C	1.47262300	-3.14397100	3.16267700
H	1.61227800	-3.49995100	2.13506500
H	1.85154800	-2.11563800	3.21727700
H	2.09707400	-3.76676300	3.81456600
C	-0.53853400	-4.65451300	3.44999100
H	0.00674000	-5.33680800	4.11307600

H	-1.60099000	-4.71179900	3.71888200
H	-0.42847000	-5.03767800	2.42898200
C	-0.28754100	-2.58135600	4.94093700
H	0.03390200	-1.52863000	4.91039700
H	-1.37578900	-2.56029800	5.10420100
C	0.37336700	-3.25553000	6.15306600
H	0.04377000	-4.30012700	6.22415600
H	1.46220400	-3.28607700	6.01626000
C	0.05260200	-2.53715400	7.46915400
H	0.52976300	-3.03224900	8.32261300
H	0.40309000	-1.49739200	7.44944700
H	-1.02816900	-2.51702000	7.65733700

$TSA_{4\text{-}5}$

-4315.039871

Rh	0.64898000	-0.61299500	-2.81022300
O	0.97539400	1.40818400	-2.73095200
O	0.31678900	-2.64492000	-2.75069000
O	0.97780100	1.42047300	-0.45935400
O	0.10440100	-2.64617900	-0.48809900
O	2.66961800	-0.95530200	-2.62595600
O	-1.38108800	-0.23783900	-2.85106100
O	-1.45875300	-0.17577700	-0.58279800
O	2.58842200	-1.06965300	-0.35897800
C	-1.95620700	-0.04543100	-1.74602900
C	3.17983000	-1.12083400	-1.48741100
C	1.08748500	1.96467500	-1.60305900
C	0.10553800	-3.19456600	-1.63727700
Rh	0.53935300	-0.60991700	-0.35149900
C	4.70086700	-1.35107900	-1.45603500
C	4.41465500	-3.62470900	-0.37849900
C	6.10619000	-2.24036700	0.43061200
O	3.48568800	-3.99907400	-1.06268400
C	5.13378800	-4.35957100	0.72033000
O	6.80991400	-1.26114700	0.53762300
C	6.16050000	-3.53550000	1.19333200
C	4.91984300	-5.61814400	1.25795400
C	7.00648500	-3.95417500	2.20668100
Cl	3.59219600	-6.63640800	0.69001100
C	5.77422400	-6.05866100	2.28519900
C	6.81026000	-5.23542900	2.75325500
Cl	8.30000800	-2.90843900	2.80098600
Cl	5.53610500	-7.66068900	2.99166500
Cl	7.87401300	-5.80640200	4.04308000
C	1.31704000	3.48536200	-1.62188300
N	2.41394000	3.85455400	-0.71893400
C	3.62568200	3.17265800	-0.61391100
C	2.40535500	5.05933100	-0.00183100
O	3.90852600	2.13800700	-1.18226600
C	4.47587700	3.99885500	0.31220600
O	1.48782600	5.84815400	0.02896300
C	3.75048000	5.14145900	0.66378900
C	5.75885900	3.79158300	0.78993500
C	4.29566100	6.11161000	1.48753300
Cl	6.65246200	2.31672700	0.39020600
C	6.32770300	4.76982200	1.62441700
C	5.60383200	5.92193500	1.96677400
Cl	3.37534300	7.55465200	1.92394100
Cl	6.33640100	7.14291700	3.01359800
C	-3.43979700	0.36704900	-1.77452900
N	-3.69008200	1.31340200	-0.68574400
C	-2.95190100	2.48504100	-0.49480700
C	-4.53402800	1.02879200	0.39094000
O	-2.10779400	2.90907700	-1.25587200
C	-3.43440100	3.05997600	0.80538200
O	-5.21902600	0.03375100	0.49884600
C	-4.39468100	2.19070300	1.33060300
C	-3.06671000	4.21344400	1.47717500
C	-5.01668600	2.45750800	2.53689600
Cl	-1.82480400	5.28958100	0.82974400
C	-3.69341500	4.49767400	2.70343000
C	-4.66201800	3.62865100	3.22750500
Cl	-6.22608500	1.34882100	3.20263200
Cl	-3.25317300	5.96258700	3.59139400
Cl	-5.44104600	4.00376000	4.77131600
C	-0.12568700	-4.71761600	-1.65473800
N	-1.23873600	-5.06267500	-0.76578300
C	-2.51469400	-4.49927600	-0.86331700
C	-1.12465800	-5.97125100	0.28875400
O	-2.85068500	-3.65492500	-1.66440000
C	-3.32816800	-5.15703600	0.21743200
O	-0.11395100	-6.56078800	0.60623800
C	-2.49233500	-6.03731100	0.91235400
C	-4.66135300	-5.00986700	0.56278500
C	-2.96839700	-6.78612800	1.97550000
Cl	-5.71052100	-3.89479200	-0.31599800
C	-5.15998600	-5.76936400	1.63714500
C	-4.31993000	-6.64821100	2.33890700
Cl	-1.90558500	-7.89114000	2.85741500
Cl	-6.85615100	-5.61245800	2.10404800
Cl	-4.96246400	-7.58974500	3.68954000
H	0.75840800	-5.16481800	-1.18733000
H	-4.01598700	-0.52603400	-1.50666100
H	0.41744700	3.92982700	-1.18381400
H	5.13616000	-0.42386600	-1.06662800
Cl	7.96625000	4.54194100	2.24657500
N	5.04050700	-2.37988600	-0.46734600
C	1.54263800	4.05197800	-3.02581500
H	0.68634000	3.81821600	-3.66198000
H	1.65066000	5.13963300	-2.96751600
H	2.43708900	3.62099900	-3.48393400
C	-3.90357300	0.89982500	-3.13122900
H	-3.73118800	0.14327800	-3.89989800
H	-4.97322500	1.12864400	-3.09242900
H	-3.35140900	1.80169000	-3.40538300
C	-0.32062400	-5.29551700	-3.05784900
H	0.55194900	-5.06699200	-3.67345700
H	-0.43472600	-6.38264500	-2.99638700
H	-1.20140200	-4.86470000	-3.53970400
C	5.30256200	-1.66880800	-2.82675200
H	5.07750400	-0.85946800	-3.52402400
H	6.38922100	-1.76681800	-2.73787700
H	4.88678800	-2.59530500	-3.23183900
C	0.31859500	-0.46531500	1.89745700
C	1.07974700	0.60427400	2.58687700
C	2.42913100	0.83738400	2.23885300
C	0.54063700	1.37391300	3.64284700
C	3.21357700	1.75455700	2.93359500
H	2.86223200	0.29382900	1.40739800
C	1.30734500	2.31369300	4.32730400
H	-0.49795000	1.24830000	3.92097400
C	2.64673300	2.48718200	3.97816800
H	4.25444400	1.89570200	2.66475300
H	0.87010800	2.89587000	5.13110000
Br	3.72187600	3.74895900	4.94858600
C	-1.14439400	-0.52115400	2.17499200
O	-1.86499100	0.46066400	2.25060900
O	-1.63126900	-1.78273000	2.27406800
C	-3.06003000	-1.88633500	2.42597100
H	-3.24788200	-2.93025200	2.68046100
H	-3.41440800	-1.22865800	3.22278900
H	-3.56367700	-1.62217100	1.49490000
C	1.31154000	-2.57556700	3.15202700
H	0.80322300	-1.52895000	2.12788300
C	2.77627900	-2.28011200	3.00457400
H	3.06520500	-2.21519700	1.95242600
H	3.07457400	-1.36484200	3.52086100
H	3.33255600	-3.11581100	3.45639200
C	0.80776500	-3.78469900	2.41850700
H	1.13700600	-4.67740100	2.97460400
H	-0.28134800	-3.79507000	2.37319100
H	1.21188700	-3.85079000	1.40777500
C	0.68133500	-2.24909000	4.47747500
H	0.89431600	-1.20550500	4.74246300
H	-0.40404000	-2.36834900	4.40741300
C	1.21410800	-3.15626500	5.62132400
H	1.04589800	-4.20959400	5.36430300
H	2.29792800	-3.02319500	5.72391400
C	0.52931900	-2.83542200	6.95354000
H	0.91248500	-3.48064400	7.75154200
H	0.70488500	-1.79475800	7.24978500
H	-0.55433200	-2.98794300	6.88994200

5A

-4315.130481

Rh	-0.19589100	-0.13106100	-4.00893400
O	0.02834700	1.91126200	-4.02326600
O	-0.45236700	-2.16442800	-3.87621600
O	-0.11190000	2.01355800	-1.76148700
O	-0.81514200	-2.05460800	-1.64053600
O	1.81716400	-0.34057200	-3.69599400
O	-2.22795900	0.10789300	-4.21336100
O	-2.48103000	0.33109500	-1.97040500
O	1.56768000	-0.35640200	-1.44059900
C	-2.90470500	0.32742800	-3.16745600
C	2.25132100	-0.41992600	-2.51170600
C	0.05228500	2.51990900	-2.91441500
C	-0.73443300	-2.66665300	-2.75162500
Rh	-0.48065000	-0.00932400	-1.62284800
C	3.77664700	-0.53875700	-2.35556300
C	3.57226500	-2.90043600	-1.45990900
C	5.11743300	-1.47885800	-0.44720700
O	2.70012200	-3.26794800	-2.21784800
C	4.29861000	-3.67996600	-0.39974200
O	5.73835300	-0.46310900	-0.21924200
C	5.23098800	-2.82849400	0.20286500
C	4.16959400	-4.99950200	0.00096800
C	6.05963500	-3.27592900	1.21821700
Cl	2.97485200	-6.06454900	-0.74489000
C	5.00770200	-5.46925200	1.02853400
C	5.94476700	-4.61561000	1.63116400
Cl	7.23385300	-2.19561300	1.97566800
Cl	4.87667200	-7.14787600	1.56217000
Cl	6.98866200	-5.22412200	2.91957300
C	0.24845900	4.04267100	-2.96492000
N	1.20377900	4.45159000	-1.93274500
C	2.45294200	3.85831500	-1.74291700
C	0.97302700	5.52671100	-1.06535600
O	2.88399100	2.91463200	-2.37297500
C	3.10686900	4.63974900	-0.63822500
O	-0.03007100	6.20425600	-1.04083300
C	2.21902600	5.64216800	-0.23264600
C	4.35886900	4.51586200	-0.05953800
C	2.56042600	6.54009800	0.76446900
Cl	5.47110200	3.23641100	-0.56031500
C	4.72723600	5.43286300	0.94128400
C	3.83270800	6.43269000	1.35377800
Cl	1.43056900	7.79749600	1.28025900
Cl	4.30770500	7.57002000	2.61946000
C	-4.41048600	0.57580200	-3.35500900
N	-4.85562800	1.59286600	-2.40096500
C	-4.21907700	2.82312400	-2.22110200
C	-5.93028400	1.40105400	-1.52583000
O	-3.27120300	3.22284400	-2.86363400
C	-4.96328400	3.50177200	-1.10517200
O	-6.63174000	0.41530000	-1.47997400
C	-6.00131800	2.65578600	-0.70016400
C	-4.76364300	4.73276500	-0.50170600
C	-6.87275300	3.02489100	0.31061900
Cl	-3.42392100	5.77623800	-0.98265800
C	-5.64348500	5.12090900	0.52521200
C	-6.69009300	4.27615400	0.92575400
Cl	-8.18253100	1.95221700	0.81924000
Cl	-5.42366800	6.68535700	1.31693100
Cl	-7.78487600	4.78227100	2.21804200
C	-0.96160800	-4.18704900	-2.71051100
N	-2.04812300	-4.49089200	-1.77840400
C	-3.29898800	-3.86928600	-1.81360100
C	-1.91728700	-5.39543700	-0.71868900
O	-3.64806200	-3.04434700	-2.63104400
C	-4.06667100	-4.44588700	-0.65727600
O	-0.92331700	-6.03830800	-0.46359800
C	-3.24278100	-5.37215100	-0.00904000
C	-5.35320900	-4.19329200	-0.21009100
C	-3.68855700	-6.07424700	1.09783000
Cl	-6.37152600	-2.99055600	-1.00394200
C	-5.82040900	-4.90477400	0.90993300
C	-4.99645800	-5.83851800	1.55695700
Cl	-2.63906000	-7.23623400	1.91970100
Cl	-7.45857000	-4.61518500	1.50570300
Cl	-5.60152900	-6.72218600	2.96317100
H	-0.06365600	-4.61763300	-2.25239200
H	-4.91247200	-0.34727000	-3.04285000
H	-0.70892500	4.47933400	-2.66015200

H	4.10124300	0.38725000	-1.86902900
Cl	6.33052200	5.33025600	1.67283800
N	4.11092900	-1.61069300	-1.41161500
C	0.64557200	4.56755800	-4.34640100
H	-0.11209700	4.28599300	-5.08098000
H	0.71897800	5.65925800	-4.31705700
H	1.60383100	4.14840300	-4.66390400
C	-4.80177100	0.92394700	-4.79288100
H	-4.49083200	0.12126800	-5.46497000
H	-5.88787700	1.04067500	-4.86072700
H	-4.31814800	1.84962800	-5.11497300
C	-1.19332400	-4.81201800	-4.08794600
H	-0.34097500	-4.60106500	-4.73720300
H	-1.30015000	-5.89649700	-3.98584200
H	-2.09247200	-4.40286300	-4.55539800
C	4.51735600	-0.71121700	-3.68353300
H	4.29728900	0.13269800	-4.34079600
H	5.59601200	-0.74170500	-3.49971300
H	4.20831800	-1.63004300	-4.18855500
C	0.58714600	-0.86099200	1.99359400
C	1.65207900	0.00647500	2.66760000
C	2.88951800	0.15690000	2.02522700
C	1.46456500	0.66421500	3.89368600
C	3.92926500	0.89612400	2.59144100
H	3.03595800	-0.29641700	1.05018400
C	2.48966200	1.41166900	4.47416100
H	0.51093500	0.60413800	4.40435500
C	3.71952200	1.51245800	3.82381900
H	4.87764500	0.98535100	2.07325500
H	2.33136900	1.90934600	5.42482300
Br	5.13509100	2.52930400	4.63679500
C	-0.67157500	-0.05823300	1.71467500
O	-1.05562900	0.26308500	0.59526200
O	-1.36227200	0.30552800	2.79999300
C	-2.54741200	1.09917500	2.57550700
H	-2.95601700	1.28861800	3.56769000
H	-2.28462100	2.03490900	2.07710600
H	-3.26029600	0.54646100	1.95962600
C	0.31313100	-2.28608700	2.64608600
H	0.96092900	-1.08062600	0.99022800
C	1.58929400	-3.12156000	2.41717600
H	1.80706400	-3.20966200	1.34640700
H	2.45855000	-2.67236400	2.91020900
H	1.46610900	-4.13680700	2.80616500
C	-0.85138600	-2.93910000	1.87050600
H	-0.92998200	-4.00284700	2.11614200
H	-1.81260300	-2.47001900	2.11728900
H	-0.70255200	-2.85608000	0.78853600
C	-0.00814500	-2.20461100	4.16108900
H	0.85933900	-1.77920500	4.68100400
H	-0.83578300	-1.50136800	4.31271300
C	-0.37724500	-3.52678600	4.85683700
H	-1.27022200	-3.96451000	4.39345900
H	0.42608900	-4.26361900	4.73259800
C	-0.64047400	-3.32641100	6.35445800
H	-0.90958200	-4.27118800	6.84007600
H	0.24586600	-2.92958400	6.86456900
H	-1.46266300	-2.61956100	6.52235800

R-P

-747.864638

C	0.56746000	-0.84040100	2.00235900
C	1.65265900	0.00399100	2.66914000
C	2.92114300	0.06083500	2.07177700
C	1.45306500	0.74009100	3.84801600
C	3.96358000	0.80353100	2.62706800
H	3.10221500	-0.48442300	1.14908800
C	2.48269900	1.49118700	4.41689300
H	0.47986700	0.74248700	4.32396400
C	3.73414600	1.51459500	3.80319800
H	4.93546800	0.83177800	2.14656000
H	2.30883300	2.05447300	5.32741800
Br	5.15743300	2.54902900	4.58300400
C	-0.71186100	-0.04189100	1.74265000
O	-1.10928800	0.24458400	0.63426100
O	-1.37262600	0.32188000	2.86867900
C	-2.56668200	1.09643600	2.65663900
H	-2.96510300	1.29616900	3.65173800
H	-2.32934900	2.03037900	2.14100000
H	-3.28702300	0.53338200	2.05794300
C	0.31569800	-2.27730700	2.63161800
H	0.91726700	-1.04199400	0.98541500
C	1.60434000	-3.09942100	2.41830200
H	1.87345400	-3.14251600	1.35557800
H	2.45221800	-2.67295800	2.96491600
H	1.46926300	-4.13044000	2.76039000
C	-0.82945900	-2.93952500	1.83528300
H	-0.92363900	-3.99883200	2.09460700
H	-1.79580900	-2.46270300	2.03781100
H	-0.64706600	-2.87881300	0.75596700
C	-0.02831900	-2.20530600	4.14238300
H	0.81647600	-1.74322600	4.66960200
H	-0.88176000	-1.53123500	4.27789600
C	-0.35462700	-3.53699500	4.84060300
H	-1.22044000	-4.01383200	4.36366300
H	0.48108600	-4.24060200	4.73707400
C	-0.65524700	-3.33878000	6.33149900
H	-0.89327400	-4.29073600	6.81979100
H	0.20337900	-2.90068100	6.85511800
H	-1.50951000	-2.66609200	6.47779300

4B

-4315.068672

Rh	0.40098000	-0.03161000	-4.25549000
O	-0.01352500	1.99652500	-4.33174700
O	0.83481100	-2.03557100	-4.02444800
O	-0.06560500	2.13990400	-2.06579100
O	0.56621900	-1.92300500	-1.77205600
O	2.40636400	0.41466700	-4.09483200
O	-1.60791900	-0.48720500	-4.25878300
O	2.31736700	0.45247900	-1.82659700
C	-2.23107700	-0.47923300	-3.16453700
C	2.91527600	0.53518800	-2.94922300
C	-0.11375500	2.62273100	-3.24545000
C	0.80271100	-2.53139900	-2.86939900
Rh	0.26594000	0.13268300	-1.79745800
C	4.41088900	0.88911700	-2.89891600
C	4.91089900	-1.16238700	-1.50399600
C	6.00134300	0.82221200	-0.95474500
O	4.18976000	-1.93180000	-2.10562800
C	5.81438600	-1.43444400	-0.33224500
O	6.34019900	1.98121200	-1.03214100
C	6.47240300	-0.24409900	-0.00610600
C	6.05482800	-2.60065600	0.37456300
C	7.38663300	-0.19104400	1.03262500
Cl	5.20376200	-4.09778400	-0.02747800
C	6.98227900	-2.56358400	1.43090900
C	7.64295300	-1.36911600	1.75703000
Cl	8.21142500	1.31639100	1.44070000
Cl	7.31461900	-4.03398300	2.35267200
Cl	8.80459800	-1.34119600	3.08774600
C	-0.35613300	4.14107400	-3.30387900
N	0.32405000	4.77319100	-2.17259300
C	1.68304200	4.59185000	-1.89279700
C	-0.36098100	5.39398300	-1.12415000
O	2.46784800	4.00181700	-2.60501400
C	1.91507200	5.26262300	-0.57010500
O	-1.55966600	5.57394200	-1.08116900
C	0.68864300	5.75480100	-0.11420600
C	3.07156800	5.41725600	0.17525200
C	0.59021200	6.42185600	1.09399500
Cl	4.60891700	4.75565300	-0.38555200
C	2.98592500	6.09568600	1.40390900
C	1.75648600	6.59600800	1.85836700
Cl	-0.96617300	7.03876500	1.66832900
Cl	1.66970900	7.44815400	3.40589100
C	-3.71635400	-0.87856600	-3.20583900
N	-4.50041600	0.02446600	-2.36087300
C	-4.45069400	1.41684600	-2.45383200
C	-5.39649200	-0.42635500	-1.38668000
O	-3.73818300	2.04512400	-3.20702100
C	-5.44628900	1.92273900	-1.44634300
O	-5.61028900	-1.58624200	-1.11094300
C	-6.01128200	0.81636500	-0.80317200
C	-5.83304900	3.21358200	-1.12543400
C	-6.97518200	0.97445300	0.17829700
Cl	-5.11483800	4.60701100	-1.93806500
C	-6.81187000	3.38899600	-0.13035800
C	-7.37726500	2.27906900	0.51640400
Cl	-7.68770100	-0.42635800	0.98768500
Cl	-7.33182800	5.02042400	0.30548400
Cl	-8.60500600	2.51931100	1.76476400
C	1.13261600	-4.02747000	-2.72830900
N	0.27279700	-4.62114700	-1.70301500
C	-1.12336800	-4.54504000	-1.72613600
C	0.76448400	-5.19426600	-0.52610000
O	-1.77983300	-4.02466000	-2.60293200
C	-1.58405300	-5.21955900	-0.46507600
O	1.93586100	-5.30392800	-0.23390500
C	-0.44991500	-5.61334800	0.25327600
C	-2.85928800	-5.47145200	0.01313300
C	-0.56356800	-6.27049700	1.46662600
Cl	-4.28599000	-4.96226500	-0.89111000
C	-2.98919500	-6.13907600	1.24471700
C	-1.85166300	-6.53588300	1.96452000
Cl	0.87299200	-6.76868300	2.36832000
Cl	-4.59915800	-6.47930500	1.88713800
Cl	-2.03493900	-7.37481100	3.50896500
H	2.14461600	-4.07233000	-2.30871800
H	-3.77985600	-1.85614200	-2.71475000
H	-1.42495100	4.28683800	-3.10732300
H	4.45611200	1.95287700	-2.63729300
Cl	4.44187800	6.31618700	2.38214900
N	5.06654700	0.19351500	-1.78900200
C	0.02080400	4.77266900	-4.64493700
H	-0.53879700	4.28762500	-5.44773200
H	-0.22754200	5.83846100	-4.63353200
H	1.08791900	4.65378100	-4.84639400
C	-4.28550300	-0.96899200	-4.62331100
H	-3.70998900	-1.69133400	-5.20610800
H	-5.32759400	-1.30128400	-4.57994300
H	-4.23361800	-0.00130200	-5.12854100
C	1.07863300	-4.79828300	-4.04837500
H	1.76750700	-4.34590700	-4.76497100
H	1.37537700	-5.83841300	-3.88082800
H	0.07327500	-4.77357200	-4.47524500
C	5.13795600	0.64789000	-4.22439800
H	4.65809100	1.22086400	-5.02027200
H	6.17959200	0.97165100	-4.13481400
H	5.10969200	-0.41039300	-4.49828500
C	0.19332100	0.38003800	0.21354700
C	0.80995500	-0.39338100	1.24553200
C	1.66542700	-1.48739600	0.93567100
C	0.56734800	-0.11293500	2.62290900
C	2.22455800	-2.26967500	1.93605800
H	1.87670700	-1.71398000	-0.10010700
C	1.12122300	-0.88792500	3.62635800
H	-0.06873300	0.72155200	2.89823700
C	1.94690400	-1.96639200	3.27435800
H	2.85753400	-3.11220100	1.68164900
H	0.92467700	-0.66728900	4.66945400
Br	2.71136200	-3.03581800	4.65475500
C	-0.48020400	1.63630000	0.64070500
O	0.17496200	2.63805900	0.86778300
O	-1.81219600	1.55521700	0.71437800
C	-2.49488000	2.78639100	1.05082600
H	-3.53802000	2.50305300	1.18400600
H	-2.09155200	3.20718300	1.97469900
H	-2.38726400	3.51117400	0.24169900
H	-3.31635200	-0.20878600	2.36316000
C	-3.06643900	0.53095800	5.06429700
H	-2.48125300	1.14322000	4.35788600
C	-4.39786600	1.25488000	5.31929400
H	-4.23009500	2.23458700	5.78238800
H	-4.96321700	1.41809300	4.39579600
H	-5.03270300	0.67109800	5.99885800
C	-2.26100600	0.42072600	6.36806600
H	-2.80195000	-0.17835900	7.11201800
H	-1.28954400	-0.06184700	6.20153900
H	-2.07535800	1.40756300	6.80862900
C	-3.26020300	-0.85938600	4.42548800
H	-2.27865100	-1.35319800	4.36043300
H	-3.86546200	-1.48113800	5.10329000
C	-3.89817900	-0.86292400	3.02894700

H	-4.90916800	-0.43852900	3.07763300
C	-3.97845400	-2.26508300	2.41449600
H	-4.45325800	-2.24358100	1.42797600
H	-2.97727600	-2.70026300	2.29813500
H	-4.56132200	-2.94321300	3.05011300
O	-1.76185200	-0.22738300	-2.00649900

$TSB_{4\text{-}5}$

-4315.036613

Rh	0.57523900	-0.85613000	-4.04520600
O	0.22911900	1.17289300	-4.23803800
O	0.97629900	-2.84539100	-3.72513100
O	0.05266100	1.40206200	-1.98684700
O	0.58029200	-2.68456300	-1.49579500
O	2.56433800	-0.43252500	-3.78779800
O	-1.44619300	-1.30689300	-4.14774000
O	2.35120800	-0.32355900	-1.52918700
C	-2.12925100	-1.27699200	-3.09094000
C	3.01235700	-0.29132700	-2.61369700
C	0.12653100	1.84620100	-3.17616200
C	0.89495500	-3.31394200	-2.55774500
Rh	0.29718200	-0.61357500	-1.62755300
C	4.51391100	0.01875700	-2.49852600
C	4.90884700	-2.14615800	-1.23976700
C	6.13151900	-0.26892700	-0.60278700
O	4.13887600	-2.83547700	-1.87650300
C	5.83817900	-2.54920900	-0.12806700
O	6.53359600	0.87294000	-0.61435800
C	6.58614200	-1.42638100	0.24011800
C	6.03862000	-3.77378800	0.48633000
C	7.56060200	-1.50378600	1.22064100
Cl	5.05292600	-5.17835500	0.05760700
C	7.02977100	-3.86959700	1.47868300
C	7.78625400	-2.74506400	1.84066500
Cl	8.50167700	-0.08097100	1.68091400
Cl	7.31864400	-5.41954400	2.27716900
Cl	9.02696100	-2.88396900	3.09164400
C	0.04886400	3.37921400	-3.31258600
N	0.70814800	3.99639500	-2.16135400
C	2.02370100	3.71658400	-1.77964600
C	0.02428900	4.76114100	-1.21256300
O	2.79926600	3.02614800	-2.40664500
C	2.23113600	4.44391900	-0.48325000
O	-1.14695500	5.07017700	-1.27753200
C	1.03392200	5.08423000	-0.15077200
C	3.34329500	4.53065600	0.33686700
C	0.92193500	5.83595400	1.00517200
Cl	4.83876800	3.68372900	-0.06597100
C	3.24339600	5.29356800	1.51394000
C	2.04443100	5.94322100	1.84377000
Cl	-0.59835400	6.63935200	1.42440600
Cl	1.94009400	6.90060100	3.32769200
C	-3.59951200	-1.72825100	-3.18128900
N	-4.44029400	-0.81800100	-2.39711900
C	-4.59755500	0.54188000	-2.69306900
C	-5.02163300	-1.17354500	-1.17861700
O	-4.09804900	1.12022400	-3.63192300
C	-5.47600300	1.09182500	-1.60326100
O	-4.95210400	-2.26448300	-0.65275100
C	-5.72176400	0.06380500	-0.68818000
C	-6.00361200	2.35909000	-1.41874300
C	-6.49529300	0.28146300	0.43951800
Cl	-5.69036600	3.65119600	-2.57997400
C	-6.79765400	2.59219800	-0.28091500
C	-7.03991600	1.56194000	0.64174500
Cl	-6.79235400	-1.01850400	1.60333200
Cl	-7.49145600	4.19374200	-0.01292600
Cl	-8.03597600	1.87334000	2.06762200
C	1.28378000	-4.79248900	-2.38992200
N	0.34778600	-5.46932800	-1.48604000
C	-1.03984200	-5.43670100	-1.62811800
C	0.76862900	-6.30782300	-0.44604600
O	-1.64764200	-4.78544300	-2.45214000
C	-1.57792600	-6.35079700	-0.56102100
O	1.91914000	-6.51294600	-0.13033300
C	-0.49159500	-6.87114200	0.15061200
C	-2.87841000	-6.70297500	-0.23957300
C	-0.67866800	-7.75203100	1.20282500
Cl	-4.24932400	-6.04285600	-1.13744800
C	-3.08416700	-7.59946200	0.82482200
C	-1.99408000	-8.11890100	1.54018300
Cl	0.69710100	-8.40058100	2.10086300
Cl	-4.72916600	-8.07188700	1.26290900
Cl	-2.27232000	-9.24203500	2.87491100
H	2.24295600	-4.78702300	-1.86058100
H	-3.64687700	-2.68304300	-2.64552500
H	-1.00732400	3.65294500	-3.20663100
H	4.57860300	1.05668600	-2.15517000
Cl	4.64292100	5.43142900	2.58614200
N	5.12521900	-0.78167300	-1.43274200
C	0.58638600	3.90277500	-4.64632700
H	0.03572100	3.44232800	-5.46944700
H	0.45608800	4.98831400	-4.69633600
H	1.64539100	3.66114300	-4.76136900
C	-4.11084700	-1.91099200	-4.61054300
H	-3.49041800	-2.64940700	-5.12304000
H	-5.14390000	-2.27288000	-4.58986000
H	-4.06580400	-0.97451900	-5.16925600
C	1.42872500	-5.54482400	-3.71480800
H	2.17438300	-5.04851200	-4.33909300
H	1.75775000	-6.57074400	-3.52090900
H	0.48231000	-5.56453800	-4.26150100
C	5.27408100	-0.13832700	-3.81808800
H	4.83504500	0.51028800	-4.57900600
H	6.32061500	0.14789200	-3.67330200
H	5.22595800	-1.16977300	-4.17793900
C	0.04499200	-0.25204600	0.63611700
C	1.19377700	-0.64243800	1.47222600
C	1.66641500	-1.97376500	1.40551200
C	1.83313800	0.22952600	2.38098800
C	2.69479500	-2.42813900	2.22697100
H	1.23259700	-2.65156700	0.67830700
C	2.87544200	-0.20954300	3.19408600
H	1.51804400	1.26312800	2.43836700
C	3.28968600	-1.54059200	3.12591900
H	3.03009400	-3.45771600	2.16134900
H	3.35384500	0.47765300	3.88361400
Br	4.68720400	-2.15750100	4.29157300
C	-0.51077500	1.12046000	0.75670500
O	0.15730900	2.12934500	0.91812700
O	-1.86043700	1.16630300	0.61224700
C	-2.44648200	2.48088700	0.63407600
H	-3.52227900	2.31454400	0.70186800
H	-2.09254500	3.04742200	1.49825100
H	-2.20252500	3.02813100	-0.27772700
H	-0.78008400	-1.05566600	0.61306800
C	-1.66777300	-0.38732600	3.86986800
H	-1.18341300	0.45139000	3.35344500
C	-3.15857000	-0.05579000	4.03612300
H	-3.28750900	0.85989600	4.62378100
H	-3.66131300	0.09702300	3.07454400
H	-3.68336800	-0.86406800	4.56185000
C	-0.98779000	-0.55240800	5.23725200
H	-1.41639700	-1.39794000	5.79107700
H	0.08823300	-0.72915900	5.12909200
H	-1.12168200	0.34598200	5.84989800
C	-1.45171000	-1.65589200	3.02234400
H	-0.39432200	-1.96685100	3.05577500
H	-1.99184600	-2.50237500	3.48613000
C	-1.88509500	-1.62015500	1.59683800
H	-2.56393600	-0.83132700	1.28716000
C	-1.99545500	-2.91074200	0.85152100
H	-1.94534300	-2.77156900	-0.23028900
H	-1.24163700	-3.63446900	1.17625300
H	-2.99446800	-3.32232600	1.06858000
O	-1.73143800	-0.95837200	-1.92165900

5B

-4315.123896

Rh	0.30080600	-0.28567800	-3.66370600
O	-0.24796400	1.68731800	-3.53573300
O	0.87553500	-2.25522100	-3.69077200
O	-0.17313200	1.63430200	-1.27032700
O	0.82287400	-2.36480100	-1.42841200
O	2.25745700	0.31013800	-3.60773900
O	-1.65345200	-0.91979400	-3.61008100
O	2.31683300	0.12976200	-1.34854700
C	-2.21220800	-1.07034000	-2.48554000
C	2.83831800	0.36406400	-2.48198900
C	-0.30212400	2.22189400	-2.38872200
C	0.98316000	-2.86349400	-2.58583400
Rh	0.32210700	-0.36565300	-1.26967200
C	4.30464700	0.81765600	-2.48671500
C	5.03231000	-1.42981700	-1.58625400
C	6.06540000	0.47524600	-0.72663900
O	4.29531900	-2.10281100	-2.27702300
C	6.05891500	-1.86958100	-0.58169700
O	6.32319400	1.64877900	-0.57765200
C	6.68905100	-0.72713500	-0.07720500
C	6.41824400	-3.13592500	-0.15159800
C	7.70102500	-0.82303000	0.86262400
Cl	5.58784500	-4.57152100	-0.75617400
C	7.44739300	-3.24853700	0.80060500
C	8.08456900	-2.10285300	1.30160900
Cl	8.49403900	0.62366300	1.49543200
Cl	7.93992200	-4.84794100	1.36777500
Cl	9.37799700	-2.26597600	2.49511800
C	-0.59066400	3.73181000	-2.34767300
N	0.13847800	4.33456500	-1.23421000
C	1.49847300	4.13046300	-0.98830300
C	-0.46820100	5.16366000	-0.28599100
O	2.24468500	3.48696400	-1.69639700
C	1.79282200	4.88035100	0.27820300
O	-1.62796400	5.51515600	-0.31361500
C	0.61524100	5.51247600	0.69165300
C	2.96759800	5.00472000	1.00138000
C	0.58715800	6.29565200	1.83197000
Cl	4.44078600	4.17680900	0.49104100
C	2.95064300	5.79415100	2.16501000
C	1.77211800	6.43623000	2.57497600
Cl	-0.89917000	7.10537600	2.34411500
Cl	1.77395100	7.42870500	4.03832900
C	-3.64542900	-1.62476700	-2.48465800
N	-4.48475900	-0.82994800	-1.58581800
C	-4.64664500	0.55404300	-1.69548200
C	-5.23512800	-1.38532900	-0.54260700
O	-4.07043000	1.26449700	-2.49089400
C	-5.64458700	0.92703200	-0.63554600
O	-5.25411500	-2.55650500	-0.23596100
C	-5.98470000	-0.23341800	0.06722600
C	-6.21138600	2.14905300	-0.31696100
C	-6.88768500	-0.19684500	1.11671900
Cl	-5.79989500	3.60637000	-1.22880500
C	-7.13192300	2.20092700	0.74405800
C	-7.46506000	1.03929200	1.45763000
Cl	-7.30714100	-1.66455700	2.00651700
Cl	-7.87343800	3.74547500	1.18250000
Cl	-8.62104300	1.12558400	2.79066200
C	1.39763000	-4.34082900	-2.65253400
N	0.73090900	-5.08730100	-1.58599700
C	-0.63615100	-5.01101300	-1.31466500
C	1.40968300	-5.96650400	-0.73116700
O	-1.43831000	-4.35136100	-1.94297000
C	-0.86125000	-5.90700200	-0.12985600
O	2.59232400	-6.21786600	-0.78343800
C	0.36238000	-6.49625400	0.20725400
C	-2.01416300	-6.18875200	0.58441000
C	0.46022500	-7.39403300	1.25697300
Cl	-3.54244900	-5.40066900	0.18714000
C	-1.92921300	-7.09982000	1.65271200
C	-0.70466000	-7.70029500	1.98341800
Cl	2.00709300	-8.13631700	1.67619200
Cl	-3.37932700	-7.48656500	2.58501800
Cl	-0.62031500	-8.84593100	3.32560300
H	2.46383700	-4.36420200	-2.39773000
H	-3.57839700	-2.61210000	-2.01460200
H	-1.64968100	3.84139400	-2.08579500
H	4.30954100	1.80856000	-2.01953300
Cl	4.42941000	5.97721000	3.11571500
N	5.09273400	-0.03523600	-1.59615500
C	-0.31329500	4.44270800	-3.67516200
H	-0.91019700	3.99175600	-4.47074000
H	-0.58303900	5.49951700	-3.58635300
H	0.74251800	4.36137700	-3.94580100

C	-4.26056600	-1.74801900	-3.87999300
H	-3.63620400	-2.39328900	-4.50209500
H	-5.25752700	-2.19329600	-3.80315600
H	-4.33534100	-0.77149400	-4.36403100
C	1.17844800	-4.97927600	-4.02655200
H	1.72647200	-4.41967900	-4.78742100
H	1.54622000	-6.00980500	-4.01315800
H	0.11809700	-4.97817800	-4.29268900
C	4.91957200	0.89598900	-3.88625200
H	4.34113600	1.58115400	-4.51002400
H	5.94558700	1.26965900	-3.81270700
H	4.92512800	-0.08570600	-4.36730300
C	-1.96188900	0.75764500	2.22575500
C	-0.51874100	0.28586100	2.27220600
C	-0.15061800	-0.86136300	1.54268600
C	0.45783000	0.89251100	3.07231300
C	1.14142900	-1.40009800	1.62322000
H	-0.90241200	-1.38616600	0.95998000
C	1.74938200	0.36776500	3.16447900
H	0.22100100	1.79156100	3.62708400
C	2.07944900	-0.77813900	2.44569300
H	1.39729500	-2.28711600	1.05605900
H	2.48701900	0.84692500	3.79928800
Br	3.83884800	-1.53205800	2.62801800
C	-2.09888900	2.27997200	2.12287000
O	-1.19432400	3.09123200	2.12533300
O	-3.39552600	2.63166300	1.99799900
C	-3.65611500	4.05212100	1.94048800
H	-4.74161900	4.14617600	1.95006500
H	-3.21938300	4.54998300	2.80922700
H	-3.23593900	4.48361300	1.03148900
H	-2.39464400	0.38797600	1.28628700
C	-2.53493800	1.85606300	5.36202800
H	-2.00615500	2.55098700	4.69513700
C	-3.99803200	2.31567500	5.46531600
H	-4.06007500	3.32746900	5.88343600
H	-4.49538400	2.32932200	4.49050300
H	-4.56839000	1.64941800	6.12614300
C	-1.85223200	1.93856200	6.73734400
H	-2.33109900	1.25726600	7.45288400
H	-0.79202700	1.66495500	6.67724200
H	-1.91491100	2.95203400	7.15082100
C	-2.40773500	0.42026700	4.80621200
H	-1.36607700	0.08804800	4.90894800
H	-2.99088600	-0.23817700	5.46699200
C	-2.87303900	0.14190700	3.35991000
H	-3.85982900	0.59270400	3.21176700
C	-3.03372800	-1.37492400	3.15641100
H	-3.37445100	-1.62138500	2.14371200
H	-2.09416700	-1.91003500	3.33450400
H	-3.77712000	-1.77070800	3.85712100
O	-1.69037600	-0.85887400	-1.34461800

R-P_B

-747.868272

C	-1.97436900	0.74125700	2.31416700
C	-0.53230900	0.26210100	2.31463600
C	-0.16424900	-0.78164000	1.45384100
C	0.45570300	0.79716000	3.15604200
C	1.13395100	-1.29335600	1.43097400
H	-0.90478600	-1.20759200	0.78104600
C	1.75978100	0.30048400	3.14619800
H	0.21881800	1.62987500	3.80652800
C	2.08858700	-0.74523200	2.28475600
H	1.39603000	-2.10088800	0.75611600
H	2.51196400	0.72847800	3.79994400
Br	3.88596000	-1.43517500	2.26777100
C	-2.10924900	2.26075600	2.21187300
O	-1.25960400	3.09393400	2.44448800
O	-3.35640700	2.58518100	1.79379600
C	-3.61458500	3.99250900	1.65543500
H	-4.64175700	4.06664900	1.29719100
H	-3.50549000	4.49962300	2.61776600
H	-2.92235600	4.43975400	0.93750100
H	-2.44175300	0.36940500	1.39375800
C	-2.51993700	1.85857400	5.46840900
H	-1.92755000	2.53590300	4.84099900
C	-3.96906900	2.37201400	5.48334100
H	-4.02078200	3.37513500	5.92336300
H	-4.39908500	2.43089600	4.47779300
H	-4.61134100	1.71419200	6.08432900
C	-1.92338300	1.90647700	6.88466600
H	-2.47699900	1.24747100	7.56668700
H	-0.87523000	1.58420900	6.88956000
H	-1.96402300	2.92150500	7.29724000
C	-2.40665300	0.42183000	4.91152200
H	-1.36913400	0.07834900	5.01781800
H	-2.99985900	-0.23048300	5.57006600
C	-2.87413200	0.14310700	3.46633800
H	-3.86352800	0.59141200	3.31980400
C	-3.02919500	-1.37389400	3.26143500
H	-3.39228200	-1.60895200	2.25359600
H	-2.07921700	-1.89986000	3.40782000
H	-3.75060100	-1.78165600	3.97836100

4C

-4315.068882

Rh	0.37118300	0.16694000	-4.20316400
O	0.12626000	2.22406200	-4.17291600
O	0.63744900	-1.87530500	-4.07082100
O	0.22100200	2.27475900	-1.90464300
O	0.50697400	-1.83736900	-1.80371800
O	2.41509900	0.43225900	-4.14440900
O	-1.66574800	-0.11363900	-4.10154100
O	-1.67321200	0.06632400	-1.83606400
O	2.45380500	0.38163800	-1.87428400
C	-2.22569100	-0.09421900	-2.97334300
C	2.99425700	0.45766600	-3.02652000
C	0.14460000	2.80945000	-3.05998300
C	0.62074800	-2.41603100	-2.93569500
Rh	0.38896400	0.23711000	-1.73505800
C	4.51669300	0.67220000	-3.05129900
C	4.90249800	-1.46769700	-1.75655500
C	6.19754300	0.38928800	-1.20523700
O	4.08240900	-2.14644700	-2.34030000
C	5.84030100	-1.86398800	-0.64896900
O	6.63641300	1.51531200	-1.26390700
C	6.62014600	-0.75019500	-0.32125200
C	6.01137600	-3.07324500	0.00369100
C	7.58990400	-0.81842000	0.66491100
Cl	5.00745200	-4.47224800	-0.39978100
C	6.99354000	-3.15910700	1.00636600
C	7.77643900	-2.04136200	1.33410300
Cl	8.56951900	0.59271100	1.07494000
Cl	7.23987200	-4.68742000	1.85819000
Cl	9.00555100	-2.16722300	2.59692800
C	0.03082300	4.34382800	-3.04581600
N	0.84144600	4.86825800	-1.94566400
C	2.19600400	4.56260300	-1.77356600
C	0.28891600	5.50306300	-0.82963500
O	2.87382600	3.93583300	-2.56036600
C	2.57939000	5.16098900	-0.45104900
O	-0.88341500	5.78229500	-0.69230200
C	1.43523700	5.73492500	0.11084200
C	3.79569600	5.19263000	0.20970700
C	1.48119100	6.36175500	1.34339300
Cl	5.22687900	4.42821500	-0.48464700
C	3.85722300	5.83097100	1.46115100
C	2.71046100	6.41250700	2.02245400
Cl	0.02763500	7.07964600	2.05345000
Cl	2.80763700	7.21121600	3.59739300
C	-3.74084000	-0.35948800	-2.94477200
N	-4.39328900	0.55456700	-2.00507800
C	-4.21034600	1.93888100	-2.00881200
C	-5.29551500	0.12530800	-1.02621400
O	-3.47627200	2.54857300	-2.75672500
C	-5.10548600	2.46544800	-0.92050400
O	-5.61510600	-1.02408600	-0.81857300
C	-5.75997600	1.37721400	-0.33405600
C	-5.34138200	3.76058400	-0.48933600
C	-6.66816200	1.55810600	0.69516800
Cl	-4.50200400	5.13027700	-1.22251300
C	-6.26160000	3.95904700	0.55610300
C	-6.91970900	2.86705700	1.14283800
Cl	-7.49776600	0.17943400	1.42894300
Cl	-6.58961200	5.59708100	1.13198300
Cl	-8.07469300	3.13577700	2.45349000
C	0.80615900	-3.94225100	-2.87554200
N	-0.03327300	-4.49402200	-1.81093800
C	-1.41236300	-4.27882500	-1.72303100
C	0.48168800	-5.16846000	-0.69968100
O	-2.07523600	-3.65912300	-2.52746300
C	-1.84578600	-4.96031700	-0.45571100
O	1.65390200	-5.40659300	-0.50288900
C	-0.70910600	-5.50212800	0.15379800
C	-3.10109600	-5.10186600	0.11280900
C	-0.80024700	-6.20313700	1.34430600
Cl	-4.52767300	-4.39493300	-0.64608500
C	-3.20815100	-5.81479400	1.32112100
C	-2.06847500	-6.36187600	1.93049600
Cl	0.63945800	-6.88611800	2.10947100
Cl	-4.79268500	-6.02193400	2.07422100
Cl	-2.22379900	-7.25640800	3.44660800
H	1.83616900	-4.10650600	-2.53738200
H	-3.86244500	-1.35609900	-2.50516200
H	-1.00459500	4.57008900	-2.76528500
H	4.67506900	1.71695100	-2.75922800
Cl	5.39409100	5.89779400	2.33240100
N	5.16505000	-0.12105100	-2.00447700
C	0.36589100	4.99765200	-4.38717100
H	-0.29129200	4.59862400	-5.16295600
H	0.21605700	6.07954200	-4.31780200
H	1.40057900	4.79483100	-4.67308900
C	-4.39519800	-0.31589100	-4.32727700
H	-3.91600900	-1.04377500	-4.98535400
H	-5.45723400	-0.56583500	-4.23877600
H	-4.29217900	0.67449600	-4.77810700
C	0.57673300	-4.64371600	-4.21553200
H	1.25245300	-4.22945600	-4.96677300
H	0.77777200	-5.71448800	-4.11052000
H	-0.45012400	-4.50107200	-4.56024300
C	5.14429900	0.41568500	-4.42408200
H	4.67808700	1.06092400	-5.17123500
H	6.21523200	0.63775400	-4.38416600
H	5.00090100	-0.62406600	-4.73083100
C	0.44108900	0.39937800	0.28297400
C	1.00181200	-0.49245200	1.24948400
C	1.76322800	-1.62686400	0.85340500
C	0.79173400	-0.28978600	2.64531400
C	2.26642300	-2.51774400	1.79095500
H	1.94983700	-1.79446200	-0.19817600
C	1.28532100	-1.17621100	3.58602900
H	0.21956200	0.56752000	2.98365300
C	2.02076500	-2.28861600	3.15020600
H	2.83055300	-3.38688500	1.47205100
H	1.11141300	-1.01656300	4.64408200
Br	2.70392400	-3.51032300	4.44446700
C	-0.06669700	1.69925900	0.79923000
O	0.70451100	2.61806000	1.00970200
O	-1.39076900	1.74869600	0.97537200
C	-1.91848800	3.02286000	1.41629700
H	-2.96437800	2.82888000	1.65089900
H	-1.38434500	3.37096100	2.30323000
H	-1.82790100	3.76531300	0.62121800
H	-2.62134900	-0.62400600	1.83167700
C	-4.34698900	0.41891900	5.61526700
H	-4.92840100	-0.43384600	5.99905700
C	-3.06573900	0.53102500	6.45589900
H	-3.30314600	0.73870900	7.50600800
H	-2.47212400	-0.38924800	6.42857500
H	-2.43174400	1.35183600	6.09291000
C	-5.20641500	1.68235100	5.77623300
H	-4.66862900	2.57052200	5.41785000
H	-6.14056700	1.60795900	5.20699000
H	-5.46604800	1.85664300	6.82723600
C	-4.05776000	0.14831300	4.12503800
H	-5.01114900	0.16532600	3.57788300
H	-3.45965500	0.98165200	3.72115500
C	-3.34633100	-1.17696800	3.81656700
H	-2.35452600	-1.18927000	4.28855000
H	-3.91073700	-2.00381100	4.27101500
C	-3.19036900	-1.42938500	2.31211300
H	-2.66000600	-2.36978500	2.12024800
H	-4.16389500	-1.49140500	1.81156300

$TSC_{4\text{-}5}$

-4315.029506

Rh	0.59629400	-0.45958400	-3.97581300
O	0.44923500	1.59974500	-4.12677200
O	0.80570100	-2.49047700	-3.68019300
O	0.24582900	1.80367300	-1.87563500
O	0.22919200	-2.31350100	-1.49280300
O	2.60137600	-0.22630300	-3.62806500
O	-1.45021300	-0.73844500	-4.16842900
O	-1.81000700	-0.39488000	-1.95308900
O	2.28831900	-0.18683100	-1.37964000
C	-2.17046200	-0.71155900	-3.13359300
C	3.00416500	-0.18379400	-2.42960200
C	0.40821900	2.25968400	-3.05123000
C	0.57122300	-2.96296700	-2.53659000
Rh	0.22637500	-0.23852100	-1.57934600
C	4.52191400	-0.05054700	-2.22709600
C	4.62636200	-2.32449600	-1.11176300
C	5.97917700	-0.62645900	-0.26727200
O	3.82223800	-2.88203800	-1.83021200
C	5.45349400	-2.89861300	0.00567600
O	6.48635400	0.46837300	-0.16873500
C	6.27117200	-1.88035900	0.50675700
C	5.51828200	-4.18242800	0.52021400
C	7.17360400	-2.12162000	1.52866700
Cl	4.47221200	-5.46761800	-0.09874400
C	6.43386800	-4.44470300	1.55441300
C	7.25540200	-3.42309100	2.05354000
Cl	8.20136400	-0.82945300	2.15682700
Cl	6.54681700	-6.07378300	2.22984800
Cl	8.39982300	-3.77031300	3.35447900
C	0.53648800	3.79215000	-3.15774000
N	1.20028900	4.30412200	-1.95908200
C	2.44486500	3.85379200	-1.50754900
C	0.55966400	5.13207200	-1.03267000
O	3.16599800	3.08414400	-2.10665500
C	2.65884500	4.52337700	-0.18115300
O	-0.55762000	5.58698600	-1.15979200
C	1.53141800	5.30189400	0.09687000
C	3.71998800	4.45617500	0.70599300
C	1.43956700	6.03850500	1.26454200
Cl	5.12206000	3.43766800	0.37137500
C	3.64103400	5.20305000	1.89501900
C	2.51201200	5.98890400	2.17128500
Cl	0.00610900	7.01469600	1.61350700
Cl	2.43223000	6.92097700	3.67211300
C	-3.61612200	-1.21449000	-3.29090500
N	-4.46886000	-0.66624800	-2.23419300
C	-4.86324800	0.67668300	-2.15785100
C	-4.76380700	-1.37485600	-1.06843300
O	-4.61306700	1.53635200	-2.97149000
C	-5.62550800	0.79871100	-0.86568700
O	-4.41837600	-2.51200900	-0.82212900
C	-5.56007200	-0.43334000	-0.20890300
C	-6.29987800	1.87226400	-0.30816400
C	-6.16163600	-0.61924700	1.02449400
Cl	-6.37683600	3.42870000	-1.14056900
C	-6.92272900	1.69526900	0.94075000
C	-6.85268700	0.45943400	1.60304100
Cl	-6.06334000	-2.17781200	1.85911500
Cl	-7.79542600	3.04046500	1.68066700
Cl	-7.63476300	0.25651700	3.17413900
C	0.74311800	-4.47723400	-2.33246000
N	-0.41585100	-4.99964500	-1.59934200
C	-1.72717300	-4.95438100	-2.08195900
C	-0.34626500	-5.44810100	-0.27478300
O	-2.06575200	-4.48494900	-3.14813400
C	-2.57766900	-5.56104300	-1.00276300
O	0.65895100	-5.49327100	0.40048700
C	-1.75232200	-5.83309900	0.09333200
C	-3.93186300	-5.84742200	-0.97024600
C	-2.26744300	-6.37487300	1.25919800
Cl	-4.95761800	-5.56003500	-2.37839300
C	-4.46870600	-6.39656600	0.20744600
C	-3.64452900	-6.65343100	1.31430300
Cl	-1.22210500	-6.70983300	2.64535700
Cl	-6.19398500	-6.76740100	0.29096100
Cl	-4.33846700	-7.33785200	2.78895000
H	1.58599700	-4.58456400	-1.64146000
H	-3.55721600	-2.28819000	-3.07382700
H	-0.47993500	4.19971600	-3.10532700
H	4.68143900	0.95013800	-1.81243600
Cl	4.97762400	5.14636100	3.05104000
N	4.98485300	-0.97843900	-1.19018500
C	1.21374300	4.26044000	-4.44808400
H	0.65803900	3.88735500	-5.31102800
H	1.22749700	5.35424600	-4.48114800
H	2.23806300	3.88579300	-4.50846500
C	-4.19888500	-1.02095500	-4.69302500
H	-3.55752400	-1.53043800	-5.41460100
H	-5.20009500	-1.46069500	-4.74047900
H	-4.25819200	0.03548800	-4.95943800
C	1.02108200	-5.25461100	-3.61837600
H	1.92975300	-4.86555600	-4.08324000
H	1.17205600	-6.31321200	-3.38398200
H	0.19851700	-5.15426500	-4.32911800
C	5.32810400	-0.21164300	-3.51834400
H	5.00388400	0.52829600	-4.25320200
H	6.39057900	-0.05471700	-3.30716100
H	5.18615900	-1.20689200	-3.94828800
C	-0.09231700	0.03947900	0.70756700
C	0.95599400	-0.54402700	1.56322000
C	1.23304400	-1.92549300	1.46410600
C	1.69655700	0.20603000	2.50088700
C	2.17014100	-2.54524900	2.28470100
H	0.71285700	-2.52446100	0.72567600
C	2.65666900	-0.39953500	3.30965500
H	1.53218300	1.27254300	2.57983000
C	2.87534500	-1.77387400	3.21099600
H	2.34145500	-3.61259400	2.19610000
H	3.22057300	0.19505100	4.02031400
Br	4.15467300	-2.61434200	4.37302100
C	-0.51087100	1.45779600	0.86284500
O	0.26178200	2.36168600	1.13749600
O	-1.81720500	1.67509000	0.59149500
C	-2.23522100	3.05409300	0.59700500
H	-3.31735100	3.02759500	0.46920600
H	-1.97053300	3.53219100	1.54296300
H	-1.77283100	3.59806600	-0.22693000
H	-0.96812100	-0.69293600	0.45977900
C	-2.03394900	-0.39642500	5.21438900
H	-2.88728300	-1.07405700	5.37564300
C	-0.76702500	-1.09607100	5.73164600
H	-0.83381900	-1.26992300	6.81179500
H	-0.60278300	-2.06851500	5.25466500
H	0.12314600	-0.48167800	5.54612100
C	-2.30302100	0.89238200	6.00555400
H	-1.47984200	1.60794400	5.88161200
H	-3.22540300	1.38302300	5.67228000
H	-2.40201200	0.68363000	7.07688600
C	-1.96246900	-0.08710500	3.70527000
H	-2.86232900	0.47361700	3.41610500
H	-1.10997100	0.57861800	3.51798900
C	-1.84785800	-1.32852100	2.81049500
H	-0.90930700	-1.86940200	2.98457700
H	-2.64359200	-2.04799500	3.07852400
C	-2.03178300	-1.08737300	1.34797000
H	-2.08759400	-1.98079300	0.72172300
H	-2.72437400	-0.30719200	1.05070700

5C

-4315.126779

Rh	0.55539700	-0.05128800	-4.07502200
O	0.20959400	1.95427500	-3.83782400
O	0.90390400	-2.06819600	-4.21886900
O	0.02829600	1.73562800	-1.58892900
O	0.57652900	-2.33870900	-1.99351500
O	2.54626000	0.28887700	-3.76157000
O	-1.45602600	-0.41896800	-4.28897900
O	-1.73716300	-0.54522600	-2.04301800
O	2.32960700	-0.06650000	-1.53210900
C	-2.15328200	-0.56701300	-3.24462400
C	2.99903600	0.17943700	-2.58252400
C	0.08262800	2.41017200	-2.66334100
C	0.80352400	-2.76605600	-3.16815500
Rh	0.29329400	-0.31071900	-1.70812200
C	4.50297700	0.42457300	-2.39710900
C	4.85613800	-1.98236000	-1.70578400
C	5.98842100	-0.32887800	-0.51475700
O	4.12821100	-2.47730800	-2.54124600
C	5.70785400	-2.65642100	-0.66753500
O	6.35749000	0.77895800	-0.19439500
C	6.39366800	-1.66438500	0.04121400
C	5.87870900	-3.99806400	-0.36960300
C	7.27053800	-1.98951100	1.06200300
Cl	4.98665000	-5.24604800	-1.24345900
C	6.76931100	-4.34323200	0.66313900
C	7.46010200	-3.34809700	1.37159400
Cl	8.13201800	-0.73194200	1.95572200
Cl	7.01795200	-6.04525100	1.06821700
Cl	8.57702800	-3.80152400	2.66415100
C	-0.06600900	3.93485200	-2.53433400
N	0.68610700	4.40564300	-1.37096200
C	1.99303200	4.01657900	-1.06704900
C	0.17916100	5.35226700	-0.47610700
O	2.67016900	3.26527300	-1.73713100
C	2.34341200	4.74365200	0.19874000
O	-0.91191000	5.87381100	-0.56516500
C	1.26539300	5.56824100	0.53730500
C	3.49108800	4.70559000	0.97350800
C	1.31983400	6.39361300	1.64653200
Cl	4.83045800	3.62997100	0.56501700
C	3.55367000	5.53200700	2.10939600
C	2.48007000	6.37299800	2.43958400
Cl	-0.02904000	7.46267000	2.05536500
Cl	2.58404700	7.41442200	3.86481800
C	-3.65020200	-0.85477000	-3.43812900
N	-4.42673300	-0.04540600	-2.49648200
C	-4.28205000	1.33678600	-2.35881300
C	-5.39607100	-0.58107200	-1.63926700
O	-3.49148100	2.02316800	-2.97111200
C	-5.28321200	1.74447000	-1.31504100
O	-5.70439500	-1.74945600	-1.57039600
C	-5.94332200	0.59238600	-0.87406900
C	-5.59945300	2.99208600	-0.80451700
C	-6.92669200	0.65871400	0.09864500
Cl	-4.78217800	4.44566700	-1.38826000
C	-6.59820200	3.07469600	0.18148800
C	-7.25317300	1.91849300	0.63269900
Cl	-7.75342900	-0.79934800	0.65612000
Cl	-7.03709800	4.65115400	0.85134500
Cl	-8.50126400	2.04250700	1.87701500
C	1.02340700	-4.27845200	-3.32048100
N	0.11744800	-4.99619400	-2.42338900
C	-1.25140700	-4.74104800	-2.32570400
C	0.54654800	-6.01574000	-1.56268900
O	-1.86148400	-3.92706200	-2.98801200
C	-1.76006800	-5.67696400	-1.26587200
O	1.68171700	-6.42564600	-1.47593600
C	-0.68502300	-6.45451900	-0.82125800
C	-3.03069100	-5.84209600	-0.73949400
C	-0.85688500	-7.42581700	0.15062900
Cl	-4.37292300	-4.82517200	-1.26958900
C	-3.21957300	-6.82581400	0.24799000
C	-2.14369600	-7.61294500	0.68662300
Cl	0.50344100	-8.40605300	0.70603300
Cl	-4.82690900	-7.06808700	0.94048000
Cl	-2.40234200	-8.84608100	1.92534900
H	2.02989300	-4.47682900	-2.93366400
H	-3.79842600	-1.89179500	-3.11685800
H	-1.11814900	4.12312700	-2.29106800
H	4.58360900	1.35360100	-1.82283600
Cl	4.99998200	5.51083700	3.12528100
N	5.07501200	-0.61365600	-1.53774900
C	0.31205900	4.69706100	-3.80709100
H	-0.30392500	4.35716200	-4.64245200
H	0.14090600	5.76717400	-3.65487300
H	1.36186900	4.53143300	-4.06313700
C	-4.13283900	-0.67653100	-4.87885000
H	-3.56380100	-1.33105700	-5.54286100
H	-5.19232000	-0.94273400	-4.94643700
H	-3.99615000	0.35486900	-5.21312800

C	0.91414900	-4.77270900	-4.76507300
H	1.63551200	-4.24557300	-5.39300900
H	1.13105000	-5.84469600	-4.80240400
H	-0.08768300	-4.59310300	-5.16388000
C	5.27170300	0.55521800	-3.71421000
H	4.85489700	1.37106000	-4.30901600
H	6.32254500	0.77621600	-3.50261300
H	5.20538200	-0.36576400	-4.29929400
C	-2.00838500	1.38742800	1.68564800
C	-0.71648600	0.58804800	1.71821500
C	-0.67120900	-0.61397100	0.98392300
C	0.38650800	0.91183600	2.51381000
C	0.42988900	-1.47714300	1.05747500
H	-1.53296900	-0.91296600	0.39316000
C	1.49615300	0.06211200	2.59560500
H	0.39531100	1.83784200	3.07421800
C	1.50659400	-1.12705600	1.87636300
H	0.43595800	-2.40797900	0.50330400
H	2.33653200	0.32713400	3.22827300
Br	2.99495400	-2.33001100	2.04636500
C	-1.84381600	2.90167200	1.82628100
O	-0.79820300	3.51414000	1.92744500
O	-3.04694200	3.50439600	1.79520600
C	-3.03860100	4.94035200	1.95410800
H	-4.08794900	5.23348700	1.94872500
H	-2.56781200	5.20791400	2.90328300
H	-2.49765300	5.41205900	1.13327300
H	-2.44344500	1.25997500	0.68442000
C	-2.52152000	2.07744400	6.39953300
H	-3.35467700	1.46294800	6.77542900
C	-1.20833200	1.42150300	6.85444700
H	-1.13992500	1.40169600	7.94858900
H	-1.11639400	0.38911000	6.50048400
H	-0.34201000	1.98279300	6.47917100
C	-2.66172900	3.48084900	7.00828500
H	-1.85394000	4.14006000	6.66398300
H	-3.61423900	3.94576200	6.72666800
H	-2.61588800	3.44532500	8.10316600
C	-2.64940300	2.14288100	4.86328300
H	-3.56358100	2.69963800	4.61287700
H	-1.81161400	2.73774600	4.47175500
C	-2.70238800	0.77293400	4.16778800
H	-1.74978900	0.24475600	4.29498300
H	-3.45863400	0.15647100	4.67440800
C	-3.07008500	0.80109300	2.67399900
H	-3.26050600	-0.22893900	2.34788500
H	-4.00411800	1.35528400	2.53226700

R-P_C

-747.869693

C	-2.03561900	1.32622400	1.77549000
C	-0.74760800	0.52078200	1.73791300
C	-0.65388500	-0.54068600	0.82668100
C	0.33467300	0.74420300	2.60211400
C	0.47135300	-1.36336800	0.77073900
H	-1.47678200	-0.73226400	0.14114700
C	1.47016400	-0.06688800	2.55885000
H	0.30867200	1.57521000	3.29569800
C	1.52883000	-1.11718600	1.64446500
H	0.52469000	-2.17718700	0.05581400
H	2.30121600	0.12228400	3.22963000
Br	3.09287200	-2.23874500	1.58264500
C	-1.84042100	2.83553700	1.90403500
O	-0.84749800	3.42397200	2.27677300
O	-2.97318800	3.47482700	1.53072300
C	-2.93531300	4.90790000	1.62929000
H	-3.91344100	5.24968500	1.28957800
H	-2.75710000	5.21747200	2.66264800
H	-2.14336800	5.31510100	0.99536900
H	-2.53377600	1.19522000	0.80675500
C	-2.55439300	2.11071900	6.52717200
H	-3.36687000	1.46962800	6.90426500
C	-1.22092100	1.50479700	6.99275800
H	-1.15768400	1.49299500	8.08746500
H	-1.09123800	0.47461000	6.64405500
H	-0.37341000	2.09449000	6.61825600
C	-2.74723000	3.51260700	7.12467400
H	-1.96189000	4.19718200	6.77827300
H	-3.71449900	3.94109100	6.83521900
H	-2.70550000	3.48728900	8.22013800
C	-2.67441800	2.15954700	4.98970100
H	-3.61103500	2.67631700	4.73133700
H	-1.86094600	2.78243400	4.59551900
C	-2.67222700	0.78206100	4.30639000
H	-1.69634600	0.29618500	4.42351000
H	-3.39300800	0.13700100	4.82954300
C	-3.06765500	0.77862100	2.81953000
H	-3.27258200	-0.25650400	2.51959600
H	-4.00296200	1.33546000	2.68434500

4D

-4315.063866

Rh	0.31550200	0.04363000	-4.32218700
O	-0.04552600	2.08259400	-4.32898600
O	0.69789900	-1.97693100	-4.15810900
O	-0.04868000	2.16054700	-2.05960200
O	0.48946400	-1.92463500	-1.89727500
O	2.33521100	0.43123200	-4.19157600
O	-1.70461600	-0.35631100	-4.29311400
O	2.29375500	0.40827800	-1.92148000
C	-2.30370300	-0.36907100	-3.18527600
C	2.87056100	0.50507300	-3.05402800
C	-0.10478800	2.67916000	-3.22332600
C	0.68035400	-2.50604300	-3.01762200
Rh	0.23710400	0.13822900	-1.85621700
C	4.37678500	0.81347800	-3.02551100
C	4.84192400	-1.28835700	-1.69429200
C	6.00303400	0.64753700	-1.11713700
O	4.08730500	-2.02054700	-2.30126900
C	5.75804400	-1.61725300	-0.54715400
O	6.37712000	1.79689800	-1.17309700
C	6.45811900	-0.45604500	-0.20418300
C	5.97466600	-2.80750900	0.12656600
C	7.39141200	-0.45659500	0.81884300
Cl	5.07099500	-4.26761400	-0.29657700
C	6.92070400	-2.82475900	1.16683700
C	7.62332000	-1.65936700	1.51005500
Cl	8.26950100	1.01435600	1.24832600
Cl	7.22316500	-4.32695800	2.04665900
Cl	8.80719500	-1.69932900	2.82077000
C	-0.30070500	4.20521900	-3.23400700
N	0.42989800	4.78546600	-2.10637200
C	1.78856000	4.55320300	-1.86620800
C	-0.20532500	5.41473800	-1.03206100
O	2.53369900	3.94973500	-2.60919800
C	2.07799700	5.19322900	-0.53932800
O	-1.39494600	5.63902700	-0.95685600
C	0.88163400	5.72003800	-0.04370000
C	3.25807900	5.29657600	0.17745000
C	0.83752100	6.37000900	1.17701400
Cl	4.75658900	4.59229900	-0.43357100
C	3.22785200	5.95819000	1.41787000
C	2.02863800	6.49228300	1.91266200
Cl	-0.68132200	7.02887000	1.80260300
Cl	2.01133600	7.32176400	3.47463200
C	-3.79853100	-0.73277400	-3.20853500
N	-4.54094900	0.13826600	-2.29573900
C	-4.45729000	1.53153500	-2.30880100
C	-5.43218600	-0.34758400	-1.33274400
O	-3.74870700	2.18624300	-3.04315300
C	-5.41449100	2.00151100	-1.24757100
O	-5.67888300	-1.51459900	-1.12713900
C	-5.99593600	0.87365300	-0.65902400
C	-5.75510200	3.28003400	-0.83716500
C	-6.92764800	0.99700500	0.35779000
Cl	-5.01296500	4.70122600	-1.57792600
C	-6.70306100	3.42035300	0.19269300
C	-7.28293000	2.28840300	0.78630200
Cl	-7.65529500	-0.43211800	1.10302900
Cl	-7.16424600	5.03535600	0.74159700
Cl	-8.46797500	2.48435800	2.08296900
C	0.96999300	-4.01464500	-2.93282200
N	0.12816700	-4.61649500	-1.89759300
C	-1.26432300	-4.49203700	-1.86385600
C	0.64167200	-5.26732400	-0.77171900
O	-1.93396300	-3.91383700	-2.69314400
C	-1.70188600	-5.20636500	-0.61640700
O	1.81795600	-5.43557700	-0.53206500
C	-0.55760500	-5.68051700	0.03391800
C	-2.96667800	-5.43052800	-0.09783100
C	-0.64992000	-6.39481600	1.21641700
Cl	-4.40468000	-4.80830000	-0.90723800
C	-3.07440200	-6.15815300	1.10131500
C	-1.92725300	-6.63705200	1.75223300
Cl	0.79937700	-6.99292100	2.03268700
Cl	-4.67146700	-6.47042600	1.79082000
Cl	-2.08452100	-7.54956100	3.25715000
H	1.99432500	-4.10248200	-2.55162900
H	-3.87054900	-1.73443300	-2.76954200
H	-1.35844600	4.37864800	-3.00318300
H	4.45897800	1.86814900	-2.73740400
Cl	4.71567400	6.11465600	2.35984100
N	5.03300500	0.06934800	-1.94771000
C	0.05925300	4.86164300	-4.56780000
H	-0.53711000	4.41688900	-5.36745400
H	-0.15443900	5.93395400	-4.52066600
H	1.11610000	4.71498500	-4.80252300
C	-4.40550700	-0.73460200	-4.61322400
H	-3.85804700	-1.43184000	-5.25091600
H	-5.45176500	-1.05202100	-4.56026300
H	-4.35058500	0.25923900	-5.06476500
C	0.84699500	-4.74135500	-4.27333800
H	1.52167000	-4.28525600	-5.00091900
H	1.12013100	-5.79394500	-4.14895900
H	-0.17227500	-4.67606200	-4.66140100
C	5.06973400	0.58611700	-4.37154500
H	4.59126100	1.19361500	-5.14224000
H	6.12210800	0.87685500	-4.29528700
H	5.00449300	-0.46332400	-4.67184200
C	0.21072500	0.33100400	0.16223100
C	0.81044600	-0.49649700	1.16168000
C	1.62809700	-1.60557600	0.80682500
C	0.58713800	-0.25585700	2.54965000
C	2.16991700	-2.43875000	1.77503600
H	1.82411500	-1.80210800	-0.23810400
C	1.12097700	-1.08395800	3.52101900
H	-0.02004300	0.58824700	2.85868200
C	1.90986300	-2.17443800	3.12525200
H	2.77654100	-3.28982300	1.48672900
H	0.93699300	-0.89556800	4.57262100
Br	2.64806700	-3.31599100	4.46180900
C	-0.40349000	1.60197300	0.63281300
O	0.29702500	2.57109200	0.86570700
O	-1.73588300	1.57252600	0.73438000
C	-2.36150800	2.82823300	1.09081500
H	-3.40876000	2.58372500	1.26243600
H	-1.90995200	3.23793500	1.99710300
H	-2.25871200	3.54584300	0.27480700
H	-3.04892100	-1.88211000	2.46552300
C	-4.59227200	0.58325500	4.35043300
H	-5.19404700	0.79598000	3.45269300
C	-5.52070900	-0.08512900	5.37541100
H	-6.32108900	0.60102200	5.67772100
H	-5.99647500	-0.98453000	4.97164300
H	-4.96923500	-0.37086300	6.28091200
C	-4.07301100	1.92278300	4.89593300
H	-3.47657500	1.77015200	5.80521400
H	-3.43612300	2.43667100	4.16519300
H	-4.89920500	2.59650100	5.15201500
C	-3.41217100	-0.30750600	3.90568000
H	-2.81823900	0.27517300	3.18732400
H	-2.75312900	-0.48454700	4.77040600
C	-3.77950200	-1.66154600	3.25527300
H	-4.74716200	-1.57213300	2.74259700
C	-3.81013100	-2.85371100	4.22163100
H	-4.08289200	-3.77811800	3.69964200
H	-2.82514200	-3.00836200	4.68027400
H	-4.52924700	-2.70954600	5.03422700
O	-1.80292300	-0.16818600	-2.03050900

$TSD_{4\text{-}5}$

-4315.027328

Rh	0.37740800	-0.93916300	-3.88774900
O	0.08577400	1.09343100	-4.09234700

O	0.76606300	-2.93242200	-3.54941500
O	0.06629100	1.36751000	-1.83896800
O	0.35828100	-2.75277100	-1.32505400
O	2.38323400	-0.56261000	-3.71394200
O	-1.67225100	-1.26210000	-3.91299300
O	2.27372300	-0.51034900	-1.44671300
C	-2.32323000	-1.06609500	-2.85321200
C	2.88470100	-0.44556300	-2.55917400
C	0.06665000	1.78789500	-3.03957800
C	0.73696800	-3.37827500	-2.37150200
Rh	0.19540000	-0.65817100	-1.45928600
C	4.38564600	-0.11488800	-2.50267500
C	4.94775800	-2.34572500	-1.44791800
C	6.05395300	-0.45587400	-0.65610800
O	4.18394800	-3.01799900	-2.11111700
C	5.95053600	-2.78978800	-0.41870100
O	6.38114200	0.70602800	-0.56862600
C	6.60570300	-1.65246700	0.06507000
C	6.28923600	-4.05415100	0.03349700
C	7.60102800	-1.74962100	1.02228400
Cl	5.48547200	-5.49516500	-0.59962300
C	7.29961200	-4.16894000	1.00476900
C	7.94696900	-3.02647500	1.49774100
Cl	8.42048200	-0.30764600	1.63114500
Cl	7.75769400	-5.76722600	1.60460100
Cl	9.20869600	-3.19014100	2.72448600
C	-0.00076600	3.31724600	-3.20770300
N	0.72732300	3.95936600	-2.11282800
C	2.05491700	3.66744200	-1.78462500
C	0.11623600	4.80249000	-1.18251300
O	2.78061000	2.92599400	-2.41292200
C	2.34731700	4.46051800	-0.54380200
O	-1.04671900	5.14790500	-1.21004400
C	1.18557800	5.15294300	-0.19042700
C	3.50285300	4.56584900	0.21160400
C	1.15224100	5.97344500	0.92303200
Cl	4.95263700	3.65539900	-0.21363100
C	3.48337300	5.39989200	1.34396000
C	2.31930900	6.09935500	1.69562800
Cl	-0.32427600	6.84177600	1.37003000
Cl	2.31548000	7.14403800	3.12304700
C	-3.85670500	-1.20606900	-2.93257500
N	-4.48752500	-0.11523000	-2.18328300
C	-4.30890900	1.24104800	-2.48137700
C	-5.21667100	-0.31631900	-1.01036300
O	-3.62676700	1.67848900	-3.38157600
C	-5.11278100	1.98745800	-1.45319300
O	-5.43189800	-1.39098100	-0.48852100
C	-5.64696700	1.05180200	-0.56162800
C	-5.35434300	3.34287400	-1.30210600
C	-6.42527400	1.45082500	0.51176100
Cl	-4.68205400	4.51726000	-2.43372600
C	-6.15233200	3.76164600	-0.22128900
C	-6.68009900	2.82355600	0.68024600
Cl	-7.08570400	0.26491800	1.64701700
Cl	-6.49024900	5.48010000	-0.00006000
Cl	-7.67346700	3.36754700	2.03637000
C	1.31593300	-4.78783800	-2.15813100
N	0.51711100	-5.55781700	-1.20003700
C	-0.79407800	-5.98189300	-1.43509000
C	1.01307500	-5.99246900	0.03353500
O	-1.47049100	-5.68299800	-2.39460500
C	-1.15578300	-6.84561900	-0.25659600
O	2.09804800	-5.71389400	0.49562000
C	-0.07300300	-6.84597700	0.62816200
C	-2.31065800	-7.55514500	0.02538700
C	-0.11967600	-7.55492200	1.81741700
Cl	-3.68110200	-7.53947200	-1.09117500
C	-2.37091700	-8.28595700	1.22533500
C	-1.28482800	-8.28486500	2.11453800
Cl	1.24885500	-7.54833200	2.93530600
Cl	-3.82632600	-9.20876300	1.61442300
Cl	-1.37869300	-9.20623600	3.61915400
H	2.27428100	-4.61874100	-1.65377800
H	-4.11424700	-2.10794100	-2.36638800
H	-1.04854400	3.60091200	-3.05435300
H	4.44839300	0.90299300	-2.10400800
Cl	4.94083500	5.56422000	2.33129000
N	5.06855600	-0.95872700	-1.51738400
C	0.46911900	3.80077900	-4.58181100
H	-0.12870000	3.32478100	-5.36182900
H	0.34590400	4.88599700	-4.65297600
H	1.51865600	3.54578200	-4.74631500
C	-4.39652300	-1.31440900	-4.35924700
H	-3.94181700	-2.17411900	-4.85642700
H	-5.48202800	-1.45399500	-4.33487300
H	-4.15843100	-0.41943000	-4.93758100
C	1.55752600	-5.56145300	-3.45614200
H	2.23835000	-4.99165200	-4.09122200
H	2.01829600	-6.52791400	-3.22704900
H	0.62637100	-5.72440600	-4.00271000
C	5.07794700	-0.18017800	-3.86632600
H	4.58695200	0.50202000	-4.56344200
H	6.12522000	0.12019500	-3.75953800
H	5.03007400	-1.18973000	-4.28323500
C	0.11906300	-0.25739900	0.78834000
C	1.30736500	-0.73093400	1.53135600
C	1.65346000	-2.09968300	1.46437600
C	2.11155400	0.10236500	2.33804700
C	2.71287100	-2.62877400	2.19452800
H	1.09756700	-2.75422700	0.80305700
C	3.18503200	-0.41126300	3.06286200
H	1.89943600	1.16224600	2.38798800
C	3.46839000	-1.77599300	3.00215400
H	2.94337500	-3.68643600	2.12377200
H	3.78831300	0.24637700	3.67946700
Br	4.91377500	-2.49083800	4.04967100
C	-0.30407700	1.16164300	0.92212500
O	0.44405100	2.11924600	1.03518700
O	-1.65179100	1.30589400	0.83965400
C	-2.14351000	2.65471700	0.92089600
H	-3.21318900	2.56264700	1.11515700
H	-1.65422500	3.19755800	1.73263700
H	-1.97367300	3.18391500	-0.01801600
H	-1.72702000	-2.72122400	0.10500400
C	-2.43250300	-0.79138000	2.88615800
H	-2.83928900	-0.00949000	2.23357900
C	-3.65578500	-1.49092000	3.54440900
H	-4.18000800	-0.75464700	4.16277200
H	-4.36354100	-1.86801400	2.80187100
H	-3.34635900	-2.31549400	4.19591700
C	-1.54520200	-0.14716500	3.96053400
H	-1.16040900	-0.90309400	4.65603800
H	-0.68669500	0.37384300	3.52893200
H	-2.12125000	0.57869700	4.54417300
C	-1.68240200	-1.74545400	2.00338100
H	-0.80521900	-0.95749800	0.91470100
H	-0.78319300	-2.18941000	2.43602100
C	-2.37543300	-2.59435800	0.97923000
H	-3.29697700	-2.11854500	0.63410000
C	-2.67868400	-4.00576400	1.54320400
H	-3.14828100	-4.60344500	0.75555900
H	-1.76038000	-4.51159000	1.86073400
H	-3.36266500	-3.97536900	2.39456600
O	-1.86236500	-0.79847500	-1.69640500
5D			
-4315.114472			
Rh	0.33565800	-0.33000700	-3.91434700
O	-0.09852400	1.66874100	-3.81763300
O	0.76863100	-2.34037000	-3.90671600
O	-0.15725000	1.62574700	-1.55130200
O	0.56738400	-2.43157500	-1.65159600
O	2.31430800	0.14656200	-3.74748300
O	-1.65556600	-0.80745300	-3.98428000
O	2.23848500	-0.03469600	-1.48893800
C	-2.29516100	-0.90820600	-2.89792400
C	2.83243500	0.17562400	-2.59138100
C	-0.20053000	2.21039100	-2.67758500
C	0.74408800	-2.94900000	-2.79893600
Rh	0.20964900	-0.40364300	-1.51986800
C	4.31477100	0.56820200	-2.51320000
C	4.94379100	-1.77352200	-1.79199200
C	6.02484900	0.01506300	-0.75865700
O	4.18428100	-2.36082200	-2.53385800
C	5.95887400	-2.33245700	-0.83556500
O	6.31315300	1.16213100	-0.49985500
C	6.61333200	-1.25922900	-0.22161100
C	6.28863500	-3.64215500	-0.53044400
C	7.61700400	-1.46980100	0.70837600
Cl	5.44529800	-4.99509700	-1.29152100
C	7.30800100	-3.87156200	0.41124100
C	7.96713900	-2.79483300	1.02419600
Cl	8.44031000	-0.11034700	1.48079900
Cl	7.76093600	-5.52956500	0.82203400
Cl	9.24795300	-3.10251800	2.20256600
C	-0.44416200	3.72740700	-2.66011400
N	0.29307400	4.32819300	-1.54925900
C	1.63603100	4.06710500	-1.26715600
C	-0.27938400	5.24921000	-0.66721100
O	2.35959900	3.34777900	-1.92384600
C	1.95174700	4.87340700	-0.04119900
O	-1.41893500	5.65765900	-0.73594800
C	0.80941300	5.60324700	0.30415200
C	3.11946600	4.97272100	0.69709400
C	0.81506900	6.46837400	1.38404400
Cl	4.54562500	4.01861700	0.27757800
C	3.13450100	5.84079800	1.80313200
C	1.99407100	6.58589300	2.14032000
Cl	-0.61973600	7.41388200	1.80220800
Cl	2.03696200	7.67988400	3.52872100
C	-3.77699800	-1.29948400	-3.01149600
N	-4.60428300	-0.36993100	-2.23534600
C	-4.46991600	1.02056700	-2.26373500
C	-5.71594500	-0.79418400	-1.49619700
O	-3.60755100	1.63119600	-2.85871900
C	-5.59634100	1.55091500	-1.42166600
O	-6.06479300	-1.94491700	-1.35475700
C	-6.34394800	0.46230400	-0.96055600
C	-5.94440900	2.84998100	-1.09210300
C	-7.45616100	0.64636900	-0.15644100
Cl	-5.00190100	4.22291900	-1.68349200
C	-7.07009500	3.05150500	-0.27404000
C	-7.82001900	1.95989900	0.18999800
Cl	-8.39497300	-0.73299700	0.42544200
Cl	-7.54191300	4.69601800	0.17319700
Cl	-9.23177500	2.23387000	1.21590800
C	0.98454600	-4.46662800	-2.82840000
N	0.12771200	-5.10450000	-1.82773400
C	-1.24257700	-4.86732700	-1.71350900
C	0.62148200	-5.94925200	-0.82399300
O	-1.89700300	-4.16848500	-2.46006100
C	-1.68831500	-5.64649300	-0.50900000
O	1.77655400	-6.28721500	-0.70091800
C	-0.57278300	-6.30907200	0.01526600
C	-2.93669400	-5.76835000	0.07902200
C	-0.68060900	-7.11976200	1.13268700
Cl	-4.33540200	-4.89843800	-0.56105700
C	-3.06070100	-6.58937000	1.21435900
C	-1.94374700	-7.26121200	1.73483100
Cl	0.73071200	-7.95463300	1.78844200
Cl	-4.63726500	-6.77236200	1.99074400
Cl	-2.12019300	-8.28936200	3.16063000
H	2.00864800	-4.62159000	-2.46899500
H	-3.87065200	-2.26564900	-2.50512400
H	-1.50255900	3.86499400	-2.41039400
H	4.34229500	1.51583800	-1.96552800
Cl	4.60495100	5.99382400	2.77208400
N	5.04625400	-0.38591200	-1.67712700
C	-0.13470800	4.41326100	-3.99335100
H	-0.73819900	3.97037500	-4.78851100
H	-0.37393900	5.47863700	-3.91987700
H	0.92027500	4.29716300	-4.25504300
C	-4.27136200	-1.41862200	-4.45458500
H	-3.67411500	-2.15956800	-4.99078600
H	-5.31655700	-1.74336100	-4.45614500
H	-4.18574100	-0.46350500	-4.97935500
C	0.81939700	-5.08989200	-4.21599600
H	1.50271800	-4.60994000	-4.91987900
H	1.05383800	-6.15777000	-4.16876000
H	-0.20202000	-4.96059400	-4.58264900
C	4.97694600	0.73749600	-3.88278200
H	4.44477400	1.49514800	-4.46255400
H	6.01326700	1.06301800	-3.74843500

H	4.96071300	-0.19976700	-4.44504700
C	-1.90867500	1.20657100	1.98101100
C	-0.50175500	0.62101200	1.91298300
C	-0.36071900	-0.64165000	1.29912700
C	0.63757200	1.19168900	2.48924600
C	0.85485400	-1.33760000	1.31474000
H	-1.23198800	-1.12836000	0.86971800
C	1.86014100	0.51134300	2.50967300
H	0.58523200	2.17696500	2.93035400
C	1.95580000	-0.75413200	1.94259800
H	0.93101900	-2.31598600	0.85594900
H	2.72499500	0.96682200	2.98023700
Br	3.60538600	-1.73102700	2.06321600
C	-1.97987800	2.73078900	1.91305200
O	-1.04307100	3.50607500	1.91116900
O	-3.26136200	3.14064900	1.82729700
C	-3.46524000	4.57172400	1.81381300
H	-4.54537100	4.70561900	1.75820300
H	-3.06930900	5.01399700	2.73151900
H	-2.97211200	5.02255800	0.95218100
H	-4.60981300	1.00600500	2.08578400
C	-2.89136400	1.39282100	4.47317500
H	-3.54274200	2.25453500	4.27145300
C	-3.54013500	0.56390200	5.60052300
H	-3.57884300	1.15297600	6.52384800
H	-4.56318300	0.24924500	5.37686300
H	-2.94964500	-0.33773100	5.81055000
C	-1.54442900	1.92364000	4.99675500
H	-0.83342000	1.10467400	5.16115400
H	-1.08002700	2.64542500	4.32237700
H	-1.69169000	2.42973100	5.95797300
C	-2.77641200	0.56353700	3.15701900
H	-2.40581200	0.88934300	1.05691100
H	-2.24562100	-0.36076200	3.42533600
C	-4.16573600	0.14984900	2.60820100
H	-4.83418100	-0.07405400	3.44426600
C	-4.14301500	-1.08095200	1.69164100
H	-5.15746700	-1.36916200	1.39622300
H	-3.57031700	-0.91790800	0.77067800
H	-3.69932400	-1.94279500	2.20553700
O	-1.82675000	-0.77077900	-1.72333600

R-P_D

-747.861097

C	-1.95926800	1.07097500	2.13315800
C	-0.49174500	0.63080800	2.12341500
C	-0.22466900	-0.73024700	1.90613700
C	0.60120800	1.49973600	2.23716500
C	1.07770500	-1.22064100	1.82782500
H	-1.04957700	-1.42845400	1.78529300
C	1.91367900	1.02764300	2.15619100
H	0.43496200	2.55754200	2.40304500
C	2.14370900	-0.33099400	1.95640800
H	1.25868900	-2.27687600	1.66024500
H	2.74606900	1.71683400	2.25012400
Br	3.94963700	-0.98919500	1.84735500
C	-2.16356700	2.57693300	2.05082500
O	-1.65899700	3.41980600	2.76588700
O	-3.03993000	2.88789500	1.06747300
C	-3.34351000	4.28689900	0.92886200
H	-4.06350600	4.34941200	0.11262700
H	-3.77273700	4.68060700	1.85389400
H	-2.43904000	4.85194500	0.68901400
H	-4.72449900	1.44252500	2.78625200
C	-2.68553900	1.09069500	4.69435200
H	-3.03853200	2.12950800	4.63192900
C	-3.54522600	0.36738500	5.75177100
H	-3.33097600	0.77420600	6.74644200
H	-4.62050600	0.47751600	5.58471900
H	-3.31550900	-0.70641800	5.78102300
C	-1.23008900	1.12929800	5.19075400
H	-0.77752200	0.12960500	5.18541500
H	-0.60892200	1.78992700	4.58626100
H	-1.20002700	1.50069100	6.22200400
C	-2.84928000	0.44739500	3.28313500
H	-2.37655500	0.67210400	1.20577700
H	-2.51498000	-0.59747500	3.36667600
C	-4.33778400	0.41570800	2.84741100
H	-4.90909600	-0.07459000	3.64052200
C	-4.64557000	-0.32071500	1.53567300
H	-5.72763700	-0.45475200	1.42401400
H	-4.29896300	0.22530400	0.65252600
H	-4.18955700	-1.31917000	1.52075400

4E

-4315.068960

Rh	0.15831400	0.18324200	-4.22665000
O	-0.15940400	2.22830900	-4.17851600
O	0.49522800	-1.85075600	-4.11543000
O	-0.06457500	2.26195700	-1.91024900
O	0.36895500	-1.83713400	-1.84813800
O	2.19141700	0.52053400	-4.16886500
O	-1.86675900	-0.16849800	-4.12381900
O	-1.87874900	-0.01541400	-1.85629400
O	2.23453300	0.44868100	-1.89946900
C	-2.42600500	-0.18320800	-2.99501900
C	2.77044900	0.55686600	-3.05126400
C	-0.16207100	2.80401800	-3.06026700
C	0.50030100	-2.40183300	-2.98556300
Rh	0.17693300	0.23015900	-1.75681300
C	4.28368000	0.82943700	-3.07381100
C	4.75424200	-1.31273700	-1.81209100
C	5.96763400	0.58775900	-1.22414100
O	3.96596700	-2.01539400	-2.41100100
C	5.70225900	-1.68720800	-0.70560500
O	6.35899300	1.73205800	-1.26196200
C	6.43295500	-0.54710800	-0.35571900
C	5.92019000	-2.89836900	-0.07070700
C	7.39860400	-0.59014300	0.63588400
Cl	4.98000400	-4.33235300	-0.50360300
C	6.89799200	-2.95847300	0.93811200
C	7.63125800	-1.81422500	1.28831200
Cl	8.31614400	0.85403500	1.07375400
Cl	7.20138300	-4.48774900	1.76955500
Cl	8.85532000	-1.90790400	2.55879900
C	-0.33444800	4.33265600	-3.03210200
N	0.45358100	4.87811300	-1.92590800
C	1.81810900	4.62169700	-1.75257100
C	-0.12411200	5.48764700	-0.80840800
O	2.52027500	4.02501100	-2.54147900
C	2.17637400	5.22654500	-0.42594700
O	-1.30598000	5.72404300	-0.67285500
C	1.01099300	5.75621600	0.13583100
C	3.38914000	5.29818900	0.23821300
C	1.03150400	6.37823700	1.37153200
Cl	4.84831000	4.58877700	-0.45625500
C	3.42460900	5.93155000	1.49316500
C	2.25650800	6.46917900	2.05413700
Cl	-0.44824900	7.04063600	2.08131200
Cl	2.32135500	7.26303400	3.63327200
C	-3.92994900	-0.50762600	-2.97273800
N	-4.61894200	0.36159700	-2.01692100
C	-4.48767400	1.75148800	-1.99143000
C	-5.51602400	-0.12043100	-1.05820900
O	-3.77439900	2.40358200	-2.72347600
C	-5.40642500	2.22174400	-0.89705000
O	-5.80216500	-1.28417900	-0.88424700
C	-6.02542600	1.09841100	-0.33881500
C	-5.68840100	3.49787200	-0.43776400
C	-6.94250200	1.22429600	0.69102600
Cl	-4.89338900	4.91180500	-1.13581300
C	-6.61782100	3.64051800	0.60861000
C	-7.23926600	2.51341600	1.16832900
Cl	-7.72678500	-0.19778400	1.39027500
Cl	-7.00319600	5.25261400	1.22091000
Cl	-8.40258000	2.71213100	2.48380300
C	0.73836700	-3.92124300	-2.93804900
N	-0.07868500	-4.50846100	-1.87496000
C	-1.46399600	-4.33992600	-1.78325500
C	0.46180400	-5.16341600	-0.76400600
O	-2.14926600	-3.74227000	-2.58566800
C	-1.87083200	-5.03485000	-0.51479400
O	1.64206600	-5.35952600	-0.56905000
C	-0.71494600	-5.53717400	0.09238900
C	-3.11887700	-5.21611000	0.05800000
C	-0.77957000	-6.23758300	1.28501200
Cl	-4.57030800	-4.55942000	-0.69961100
C	-3.19882900	-5.92670300	1.26952400
C	-2.03994500	-6.43472500	1.87647200
Cl	0.68381200	-6.87272200	2.04663200
Cl	-4.77290700	-6.17980400	2.03023200
Cl	-2.16109100	-7.32817700	3.39638200
H	1.77448100	-4.05283400	-2.60420400
H	-4.01274500	-1.51683100	-2.55330300
H	-1.37836800	4.51610300	-2.75159000
H	4.40252500	1.87552300	-2.76788500
Cl	4.95575500	6.04768700	2.36944000
N	4.96173300	0.04755500	-2.03738700
C	-0.02233900	5.01120900	-4.36677300
H	-0.66050200	4.59287700	-5.14823700
H	-0.21586900	6.08553100	-4.28849000
H	1.02060200	4.85281000	-4.65081600
C	-4.58513800	-0.46299100	-4.35500500
H	-4.07746800	-1.15808200	-5.02694900
H	-5.63642700	-0.75653100	-4.27221500
H	-4.52159900	0.53952800	-4.78593900
C	0.52913500	-4.61962000	-4.28288600
H	1.18763300	-4.17592400	-5.03262400
H	0.76787500	-5.68349500	-4.18728000
H	-0.50315600	-4.51021400	-4.62340400
C	4.91958400	0.61471600	-4.44985600
H	4.42762300	1.25015100	-5.18886500
H	5.98097200	0.87836500	-4.40772700
H	4.81695400	-0.42607800	-4.76899400
C	0.25207000	0.38988800	0.26391800
C	0.90579800	-0.45261500	1.21582800
C	1.66338300	-1.58292900	0.79986700
C	0.79794700	-0.20827800	2.61693500
C	2.25394900	-2.43351100	1.72335300
H	1.77234800	-1.78302400	-0.25683300
C	1.38450300	-1.05078200	3.54435800
H	0.24263000	0.65313900	2.97168000
C	2.10800800	-2.16332200	3.08940000
H	2.81017800	-3.30192300	1.38885600
H	1.29006100	-0.85760400	4.60686400
Br	2.91518300	-3.32697200	4.36565000
C	-0.32236100	1.65910900	0.78779200
O	0.39530600	2.62050700	0.99900200
O	-1.64710100	1.63500800	0.96496900
C	-2.24247800	2.88083500	1.40060500
H	-3.28423900	2.63851300	1.60609900
H	-1.74828100	3.24528400	2.30399300
H	-2.16528100	3.63277200	0.61324900
H	-2.93803600	-0.82314400	1.62495900
C	-4.08837200	-0.89478700	3.48396600
H	-4.78541200	-0.10644000	3.15866300
C	-2.97650400	-0.22689300	4.30877300
H	-2.41814800	0.49066500	3.69475200
H	-3.36965700	0.31308000	5.17690600
H	-2.26227000	-0.97627400	4.67660300
C	-3.50270900	-1.54860000	2.22270000
H	-2.81633700	-2.36331200	2.49250600
H	-4.29018600	-1.96858400	1.58711200
C	-4.89833000	-1.91922400	4.30293400
H	-5.58852600	-2.43889600	3.62284900
H	-4.21268100	-2.69154600	4.68612600
C	-5.71009800	-1.33704100	5.46874900
H	-5.04012600	-0.85176200	6.19072600
H	-6.37311000	-0.54751900	5.08662700
C	-6.54687300	-2.39566600	6.19602400
H	-5.91020100	-3.18532400	6.61426700
H	-7.11841800	-1.95653100	7.02184400
H	-7.26012600	-2.87429400	5.51370700

$TSE_{4\text{-}5}$

-4315.027208

Rh	0.44913700	-0.54163700	-3.82762900
O	0.17781300	1.50776500	-3.84680300
O	0.75998500	-2.56925600	-3.67234000
O	0.16779600	1.58730800	-1.57851300
O	0.55975700	-2.52775600	-1.41327400
O	2.46680300	-0.21439600	-3.69876900
O	-1.59021000	-0.90198100	-3.79707700
O	-1.68650900	-0.70675600	-1.53717700

O	2.42877000	-0.23999600	-1.42807000
C	-2.19017700	-0.91450300	-2.69000100
C	3.00755500	-0.16016900	-2.55626100
C	0.16730800	2.10996200	-2.73837100
C	0.72987800	-3.10880200	-2.53331500
Rh	0.36557700	-0.45181300	-1.39267200
C	4.52252400	0.09826700	-2.53767200
C	4.93979800	-2.15447600	-1.45476100
C	6.25342500	-0.35239600	-0.77897300
O	4.10682900	-2.77862400	-2.07910000
C	5.93110900	-2.65312100	-0.43946200
O	6.68349300	0.77868000	-0.74154100
C	6.73073900	-1.57464200	-0.04743100
C	6.13957000	-3.92134000	0.07561000
C	7.76395200	-1.74055000	0.85923900
Cl	5.09251400	-5.27074700	-0.38210000
C	7.19000200	-4.10670600	0.99135900
C	7.99662900	-3.02612300	1.37819400
Cl	8.76996900	-0.37359000	1.35068000
Cl	7.49110100	-5.71430400	1.66059500
Cl	9.31065900	-3.27765500	2.53298600
C	0.11671200	3.64892600	-2.76517300
N	0.87500300	4.16859100	-1.62685700
C	2.20546000	3.82664600	-1.36373000
C	0.27892200	4.86121300	-0.56928200
O	2.91169000	3.16665600	-2.09655300
C	2.52399400	4.44178200	-0.03198200
O	-0.88646300	5.19484200	-0.52258800
C	1.36870600	5.07246400	0.43960400
C	3.69507400	4.44376800	0.70699200
C	1.35745100	5.72625900	1.65886800
Cl	5.13929200	3.61301700	0.12502700
C	3.69786900	5.10818300	1.94644000
C	2.54012700	5.74547100	2.41762900
Cl	-0.11018700	6.51549200	2.25449000
Cl	2.56423800	6.57545300	3.97924400
C	-3.68879700	-1.26576200	-2.69651200
N	-4.41977000	-0.30078400	-1.86912600
C	-4.40731200	1.07936700	-2.09975800
C	-5.12134400	-0.64969100	-0.71296700
O	-3.79986800	1.63653600	-2.98698000
C	-5.27532200	1.67466800	-1.02692300
O	-5.21027500	-1.76722600	-0.25031300
C	-5.70842000	0.63605900	-0.19636500
C	-5.65696300	2.98608300	-0.79733400
C	-6.53862100	0.88635800	0.88320000
Cl	-5.10435700	4.29055800	-1.85043500
C	-6.49821500	3.25441500	0.29788100
C	-6.93552800	2.21264900	1.13101700
Cl	-7.10224100	-0.42941600	1.92284800
Cl	-7.00822000	4.91343600	0.62170800
Cl	-7.99433500	2.56703500	2.50049200
C	0.98188200	-4.62480900	-2.48727400
N	0.17577000	-5.23526800	-1.42743400
C	-1.19895100	-5.04328300	-1.28082100
C	0.71503100	-6.08359900	-0.45244500
O	-1.89410200	-4.35529100	-1.99892100
C	-1.59252200	-5.85290800	-0.07553100
O	1.87954300	-6.40251800	-0.36555700
C	-0.44452800	-6.48265300	0.41720700
C	-2.82321900	-6.02905800	0.53539700
C	-0.49850200	-7.30539400	1.52998000
Cl	-4.26765600	-5.21875600	-0.07810400
C	-2.89309400	-6.86064700	1.66774000
C	-1.74185500	-7.49472500	2.15988700
Cl	0.95483700	-8.09625800	2.14711000
Cl	-4.44548700	-7.10502600	2.47633400
Cl	-1.85024200	-8.53615600	3.58249600
H	2.02182900	-4.74394400	-2.16084800
H	-3.77425200	-2.21856500	-2.16281600
H	-0.92233900	3.93195800	-2.56018500
H	4.64678200	1.10988700	-2.13625300
Cl	5.17496600	5.13695800	2.91755000
N	5.18248900	-0.78534200	-1.57251600
C	0.56556500	4.25498200	-4.09642100
H	-0.05743200	3.86586600	-4.90468600
H	0.45998800	5.34369700	-4.06017900
H	1.60640700	4.00091900	-4.30921600
C	-4.28994400	-1.39252600	-4.09677500
H	-3.75198300	-2.16137500	-4.65604100
H	-5.34248800	-1.68400500	-4.02168900
H	-4.21161200	-0.45146300	-4.64512100
C	0.77681700	-5.32269400	-3.83398400
H	1.42650300	-4.86989800	-4.58551400
H	1.02915400	-6.38367100	-3.74129200
H	-0.25873200	-5.22568400	-4.17056500
C	5.17680300	0.00367500	-3.91838500
H	4.70444100	0.71110900	-4.60317100
H	6.23997600	0.25041000	-3.83596300
H	5.06826500	-1.00154500	-4.33476200
C	0.25851000	-0.29183200	0.94808800
C	1.43724400	-0.81458200	1.66753700
C	1.89368300	-2.12510400	1.40944900
C	2.13231200	-0.05999500	2.63525300
C	2.95336800	-2.68159500	2.11942100
H	1.42207900	-2.70889900	0.62692500
C	3.20912300	-0.59919300	3.33562500
H	1.83375600	0.96133900	2.83178400
C	3.60151500	-1.91431700	3.08952400
H	3.27283100	-3.69725900	1.91164900
H	3.72787400	-0.00205500	4.07771100
Br	5.04868900	-2.67685300	4.09819200
C	-0.25869200	1.07166800	1.22011000
O	0.45135700	2.03292900	1.46816900
O	-1.60101100	1.16748800	1.09408900
C	-2.14888200	2.49007300	1.25178000
H	-3.22436800	2.34477100	1.35920100
H	-1.73701400	2.97552800	2.13908500
H	-1.93220400	3.10172800	0.37469700
H	-0.59104000	-1.03607900	0.68693500
C	-2.14089100	-1.28383700	2.84260400
H	-2.66806200	-0.36383000	2.57024200
C	-1.23285100	-1.02150700	4.04959900
H	-0.47961700	-0.26127400	3.82678800
H	-1.81451500	-0.66862100	4.90580200
H	-0.70409500	-1.93351800	4.35371400
C	-1.40741300	-1.78741200	1.63465000
H	-0.67241500	-2.57164400	1.81064600
H	-2.02954100	-1.95640500	0.75198300
C	-3.23176600	-2.36810200	3.13107500
H	-3.82528100	-2.52211400	2.22089300
H	-2.74077100	-3.32569800	3.35746300
C	-4.18827400	-2.00796800	4.28018100
H	-3.63223500	-1.91931000	5.22107700
H	-4.63464900	-1.02383400	4.08391000
C	-5.29944800	-3.05094000	4.44487900
H	-4.88468300	-4.04497500	4.65167300
H	-5.96486600	-2.78766000	5.27472300
H	-5.90746500	-3.12783700	3.53621000

5E

-4315.124083

Rh	0.37515400	-0.10320000	-4.10325200
O	-0.08915900	1.87903800	-3.86607700
O	0.84162700	-2.09733900	-4.24249400
O	-0.20780800	1.66357000	-1.61247800
O	0.62361400	-2.36273600	-2.00294300
O	2.34868200	0.36507900	-3.85725000
O	-1.61804100	-0.59368000	-4.24922200
O	-1.80950900	-0.73957300	-1.99499500
O	2.22513400	0.03964800	-1.61612800
C	-2.26631600	-0.78738500	-3.18107200
C	2.84336700	0.31213100	-2.69121100
C	-0.22976600	2.33208200	-2.69207700
C	0.83223100	-2.78747900	-3.18191400
Rh	0.20857200	-0.35617500	-1.72710300
C	4.32988600	0.67067300	-2.55872800
C	4.87169700	-1.68340800	-1.81182300
C	5.92382100	0.07957300	-0.70743800
O	4.15786000	-2.25174900	-2.61200300
C	5.79507300	-2.26523700	-0.77957100
O	6.22717100	1.21938800	-0.43366800
C	6.43384600	-1.20745800	-0.12398900
C	6.06200700	-3.58224000	-0.44483800
C	7.35979100	-1.44042700	0.87847900
Cl	5.22703100	-4.91332400	-1.24931300
C	7.00279400	-3.83380500	0.57015700
C	7.64714700	-2.77271100	1.22473700
Cl	8.16279600	-0.10008500	1.70398900
Cl	7.37411500	-5.50159000	1.02194300
Cl	8.82856200	-3.10939600	2.49547200
C	-0.50206800	3.83954700	-2.56790100
N	0.26016800	4.38786400	-1.44572800
C	1.60638500	4.11078700	-1.19676200
C	-0.28112900	5.30899200	-0.54389700
O	2.30991900	3.39671300	-1.88048500
C	1.95698700	4.89760500	0.03248100
O	-1.41526900	5.73550100	-0.58623400
C	0.83263700	5.64026900	0.40709400
C	3.14104500	4.97475100	0.74715200
C	0.87407300	6.49694100	1.49271800
Cl	4.54347100	4.00277000	0.29350300
C	3.19166100	5.83380900	1.85918400
C	2.06971400	6.59272800	2.22523300
Cl	-0.53752300	7.46299700	1.94715400
Cl	2.15703500	7.67668800	3.61966700
C	-3.74711600	-1.17306300	-3.32312100
N	-4.53934600	-0.43219300	-2.33935800
C	-4.46640000	0.95152600	-2.16875100
C	-5.45254300	-1.04245400	-1.47014200
O	-3.73894700	1.69672600	-2.79091500
C	-5.44819700	1.27536400	-1.07844300
O	-5.69618600	-2.22721300	-1.42678900
C	-6.03555700	0.07843500	-0.65424300
C	-5.80261900	2.48840400	-0.51250200
C	-6.98657700	0.06508400	0.35217400
Cl	-5.07104200	3.99775100	-1.06806500
C	-6.76616500	2.48965400	0.51144100
C	-7.35229100	1.28910800	0.94137700
Cl	-7.72368800	-1.44872300	0.88555800
Cl	-7.24493600	4.01859500	1.25897000
Cl	-8.56140700	1.31130800	2.22888100
C	1.14983300	-4.28319100	-3.32851700
N	0.33990000	-5.04811100	-2.38032000
C	-1.03737200	-4.88577800	-2.22073900
C	0.87987100	-6.01487700	-1.52119300
O	-1.73381600	-4.13282400	-2.86968900
C	-1.42761100	-5.82733000	-1.11679300
O	2.04397200	-6.34293300	-1.48185700
C	-0.28098500	-6.51878400	-0.71040600
C	-2.65614800	-6.06328400	-0.52208200
C	-0.33745000	-7.47391600	0.29062100
Cl	-4.08904400	-5.15222800	-1.00619300
C	-2.72785300	-7.03092200	0.49626000
C	-1.58008400	-7.73223400	0.89674700
Cl	1.11259700	-8.34611500	0.79686500
Cl	-4.27814800	-7.36140700	1.27664400
Cl	-1.69136900	-8.94523200	2.17649000
H	2.18483400	-4.40587500	-2.98810400
H	-3.81322100	-2.22248100	-3.01447200
H	-1.55408100	3.93869500	-2.27655300
H	4.35800900	1.61927800	-2.01200900
Cl	4.68382500	5.95878500	2.79833400
N	5.00029900	-0.29836200	-1.69019400
C	-0.25026800	4.61679100	-3.86245400
H	-0.87024600	4.21425100	-4.66651700
H	-0.50874300	5.66936000	-3.71106700
H	0.79765900	4.54140700	-4.16464600
C	-4.29638200	-1.00712200	-4.74138300
H	-3.70932400	-1.60917700	-5.43849000
H	-5.33647400	-1.34626200	-4.77355100
H	-4.24559300	0.03660800	-5.06156800
C	1.00780900	-4.80490900	-4.76050700
H	1.65861200	-4.23674100	-5.42849500
H	1.29944200	-5.85906600	-4.79623800
H	-0.02219600	-4.70351400	-5.11233300
C	5.04906400	0.81987200	-3.90160800
H	4.55702400	1.58663300	-4.50418500
H	6.08652100	1.12199500	-3.72770300
H	5.03402500	-0.11934600	-4.46075400
C	-1.99795500	1.14968500	1.56776700
C	-0.66139200	0.42934900	1.66827500
C	-0.52202900	-0.78698100	0.96901600
C	0.39976300	0.84583900	2.47689900

C	0.63022100	-1.57441400	1.09042500
H	-1.35780800	-1.16558100	0.38610700
C	1.55620800	0.06948300	2.60933100
H	0.33775500	1.78387100	3.01366800
C	1.66129800	-1.13547000	1.92184400
H	0.71260500	-2.50898800	0.54890300
H	2.36267200	0.40402800	3.25313200
Br	3.22548400	-2.22858000	2.15028500
C	-1.92027500	2.66279300	1.79356900
O	-0.91182900	3.34046200	1.74997100
O	-3.14281400	3.18479000	2.00388300
C	-3.19592500	4.61604500	2.18964100
H	-4.24662900	4.83974700	2.37208900
H	-2.58357000	4.90615200	3.04679600
H	-2.83735500	5.12960600	1.29685100
H	-2.32091600	1.05838100	0.51975400
C	-2.95770400	0.57783000	3.96461400
H	-2.34373800	1.46250800	4.19492200
C	-2.24570200	-0.65671900	4.54479000
H	-1.28442900	-0.83625000	4.05504100
H	-2.05185100	-0.54392600	5.61652700
H	-2.86339600	-1.55475200	4.41041800
C	-3.11510200	0.48001700	2.42331200
H	-3.17799100	-0.57484700	2.12716600
H	-4.06104200	0.94205200	2.12572600
C	-4.33890800	0.80493800	4.61656700
H	-4.80202000	1.68028000	4.13918400
H	-4.99008000	-0.05171600	4.38200200
C	-4.32632500	1.02833700	6.13519000
H	-3.94008500	0.13694000	6.64521400
H	-3.62957600	1.84489000	6.37508400
C	-5.71467200	1.36177000	6.69338600
H	-6.42636000	0.55116300	6.49364600
H	-5.68241200	1.51658100	7.77789200
H	-6.11833000	2.27432900	6.23746700

R-P_E

-747.868116

C	-2.16100200	1.13740400	1.68614900
C	-0.79817000	0.45811700	1.76686100
C	-0.56099100	-0.64344000	0.93132200
C	0.22379300	0.85797700	2.63930700
C	0.64662800	-1.33983900	0.96395900
H	-1.33369300	-0.96703600	0.23721200
C	1.44167100	0.17532300	2.68089900
H	0.07195400	1.71536000	3.28436700
C	1.64306900	-0.92119200	1.84492600
H	0.81141100	-2.18873500	0.30936300
H	2.22430200	0.49784800	3.35918700
Br	3.31964400	-1.86639100	1.89873100
C	-2.11853900	2.63801500	1.94242500
O	-1.64485400	3.19265300	2.91498000
O	-2.73824600	3.30977900	0.94794400
C	-2.80718000	4.73651800	1.11428100
H	-3.33555200	5.10711300	0.23558700
H	-3.35129500	4.99088100	2.02774900
H	-1.80266900	5.16411400	1.16888900
H	-2.52142600	1.01849700	0.65948800
C	-3.01297900	0.47913400	4.12530600
H	-2.33524900	1.30678400	4.37026000
C	-2.35709700	-0.83868200	4.57400900
H	-1.44921400	-1.05176900	4.00287800
H	-2.07957700	-0.81110300	5.63296900
H	-3.04753300	-1.68152700	4.43195800
C	-3.26108500	0.49201100	2.59501800
H	-3.41286800	-0.53467000	2.23648900
H	-4.19352600	1.02910700	2.37487200
C	-4.33944000	0.74178300	4.87224900
H	-4.77652300	1.67423100	4.48500700
H	-5.05831500	-0.05555900	4.62517900
C	-4.22080900	0.86111500	6.39786500
H	-3.86205700	-0.08483100	6.82276800
H	-3.45943300	1.61582000	6.64195300
C	-5.54734400	1.23890200	7.06690300
H	-6.32240600	0.48979600	6.86186700
H	-5.43861900	1.31543100	8.15489900
H	-5.91699500	2.20470800	6.70027600

4S

-4315.066376

Rh	0.17591200	0.11939200	-4.12695900
O	-0.14881500	2.15356500	-4.01472900
O	0.53077000	-1.91895100	-4.05539900
O	-0.42562300	2.08695300	-1.76181600
O	-0.05456500	-2.02542900	-1.86274100
O	2.15826000	0.44912200	-3.65966500
O	-1.84392200	-0.16403000	-4.45357000
O	-2.29438200	-0.11032400	-2.22860700
O	1.76093900	0.12849800	-1.44769800
C	-2.61746400	-0.14568100	-3.46098500
C	2.50957600	0.36634900	-2.45597300
C	-0.32226500	2.68135100	-2.88422800
C	0.39966800	-2.51027600	-2.95004000
Rh	-0.30074900	0.02015900	-1.70634700
C	3.99117100	0.60833500	-2.11667600
C	4.53409600	-1.81030300	-1.60385700
C	4.80157200	-0.25493000	0.10754600
O	4.19048900	-2.25814200	-2.67705200
C	5.07482800	-2.53136800	-0.40319700
O	4.76298900	0.81162400	0.68380600
C	5.20350800	-1.60265500	0.63450900
C	5.41949500	-3.85991700	-0.22349600
C	5.65109300	-1.98738700	1.88698800
Cl	5.31592700	-5.01554300	-1.55450600
C	5.87696600	-4.26416300	1.04270800
C	5.98554200	-3.33720800	2.09093700
Cl	5.79780900	-0.81222300	3.20059900
Cl	6.32208000	-5.95273900	1.31375100
Cl	6.55464400	-3.86557800	3.67901800
C	-0.48115300	4.21069600	-2.85267800
N	0.15174600	4.75900800	-1.65058500
C	1.43737900	4.43604400	-1.21763500
C	-0.47995000	5.70104600	-0.82708400
O	2.19351500	3.66078500	-1.76665400
C	1.65882400	5.24640400	0.03009100
O	-1.59032000	6.14976700	-0.99963000
C	0.51146100	6.01267600	0.25880700
C	2.74901700	5.32169300	0.88077900
C	0.42932300	6.87664300	1.33759400
Cl	4.18618200	4.32808600	0.60884200
C	2.68184300	6.19677400	1.97952500
C	1.53167200	6.96837500	2.20592700
Cl	-1.02411900	7.84075800	1.62078700
Cl	1.46285700	8.06032100	3.59293400
C	-4.13085600	-0.21098800	-3.73695600
N	-4.84128600	0.59164500	-2.74250300
C	-4.59044300	1.94827500	-2.51191500
C	-5.71672000	0.03829200	-1.80423700
O	-3.80453800	2.62826300	-3.13704800
C	-5.48375300	2.33169100	-1.36715100
O	-6.02503300	-1.13337700	-1.74288600
C	-6.15887000	1.18316900	-0.94185100
C	-5.69709300	3.55597100	-0.75652700
C	-7.06026100	1.22906900	0.10716500
Cl	-4.82332700	4.99680000	-1.27902200
C	-6.62044300	3.61913800	0.30245900
C	-7.29277900	2.46577200	0.73336300
Cl	-7.90138100	-0.22933600	0.64882300
Cl	-6.93507000	5.16795900	1.09466800
Cl	-8.44004200	2.56398900	2.07550700
C	0.93757600	-3.94910700	-2.87009100
N	0.39265900	-4.63846300	-1.70094400
C	-0.94150700	-5.04226700	-1.57421000
C	1.09022700	-4.71426200	-0.49050000
O	-1.79522000	-4.95351500	-2.42800200
C	-1.06587000	-5.58145500	-0.17414500
O	2.21911100	-4.31687800	-0.30061500
C	0.15195600	-5.37453200	0.47904100
C	-2.12981700	-6.18694000	0.47282600
C	0.33347900	-5.76130700	1.79630000
Cl	-3.66798000	-6.45336800	-0.36005800
C	-1.96050500	-6.58790500	1.80964800
C	-0.73876000	-6.37502700	2.46705300
Cl	1.87501900	-5.49340500	2.62047400
Cl	-3.29798400	-7.36270700	2.66695200
Cl	-0.54501600	-6.88106800	4.14931900
H	2.00584700	-3.82772300	-2.65163400
H	-4.44219000	-1.24197000	-3.53187600
H	-1.55301100	4.40087100	-2.72340900
H	4.00690900	1.51037800	-1.49571100
Cl	4.05699300	6.32185600	3.08191500
N	4.47220800	-0.46087200	-1.23622400
C	0.02015000	4.89971600	-4.12431200
H	-0.50715500	4.50046500	-4.99300300
H	-0.17005300	5.97552700	-4.05867900
H	1.09108600	4.72946600	-4.26429500
C	-4.50715200	0.16933300	-5.17081800
H	-3.98595200	-0.48475400	-5.87310200
H	-5.58615800	0.05253800	-5.31180400
H	-4.22438600	1.20202900	-5.38676700
C	0.77948600	-4.74449000	-4.16891300
H	1.27053600	-4.20015100	-4.97785600
H	1.25663300	-5.72373900	-4.06262000
H	-0.27203700	-4.88563900	-4.42453100
C	4.88447400	0.80213200	-3.34180800
H	4.51799600	1.64879400	-3.92693200
H	5.90902500	1.01500700	-3.02013100
H	4.88098900	-0.08433000	-3.97872600
C	-0.80490000	-0.06209600	0.26455000
C	-0.07748500	0.33946200	1.42568600
C	1.17950000	0.99737600	1.31788700
C	-0.56978600	0.06420100	2.73675500
C	1.91329900	1.34039100	2.44408800
H	1.57278900	1.21873400	0.33557100
C	0.15501600	0.40210000	3.86509300
H	-1.53001100	-0.42513700	2.85909300
C	1.39636200	1.03905100	3.70966500
H	2.88208500	1.81451500	2.33913300
H	-0.22630700	0.18253000	4.85571100
Br	2.39595900	1.50328400	5.26456200
C	-2.19534700	-0.54591700	0.48959000
O	-3.11103900	0.24429400	0.63830000
O	-2.31731500	-1.87607700	0.47958900
C	-3.66868100	-2.38507800	0.59381500
H	-3.56395700	-3.46757000	0.63697200
H	-4.14316800	-2.00471200	1.50158700
H	-4.25714700	-2.09435400	-0.27742300
C	-2.58425500	3.57133800	3.83274900
H	-1.53889900	3.24009200	3.73453700
C	-3.11415000	3.82332600	2.41203100
H	-2.50962200	4.57666100	1.89303300
H	-3.09825300	2.90458400	1.81292500
H	-4.14339800	4.20076000	2.43002300
C	-2.57330000	4.86549500	4.66186700
H	-3.57921900	5.29078300	4.75913900
H	-2.18506000	4.69064000	5.67322500
H	-1.94401500	5.62817600	4.18826900
C	-3.32999200	2.41746500	4.54229900
H	-3.24000700	1.51484200	3.91888600
H	-2.80913500	2.19181800	5.48579100
C	-4.81710500	2.64691100	4.85270300
H	-4.93142300	3.52571300	5.50049900
H	-5.36313700	2.87484900	3.92847500
C	-5.46638900	1.43568300	5.53243400
H	-4.96959700	1.19972300	6.48206400
H	-6.52574100	1.61721700	5.74662000
H	-5.40461300	0.54352800	4.89648800

$TS_{4S\text{-}5S}$

-4315.038380

Rh	0.28044100	-0.67654500	-3.95124700
O	0.09931800	1.37704700	-3.85445600
O	0.45489300	-2.72898200	-3.88482400
O	-0.12288700	1.36018200	-1.59455700
O	-0.08074800	-2.79787000	-1.67674400
O	2.28160600	-0.50979300	-3.49289100
O	-1.75095400	-0.78652400	-4.28970900
O	-2.19578100	-0.66313000	-2.06739900
O	1.87654500	-0.73896600	-1.27057000
C	-2.51879600	-0.66935700	-3.29571700
C	2.63329100	-0.60402800	-2.28791000
C	-0.01347900	1.93072400	-2.73040300
C	0.29131400	-3.31368100	-2.77645800
Rh	-0.18680400	-0.73540400	-1.53204100

C	4.13936400	-0.52557200	-1.97399200
C	4.49426600	-3.03534400	-1.81904800
C	5.06555200	-1.74095100	0.03015900
O	4.01409900	-3.31611000	-2.89601500
C	5.10936700	-3.94053000	-0.79082600
O	5.15237400	-0.76409800	0.74439300
C	5.44479300	-3.16460900	0.32285900
C	5.36658500	-5.30013200	-0.82110300
C	6.03917900	-3.73262600	1.43717600
Cl	4.98284600	-6.26827400	-2.24797100
C	5.95943100	-5.89190600	0.30735900
C	6.29217700	-5.11509100	1.42783700
Cl	6.48529400	-2.74314400	2.83402300
Cl	6.29620000	-7.62686900	0.30909200
Cl	7.04421400	-5.87567400	2.83518700
C	-0.07292400	3.47064500	-2.71850500
N	0.83139000	3.99559200	-1.68793700
C	2.19113700	3.68024000	-1.60813100
C	0.42193800	4.88622100	-0.68946700
O	2.77622400	2.90567900	-2.33433400
C	2.72444800	4.47936500	-0.45115600
O	-0.70846000	5.29090400	-0.52712300
C	1.66110600	5.19931300	0.10330000
C	4.00301700	4.57306300	0.07275600
C	1.84966600	6.02317000	1.20020800
Cl	5.34424800	3.66604800	-0.63332000
C	4.21146900	5.41271200	1.18211600
C	3.14295900	6.13045200	1.74219500
Cl	0.49779200	6.91698600	1.90762200
Cl	3.42047000	7.17609200	3.13862300
C	-4.02606200	-0.56312500	-3.59873500
N	-4.68042100	0.28157200	-2.59921300
C	-4.29953600	1.59130800	-2.30652800
C	-5.70340800	-0.18444600	-1.76644600
O	-3.40224100	2.20207100	-2.84929100
C	-5.22715900	2.04481400	-1.21294500
O	-6.17268200	-1.30130500	-1.79492700
C	-6.06681800	0.97561500	-0.88622800
C	-5.33760800	3.26375700	-0.56528100
C	-7.03426600	1.09673500	0.09642900
Cl	-4.27040500	4.61283200	-0.97483500
C	-6.31563300	3.40236100	0.43550500
C	-7.15647400	2.32813100	0.76410200
Cl	-8.09139300	-0.25871400	0.50419900
Cl	-6.48337900	4.94375900	1.28550100
Cl	-8.37952200	2.52087600	2.02577500
C	0.68339600	-4.80073100	-2.75170100
N	0.17297700	-5.46924400	-1.55576300
C	-1.17252600	-5.76407600	-1.31922200
C	0.98235400	-5.73179900	-0.44550100
O	-2.09592500	-5.53283300	-2.06887200
C	-1.20891000	-6.41231000	0.03967400
O	2.16527800	-5.48224000	-0.36147000
C	0.08383300	-6.37879800	0.56946000
C	-2.25303800	-6.98978800	0.74216900
C	0.36176300	-6.90886000	1.81836700
Cl	-3.88093000	-7.07486500	0.05208500
C	-1.98959200	-7.52500500	2.01504700
C	-0.69330300	-7.48133100	2.55048500
Cl	2.00008700	-6.87722700	2.47831100
Cl	-3.30177400	-8.26080000	2.94407700
Cl	-0.38058900	-8.15524300	4.15489600
H	1.77271000	-4.79528200	-2.62566000
H	-4.45088300	-1.56022500	-3.43496900
H	-1.07869100	3.73556600	-2.37585700
H	4.25632200	0.26795000	-1.22997700
Cl	5.82917400	5.56187900	1.87340100
N	4.56387200	-1.74612300	-1.27586100
C	0.19659200	4.10619100	-4.08339000
H	-0.52990800	3.73535100	-4.80962300
H	0.09729700	5.19398300	-4.00977000
H	1.19749800	3.85526900	-4.44226700
C	-4.32920500	-0.10334000	-5.02748100
H	-3.86581600	-0.78875700	-5.73989900
H	-5.41125800	-0.09789700	-5.19231100
H	-3.93187200	0.89863700	-5.20680300
C	0.33773600	-5.54840500	-4.04413500
H	0.81166500	-5.03780900	-4.88431500
H	0.71996700	-6.57277000	-3.99212800
H	-0.74071200	-5.57801200	-4.21085000
C	5.00686400	-0.22708000	-3.19652300
H	4.69844100	0.72718600	-3.63066700
H	6.05675800	-0.15272500	-2.89453500
H	4.90016900	-1.00380000	-3.95594000
C	-0.81146000	-0.92627700	0.64254900
C	0.05519500	-1.63496200	1.61577600
C	1.44046200	-1.35811900	1.66906400
C	-0.45946900	-2.52750500	2.58506200
C	2.26333900	-1.90997200	2.64869900
H	1.88194200	-0.72009300	0.91468900
C	0.35474000	-3.10288200	3.55661800
H	-1.51359900	-2.77861600	2.58149400
C	1.71170100	-2.77635300	3.59409100
H	3.32028200	-1.66673600	2.66902400
H	-0.06463800	-3.78178100	4.29134500
Br	2.82243100	-3.52035500	4.96964500
C	-2.25836000	-1.32210900	0.61230800
O	-3.20999600	-0.57128700	0.76765100
O	-2.40486400	-2.63332300	0.33911400
C	-3.75779700	-3.08982000	0.14179500
H	-3.66727400	-4.11188500	-0.22097400
H	-4.31190100	-3.05794300	1.08473400
H	-4.26988000	-2.47145600	-0.59485800
C	-1.00072400	1.43395400	1.82171100
H	-0.80451500	0.24165900	0.88944500
C	-1.96782800	2.21487600	0.97922800
H	-1.64877600	2.25290700	-0.06337700
H	-2.97179100	1.79816000	1.04231700
H	-1.97798800	3.25135200	1.35267000
C	0.43658800	1.87116900	1.76896400
H	0.51595400	2.83144500	2.30098100
H	1.10227200	1.16389800	2.27116400
H	0.76542400	2.02248500	0.73830500
C	-1.50632100	0.88787200	3.12634900
H	-2.47198900	0.40027500	2.95922300
H	-0.80737400	0.14096700	3.52097300
C	-1.68434000	2.00363900	4.19368700
H	-0.72279000	2.49955800	4.37509100
H	-2.37016200	2.76997000	3.81247200
C	-2.22493900	1.43452800	5.50920800
H	-1.54306900	0.68498300	5.92733600
H	-2.34850600	2.22873500	6.25363000
H	-3.20033900	0.95636800	5.36269600

5S

-4315.121019

Rh	0.45117900	0.04230900	-4.09217600
O	0.21611900	2.08062400	-3.99816200
O	0.68055500	-1.99953800	-4.07162400
O	0.26034300	2.05223000	-1.73199900
O	0.52178400	-2.05325800	-1.81046600
O	2.48565900	0.29176800	-3.99648900
O	-1.57353200	-0.22337200	-4.08861500
O	-1.66596700	-0.14474400	-1.82477900
O	2.45741400	0.14056800	-1.73624400
C	-2.18698700	-0.23580500	-2.98027600
C	3.03992700	0.25483600	-2.86025900
C	0.20546800	2.63382300	-2.86174800
C	0.61956800	-2.59374900	-2.95542200
Rh	0.38921400	-0.00597500	-1.69697600
C	4.56715700	0.41519800	-2.82353800
C	4.85289000	-1.91730900	-1.89683000
C	6.05597400	-0.19270000	-0.88667800
O	4.08952200	-2.46316700	-2.66558500
C	5.68176100	-2.51129500	-0.79345300
O	6.46259500	0.92862600	-0.67956200
C	6.40341200	-1.47688100	-0.18792900
C	5.80626700	-3.82079500	-0.35984200
C	7.26476600	-1.72615100	0.86715900
Cl	4.88211200	-5.12191100	-1.11522100
C	6.68075600	-4.08909400	0.70877900
C	7.40328800	-3.05106900	1.31717200
Cl	8.16966500	-0.41436800	1.63041800
Cl	6.86869600	-5.74802400	1.28731500
Cl	8.49682600	-3.40777000	2.65858800
C	0.07788900	4.16395200	-2.82259500
N	0.92022600	4.68457600	-1.74405400
C	2.27690600	4.37983200	-1.60780800
C	0.41651000	5.41609900	-0.66109300
O	2.92360000	3.70788000	-2.38409000
C	2.71345500	5.04226500	-0.33164400
O	-0.74026800	5.73952200	-0.50989900
C	1.59962400	5.67668500	0.22891800
C	3.95279200	5.09082800	0.28565700
C	1.70046100	6.38444800	1.41470800
Cl	5.34600300	4.25537200	-0.40350300
C	4.06970700	5.80914000	1.48964500
C	2.95411900	6.45231100	2.04785100
Cl	0.29011200	7.18611000	2.11691900
Cl	3.12110400	7.35162900	3.55965000
C	-3.70710400	-0.45386500	-3.04105100
N	-4.42143000	0.67662300	-2.43812700
C	-4.09100800	2.02239000	-2.60604800
C	-5.61112300	0.49710000	-1.72355700
O	-3.10490900	2.43844300	-3.17800200
C	-5.20178100	2.79538500	-1.95530900
O	-6.10286500	-0.57651600	-1.44886000
C	-6.11790100	1.88006500	-1.43077500
C	-5.40164700	4.15922000	-1.83045200
C	-7.25419800	2.30747500	-0.76867800
Cl	-4.24063800	5.31634000	-2.49444200
C	-6.55388400	4.60863900	-1.16194000
C	-7.47335000	3.68917600	-0.63529200
Cl	-8.40870200	1.14343200	-0.09821400
Cl	-6.84542100	6.34386500	-0.98790100
Cl	-8.91920400	4.26979500	0.20166700
C	0.70831500	-4.12784000	-2.97559500
N	-0.19506100	-4.66947800	-1.95976100
C	-1.53001000	-4.28721600	-1.82783700
C	0.21914700	-5.56448000	-0.96421400
O	-2.11836700	-3.52695400	-2.56868900
C	-2.03931300	-5.01232500	-0.61426800
O	1.32752000	-6.03854700	-0.86574800
C	-0.99327300	-5.78758700	-0.10239400
C	-3.28566800	-5.00280700	-0.01061200
C	-1.17111200	-6.57961900	1.01951800
Cl	-4.60130500	-4.00721800	-0.64822800
C	-3.47953400	-5.79866300	1.13218500
C	-2.43267600	-6.58262900	1.64125300
Cl	0.15143300	-7.56081100	1.65767000
Cl	-5.05566200	-5.80795700	1.93333000
Cl	-2.69679800	-7.57971200	3.07631100
H	1.71650300	-4.38019200	-2.62711600
H	-3.91500100	-1.30916900	-2.39193100
H	-0.95158200	4.37269900	-2.50955200
H	4.75699600	1.39796400	-2.37691900
Cl	5.63489500	5.89948100	2.30295700
N	5.13727100	-0.54940200	-1.88212300
C	0.36393200	4.84285300	-4.16304800
H	-0.31906800	4.45609400	-4.92243700
H	0.21164600	5.92243100	-4.06799400
H	1.38907500	4.65034000	-4.48862100
C	-4.21838000	-0.74314900	-4.45453600
H	-3.71665100	-1.62696200	-4.85610500
H	-5.29472400	-0.93793800	-4.41899900
H	-4.02190100	0.09876800	-5.12338600
C	0.46264900	-4.74131800	-4.35561200
H	1.18444400	-4.34242900	-5.07169700
H	0.58354500	-5.82757200	-4.30050600
H	-0.54352300	-4.50753100	-4.71269500
C	5.22817600	0.33143200	-4.20090300
H	4.80945600	1.09515200	-4.86007400
H	6.30429700	0.50424400	-4.10136400
H	5.05915500	-0.64741600	-4.65674700
C	-2.04932800	1.45267800	1.94280500
C	-0.98684000	0.35771500	1.88580700
C	0.22209400	0.62653200	1.21431500
C	-1.13355900	-0.90169500	2.48026100
C	1.25444200	-0.31892900	1.14935600
H	0.37599200	1.60130100	0.76159500
C	-0.11763900	-1.86071100	2.41752100
H	-2.05193600	-1.14957300	2.99759400
C	1.06879300	-1.56515900	1.75558000
H	2.18722300	-0.07928900	0.65293100

H	-0.25336400	-2.82669300	2.89240700
Br	2.46017600	-2.88514100	1.68269300
C	-3.44067600	0.95008400	1.55951100
O	-4.04971100	1.36304900	0.59215500
O	-3.94931600	0.02499800	2.39679300
C	-5.25866200	-0.48358400	2.06166700
H	-5.49272100	-1.20705700	2.84262800
H	-5.99122400	0.32649100	2.05638400
H	-5.24606600	-0.96251600	1.08085600
C	-2.04865000	2.34661300	3.26106000
H	-1.82287400	2.14898700	1.13013900
C	-3.23242700	3.33250100	3.16042900
H	-3.23109500	3.85503400	2.19708100
H	-4.19736200	2.82278600	3.26673000
H	-3.17242200	4.09119900	3.94689600
C	-0.73647700	3.15821700	3.26280300
H	0.14310100	2.50971000	3.34063000
H	-0.64495400	3.75707900	2.34839800
H	-0.71299400	3.85482000	4.10651700
C	-2.15083400	1.48335300	4.54547200
H	-3.03490000	0.83944000	4.46909400
H	-1.28342500	0.81129300	4.58357300
C	-2.22615800	2.24131600	5.88214100
H	-1.35793700	2.90221300	5.99840300
H	-3.11196200	2.88856400	5.90108900
C	-2.28374200	1.28202500	7.07747500
H	-1.39213400	0.64422900	7.11761200
H	-2.34486000	1.82974900	8.02473600
H	-3.15874300	0.62296400	7.01639500

S-P

-747.864661

C	-2.03748900	1.45397200	1.96300900
C	-0.96786300	0.36404600	1.89959600
C	0.20397300	0.61236300	1.16881800
C	-1.09292300	-0.88557300	2.52731100
C	1.22612300	-0.33260400	1.07378100
H	0.32382100	1.56398100	0.65758800
C	-0.08292800	-1.84484700	2.44077900
H	-1.99363400	-1.12299900	3.08069000
C	1.07317600	-1.55968000	1.71597900
H	2.12274900	-0.11732400	0.50279900
H	-0.19883100	-2.80532200	2.93129300
Br	2.46807700	-2.87994300	1.59173000
C	-3.41607400	0.93543500	1.54730000
O	-3.97740100	1.26914200	0.52653600
O	-3.96495800	0.06270000	2.42715400
C	-5.25199000	-0.45991600	2.05152300
H	-5.54011800	-1.13298900	2.85946600
H	-5.97780400	0.35029400	1.94614200
H	-5.18294500	-1.00057400	1.10422300
C	-2.04780100	2.34218100	3.28055400
H	-1.80918800	2.15652000	1.15571200
C	-3.22837000	3.33052500	3.16811200
H	-3.21862500	3.85039900	2.20289200
H	-4.19436000	2.82110200	3.26445400
H	-3.17636100	4.09127500	3.95347600
C	-0.73033100	3.14588900	3.29535100
H	0.14320500	2.49019300	3.37656600
H	-0.62218000	3.74285700	2.38124600
H	-0.70757900	3.84118400	4.14041700
C	-2.16379200	1.48331400	4.56726400
H	-3.04862900	0.84185600	4.48492600
H	-1.29782700	0.81047000	4.61491000
C	-2.24904200	2.24625200	5.90063400
H	-1.38125400	2.90686000	6.02224600
H	-3.13447300	2.89446000	5.91072900
C	-2.31682400	1.29135900	7.09901100
H	-1.42591800	0.65325000	7.14822100
H	-2.38528800	1.84218300	8.04411200
H	-3.19149600	0.63230400	7.03298000

Rh_2-$(O_2CH)_4$

-975.819482

Rh	-0.00024900	-0.00001200	-3.57440500
O	-0.06496200	2.05738400	-3.51719300
O	0.06444700	-2.05743400	-3.51756900
O	-0.06636000	2.05713400	-1.24168100
O	0.06612600	-2.05756400	-1.24205700
O	2.05716800	0.06467800	-3.51748400
O	-2.05765100	-0.06473100	-3.51727800
O	-2.05747500	-0.06646300	-1.24176600
O	2.05722300	0.06602400	-1.24197200
C	-2.61443900	-0.08274500	-2.37949400
C	2.61407100	0.08249700	-2.37975300
C	-0.08281000	2.61413500	-2.37938700
C	0.08243300	-2.61437500	-2.37986100
Rh	-0.00011900	-0.00022700	-1.18484000
H	-0.11668100	3.71172100	-2.37928300
H	-3.71202500	-0.11661400	-2.37942900
H	0.11629600	-3.71196200	-2.37994100
H	3.71165800	0.11636000	-2.37979400

1H

-1596.067328

Rh	0.02038800	0.40959300	-3.21688200
O	-0.86956300	2.26176900	-3.42081800
O	0.88006200	-1.43569100	-2.88784900
O	-1.30413400	2.38106200	-1.18850200
O	0.41582100	-1.33350500	-0.65894300
O	1.82943600	1.32645000	-2.82579900
O	-1.80829800	-0.49120200	-3.50088300
O	-2.28185200	-0.37955900	-1.27601400
O	1.37379300	1.45009900	-0.59928200
C	-2.53405700	-0.67406100	-2.48354900
C	2.09117400	1.63636800	-1.63186600
C	-1.31905000	2.81923700	-2.37941900
C	0.87997700	-1.88144700	-1.70365700
Rh	-0.46729400	0.52592000	-0.84815400
H	-1.78095000	3.80666400	-2.51689100
H	-3.50815200	-1.14993100	-2.66504600
H	1.34133200	-2.86842800	-1.55899100
H	3.05782900	2.12925800	-1.45716800
C	-0.94032900	0.68570000	1.61894500
C	0.01364700	-0.20231900	2.36413600
C	1.39602200	0.03424700	2.27566600
C	-0.43702100	-1.24379200	3.18980900
C	2.30424500	-0.73880300	2.99413700
H	1.77173300	0.80861400	1.61535200
C	0.46795500	-2.03254600	3.89916700
H	-1.49468000	-1.45252200	3.27596000
C	1.83354700	-1.77284100	3.80290800
H	3.36803100	-0.54399800	2.91370700
H	0.10542100	-2.83647200	4.53031900
Br	3.07938900	-2.85125500	4.79125000
C	-2.43487200	0.55499400	1.55349800
O	-3.18316800	1.50417600	1.44753900
O	-2.82389900	-0.72709200	1.60074700
C	-4.23407100	-0.94138500	1.40011300
H	-4.37113600	-2.02023600	1.47136600
H	-4.81339500	-0.42352500	2.16827500
H	-4.52290700	-0.57755200	0.41268900
N	-0.62271800	2.00333300	1.69467400
N	-0.33266900	3.08971800	1.69360700

$TS_{1H\text{-}2H}$

-1596.051532

Rh	0.38033200	-0.00711700	-3.71157000
O	-0.55316900	1.83895000	-3.74570600
O	1.27868200	-1.86033000	-3.52730300
O	-0.94549100	1.78705200	-1.50124400
O	0.85994300	-1.93148600	-1.28614600
O	2.18355900	0.91640400	-3.27054400
O	-1.44474600	-0.91968400	-4.01410200
O	-1.87875800	-0.97166400	-1.77647300
O	1.76994100	0.86450900	-1.03041000
C	-2.14556800	-1.18204400	-3.00064600
C	2.46061800	1.14127600	-2.06552400
C	-0.99326300	2.30564300	-2.66122300
C	1.30791200	-2.38986700	-2.38346100
Rh	-0.06655600	-0.07389800	-1.29627800
H	-1.48235600	3.28897200	-2.71387900
H	-3.11854800	-1.65762000	-3.19299300
H	1.78433000	-3.37906800	-2.31717500
H	3.42026200	1.64049200	-1.86672500
C	-0.48384200	-0.18219700	0.83225800
C	0.39820000	-0.90051200	1.78056200
C	1.77562900	-1.02405800	1.51158600
C	-0.10327100	-1.46319300	2.97336800
C	2.62103500	-1.68957200	2.39417000
H	2.18239600	-0.58489500	0.60974600
C	0.72888000	-2.14579600	3.85342900
H	-1.15789200	-1.38290700	3.21129000
C	2.09001400	-2.25149900	3.55659300
H	3.67999000	-1.77693700	2.17818400
H	0.32972300	-2.58229500	4.76205300
Br	3.24661700	-3.17921400	4.77050600
C	-1.97624900	-0.24175400	1.03132800
O	-2.71897300	0.71294000	1.11875600
O	-2.37260000	-1.52533800	1.01732300
C	-3.79462900	-1.72812400	0.91236900
H	-3.93091700	-2.80927800	0.91470100
H	-4.31053800	-1.26851600	1.75895900
H	-4.15937800	-1.29367400	-0.02041000
N	-0.25215400	1.52431700	1.25747800
N	0.20877600	2.53239400	1.22908500

2H

-1596.083356

Rh	0.04236600	0.73069200	-3.27187300
O	-0.97123300	2.51425700	-3.01960800
O	1.02399900	-1.09191100	-3.38267900
O	-1.44443400	2.02633400	-0.84190000
O	0.58395300	-1.56398800	-1.19540600
O	1.78656900	1.63707600	-2.61408000
O	-1.73382500	-0.20415200	-3.77058100
O	-2.20739200	-0.66723300	-1.58720500
O	1.32752400	1.15910400	-0.43139800
C	-2.43767600	-0.67197600	-2.83855400
C	2.02345500	1.64959400	-1.37984700
C	-1.47353800	2.74846000	-1.88865500
C	1.07100200	-1.80403400	-2.34855600
Rh	-0.45932200	0.21303000	-0.90508800
H	-2.01145900	3.70052300	-1.77573900
H	-3.38175600	-1.15407300	-3.13242300
H	1.60059100	-2.76434000	-2.43547400
H	2.95268100	2.14523200	-1.06201600
C	-0.88986500	-0.22208500	1.01868400
C	0.00917500	-0.61356400	2.05743800
C	1.36140300	-0.94261500	1.76566100
C	-0.42004200	-0.70164400	3.41371400
C	2.22861400	-1.35406400	2.76675800
H	1.70365400	-0.89109100	0.74225700
C	0.44652400	-1.08976400	4.41998100
H	-1.43872800	-0.43063500	3.67024900
C	1.76791400	-1.42060000	4.08637800
H	3.25401300	-1.61767000	2.53370200
H	0.11354100	-1.14182300	5.45024300
Br	2.96237000	-1.97513100	5.46720500
C	-2.31969300	-0.05090800	1.38534300
O	-2.75972300	1.00726800	1.79088400
O	-3.03353500	-1.16776700	1.19550100
C	-4.45892700	-1.03399700	1.36262700
H	-4.86687200	-2.02172300	1.15055900
H	-4.70069800	-0.72709500	2.38343800
H	-4.84997800	-0.29557100	0.65872000
N	-0.21669800	3.09437300	2.37791900
N	-0.37555400	3.87090900	1.60833500

3H

-1486.559446

Rh	0.05102600	0.75552500	-3.26098900
O	-0.95813900	2.53647500	-2.97633600
O	1.02766300	-1.06765300	-3.40735800
O	-1.44070600	2.00356900	-0.81099100
O	0.57203100	-1.58853900	-1.23423600
O	1.79327300	1.64368500	-2.57292000
O	-1.72532900	-0.16409700	-3.78829700
O	-2.21329300	-0.67229600	-1.61788500
O	1.32203800	1.11302400	-0.40496700
C	-2.43618600	-0.64921400	-2.87031200
C	2.02359900	1.62514000	-1.33723200
C	-1.46417000	2.74711300	-1.84230600
C	1.06607200	-1.80332000	-2.38958700

Rh	-0.46516400	0.18628300	-0.90926200
H	-2.00114700	3.69770700	-1.71162700
H	-3.38019600	-1.12151700	-3.18003000
H	1.59351300	-2.76297000	-2.49510500
H	2.95212300	2.11087000	-1.00251700
C	-0.90130000	-0.25676100	1.00970500
C	0.00509800	-0.62084500	2.05316300
C	1.34132400	-1.00307100	1.75389700
C	-0.40068300	-0.62773800	3.41927800
C	2.21561800	-1.38965800	2.75903900
H	1.66196300	-1.02005000	0.72209800
C	0.47604600	-0.98488100	4.42853300
H	-1.40608300	-0.31323100	3.67859800
C	1.78049500	-1.37180700	4.08870200
H	3.22753700	-1.69716300	2.52094000
H	0.16276500	-0.97197300	5.46622700
Br	2.98692800	-1.88671600	5.47482500
C	-2.33033700	-0.08741600	1.38063100
O	-2.76608700	0.96165900	1.81381800
O	-3.04746000	-1.19659400	1.16323700
C	-4.47069500	-1.06669000	1.34978300
H	-4.88159400	-2.04854100	1.11724700
H	-4.70049300	-0.78588900	2.38084800
H	-4.86939800	-0.31030000	0.66964700

4HA

-1723.640895

Rh	3.29786400	-0.75057500	-0.57629000
O	2.85348800	-2.74042400	-0.20275300
O	3.60927500	1.27083700	-0.87496300
O	0.83572500	-2.20903800	0.72002100
O	1.61543800	1.81080400	0.09546700
O	2.32094400	-0.86997500	-2.40048300
O	4.14760800	-0.59073600	1.30016600
O	2.13687100	-0.06967500	2.24424700
O	0.31278000	-0.32839600	-1.46442700
C	3.38879400	-0.29473500	2.26088600
C	1.08710700	-0.63505600	-2.43056000
C	1.75471600	-3.00910500	0.34642300
C	2.72349500	2.07044800	-0.47504500
Rh	1.12473000	-0.17232800	0.44817300
H	1.54511700	-4.07249000	0.53376300
H	3.85687400	-0.21668100	3.25267000
H	2.91976900	3.14017500	-0.63667700
H	0.59690100	-0.69964200	-3.41313300
C	-0.63757200	0.28945300	1.32284300
C	-1.87954600	-0.40937200	1.21504300
C	-2.06098600	-1.42120800	0.23235300
C	-2.97859700	-0.10918800	2.07183500
C	-3.27363700	-2.08147000	0.10091400
H	-1.24440000	-1.65328900	-0.43600900
C	-4.18341000	-0.78011800	1.96004200
H	-2.86152100	0.63837900	2.84918300
C	-4.32443300	-1.76116400	0.96763300
H	-3.40784000	-2.84116600	-0.66079000
H	-5.00904300	-0.55242300	2.62456700
Br	-5.98925500	-2.67764000	0.79885500
C	-0.58371700	1.43080200	2.27269500
O	-0.37464500	1.27054300	3.45952300
O	-0.76586100	2.61382200	1.67145900
C	-0.58916600	3.77385200	2.50944200
H	-0.76919300	4.62807800	1.85794700
H	-1.30139300	3.76222400	3.33842900
H	0.42855200	3.79744500	2.90591900
C	-1.21688200	3.24010300	-2.70727600
H	-0.84156700	2.20773600	-2.65394400
C	-1.57536400	3.52628900	-4.17419100
H	-0.70853400	3.36690800	-4.82707600
H	-2.38234100	2.87036400	-4.52448600
H	-1.90382300	4.56319300	-4.31676000
C	-0.07849500	4.15304700	-2.22465900
H	-0.36070900	5.21243500	-2.26607400
H	0.20281800	3.91048700	-1.19346500
H	0.81162100	4.02999100	-2.85453300
C	-2.44751800	3.28875900	-1.77289300
H	-3.16840000	2.52764200	-2.10858200
H	-2.12691600	2.98386200	-0.76651800
C	-3.17890600	4.63645300	-1.66841200
H	-2.48443400	5.41422700	-1.32373800
H	-3.52554100	4.95438500	-2.66054800
C	-4.37888700	4.57769200	-0.71552900
H	-4.89029100	5.54534300	-0.65165100
H	-5.11324300	3.83413900	-1.04982700
H	-4.06644400	4.29770900	0.29862500

$TS_{4HA\text{-}5HA}$

-1723.615647

Rh	3.48327200	-1.17189600	-0.30658200
O	2.57227500	-2.97944400	0.09872800
O	4.27792300	0.70669400	-0.68513900
O	0.57168200	-1.96324200	0.50623100
O	2.25782100	1.72454500	-0.38865300
O	2.94714600	-1.35647100	-2.30766400
O	3.87777200	-0.92386900	1.70354000
O	1.89374100	0.14981700	2.04212700
O	0.92336000	-0.36059900	-1.96825700
C	3.01360400	-0.32651700	2.40247000
C	1.82244300	-0.92831300	-2.67081400
C	1.35217300	-2.95978200	0.42116500
C	3.50208500	1.69828700	-0.64369400
Rh	1.31008900	-0.07369100	0.07168100
H	0.89786300	-3.93294800	0.65908700
H	3.25603000	-0.19652400	3.46741300
H	3.95795700	2.67739500	-0.85801300
H	1.57447100	-1.05566200	-3.73582800
C	-0.70844700	0.86695000	0.49285000
C	-1.88142000	-0.03241400	0.42434300
C	-1.99956200	-0.94759600	-0.64725900
C	-2.92590400	-0.01215900	1.37701400
C	-3.10334300	-1.78551400	-0.77508800
H	-1.19984500	-1.01087300	-1.37543200
C	-4.02839700	-0.85559900	1.26687500
H	-2.85674100	0.65058400	2.22954100
C	-4.11401700	-1.73391000	0.18626800
H	-3.16969600	-2.48304600	-1.60309700
H	-4.81353900	-0.82825600	2.01470800
Br	-5.63749400	-2.89301700	0.02364100
C	-0.52671400	1.66608400	1.73544500
O	-0.79429000	1.28043000	2.85850100
O	0.06375000	2.87073400	1.50974500
C	0.48903700	3.56562500	2.69234500
H	0.94985000	4.48887600	2.33828600
H	-0.36071500	3.78514400	3.34464100
H	1.21426500	2.96035300	3.24090000
C	-1.35200600	2.67285200	-1.34900400
H	-0.62929200	1.55854900	-0.45075100
C	-1.72382000	1.75781300	-2.47659500
H	-0.85994700	1.19961300	-2.84537800
H	-2.51964900	1.06118600	-2.19915500
H	-2.10540800	2.38033100	-3.30163300
C	-0.12567900	3.51431900	-1.54924400
H	-0.38114300	4.29487800	-2.28571600
H	0.18780200	3.99831400	-0.62420200
H	0.70753100	2.93293900	-1.94744200
C	-2.47365400	3.25083100	-0.53278800
H	-3.13937400	2.44639800	-0.19503500
H	-2.06382000	3.74895000	0.35140700
C	-3.31992900	4.27653700	-1.33753000
H	-2.66859000	5.07322200	-1.71855300
H	-3.76389500	3.78414100	-2.21117500
C	-4.42825800	4.88725300	-0.47410700
H	-5.01732400	5.60806100	-1.05171900
H	-5.11239000	4.11578000	-0.10233300
H	-4.01193000	5.41236600	0.39339100

5HA

-1723.703810

Rh	3.71754700	-1.30340400	-0.33986600
O	2.20029700	-2.69459900	-0.24061000
O	5.16433700	0.16223800	-0.40572300
O	0.69223100	-1.08806500	0.32862600
O	3.65727000	1.77622900	0.14474600
O	3.27586200	-0.94483200	-2.32183100
O	4.07815200	-1.58007200	1.67065900
O	2.57787000	0.03757300	2.23073200
O	1.74623900	0.64960000	-1.76935600
C	3.43634600	-0.86028200	2.48857700
C	2.40576800	-0.06599300	-2.58449200
C	1.04840200	-2.27914200	0.07611000
C	4.81458400	1.35087700	-0.15580100
Rh	2.12038300	0.39166700	0.25128700
H	0.25634900	-3.03748200	0.13876900
H	3.64665100	-1.03069600	3.55323400
H	5.60744500	2.10992700	-0.20411400
H	2.19261600	0.10053000	-3.64953500
C	-1.41154500	1.51926200	-0.15743900
C	-2.41098500	0.43969300	0.25642200
C	-2.45163900	-0.75475900	-0.47871200
C	-3.30350400	0.57975100	1.32962600
C	-3.35512500	-1.77271800	-0.17422900
H	-1.75915700	-0.89792600	-1.30275500
C	-4.20830100	-0.43308900	1.65510200
H	-3.28356200	1.48039500	1.93146900
C	-4.23060600	-1.60175700	0.89718600
H	-3.37300400	-2.68639000	-0.75863500
H	-4.88678500	-0.30882700	2.49212100
Br	-5.47735200	-3.00111900	1.33766400
C	-0.75868300	2.17965600	1.04581300
O	-1.32536000	2.73534500	1.95949200
O	0.61775000	2.16408900	0.98658300
C	1.27530200	2.94612200	2.02301900
H	2.32182400	2.98310900	1.73053400
H	0.83511200	3.94359900	2.05312400
H	1.15390000	2.45462300	2.98912400
C	-1.99372000	2.63396800	-1.14636500
H	-0.61673700	1.02796700	-0.72273500
C	-2.39000600	1.92710600	-2.45811300
H	-1.53755500	1.38497000	-2.88547300
H	-3.20730000	1.21478100	-2.30737700
H	-2.71703900	2.65952600	-3.20325900
C	-0.86102200	3.63637700	-1.45665300
H	-1.16049300	4.31669800	-2.26042800
H	-0.60969800	4.25320200	-0.58526500
H	0.04820100	3.11726200	-1.78017300
C	-3.21719300	3.35105200	-0.52085000
H	-4.00049200	2.60432500	-0.33726000
H	-2.93216000	3.74175200	0.46316000
C	-3.83518500	4.50236700	-1.33306600
H	-3.09108800	5.29177700	-1.49945100
H	-4.14098700	4.15085100	-2.32686900
C	-5.05182500	5.10707200	-0.62147200
H	-5.48344600	5.93124600	-1.20088100
H	-5.83748400	4.35634800	-0.47181100
H	-4.77830000	5.49945500	0.36568200

THE JOURNAL OF PHYSICAL CHEMISTRY C

Article

Cite This: J. Phys. Chem. C 2018, 122, 11926−11932

pubs.acs.org/JPCC

Surfaces, Shapes, and Bulk Properties of Crystals

Michael Springborg,*[,†,‡] Meijuan Zhou,[†] Mohammad Molayem,[†] and Bernard Kirtman[§]

[†]Physical and Theoretical Chemistry, University of Saarland, 66123 Saarbrücken, Germany

[‡]School of Materials Science and Engineering, Tianjin University, Tianjin 300072, China

[§]Department of Chemistry and Biochemistry, University of California, Santa Barbara, California 93106, United States

Supporting Information

ABSTRACT: We study the interplay between surface and bulk properties of macroscopic materials. It is demonstrated that the so-called polar surfaces may be stabilized through a charge redistribution between the complete set of surfaces that depends upon the overall shape of the sample and the nature of the material. This charge redistribution, in turn, is governed by certain constraints that we call generalized Tasker conditions. The same surface, but for samples of different shapes, may have different surface charges. Besides its stabilizing effect, the charge redistribution is also shown to particularly affect the dipole moment per repeat unit, a bulk property. For the latter, it is established that essentially any physically meaningful value is possible (depending upon the shape and material), in contrast to the often made assumption that different samples of the same material will have values that differ by, at most, a lattice vector. Finally, some recent experimental and theoretical results for polar surfaces are discussed in terms of the analysis presented here.

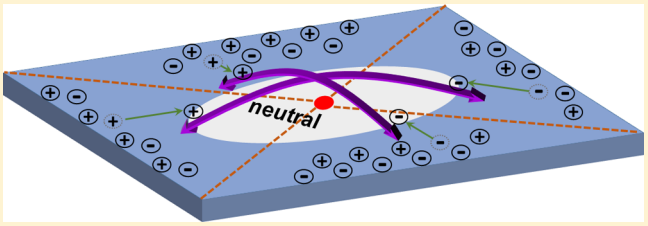

INTRODUCTION

For macroscopic, crystalline materials, the properties of the surfaces as well as the bulk are interesting and are also of technological importance. Heterogeneous catalysis, for instance, depends crucially on the local properties at the surfaces of the catalyst. On the other hand, the responses to the mechanical, magnetic, and electric perturbations are determined primarily by the bulk properties of the system.

Most often, it is indirectly assumed that the bulk and surface properties are essentially independent of one another. Thus, limited attention has been paid to the coupling between the two. An exception can be found within the treatment of the so-called polar surfaces. In a seminal paper, Tasker[1] discussed various arrangements of the parallel layers of different ions at the surfaces of a thin film and demonstrated that certain arrangements lead to a nonvanishing electric field acting on the ions in the bulk, so that such arrangements should not be realizable. This is the result of a coupling between the surface and the bulk.

It turns out that oxides represent an especially challenging case as far as the understanding of ionic surfaces is concerned (see, e.g., the review papers by Noguera et al.[2,3]). The polar surfaces of crystalline ZnO have attracted particular attention (see, e.g., the theoretical studies of Wander et al.,[4] Meyer and Marx,[5] and Mora-Fonz et al.[6]). Tasker's criterion indicates that these surfaces should not exist, but they are nevertheless observed in the experiment. Several studies have been devoted to rationalizing this discrepancy, including the three theoretical papers mentioned above. In these papers, a number of different scenarios have been proposed, including the charge transfer between the opposite, parallel sides of a slab[4,5] as well as the existence of lower symmetry surfaces.[6] The first suggestion is noteworthy with regard to our present work as it implies that it is not sufficient to study an individual polar surface without taking into consideration the other surfaces. We shall explore this circumstance in detail here.

In a further very recent study, Setvin et al.[7] discussed the stability of the (001) surface of $KTaO_3$, another surface that, according to the criteria of Tasker, should not be stable but nevertheless is found experimentally. In their combined experimental and theoretical study, the authors of this work could explain the stability of the surface as being due to several different mechanisms. We shall return to this work at the end of this paper.

Surfaces can also influence bulk properties. In a recent work,[8] we have demonstrated that the dipole moment per unit cell (or per unit volume, which corresponds to the polarization) contains a finite contribution from the surfaces independent of the size of the system. This contribution can be important for a quantitative description of properties that depend upon the linear response of the system to electric fields, such as the so-called converse piezoelectric effect (the creation of strain due to an electrostatic field). In that regard, we have shown that the samples of the same material that vary in shape can have different response properties because of the differences in the surface contributions.

Received: March 30, 2018
Revised: May 15, 2018
Published: May 16, 2018

DOI: 10.1021/acs.jpcc.8b03041
J. Phys. Chem. C 2018, 122, 11926−11932

In the present work, we shall generalize the conditions set up by Tasker and thereby demonstrate that (almost) all surfaces, whether polar or not, can be stabilized through a charge transfer that causes the electric field acting on the ions in the inner part of the sample to vanish. We, then, demonstrate that such a charge transfer between surfaces affects the dipole moment per unit indicating that typical bulk properties can thereby be affected. In addition, the same surface in the samples of different shapes may have a different charge density. Subsequently, we illustrate these theoretical findings through the results from model calculations on finite quasi-two-dimensional systems with up to almost 10 000 atoms that are designed as models for certain three-dimensional systems.

THEORY

The System. We consider a neutral, large, finite, regular system that consists of very many mostly identical units. Only at the boundaries, many deviations from this regularity occur. The system is assumed to be so large that the thermodynamic limit has been reached. In that limit, we can define a central region and various boundary regions. Inside each region, the units are assumed to be identical. The central region consists of units whose properties are independent of the size and the shape of the system, whereas this is not the case for the boundary regions. For a three-dimensional (3D) system, the boundary regions can be separated into a set of two-dimensional (2D) side regions, a set of one-dimensional (1D) edge regions, and a set of zero-dimensional (0D) corner regions. In each of the boundary regions, the repeated units may be larger than those of the central region (because of the structural relaxations at the boundaries and/or to the adsorbants).

Often, such systems are treated as being infinite and periodic. Here, we will explicitly consider instead the large, finite system. In passing, we add that, even when treating the system as being infinite and periodic (i.e., without surfaces), it is possible to include effects that can be ascribed to the surfaces of the finite system as we have demonstrated elsewhere for the calculations of the dipole moment per unit.[8]

The units of the central region are equivalent to the unit cells of the infinite, periodic system and are, accordingly, nonunique. As the complete system is separated into nonoverlapping units, the units of the boundary regions are also nonunique. Ultimately, this implies that the separation of any extensive quantity, Z, into contributions from the individual units

$$Z = \sum_n Z_n = \sum_n \int_{\vec{r}\in\Omega_n} Z(\vec{r})\, \mathrm{d}\vec{r} \tag{1}$$

is nonunique, although the total value Z is unique. In this expression, Ω_n is the volume associated with the nth unit. For different regions, Ω_n may have different sizes and even different compositions (corresponding, e.g., to the surface reconstructions and/or adsorbants).

By construction, all units in each region will be identical and, initially, independent of the presence or properties of the other regions, that is, Z_n will take the same value for all units n of the same region. If we now imagine scaling the size of the system by some factor f, the properties of the units in the different regions will, per construction, remain unchanged. As the number of units in the central region scales as f^3 and the number in each of the other regions scales as f^p with $p < 3$, the units of the central region must be neutral (otherwise, the charge distribution in the sample will depend on its size, f, which is in conflict with the assumption of having reached the thermodynamic limit). Thus, the charge will accumulate only in the boundary regions. This fact will become important below.

We add that similar arguments apply to extended 2D or 1D systems. A 2D system will separate into a central region, various side regions, and corner regions. A 1D system will separate into a central region and two termination regions. Again, only the boundary regions can accumulate charge.

Generalizing Tasker's Condition. In his seminal work,[1] Tasker considered a crystal as consisting of atomic layers. Assuming that a layer is infinitely large and that its charge density, q, can be approximated as being constant throughout, he calculated the electrostatic field at a point far away from the layer, corresponding to the position of an atom in the middle of the central region. Tasker found the strength of the field to be $E = 2\pi q$, independent of the distance to the point of interest. Subsequently, he studied the total field created by several such layers both above and below that point. Thereby, he identified certain situations where the total field would not vanish and concluded that such situations would be unstable.

The discussion by Tasker demonstrates that the electrostatic field is determined not by a single surface but—in his case—by the two parallel surfaces at the "top" and at the "bottom". As a generalization of his discussion, we consider a system like that of Figure 1 in which each surface may be composed of several atomic layers. Then, the field at the reference point in the middle of the central region becomes

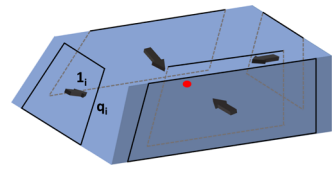

Figure 1. Schematic representation of a 3D system with several different sides. The red circle marks the position of an atom in the middle of the central region. q_i is the charge density of the ith layer of atoms, and $\vec{1}_i$ is a normal to this layer. For the sake of simplicity, the top and bottom surfaces are ignored. Moreover, the system of the figure has just one layer of charges at each surface, except for the front surface that has two such layers.

$$\vec{E} = 2\pi \sum_i q_i' \vec{1}_i = 2\pi \sum_k \left[\sum_{i\in k} q_i' \right] \vec{1}_k = 2\pi \sum_k q_k \vec{1}_k \tag{2}$$

Here, $\vec{1}_i$ is an inward-pointing normal for the ith atomic layer, q_i' is the charge density of that layer, which is assumed to be constant, and the layer is assumed to be infinitely large. These two assumptions will be retained throughout our discussion. Moreover, q_k is the sum of the charge densities of all atomic layers associated with the kth surface.

Equation 2 demonstrates that, even in the case of more parallel atomic layers (as illustrated in Figure 1), only the sum of the charge densities is relevant. Since, as demonstrated above, the units of the central region are neutral, only the total charge densities associated with the surfaces contribute to $\vec{E}$. Accordingly, it is straightforward to separate the total charge density into contributions from individual surfaces. Moreover, as this charge density is confined to the surfaces, it is far from the reference point, and, thus, it is a good approximation to assume that its spatial variation can be ignored.

DOI: 10.1021/acs.jpcc.8b03041
J. Phys. Chem. C 2018, 122, 11926−11932

Stability (i.e., the generalized condition of Tasker) requires that the electrostatic field vanish at the ions of the central region

$$\vec{E} = 2\pi \sum_k q_k \vec{1}_k \equiv \vec{0} \tag{3}$$

If the charge densities at the surfaces are such that this condition is not satisfied, then a charge redistribution at the surfaces must occur to achieve structural stability. This simple generalization of the result obtained by Tasker is of central importance for the present work and its consequences will be developed in the following. For 2D and 1D systems, the contribution from the individual boundary regions decays with the distance to the reference point, so that the treatment leading to eq 3 must be modified. Moreover, for 3D systems, only the side regions contribute to $\vec{E}$ in the thermodynamic limit; the edge and corner regions provide contributions that become negligible for sufficiently large systems.

Stabilizing Polar Surfaces. Let us now discuss the theoretical construction of a system with a more or less arbitrary shape. We may start by cutting out a finite, neutral sample with the shape we want to study from a very large 3D piece of the material of interest (cf. Figure 1), while keeping the charge distribution as it was before cutting. In general, this will lead to an unstable situation if the surfaces are polar, as the stability condition of eq 3 will not be fulfilled. Thus far, structural and electronic relaxation effects have been ignored. However, the electronic relaxation effects (including the possible occurrence of surface states) will modify the original surface charge densities q_{k0}'

$$q_{k0}' \rightarrow q_{k0} \tag{4}$$

so that the charge neutrality constraint

$$\sum_k q_{k0} L_k = 0 \tag{5}$$

(L_k is the size (area) of the kth surface) will make the individual q_{k0} dependent on the overall shape.

There are many ways that the instability can be overcome (as discussed in detail for a single case by Setvin et al.[7]), for example, through structural relaxation. We notice, however, that the structural relaxation of each individual surface region will be independent of the overall shape of the system. Moreover, such structural relaxations will mainly lead to local redistributions of the electronic charge densities that will not have any consequences for the generalized condition of Tasker, eqs 2 and 3. Thus, to determine the effect of the overall shape, we consider just the possibility of charge transfer between the surfaces without structural relaxation.

If we ignore, at first, the charge transfer between surfaces, then the field defined in eq 2 will be

$$\vec{E} = 2\pi \sum_k q_{k0} \vec{1}_k \equiv \vec{E}_0 \tag{6}$$

in which we have made the simplification that a single charge density is ascribed to each surface as in eq 2. As mentioned above, q_{k0} depends on the overall shape.

Subsequently, assuming that $\vec{E}_0$ does not vanish, there must be a charge flow between the different surfaces to satisfy the generalized condition of Tasker, eq 3, that is

$$q_{k0} \rightarrow q_{k0} + \Delta q_k \equiv q_k \tag{7}$$

with the additional charges Δq_k determined by the facts that $\vec{E}$ must vanish and that the complete system is neutral. This is a nonlocal charge redistribution that differs from the local redistribution related to structural relaxation.

Charge neutrality requires that

$$\sum_k \Delta q_k L_k = 0 \tag{8}$$

Moreover, the condition of eq 3 becomes

$$2\pi \sum_k \Delta q_k \vec{1}_k = -\vec{E}_0 \tag{9}$$

For a 3D system, eqs 8 and 9 provide four conditions on the charge transfers $\{\Delta q_k\}$. Often, however, there will be more surfaces so that many different solutions to these equations can be found. This means that the general solution can be written as

$$\Delta q_k = \Delta q_{k0} + \Delta q_{k1} \tag{10}$$

where $\{\Delta q_{k0}\}$ is a particular solution and $\{\Delta q_{k1}\}$ is the general solution with $-\vec{E}_0$ in (9) replaced by $\vec{0}$. The set of solutions $\{\Delta q_{k1}\}$ forms a $P - 4$ dimensional subspace of the P-dimensional space of $\{\Delta q_k\}$, and it is interesting to notice that these solutions depend solely on the overall shape of the system and not on the size of the units or on the number or types of atoms in the system. Moreover, the resulting set $\{\Delta q_k\}$ does not depend on the choice of $\{\Delta q_{k0}\}$.

We see that, in general, it is always possible in principle to stabilize any surface through appropriate charge transfers between the different surfaces. This can occur with or without simultaneous structural relaxation and/or the addition of adsorbates. Typically, there will be a number of possible solutions for $\{\Delta q_{k1}\}$. What actually occurs in practice depends upon the energetics and is well beyond the scope of the present study.

The Dipole Moment Per Cell. An intensive nonlocal property that explicitly depends on the surfaces of the system is the dipole moment per cell.[8] In considering a set of systems of the same material and shape but increasing size, this property can be calculated either as the dipole moment per unit or as the change in the dipole moment per added unit, both evaluated in the limit of infinitely large systems. Thus, for the extensive property Z (in our case, one of the components of the total dipole moment), we can define the corresponding intensive quantity in the thermodynamic limit as

$$\bar{Z} = \lim_{N\to\infty} \frac{Z(N)}{N} = \lim_{N\to\infty} \frac{Z(N+\Delta N) - Z(N)}{\Delta N} \tag{11}$$

with $Z(N)$ being the value of Z for the system with N cells.

In the results to be reported below, we shall use the first equality of eq 11. The size of the system will be increased, while preserving the shape, by displacing the surfaces along their outward pointing normal (i.e., along $-\vec{1}_i$ in Figure 1). For discussion purposes, it can be more revealing to use the second relation. Thus, one contribution to the dipole moment per cell due to the increase in size arises because the number of (neutral) units in the central region grows. As the units in the surface regions in general contain charge, a second contribution to the dipole moment per cell comes from the displaced surface charges, as discussed in detail earlier.[8] In the case of 1D systems, the so-called charge quantization[9,10] reduces the

DOI: 10.1021/acs.jpcc.8b03041
J. Phys. Chem. C 2018, 122, 11926−11932

number of possible values for the dipole moment per cell, but this effect does not occur in 2D or 3D.

In calculating the surface contribution to the dipole moment per cell, according to (7), it will be assumed that the extra charge density Δq_k is placed along the kth boundary of the sample. We emphasize that the surface charge densities will provide a field in the middle of the sample only for 3D systems. When scaling the size of a 3D system by the factor f mentioned above, the numbers of cells in the central region and in the complete system both scale as f^3. On the other hand, the distances of the boundary regions to the origin of coordinates (which conveniently is chosen as the center of the system) will scale as f, so that, of the boundary regions, only the surface (as opposed to the edge and corner) regions will give a finite contribution to the dipole moment per unit in the infinite system limit. In total, the dipole moment per unit can therefore be written as

$$\vec{\vec{\mu}} = \vec{\mu}_C + \sum_k Q_k \vec{1}_k \tag{12}$$

where $\vec{\mu}_C$ is the dipole moment of a single (neutral) unit cell in the central region, which is independent of the surfaces and/or shape of the sample. Q_k is the contribution to the dipole moment per bulk unit cell that originates from the charge associated with the kth surface and is accordingly related to q_{k0}. $\vec{\mu}_C$ is equivalent to Z_n of eq 1 for n representing a unit of the central region and is, accordingly, nonunique, which must also be the case for the contributions because of the charges associated with the surface regions, Q_k.

As discussed in detail in our previous work,[8] Q_k can be interpreted as originating from the displacement of this charge along the outward pointing normal to the kth surface when increasing the size of the system. It will be confirmed by our numerical results below that Q_k depends on the overall shape of the sample. We also find that, for some shapes, the occurrence of (occupied or empty) surface states gives a contribution to the charges of the individual surfaces, whereas for other shapes the same surfaces may not possess such surface states.

RESULTS

To study the consequences of our theoretical analysis further, we set up a simple model 2D system lying in the (x,y) plane. It should be noted that this model is completely equivalent to a 3D system for which two neutral surfaces are parallel to the (x,y) plane and for which the properties of different layers of cells parallel to the (x,y) plane are identical. Our reason for this choice, instead of the "true" 3D systems, is that we could thereby study many cases having large spatial extensions without requiring excessive computer resources. Thus, we shall treat the numerical results for the 2D systems as if they were for the abovementioned 3D systems.

Each unit cell contains M atoms. The position of the nth atom in the (n_x,n_y)th unit cell is given as

$$\vec{R}_{n,n_x,n_y} = n_x\vec{a} + n_y\vec{b} + \vec{u}_n, \qquad n = 1, 2, \ldots, M \tag{13}$$

where $\vec{a}$ and $\vec{b}$ are the two lattice vectors. We shall limit ourselves to the case that the sample has four sides. It is convenient to define the borders of the sample through four straight lines

$$a_i x + b_i y + d_i \geq 0, \qquad i = 1, 2, 3, 4 \tag{14}$$

Here, the constants (a_i,b_i,d_i), i = 1,2,3,4 define the shape of the sample, and the parameters d_i can be varied so that the size of the sample is altered without changing its shape. Thus, the thermodynamic limit is studied by gradually increasing all d_i. In our case, we shall do so by letting

$$d_i = d_{i0} + n_d \Delta d_i$$
$$n_d = n_{d,\min}, \; n_{d,\min} + 1, \ldots, n_{d,\max} \tag{15}$$

For a given n_d, we include all $N(n_d)$ atoms whose positions obey eqs 14 and 15. This implies that we may not include equally many of the M atoms in every cell and, therefore, we study the dipole moment not per cell but per atom. However, when the number of cells becomes very large, this difference becomes irrelevant. In the calculations whose results will be reported below, we considered systems with sizes up to 8000 atoms, which meant having typically 40−80 different sizes for a given shape and material.

We did not attempt to relax the structure of the system. It is assumed that there is one electron per atom, and the electronic orbitals are calculated using a Hückel-like Hamiltonian with one basis function per atom. The entire basis set is orthonormal, that is

$$\langle \chi_{n,n_x,n_y} | \chi_{m,m_x,m_y} \rangle = \delta_{n,m}\delta_{n_x,m_x}\delta_{n_y,m_y} \tag{16}$$

with χ_{n,n_x,n_y} being the basis function centered at the atom at the position of eq 13. We take the diagonal elements of the Hamilton matrix to be

$$\langle \chi_{n,n_x,n_y} | \hat{h} | \chi_{n,n_x,n_y} \rangle = \varepsilon_n \tag{17}$$

whereas the off-diagonal elements are given by

$$\langle \chi_{n,n_x,n_y} | \hat{h} | \chi_{m,m_x,m_y} \rangle = t_{nm}(|\vec{R}_{n,n_x,n_y} - \vec{R}_{m,m_x,m_y}|) \tag{18}$$

wherein the hopping integrals go smoothly to 0 at a prechosen cutoff distance

$$t_{nm}(R) = t_{mn}(R) = \begin{cases} t_{0,nm}\dfrac{(R - d_{nm})^2}{d_{nm}^2} & R \leq d_{nm} \\ 0 & R \geq d_{nm} \end{cases} \tag{19}$$

Here, $t_{0,nm}$ and d_{nm} are constants that have prechosen values. If the typical values for the hopping integrals $|t_{nm}|$ are larger than the typical values for the differences in the on-site energies, $|\epsilon_p - \epsilon_q|$, we model a more covalent system, whereas the opposite case corresponds to a more ionic system.

The dipole moment per atom is calculated using the Mulliken populations. Thus, we write the jth orbital as

$$\psi_j = \sum_{n,n_x,n_y} c_{j,n,n_x,n_y}\chi_{n,n_x,n_y} \tag{20}$$

and assuming that all nuclear charges are equal to 1 obtain the effective charge on the (n,n_x,n_y)th atom equal to

$$q_{n,n_x,n_y} = 1 - \sum_j n(\epsilon_j)|c_{j,n,n_x,n_y}|^2 \tag{21}$$

where $n(\epsilon_j)$ is the occupancy of the orbital with energy ϵ_j. This gives the following expression for the dipole moment

$$\vec{\mu} = \sum_{n,n_x,n_y} q_{n,n_x,n_y}\vec{R}_{n,n_x,n_y} \tag{22}$$

DOI: 10.1021/acs.jpcc.8b03041
J. Phys. Chem. C 2018, 122, 11926−11932

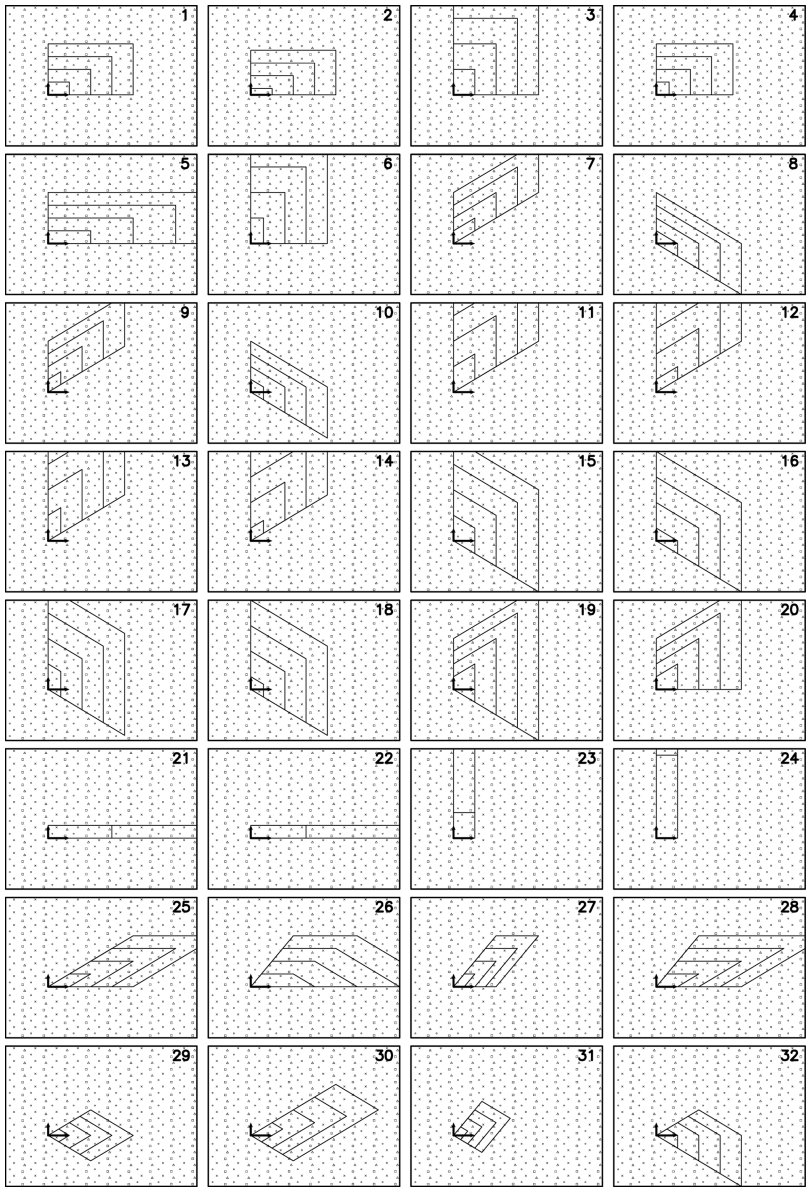

Figure 2. Thirty-two shapes that were studied. For each shape, the four smallest systems are shown. Each system has four atoms per unit. The small arrows show the lattice vectors.

For a given shape and system, we have a set of values for the total dipole moment for different values of n_d [eq 15]. Subsequently, we use a least-squares fit of the type

$$\frac{1}{N(n_d)} Z(N(n_d)) \simeq \bar{Z}_0 + a[N(n_d)]^{-1/2} + b[N(n_d)]^{-1} \tag{23}$$

where $Z(N(n_d))$ is a component of the total dipole moment for the system with $N(n_d)$ atoms. Then, the value $\bar{Z}_0$ is identified as the limiting infinite system value. The form of eq 23 was chosen, so as to take into account the fact that the linear dimensions of the system scale as $\sqrt{N(n_d)}$. Some simple tests using a subset of the results allow us to estimate that the error bars in $\bar{Z}_0$ are smaller than the sizes of the symbols in the figures below.

DISCUSSION

We now discuss in detail the results obtained for the shapes shown in Figure 2 with the two lattice vectors taken as $\vec{a}$ = (5,0) and $\vec{b}$ = (0,3). For the present discussion, the units are irrelevant. Some further examples are given in the Supporting Information.

The systems of Figure 2 contain four atoms per unit cell. Two different cases were considered, that is, a more covalent and a more ionic one. Moreover, we also considered the same systems, but keeping only two of the four atoms per unit cell. The dipole moment per atom is calculated in all cases; as our systems are, in effect, 2D, the dipole moment per atom has only two nonzero components, $\vec{\bar{\mu}} = (\bar{\mu}_x, \bar{\mu}_y)$.

The shapes 21−24 correspond to the quasi-1D systems, that is, chain-like compounds. For these systems, the charge quantization discussed above implies that the dipole moment per atom cannot take any value. Nevertheless, we shall include these systems in our analysis as well.

DOI: 10.1021/acs.jpcc.8b03041
J. Phys. Chem. C 2018, 122, 11926−11932

At first, we show in Figure 3 the calculated values of the dipole moment per atom before taking the generalized

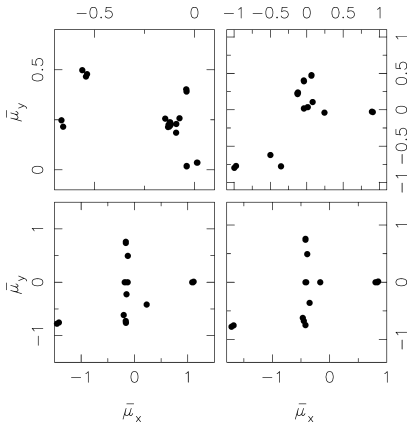

Figure 3. Dipole moment per atom for the 32 shapes of Figure 2 before applying the generalized Tasker criterion. In the upper row, we show results for the systems with four atoms per cell; the lower row contains results for the systems with two atoms per cell. The more covalent systems are represented in the left column; the more ionic ones in the right column. Each small sphere represents the results for one of the shapes of Figure 2. The size of the sphere indicates the uncertainty in the fit of eq 23.

condition of Tasker into account. Thus, for each shape and system we have a unique value for $\vec{\mu}$. At first, we verified that the charge distribution in the central region is independent of the overall shape of the system, with the shapes 21−24 being exceptions. This implies also that $\vec{\mu}_C$ of eq 12 is independent of the shape.

It may be suggested that the charges Q_k of eq 12 are independent of the shape, too. This would imply that the dipole moment per atom for the three shapes 1, 3, and 5 of Figure 3 takes the same value. This was found not to be the case. In addition, it was not possible to fit the dipole moment per atom with the expressions of the type of eq 12 when assuming that Q_k is a constant for a given surface but independent of the shape of the sample. This confirms that, in general, Q_k do depend on the overall shape of the sample. This can be explained through the charge conservation constraint, that is, the sum of the surface charges over all surfaces has to vanish.

For the four types of system studied here (i.e., with four or two atoms per cell and with a more covalent or ionic character), the infinite, periodic system possesses a well-defined energy gap between the occupied and unoccupied orbitals. On the other hand, for some (but certainly not all) shapes of Figure 2, even the largest systems possess an energy gap identical to or close to zero, which we ascribe to the existence of surface states that will prevail even when the system approaches becoming infinitely large. These surface states are certainly one reason for the different values of the dipole moment per atom. However, when focusing on only those shapes that have energy gaps significantly different from zero, Q_k is found to depend not only on the specific surface but also on the complete shape of the sample.

Finally, it is occasionally assumed that the dipole moment per cell can take values that differ only by lattice vectors (see, e.g., the introduction by Spaldin in ref 11). For the systems of Figure 2, the lattice vectors are $\vec{a} = (5,0)$ and $\vec{b} = (0,3)$, which would imply that the values of the dipole moment per atom would have to differ by $n_a(1.25,0) + n_b(0,0.75)$, with n_a and n_b being the integers for the systems with four atoms per unit cell and n_a and n_b being the even integers for the systems with two atoms per unit cell. The results of Figure 3 show clearly that this is not the case, confirming our earlier theoretical treatment.[8]

Next, we introduce the generalized Tasker constraints, that is, eqs. 2 and 3. We do that by following the approach of the Theory section. In the present case, it is assumed that, per construction, the z component of $\vec{E}$ vanishes, whereby eqs 2 and 3 or 9 give two constraints for the charge density shifts Δq_k. In addition, the charge neutrality constraint of eq 8 gives a third constraint for Δq_k. With four sides, this means that eq 10 can be written as

$$\Delta\vec{q} = \Delta\vec{q}_0 + t\Delta\vec{q}_1 \tag{24}$$

where $\Delta\vec{q}_0$ and $\Delta\vec{q}_1$ are constants, whereas $-\infty \le t \le +\infty$ is a parameter.

Ultimately, this means that, in general, the possible values for $(\bar{\mu}_x,\bar{\mu}_y)$ will form a straight line where different points correspond to different values of t. An exception, however, occurs when the shape has the form of a parallelogram, which indeed is the case for many of the shapes of Figure 2. Then, $(\bar{\mu}_x,\bar{\mu}_y)$ will reduce to a single point (i.e., $\Delta\vec{q}_1 = \vec{0}$). That this is the case can be understood as follows. For a rectangle, the generalized Tasker criterion requires that the charge densities associated with opposite sides have to be identical with no contribution to the dipole moment from these surfaces. Once this is established, changing the charge densities will not change the total dipole moment. For a parallelogram, the same arguments apply as one can see by using a coordinate system with axes that are parallel to the opposite sides.

In Figure 4 we show the results for the redistributed charge densities that satisfy the generalized Tasker criterion. As in

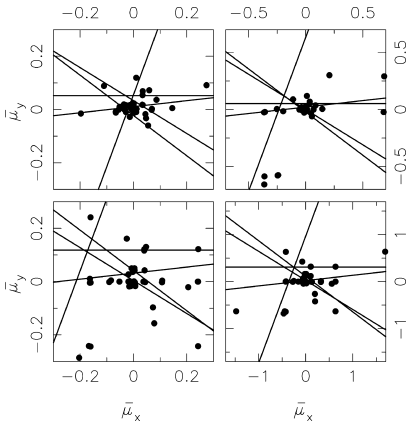

Figure 4. As Figure 3, but after redistributing the charge densities on the surfaces so that the generalized Tasker criterion is satisfied. For the five shapes that are not parallelograms, the dipole moment per atom is not uniquely determined but can lie anywhere along the lines shown.

Figure 3, we see that the dipole moment per atom can take essentially any value. As most of the shapes are parallelograms, there are only a few (five) cases for which the dipole moment per atom is not uniquely identified. In those cases, the possible values lie on one of the straight lines shown in the figure. The different values along the straight line correspond to different values of t in eq 24. As mentioned in the Theory section, Δq_{k1} does not depend on the system but solely on the overall shape.

DOI: 10.1021/acs.jpcc.8b03041
J. Phys. Chem. C 2018, 122, 11926−11932

Therefore, the straight lines have the same slope in the four different panels of Figure 4, which can easily be verified by inspection. We emphasize, however, that for a given system a unique value of the dipole moment per atom will be found corresponding to the value for the lowest total energy structure.

When comparing Figures 3 and 4, we see only a few similarities. Thus, the generalized Tasker conditions lead to significant changes in the charge distributions on the surfaces. The redistributed charges, in turn, alter the dipole moment per atom, which is a bulk property. Exactly how these charge redistributions are realized is beyond the scope of the present work, but could be accompanied by surface reconstructions and/or induced by the effect of adsorbants.

CONCLUSIONS

The purpose of the present work was to study the interplay between the surface and bulk properties of macroscopic crystalline materials with an emphasis on polar surfaces. To that end, we generalized a classification scheme, originally proposed by Tasker,[1] to identify stable polar surfaces. It was shown that it is always possible to stabilize a given surface through a charge redistribution involving the entire set of surfaces. A surface that should not be stable when considered individually may very well be observed experimentally through such a charge redistribution. Moreover, in two different experiments focusing on the same surface, but for samples of different shapes, one may observe different charge distributions on that surface. As the charge density of the surface is modified, even spatially local properties like catalytic activity can be influenced.

An especially relevant property associated with the charge distribution is the bulk dipole moment per unit. It was shown how the values for this property can be calculated subject to the generalized Tasker constraints. From the results of calculations for very large systems, based on a sufficiently simple model, we were able to show that applying these constraints leads to a change in the dipole moment per atom (or per unit in the thermodynamic limit). For some shapes, the resulting value of the dipole moment per unit is not uniquely determined. However, in the case of any real system, it will have a specific value determined by detailed energetic considerations that lie beyond the scope of this work. Essentially, any physically reasonable value can be obtained in contrast with the assumption often made that, for samples of the same material, the possible values differ by at most a lattice vector.

Our analysis allows for further understanding of the theoretical studies on the polar surfaces of ZnO mentioned in the Introduction. When the system is modeled in these studies using an infinite, periodic slab, there are only two surfaces, and only the component of the electric field $\vec{E}$ perpendicular to these surfaces may be nonvanishing. This leads to two conditions related to the charge redistribution (i.e., vanishing $\vec{E}$ and charge neutrality), whereby the changes in the charges on the two surfaces are uniquely determined according to our procedure. This coincides with the results of Meyer and Marx,[5] for example. Whether this is realized through surface states or through a lower symmetry on the surface is a question we do not try to address in the present work. On the other hand, our study suggests that consideration of other shapes (particularly containing more surfaces) would provide many more possibilities to realize this same surface.

Our results can also be used to throw some further light on the recent study on the (001) surface of $KTaO_3$.[7] The authors observed that after the surface is created it undergoes an insulator-to-metal transition, which we interpret as being a first consequence of stabilizing the surface through a charge redistribution. When the surface is subsequently exposed to water vapor, a further stabilization occurs which we consider is likely accompanied by a further charge redistribution. A detailed analysis of this qualitative picture, however, lies outside the scope of the present work.

ASSOCIATED CONTENT

Supporting Information

The Supporting Information is available free of charge on the ACS Publications website at DOI: 10.1021/acs.jpcc.8b03041.

Results of further model calculations (PDF)

AUTHOR INFORMATION

Corresponding Author

*E-mail: m.springborg@mx.uni-saarland.de. Phone: +49 (0) 681 302 3856. Fax: +49 (0) 681 302 3857.

ORCID

Michael Springborg: 0000-0002-5036-8239

Notes

The authors declare no competing financial interest.

ACKNOWLEDGMENTS

This work was supported by the German Research Council (DFG) through project SP 439/37-1. Moreover, one of the authors (M.S.) is very grateful to the International Center for Materials Research, University of California, Santa Barbara, for generous hospitality.

REFERENCES

(1) Tasker, P. W. The stability of ionic crystal surfaces. *J. Phys. C: Solid State Phys.* **1979**, *12*, 4977−4984.

(2) Noguera, C. Polar oxide surfaces. *J. Phys.: Condens. Matter* **2000**, *12*, R367−R410.

(3) Goniakowski, J.; Finocchi, F.; Noguera, C. Polarity of oxide surfaces and nanostructures. *Rep. Prog. Phys.* **2008**, *71*, 016501.

(4) Wander, A.; Schedin, F.; Steadman, P.; Norris, A.; McGrath, R.; Turner, T. S.; Thornton, G.; Harrison, N. M. Stability of polar oxide surfaces. *Phys. Rev. Lett.* **2001**, *86*, 3811−3814.

(5) Meyer, B.; Marx, D. Publisher's Note: Density-functional study of the structure and stability of ZnO surfaces. *Phys. Rev. B: Condens. Matter Mater. Phys.* **2003**, *67*, 035403.

(6) Mora-Fonz, D.; Lazauskas, T.; Farrow, M. R.; Catlow, C. R. A.; Woodley, S. M.; Sokol, A. A. Why are polar surfaces of ZnO stable? *Chem. Mater.* **2017**, *29*, 5306−5320.

(7) Setvin, M.; Reticcioli, M.; Poelzleitner, F.; Hulva, J.; Schmid, M.; Boatner, L. A.; Franchini, C.; Diebold, U. Polarity compensation mechanisms on the perovskite surface $KTaO_3$ (001). *Science* **2018**, *359*, 572−575.

(8) Molayem, M.; Springborg, M.; Kirtman, B. Surface effects on converse piezoelectricity of crystals. *Phys. Chem. Chem. Phys.* **2017**, *19*, 24724−24734.

(9) Kudin, K. N.; Car, R.; Resta, R. Quantization of the dipole moment and of the end charges in push-pull polymers. *J. Chem. Phys.* **2007**, *127*, 194902.

(10) Springborg, M.; Kirtman, B. How much can donor/acceptor-substitution change the responses of long push-pull systems to DC fields? *Chem. Phys. Lett.* **2008**, *454*, 105−113.

(11) Spaldin, N. A. A beginner's guide to the modern theory of polarization. *J. Solid State Chem.* **2012**, *195*, 2−10.

DOI: 10.1021/acs.jpcc.8b03041
J. Phys. Chem. C 2018, 122, 11926−11932

Supporting information for:

Surfaces, Shapes and Bulk Properties of Crystals

Michael Springborg,*,†,‡ Meijuan Zhou,† Mohammad Molayem,† and Bernard Kirtman¶

Physical and Theoretical Chemistry, University of Saarland, 66123, Saarbrücken, Germany, School of Materials Science and Engineering, Tianjin University, Tianjin 300072, China, and Department of Chemistry and Biochemistry, University of California, Santa Barbara, California 93106, USA

E-mail: m.springborg@mx.uni-saarland.de

Phone: +49 (0) 681 302 3856. Fax: +49 (0) 681 302 3857

*To whom correspondence should be addressed

†Physical and Theoretical Chemistry, University of Saarland, 66123, Saarbrücken, Germany

‡School of Materials Science and Engineering, Tianjin University, Tianjin 300072, China

¶Department of Chemistry and Biochemistry, University of California, Santa Barbara, California 93106, USA

We shall here give further details on the model calculations as well as results of other sets of model calculations.

Table S1: The values of the parameters for the model for the different sets of calculations.

System / Parameter	1	2	3	4	5	6
M	4	4	2	2	2	2
$\vec{a}$	(5, 0)	(5, 0)	(5, 0)	(5, 0)	(4, 0)	(5, 0)
$\vec{b}$	(0, 3)	(0, 3)	(0, 3)	(0, 3)	(0, 4)	(0, 5)
$\vec{u}_1$	(1.0, 1.0)	(1.0, 1.0)	(1.0, 1.0)	(1.0, 1.0)	(2.0, 1.0)	(0.0, 2.0)
$\vec{u}_2$	(2.0, 2.5)	(2.0, 2.5)	(2.0, 2.5)	(2.0, 2.5)	(1.0, 3.0)	(2.0, 0.0)
$\vec{u}_3$	(4.0, 0.5)	(4.0, 0.5)				
$\vec{u}_4$	(4.5, 2.0)	(4.5, 2.0)				
ϵ_1	-6	-2	-6	-2	-6	-6
ϵ_2	-8	-8	-8	-8	-8	-8
ϵ_3	-7	-7				
ϵ_4	-5	-13				
$t_{0,11}$, d_{11}	10, 3	5, 3	10, 3	5, 3	10, 5	10, 5
$t_{0,12}$, d_{12}	20, 3	9, 3	20, 3	9, 3	15, 5	15, 5
$t_{0,13}$, d_{13}	15, 3	7, 3				
$t_{0,14}$, d_{14}	12, 3	6, 3				
$t_{0,22}$, d_{22}	11, 3	5, 3	11, 3	5, 3	10, 5	10, 5
$t_{0,23}$, d_{23}	13, 3	6, 3				
$t_{0,24}$, d_{24}	17, 3	8, 3				
$t_{0,33}$, d_{33}	16, 3	8, 3				
$t_{0,34}$, d_{34}	14, 3	7, 3				
$t_{0,44}$, d_{44}	18, 3	9, 3				

At first, we show in Table S1 the values for the parameters that enter the model calculations and whose meaning is described in the main paper. The systems 1–4 are the ones whose results are given in the main paper, whereby the systems 1 and 2 contain 4 atoms per unit cell, and the other systems (including 5 and 6) contain 2 atoms per unit cell. The systems 1 and 3 are constructed as having a larger covalent character and a smaller ionic one, whereas the opposite is the case for the systems 2 and 4.

Subsequently, we show results for the systems 5 and 6 of Table S1. For system 5 we studied the 8 shapes of Fig. S1, and for system 6 we studied the 9 shapes of Fig. S4. The resulting

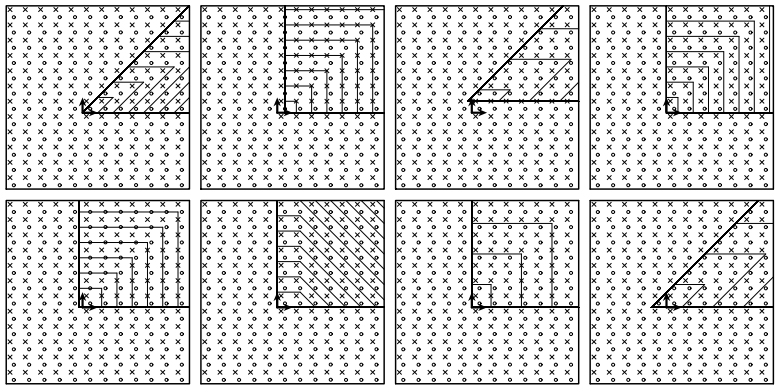

Figure S1: The 8 shapes that were studied for system 5. In each case, the smallest systems are shown.

dipole moments per atom are shown in Figs. S2 and S5, respectively, before enforcing the generalized criterion of Tasker, and in Figs. S3 and S6, respectively, after enforcing the generalized criterion of Tasker.

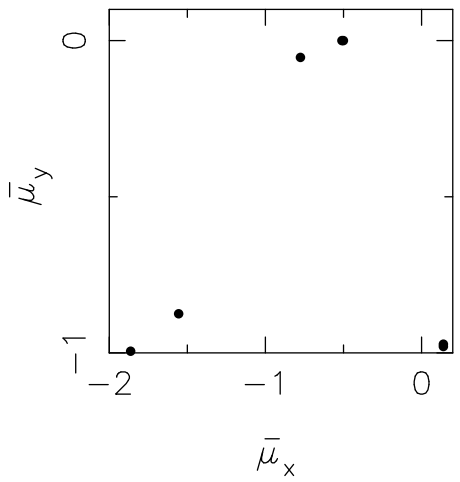

Figure S2: The dipole moment per atom for the 8 shapes of Fig. S1 for system 5 before applying the generalized criterion of Tasker.

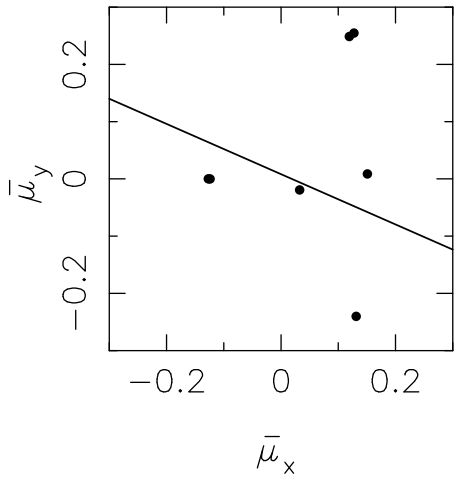

Figure S3: As Fig. S2, but after redistributing the charge densities on the surfaces so that the generalized criterion of Tasker is satisfied. For the single shape that is not a parallellogram, the dipole moment is not uniquely determined but can lie anywhere along the line shown.

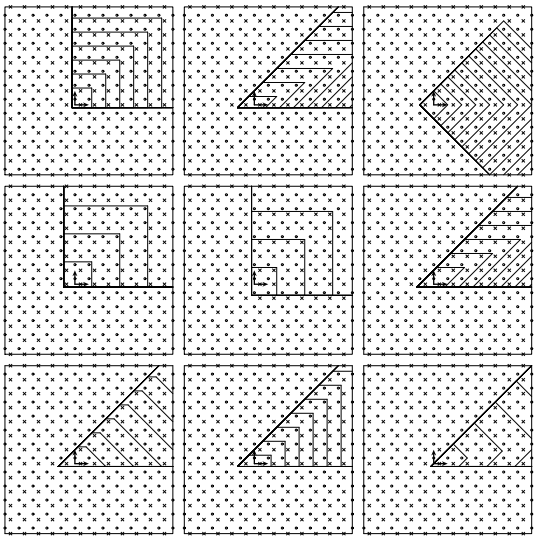

Figure S4: The 9 shapes that were studied for system 6. In each case, the smallest systems are shown.

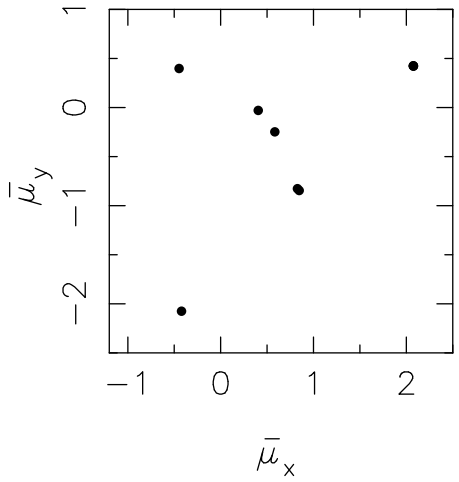

Figure S5: The dipole moment per atom for the 9 shapes of Fig. S4 for system 6 before applying the generalized criterion of Tasker.

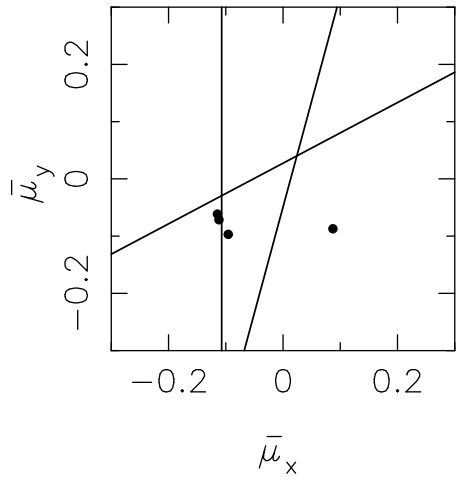

Figure S6: As Fig. S5, but after redistributing the charge densities on the surfaces so that the generalized criterion of Tasker is satisfied. For the three shapes that are not a parallellogram, the dipole moment is not uniquely determined but can lie anywhere along the lines shown.

ADVANCED THEORY AND SIMULATIONS
www.advtheorysimul.com

Theoretical Treatment for Properties of Surfaces and Their Interplay with Bulk Properties of Crystals

Meijuan Zhou, Michael Springborg,* and Bernard Kirtman*

It is demonstrated that there is an interconnection between surfaces, shapes, and bulk properties of macroscopic, crystalline materials. Thus, the requirement that no atom in the bulk shall experience a force from charges associated with the surface, a requirement formulated in terms of a generalized Tasker condition, leads to an interplay involving transfer of charge between different surfaces for a given sample. Through this mechanism, so-called polar surfaces, often considered to be essentially unstable, can always be stabilized. Density functional theory slab calculations are carried out to obtain typical surface charges and associated bulk geometric displacements for an individual surface. Then the consequences of the interplay between surfaces are studied through one property that is usually considered a bulk property, namely the polarization / dipole moment per volume, and one property that is usually related to an individual surface, that is, heterogeneous catalytic activity. Model calculations illustrate the importance of charge transfer between surfaces in both cases. These calculations provide a guide for much more difficult ab initio computations that might be carried out in the future.

1. Introduction

The properties of crystalline materials continue to be exploited for a very large range of applications. In many cases, it is the bulk properties that are of interest. In the thermodynamic limit, that is, for sufficiently large systems, these properties are either intensive or extensive depending upon whether they are independent of the system size or proportional to it. In either case, since the boundary regions make up a very small part of the complete system, it may be suggested that the boundary regions are of no importance. On the other hand, the properties of the boundaries themselves can also be of interest for applications. An example is heterogeneous catalysis, in which case the bulk part of the sample is often assumed to be irrelevant.

These considerations suggest that bulk properties and surface properties are essentially independent of each other and can be treated separately. Theoretical studies of the properties of crystals often utilize this approach. For bulk properties, one typically treats the system as being infinite and periodic, thus completely ignoring the boundary regions. For the study of surface properties, one often constructs a simple model system that contains the surface of interest while ignoring other surfaces as well as the bulk region with the exception that the latter defines the structure of the surface.

Recently, we have demonstrated that, for any real material, there is a delicate interplay whereby the concerted interactions between all surfaces and the bulk region will influence the properties of the individual surfaces.[1] Moreover, in some cases, these interactions will also affect the bulk properties. As an example of the latter, we considered the dipole moment per atom, an intensive property closely related to the polarization (i.e., the dipole moment per unit volume), that has relevance for piezoelectricity and other responses to electric fields. The purpose of the present work is to provide further details about this interplay and about its consequences. As in the previous study, we use simple model calculations that allow for application to very large, finite systems and thereby examine and illustrate concepts without attempting to provide accurate results for any real system.

Our paper is organized as follows. At first, we study in Section 2 the physical reasons behind the interplay between all surfaces and the bulk through surface charges. Subsequently, in Section 3, we discuss the implications for theoretical calculations designed to study the properties of individual surfaces. Then, in Sections 4 and 5, we illustrate the consequences of this interplay by studying the effects of the surfaces on a bulk property (the dipole moment per atom; Section 4) and the effects of the bulk on a surface property (heterogeneous catalysis; Section 5). Our results are summarized in Section 6.

2. Interplay between Surfaces and Bulk

Our goal is to consider neutral, macroscopic, 3D crystalline samples. For the sake of simplicity, however, we shall illustrate the

M. Zhou, Prof. M. Springborg
Physical and Theoretical Chemistry
University of Saarland
66123 Saarbrücken, Germany
E-mail: meijuan.zhou@uni-saarland.de;
m.springborg@mx.uni-saarland.de
Prof. M. Springborg
School of Materials Science and Engineering
Tianjin University
Tianjin 300072, China
Prof. B. Kirtman
Department of Chemistry and Biochemistry
University of California
Santa Barbara, CA 93106, USA
The ORCID identification number(s) for the author(s) of this article can be found under https://doi.org/10.1002/adts.201800117

DOI: 10.1002/adts.201800117

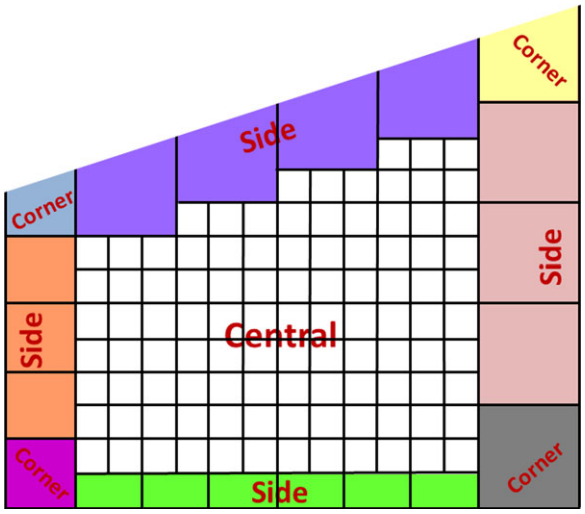

Figure 1. A schematic representation of a 2D system. It consists of a central region as well as various boundary regions.

concepts through 2D systems. Such systems, cf. **Figure 1**, can be separated into a central region and a number of boundary regions. Each region is assumed to consist of units that are identical, although the units of different regions will usually be different. In the central region, the units are chosen to be the same as the unit cells of the corresponding infinite, periodic system. Note that, in either case, this choice is not unique.

In the boundary regions, the units will often be larger than those of the central region due to the effects of structural and electronic relaxations near the surfaces. Since the sample is completely divided into units, those of the boundary regions will depend, in part, upon how the units of the central region are chosen and, in part, they may be constructed according to convenience. In the thermodynamic limit, the size of the central region will be much larger than that of any other region, which is why most bulk properties are independent of the boundary regions. We add that the units of the central region may be chosen independently of the boundary regions and of the overall shape of the sample.

The units of the central region are neutral as can easily be seen as follows. Consider, for example, a 2D system like that of Figure 1. If the units of the central region carried charge, the fact that the complete system is neutral implies that a compensating charge must be accumulated in the boundaries. If you double the linear dimension of the system, then the total charge of the central region will be four times larger. On the other hand, per construction, each boundary region does not change extension in the direction(s) perpendicular to the surface(s) at which it is placed. Therefore, the charge per cell in the boundary regions would have to increase on average in order to maintain neutrality. This is in conflict with the assumption that the thermodynamic limit has been reached. Thus, only the units of the boundary regions may be charged.

Having established that the charge is concentrated in the boundary regions, we may continue by studying the effects of this charge distribution on the atoms in the central region. To that end, we consider an approach originally proposed by Tasker.[2] Tasker studied the electrostatic field created by a set of parallel layers of ions at a point far away from those layers, which represents the position of an atom in the bulk. In order to ensure that the crystal structure is stable, the electrostatic field at the atom would have to vanish. Since the details of the charge distribution were not relevant for his argument, he approximated each infinite layer of ions by means of a 2D plane with a constant charge density. Thereby, he was able to identify certain arrangements of the ion layers for which the electrostatic field at the bulk atom does not vanish and concluded that such so-called polar surfaces either could not exist or would experience substantial reconstruction.

In our recent work,[1] we generalized Tasker's analysis by considering an arbitrary shape for the sample and the corresponding charged layers with different orientations as shown schematically in **Figure 2**. Then, the electrostatic field at an atom in the central region, due to charges localized in the surface regions, becomes

$$\vec{E}_{\text{charge}} = \frac{1}{4\pi\epsilon} 2\pi \sum_i q_i' \vec{1}_i$$

$$= \frac{1}{4\pi\epsilon} 2\pi \sum_k \left[\sum_{i \in k} q_i' \right] \vec{1}_k = \frac{1}{4\pi\epsilon} 2\pi \sum_k q_k \vec{1}_k \tag{1}$$

where $\vec{1}_i$ is an inward pointing normal to the ith layer of ions and q_i' is the charge density of that layer and

$$\epsilon = \epsilon_0 \epsilon_r \tag{2}$$

is the dielectric constant of the material. Finally, q_k is the sum of the charge densities of all layers associated with the kth surface.

Another contribution to the electric field that occurs in certain cases has been analyzed by Meyer and Vanderbilt, and Meyer and Marx.[3,4] Thus, for crystals with a periodic stacking sequence as in **Figure 3**c, which results in a dipole moment perpendicular to

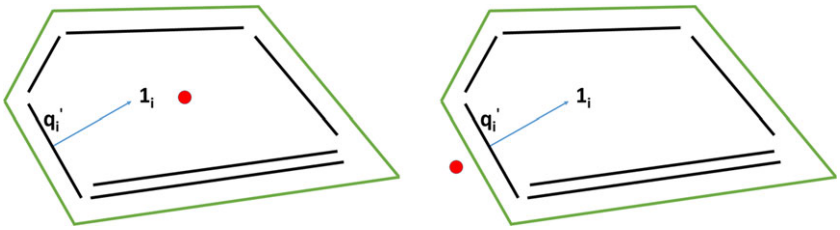

Figure 2. A schematic representation of a 2D system. It shows the layers with the charge densities q_i' as well as an inward pointing normal to a given layer, $\vec{1}_i$. The boundary of the system is shown through green lines. In the left part, the red dot represents a point in the central part of the system, whereas in the right part it represents a point just outside one of the sides.

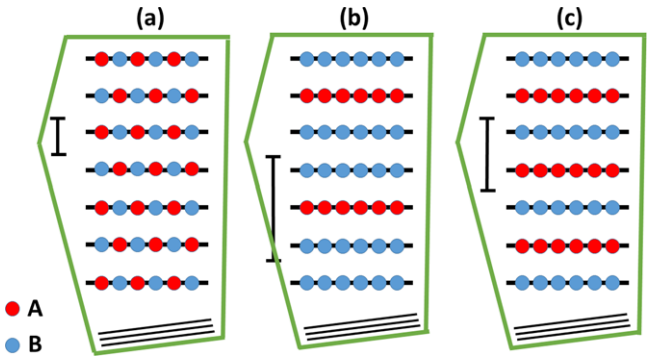

Figure 3. A schematic representation of three different systems similar to those discussed in the original work by Tasker.[2] The repetition of the atomic layers is indicated. The shape is indicated through the green frame, and examples of some atomic layers are indicated for the bottom-most surface through the thinner lines.

the surface, there is a field from the dipole layers, $\vec{E}_{\text{dipole}}$. Except for the slab geometry, that will be discussed in the next section, closed expressions for $\vec{E}_{\text{dipole}}$ have not been presented.

The total field is then

$$\vec{E} = \vec{E}_{\text{charge}} + \vec{E}_{\text{dipole}} \tag{3}$$

and the generalized Tasker condition is

$$\vec{E} \equiv \vec{0} \tag{4}$$

In our previous work, we have ignored $\vec{E}_{\text{dipole}}$ which is also what we shall do in most of the present work. In that event, Equation (4) becomes

$$\vec{E} = \frac{1}{4\pi\epsilon} 2\pi \sum_k q_k \vec{1}_k \equiv \vec{0} \tag{5}$$

It is important to emphasize that this is a condition not for a single surface but for the complete set of surfaces of a given sample.

At this point, it is relevant to relate our present results with the analysis of Tasker in his original work.[2] Tasker considered systems like those of Figure 3, that is, crystalline AB or AB_2 compounds. In contrast to the present work, he considered solely a single sequence of parallel atomic layers (i.e., a slab), whereas we include other surfaces as well, as indicated in Figure 3. Due to different chemical surroundings, the surface unit cells, as opposed to those in the bulk, may not be neutral. Then, the total charge density associated with such cells can give rise to the electrostatic fields discussed above in Equations (3) and (4). The realization of this possibility will depend, in general, on all surfaces of the sample.

3. Implications for the Study of Individual Surfaces

Often the properties of one or more individual surfaces of a 3D system, such as the ones shown schematically in Figure 2, are of interest. To that end, each surface of interest can be modeled using a slab geometry as shown in **Figure 4**. In that event (cf. Figure 4), the inward pointing normals from the surfaces are both parallel to the z axis. Thus, if $\vec{1}_z$ is a unit vector along the z axis, then

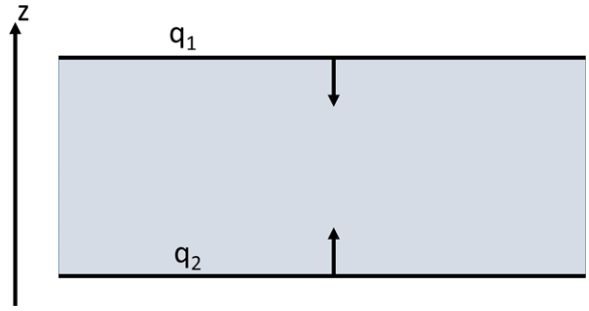

Figure 4. A schematic representation of a slab used for treating a single surface.

$$\vec{1}_2 = -\vec{1}_1 = \vec{1}_z \tag{6}$$

and, putting $\vec{E}_{\text{dipole}}$ aside for the moment, the generalized Tasker condition of Equation (5) reduces to

$$(q_1 - q_2)\vec{1}_z = \vec{0} \tag{7}$$

Combining this condition with the charge-neutrality requirement given by

$$q_1 + q_2 = 0 \tag{8}$$

leads to the unique solution

$$q_1 = q_2 = 0 \tag{9}$$

However, it is not realistic in general to ignore $\vec{E}_{\text{dipole}}$ and, therefore, $q_1 = -q_2 \neq 0$ corresponds to a more correct description. Here, we shall use polar ZnO to obtain a quantitative description of the effects of the surface charges on the bulk structures, in which case[3]

$$\vec{E}_{\text{dipole}} = -\frac{1}{4\pi\epsilon}\frac{4\pi}{a} m\vec{1}_z \tag{10}$$

where m is the dipole density and a is the distance between repeating layers.

To determine surface charges and their effect, density functional theory (DFT) calculations were carried out for stoichiometric slabs of ZnO containing both O- and Zn-terminated surfaces using the Vienna ab initio simulation package (VASP).[5–8] Exchange and correlation effects were described using the generalized gradient approximation (GGA)[9] of Perdew, Burke, and Ernzerhof (PBE)[10] with the energy cutoff for the plane-wave expansion set to 400 eV.[11] Two structures, as shown in **Figure 5**, were constructed using the ZnO bulk crystal geometry.[12] Both structures contain the $(000\bar{1})$ Zn-terminated surface to the left and the (0001) O-terminated surface to the right. For structure I, we considered 15 atomic bilayers with a (1×1) unit cell whereas for structure II, eight bilayers and a (2×2) unit cell were used. A vacuum region of 20 Å was included in all calculations. In each

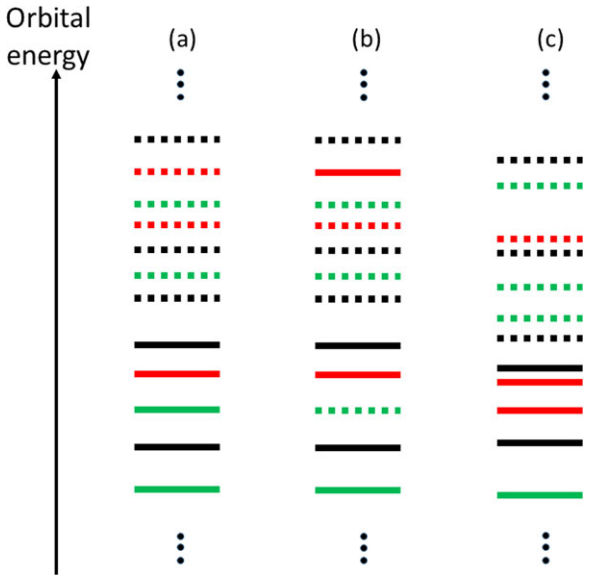

Figure 5. Schematic presentation of the orbitals closest to the Fermi level of a large, finite system. The full and dashed lines represent occupied and empty orbitals, respectively. Moreover, the black lines represent orbitals localized to the bulk region, whereas the green and red lines represent orbitals that are localized to electron-donating and electron-accepting surfaces, respectively. For further details, see the text.

case, we examined both the fixed geometry and a relaxed geometry (see later) with lattice parameters fixed at the experimental bulk values.

A Bader analysis[13] was used to decompose the total charge density into atomic contributions. Each structure contains alternating layers of Zn and O atoms. Denoting the Bader charges of the Zn and O atoms of the mth bilayer by $\tilde{Q}_{\mathrm{Zn},m}$ and $\tilde{Q}_{\mathrm{O},m}$, respectively, we constructed the accumulated charges as

$$Q_n = \sum_{m=1}^{n} \tilde{Q}_m = \sum_{m=1}^{n} \left[\tilde{Q}_{\mathrm{Zn},m} + \tilde{Q}_{\mathrm{O},m}\right] \tag{11}$$

wherein the atomic bilayers are enumerated starting from the left in Figure 5 and $\tilde{Q}_m$ is the total charge of the mth bilayer. For structure II, we used the averaged values of the atomic charges per bilayer. These accumulated charges are shown in the panels at the bottom of Figure 5.

We note that Q_n converges rapidly to a roughly constant value when starting from either side of the slab (i.e., for n close to 1 or 15 for structure I and close to 1 or 8 for structure II). That the converged value in all cases is markedly different from zero is in conflict with the condition of Equation (9). Instead, the fact that we have a regular charge distribution in the middle of the slab implies that the field due to the surface charges compensates the field due to the repeated sequence of dipoles, that is, $\vec{E}_{\mathrm{dipole}} = -\vec{E}_{\mathrm{charge}}$ for this structure. However, our results do not imply that the results of slab calculations will be found for an arbitrary shape containing the same individual surfaces as the slab. For other shapes, the generalized Tasker condition will most often lead to different results.

It is of interest to estimate how much a surface charge density of the magnitude found in our ZnO calculations will affect the bulk structure. For this purpose, we see from Figure 5 that a realistic value for the magnitude of the charge per surface unit cell is a bit less than $0.3e$. In order to obtain the charge density q, one must divide by the area of the surface unit cell, which is calculated to be 9.14 Å^2 from the experimental crystal structure.[12] We also use for the relative dielectric constant of Equation (2), the value $\epsilon_r = 8.5$.[15] Finally, a Bader analysis of the atoms in bulk ZnO gives atomic charge of roughly ± 1, which allows us to estimate a typical value for the force acting on an ion in the central part of the slab.

In addition, we need the force or energy associated with typical nuclear displacements. Toward that end, VASP calculations were carried out on crystalline ZnO with four atoms per unit cell. As a representative motion, that maintains the crystal symmetry, we chose to displace all Zn and O atoms in opposite directions along the c axis. The unit displacement is shown in **Figure 6** where it is labeled u. The resulting total energy and force curves are also shown in the figure where it is seen that the motion is strongly anharmonic. Nonetheless, we can obtain an estimate for u based on the dashed horizontal red line in Figure 6, which represents the force due to the surface charge. We see that the displacement corresponding to this force is roughly $|u| \simeq 0.03$ Å. Of course, this is just a crude estimate. Although non-negligible, such a displacement is small enough that bulk structural distortions due to surface charges will likely be difficult to calculate with reliability. On the other hand, geometric distortions at the surface may be substantially larger.

Having considered the slab geometry in some detail, we are now ready to describe a more general system such as the 3D analogue of the one in Figure 2. For that case, we have three scalar relations provided by the generalized Tasker condition, Equation (5),

$$\sum_k q_k \vec{1}_k = \vec{0} \tag{12}$$

plus a single charge-neutrality condition

$$\sum_k q_k L_k = 0 \tag{13}$$

with L_k being the size of the kth surface. It is clear that

$$q_k = 0 \tag{14}$$

satisfies these equations. However, often the shape will have $N_S > 4$ surfaces so that, in general, the charge densities may be written in the form

$$q_k = \sum_{p=1}^{N_S-4} t_p q_{kp} \tag{15}$$

with t_p a parameter where, for a given p, $\{q_{kp}\}$ is one of the linearly independent solutions of

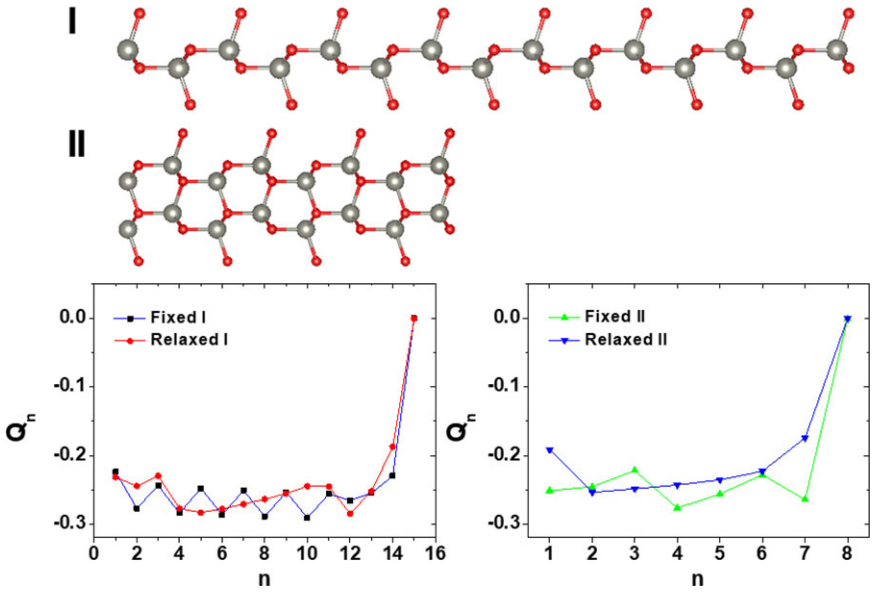

Figure 6. Accumulated layer charges per 1 × 1 surface unit cell from VASP calculations on polar slabs of ZnO. Atomic charges were obtained using a Bader analysis[13] and accumulated charges are defined in Equation (11) where the layers are enumerated starting from the right. The structures correspond to the (000$\bar{1}$) O-terminated surface to the left and the (0001) Zn-terminated surface to the left. For structure I, we considered 15 atomic bilayers and for structure II, eight bilayers. The 3D visualization of these structures were constructed using the VESTA 3 software.[14] Here, the smaller red and the larger grey spheres represent oxygen and zinc atoms, respectively. Further details are provided in the text.

$$\sum_k q_{kp}\vec{1}_k = \vec{0}$$

$$\sum_k q_{kp} L_k = 0 \tag{16}$$

Thus, not only is the solution identified from the slab calculations possible, but very many other solutions are possible as well. Which set of surface charge densities $\{q_k\}$ actually occurs for the system of interest will be determined by the electronic potential-energy landscape, which is beyond the scope of the present treatment. However, our discussion shows that what is obtained in a slab calculation does not necessarily correspond to what will be observed for a given surface of a real sample.

Let us now imagine that we have carried out an Hartree–Fock (HF) or DFT electronic-structure calculation on some large, finite system with a given fixed shape. In general, the lowest total energy (electronic + nuclear) solution will be such that

$$q_k \equiv q_{k0} \neq 0 \tag{17}$$

whereas the electrostatic field at any atom in the central region must vanish at the energy minimum. This calculation will yield a set of electronic orbitals that are (doubly) occupied from below as indicated schematically in **Figure 7**a.

Subsequently, we may consider another sample with a different shape. A simple example is shown in **Figure 8** where the new sample contains the same types of surfaces but their relative sizes are different. In this case, the sample on the right can be obtained by making a parallel cut on one side of the original left-hand sample. Because the surfaces have changed relative size, the charge-neutrality condition (13) will, in general, not be satisfied for the second sample if the original charge densities are retained. Thus, the two samples will differ not only in shape but also in their electronic charge distribution and/or their minimum energy structure. Of course, this is just one possible example. In other constructions, the shape may be altered in a way that preserves charge neutrality, but directly violates the generalized Tasker condition.

In general, the change from one sample to the other may be described, at least partly, as a flow of electronic charge between the different surfaces

$$q_{k0} \rightarrow q_{k0} + \Delta q_k \equiv q_k \tag{18}$$

in such a way that charge neutrality, that is

$$\sum_k q_k L_k = \sum_k (q_{k0} + \Delta q_k) L_k = 0 \tag{19}$$

is maintained. Through this charge flow, the generalized Tasker condition shall still be satisfied

$$2\pi \sum_k (q_{k0} + \Delta q_k)\vec{1}_k = 2\pi \sum_k \Delta q_k \vec{1}_k \equiv \vec{0} \tag{20}$$

For a 3D system, Equation (19) provides one condition and Equation (20) another three scalar conditions that the charge-density shifts $\{\Delta q_k\}$ must satisfy. Thus, for samples with more than four surfaces, there is, at first, a whole continuum of possible solutions.

As already noted, in order to accomplish the charge transfer implied by any particular solution of Equations (19) and (20), an electronic relaxation is required. It may be that the particular solution corresponds to a charge redistribution that can be closely simulated by transferring electrons between localized

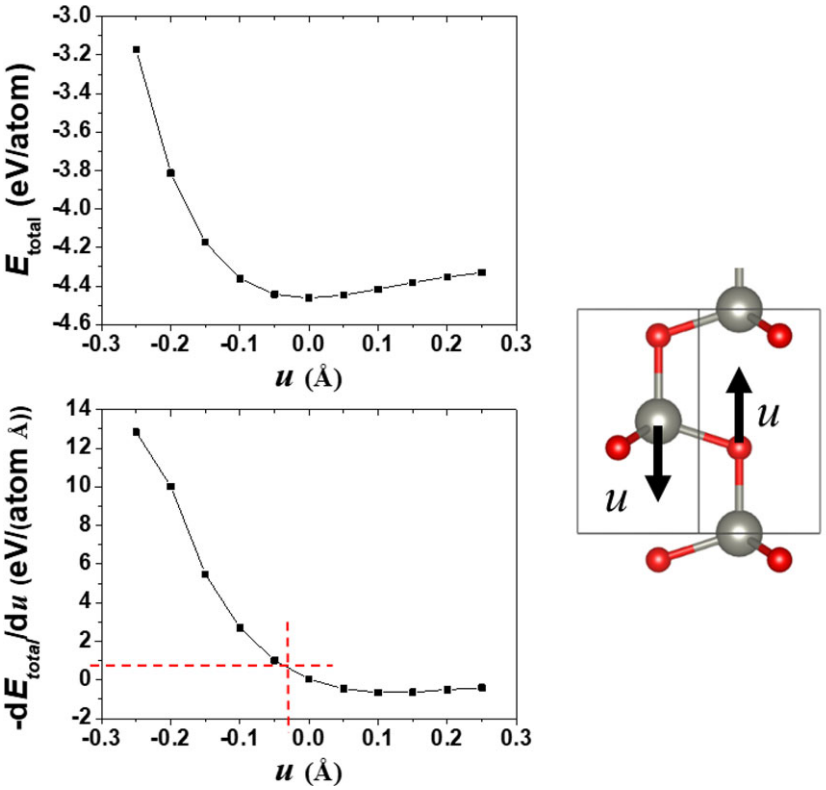

Figure 7. Results from VASP calculations on crystalline ZnO. All Zn and O atoms were displaced along the *c* axis in opposite directions as shown to the right. The upper panel to the left shows the resulting total energy, and the lower panel the resulting forces on the atoms. In this panel, the horizontal line marks the upper limit for the forces that can act on the ions due to the charges on the (0001) or (000$\bar{1}$) surfaces.

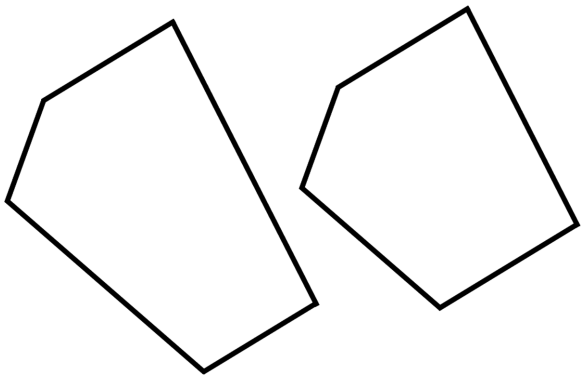

Figure 8. A schematic representation of two different samples with the same types of surfaces but different shapes. In this case, the right sample can be created from the left one by cutting one surface.

orbitals on different surfaces. In that event, a good initial guess for a subsequent SCF calculation could be obtained by occupying orbitals as shown in Figure 7b. Of course, this depends upon the particular solution. Alternatively, one could simply begin the SCF procedure with the charge density derived from the orbital occupancy of Figure 7a. In either case, an additional structural relaxation will normally be needed, so as to arrive at the stable ground state with the occupied orbitals of Figure 7c. Whether a stable ground state geometry can be reached without a major reconstruction, or not at all, will depend upon the details of the system of interest and cannot be answered in general.

These arguments demonstrate that the surface properties are determined partly by the bulk in the sense that the generalized Tasker condition for the electrostatic field at a bulk atom puts limits on the charge distribution at the surfaces. Moreover, since this condition involves all surfaces simultaneously, there is a coupling between the individual surfaces, which ultimately implies that the same surface for samples of different shapes may have different properties. Moreover, even for the same shape, there are many possibilities for the charge distribution and structure of a given surface with a relative stability that depends upon the system. This is a relevant issue, in particular, for oxide surfaces. It has often been argued that the latter belong to the class of polar surfaces and, accordingly, should not be stable, although they are observed in experiment. Several studies have been devoted to this conundrum[4,16–20] that often reach different conclusions. This may be due, at least in some degree, to the fact that the generalized Tasker condition, by itself, does not provide the unique solution for a given surface, since the charge density depends upon an interplay between all the surfaces of the system of interest.

4. Dipole Moment per Atom

Having discussed how the set of surface charges is limited by the condition that the electrostatic field must vanish in the bulk, let

us consider how an allowed set of surface charges can affect bulk properties. Although this is not the case for all properties, one property that does contain a finite contribution from the surfaces regardless of the size of the system is the dipole moment per atom.[21] Formally, any intensive property, which corresponds to an extensive property Z, can be calculated as

$$\tilde{Z} = \lim_{N\to\infty} \frac{Z(N)}{N} = \lim_{N\to\infty} \frac{Z(N+\Delta N) - Z(N)}{\Delta N} \tag{21}$$

with $Z(N)$ being the value for the system with N atoms. In the present case, Z is one of the vector components of the total dipole moment,

$$\vec{\mu} = \int \rho(\vec{r})\vec{r}\,d\vec{r} \tag{22}$$

Since the system is neutral, $\vec{\mu}$ is independent of our choice of the origin for the coordinate system and, for convenience, we place this origin at the middle of the bulk region. Then, from the last expression in Equation (21), it follows that the dipole moment per atom consists of two terms,

$$\tilde{\vec{\mu}} = \vec{\mu}_C + \sum_k \vec{\mu}_k \tag{23}$$

where $\vec{\mu}_C$ is the dipole moment per atom of a single (neutral) unit cell in the central region whereas $\vec{\mu}_k$ is the contribution from the kth side (cf. Figure 2). The latter can be interpreted as originating from a displacement of the charge density q_k along the negative normal, that is, along $-\vec{1}_k$ when the size of the system is increased, as we have discussed in detail previously.[21] In general, $\tilde{\vec{\mu}}$ will have a nonvanishing contribution from the surface regions. We emphasize, however, that the separation in Equation (23) is not unique since it depends critically on the definition of the bulk unit cell. In fact, one may construct bulk unit cells so that one of the two terms in Equation (23) vanishes. We shall make use of this possibility below.

As an aside, it is interesting to note that, in principle, the surface contribution can be obtained from calculations on infinite, periodic crystalline systems even though such systems, by construction, have no surfaces.[21] On the other hand, the relation between the polarization—that is, dipole moment per unit volume—as calculated for the infinite, periodic system and the corresponding property for the large, finite system is nontrivial and, in fact, at the moment of writing, the relation between the shape and the values of the polarization calculated for the infinite, periodic system is not known.

In order to explore the surface contribution to the dipole moment per atom further, we performed calculations for a simple finite 2D model system lying in the (x, y) plane. This model is completely equivalent to a 3D system which has two neutral, oppositely placed surfaces parallel to the (x, y) plane with identical properties for the parallel layers of cells that are in between. The advantage of using the simpler 2D model is that we can study many cases having large spatial extensions without requiring excessive computer resources. Accordingly, we shall treat the system as if it were 3D.

Our model has been described in detail elsewhere[1] and will, therefore, be described here only briefly. It is a single-particle, Hückel-like model with distance-dependent hopping integrals. In the current application, the bulk unit cell contains two atoms, each having one electron and a nuclear charge of unity. A single atomic orbital is placed on each atom and all atoms are fixed at the positions they occupy in the bulk. More details may be found in refs. [1,22]. Initially, we construct a very large system and, then, cut out a finite segment with four sides. In each set of calculations, the shape of the segment is retained but the sample is made gradually larger up to around 8000 atoms in total. For every size, we calculate the (2D) dipole moment per atom and afterward extrapolate the entire set of values to the infinite-system-size limit in the spirit of Equation (21).

Two systems were studied, one of them more covalent and the other more ionic. Here, for the covalent system, the ratio between the absolute values of the difference in the on-site energies and the typical hopping integrals is smaller than what is the case for the ionic system (see parameter values in ref. [22]). Moreover, calculations were done for the eight different shapes shown in **Figure 9**. Finally, we considered the variation from a high-symmetry structure to displaced structures with reduced symmetry. The displacements were generated by moving one type of atom, with the other type fixed, as shown in **Figure 10**. These displacements are quantified by a parameter s that goes from $s = 0$ at the configuration where the bulk unit cell can be constructed as being centro-symmetric to a maximum at $s = 1$ in six equidistant steps. We shall discuss this structural change and the rationale behind it in more detail below. Here, however, it is worthwhile to mention that when choosing the bulk unit cell as in Figure 10, $\vec{\mu}_C$ vanishes for $s = 0$ so that any nonzero value for the dipole moment per atom can be ascribed solely to surface contributions. When $s = 0$, not only the bulk unit cell has inversion symmetry but also the complete sample has inversion symmetry, the total dipole moment will vanish for obvious reasons.

The shapes 1–8 of Figure 9 are all parallelograms, which has an interesting consequence for the possible values of the total dipole moment. For the sake of convenience our argument below is presented using a coordinate system where the two axes are parallel to the nonparallel sides of the parallelogram. Let us suppose that we have identified a set of charge transfers $\{\Delta q_k\}$ for which the charge-neutrality constraint (19) and the generalized Tasker condition (20) are satisfied. Many other solutions to these equations may exist, implying that we may modify the $\{\Delta q_k\}$. However, the opposite sides of a parallelogram have the same size and, therefore, requiring that the generalized Tasker condition and the charge-neutrality condition remain satisfied implying that the same charge has to be added to each of the two opposite sides. It is easily realized that these changes will not alter the total dipole moment. Thus, for the parallelogram, this property has a unique value when the generalized Tasker condition and the charge-neutrality condition are satisfied. This is, in general, not the case for other shapes as shown, for example, in our previous study.[1]

In **Figure 11**, we show the dipole moment per atom for the eight shapes of Figure 9 including both the covalent and ionic models. As mentioned above, the bulk unit cell geometry can be chosen as being centro-symmetric (see Figure 10) so that $\vec{\mu}_C = \vec{0}$ and, thus, any deviation of $\tilde{\vec{\mu}}$ from $\vec{0}$ is solely due to the surfaces. When the overall system also has inversion symmetry, $\tilde{\vec{\mu}}$ will vanish, which only happens for shape 6. Before applying the

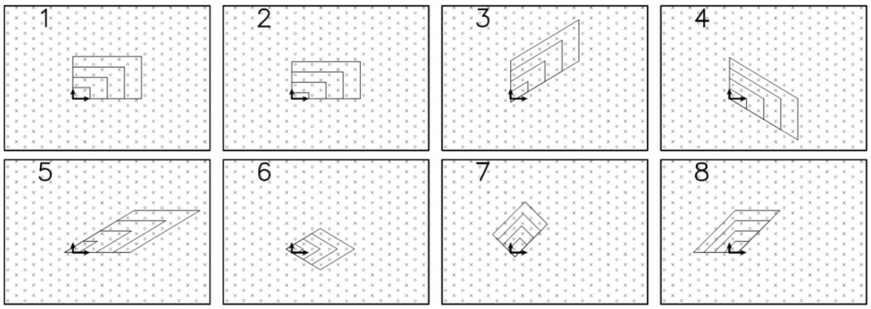

Figure 9. The eight shapes that were studied in Section 4. For each shape, the four smallest systems are shown. Each system has two atoms per unit shown through the different symbols. The small arrows show the lattice vectors. The first row contains from left to right the shapes 1–4, and the second row the shapes 5–8.

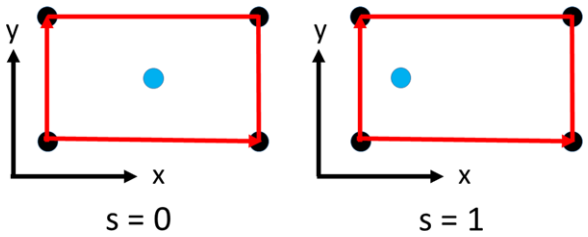

Figure 10. Schematic presentation of how the bulk unit cell changes when passing from the high-symmetry structure with $s = 0$ to the structure with a lower symmetry for $s = 1$. The red lines show the unit cell boundaries while the black and blue dots mark the positions of the two different types of atom. By moving the latter atom with respect to the former, which is fixed in position, one passes from the most symmetric structure at $s = 0$ to a maximum displacement at $s = 1$.

generalized Tasker condition (top panels), our calculations for shape 6 give very small values (less than 0.03 in the units of the present study) for the two components of $\vec{\mu}$. These deviations from zero are a measure of the numerical accuracy in our extrapolation to the infinite-system limit.

In addition to shape 6, we see that shapes 1, 2, and 7 in Figure 11 for $s = 0$ also have values for $\vec{\mu}$ that are very close to $\vec{0}$ before applying the generalized Tasker condition. However, the values for the four other shapes (3, 4, 5, and 8) clearly differ from $\vec{0}$, which means that the surfaces make significant contributions to $\vec{\mu}$. The fact that, in general, $\vec{\mu}$ takes larger (positive or negative) values for the ionic system than for the covalent system before the generalized Tasker condition is applied can be related to the larger atomic charges in the ionic case. A comparison of the upper row with the lower row shows that applying the generalized Tasker condition has a different effect for different shapes. On the other hand, the $\vec{\mu}$ values become essentially the same for both the ionic and covalent cases once this condition has been satisfied. We will see later, however, that this is not a general result for other parallelogram shapes.

For the lower-symmetry structure with $s = 1$, the inversion symmetry is lost and $\vec{\mu}$ may take any value. In particular, this property is no longer required to vanish for shape 6. In Figure 11 e,f, it is clearly seen that the spread in the values of the $\vec{\mu}$ components is smaller than what is found for $s = 0$. After applying the generalized Tasker condition, however, the spread increases

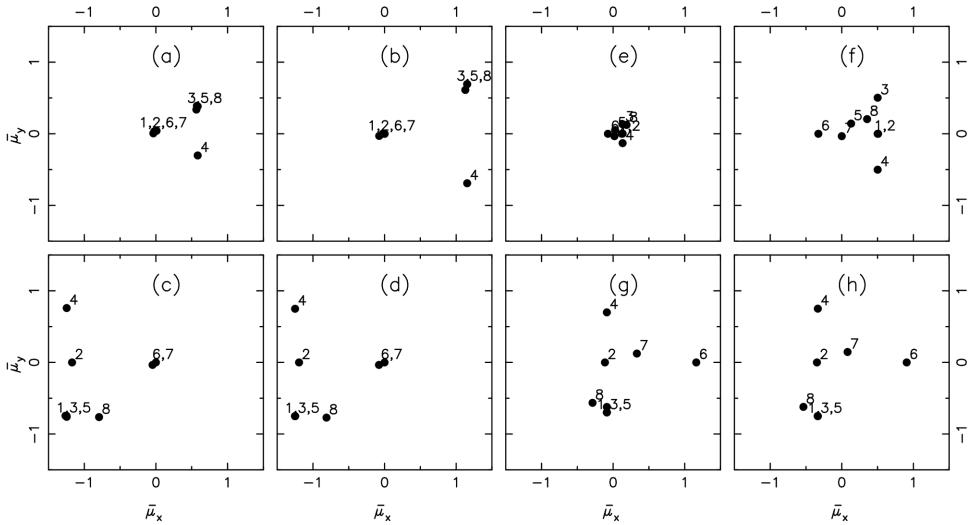

Figure 11. Dipole moment per atom for the eight shapes of Figure 9 in the cases a–d) $s = 0$ and e–h) $s = 1$. The top panels show results prior to applying the generalized Tasker criterion while the bottom panels show the analogous results after applying this criterion. Panels (a)–(d) pertain to the covalent system and (e)–(h) to the ionic system. The numbers refer to the shapes of Figure 9.

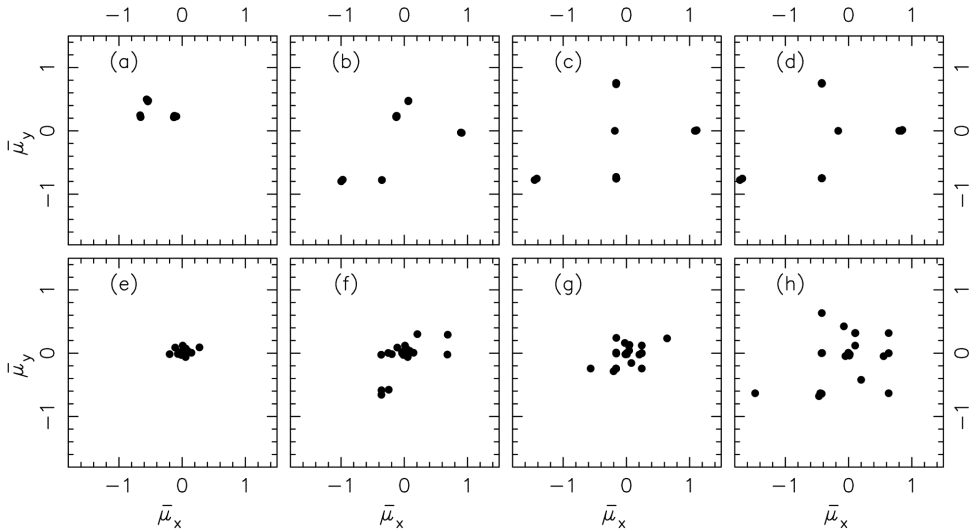

Figure 12. Dipole moment per atom for an extended set of 23 parallelogram-shaped systems considered previously. The upper panels show results before applying the generalized Tasker condition, whereas the lower ones show results after applying this condition. Panels (a),(c),(e),(g) are for a more covalent system, while the others are for a more ionic one. Panels (a),(b),(e),(f) show results for a system with four atoms per unit cell; the others are for a system with two atoms per cell. The results are extracted from ref. [1].

and once again, the values of $\vec{\bar{\mu}}$ for the ionic and covalent systems become more similar but without being identical.

For $s = 0$, the fact that the values after applying the generalized Tasker condition are identical for ionic and covalent systems with the same shape can be understood as follows. Due to inversion symmetry $\vec{\mu}_C = \vec{0}$ for the bulk unit cell in the left part of Figure 10. Thus, any deviation of $\vec{\bar{\mu}}$ from $\vec{0}$ is caused solely by the surfaces. Before applying the generalized Tasker conditions, the differences in the surface charges between ionic and covalent systems of the same shape will lead to different values for $\vec{\bar{\mu}}$ as can be seen in Figure 11 a–d. However, once the generalized Tasker condition has been applied, the dipole moment per atom does not depend any further on the surface charges since the shapes we are considering are parallelograms. These surface contributions to $\vec{\bar{\mu}}$ are, in turn, determined solely through the geometry of the sample, cf. Equations (12) and (13), and independent of the number, types, or positions of the atoms per unit cell.

For $s \neq 0$, $\vec{\mu}_C$ will no longer vanish. In fact, an approximate value for $\vec{\mu}_C$ can be obtained through the atomic Mulliken charges that vary from $\pm 0.47|e|$ to $\pm 0.17|e|$ for the covalent system and from $\pm 0.92|e|$ to $\pm 0.67|e|$ for the ionic system when going from $s = 0$ to $s = 1$. If we consider shape 1 as an example, then before applying the generalized Tasker condition, the corresponding electric fields given by Equation (1) (with $\epsilon_r = 1$) vary from (2.1,1.3) to (0.4,1.1) for the covalent system and from (2.1,1.3) to (1.4,1.3) for the ionic system. Thus, for the ionic system, a larger charge transfer among the different surfaces is needed in order to satisfy the generalized Tasker condition, that is, in order to make the fields vanish. This, in turn, leads to larger changes in $\vec{\bar{\mu}}$. For the present systems, it turns out that this ultimately leads to values for $\vec{\bar{\mu}}$ that are very close for the ionic and the covalent systems, which, however, as we shall see below is not a general conclusion.

We realize that some of the results discussed in detail here are based on calculations for a limited number of cases. Thus, it is worthwhile to compare with our more extensive previous study[1] in which 23 purely 2D systems with a parallelogram shape (only partly, the same shapes were treated in the present study) were considered (amongst others) with the results shown in **Figure 12**. In contrast with parallelograms 1–8, application of the generalized Tasker condition reduces the dipole moment per atom, in general, but at the same time it leads to a more distinct set of values for that property. Moreover, we see that for this larger sample, the values for the ionic and the covalent systems differ significantly, which is in contrast to the results of the present study, and which can be ascribed to the fact that the bulk contributions to $\vec{\bar{\mu}}$ in the previous study were larger.

When calculating the dipole moment per atom using the approximation of having an infinite, periodic system, one may apply the so-called Berry-phase approach.[23,24] Without going into detail, we mention that, as the name suggests, the dipole moment per unit cell is then related to the phase of a complex number with the phase being defined only up to an integer times 2π. For a system that is periodic in only ID, the so-called charge quantization[25–27] implies, then, that the dipole moment per unit cell is defined only up to a lattice vector times the elementary charge. In higher dimensions, similar restrictions on the dipole moment per cell do not exist.[21] Nevertheless, in this case as well, it is often assumed that possible values of the dipole moment per cell differ by lattice vectors times the elementary charge (see, e.g., the introduction to the Berry-phase approach given in ref. [28]).

This situation can be studied using our model results for the finite systems. Toward that end, we note that an often used approach in infinite periodic system calculations of the dipole moment per cell is to start with a centrosymmetric cell structure and, then, transition adiabatically to the lower symmetry cell structure of interest. In making the transition, it is assumed that the dipole moment per cell varies smoothly as a function of structure and, accordingly, cannot jump by a lattice vector times the elementary charge. Moreover, it is assumed that the dipole moment per

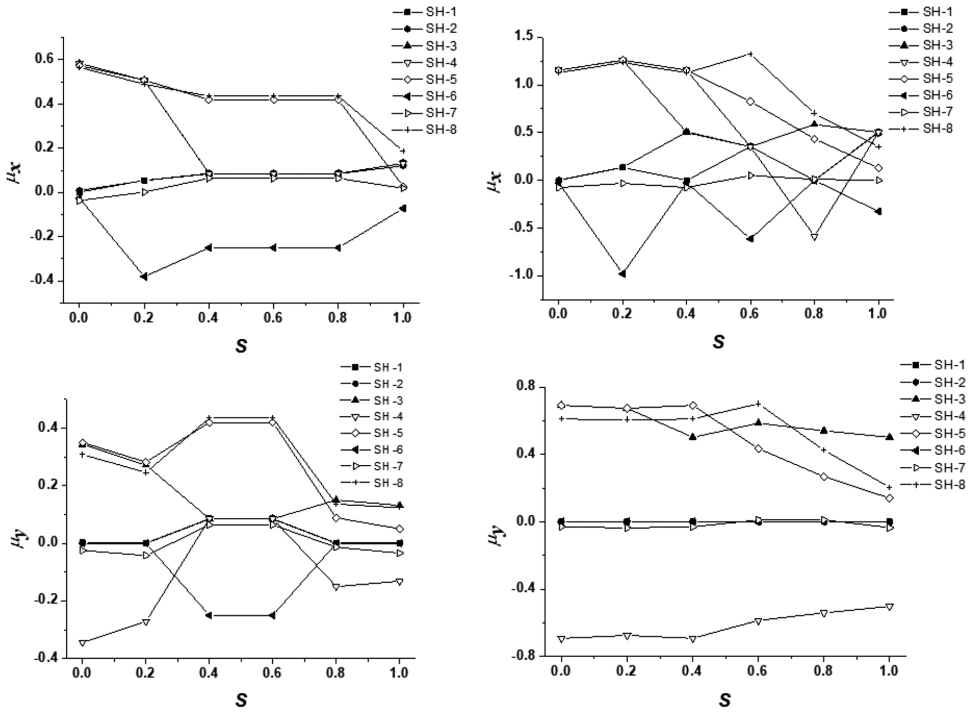

Figure 13. The dipole moment per atom as a function of s for the eight shapes of Figure 9 before applying the generalized Tasker condition. The left (right) panels show the results for the covalent (ionic) systems, and the upper (lower) panels show the x (y) component.

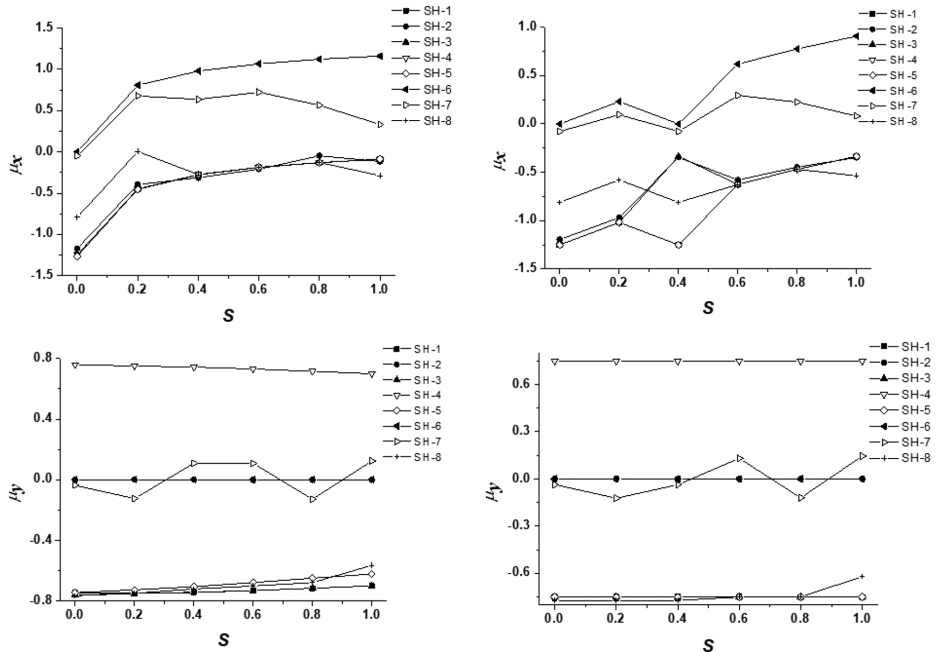

Figure 14. The dipole moment per atom as a function of s for the eight shapes of Figure 9 after applying the generalized Tasker condition. The left (right) panels show the results for the covalent (ionic) systems, and the upper (lower) panels show the x (y) component.

cell for the high-symmetry structure vanishes, that is, that surface contributions can be neglected.

The above treatment for infinite periodic systems is equivalent to our procedure wherein we slowly move from the centrosymmetric $s = 0$ structure to the $s = 1$ structure. We emphasize that in our calculations, the dipole moment per atom has a unique value. **Figure 13** shows the calculated dipole moment per atom as a function of s before applying the generalized Tasker condition whereas the values afterward are shown in **Figure 14**. Figure 13 demonstrates clearly that $\vec{\mu}$ is a continuous function of s, but

that this function has a different behavior depending on the overall shape of the sample. Most importantly, for a given s, the various curves in Figure 13 differ by values that are not simply related to the lattice vectors $\vec{a} = (5, 0)$, $\vec{b} = (0, 3)$. After applying the generalized Tasker condition (Figure 14), these conclusions do not change. Moreover, the absolute value of $\vec{\mu}$ has increased significantly, again implying that the interplay between bulk and surface properties as expressed through the generalized Tasker condition has a profound impact on the dipole moment per atom through a surface contribution, in particular, in those case where the bulk-unit-cell contribution to $\vec{\mu}$ is relatively small.

5. Heterogeneous Catalysis

As we have seen, the interplay between all surfaces and the bulk may affect the charge distribution on each surface. This means, in particular, that the properties associated with any surface will depend on the overall shape of the system of interest. This includes, for example, the catalytic properties. Accordingly, in order to study the catalytic properties of a given surface, it is, in principle, necessary to study the complete, essentially macroscopic system with a given shape. When using theoretical modeling for such a study, one has to ensure that the generalized Tasker condition is satisfied. Moreover for an arbitrary shape, one must use the particular charge distribution that corresponds to the ground-state structure. Determining this structure can be an overwhelming challenge, but it may be possible to obtain the most important information regarding catalytic properties through simpler studies. In this section, we shall discuss briefly some ideas behind this suggestion.

A simple model description of a heterogeneous catalytic process, that does not necessarily duplicate what occurs mechanistically, includes the following steps.

1. The reactants approach the surface of the catalyst and feel its presence through electrostatic fields.
2. One or more of the reactants forms a chemical bond with the catalytic surface.
3. The reaction takes place on the surface and the product(s) are formed.
4. The products leave the catalytic surface.

In theoretical studies, one usually starts by specifying the catalytic surface under consideration and, then, constructs a convenient geometry (very often a slab) with such a surface. An electronic structure calculation will, then, give an orbital energy diagram like that of Figure 7a. Subsequently, the steps 1–4 above are studied for the chemical reaction of interest.

Our present analysis suggests that in the case of a charged surface, there will be effects on the electronic structure that can be related to the shape of the catalytic substrate. In fact, for stability one can expect that there will be an initial charge transfer between the surfaces leading to a reordering/relaxation of the orbitals in order to arrive at a situation like that of Figure 7c. This will necessarily have consequences for steps 2 and 3 above, which will depend critically on the chemical reaction and on the atomic composition and structure of the substrate. The nature and importance of these consequences have, to our knowledge, not been addressed as yet.

We begin by determining the electrostatic field that acts on the molecules just outside one of the surfaces (cf. Figure 2). In the simplest approximation, that field may be obtained using the same approach as in deriving the generalized Tasker condition, that is, by assuming that we have layers of constant charge density parallel to the various surfaces and, then, calculating the resultant potential. For the situation in Figure 2, the reference point (red dot) is in the direction of all inward pointing normals to the surfaces with the single exception of the ith surface. Thus, from Equation (5), the field at the reference point in right part of Figure 2 is

$$\vec{E} = \frac{1}{4\pi\epsilon} 2\pi \left[\sum_{k \neq i} q_k \vec{1}_k + q_i(-\vec{1}_i) \right]$$
$$= \frac{1}{4\pi\epsilon} 2\pi \left[\sum_{k} q_k \vec{1}_k - 2q_i \vec{1}_i \right] = -\frac{1}{4\pi\epsilon} 4\pi q_i \vec{1}_i \tag{24}$$

This field will be felt by the molecule(s) when they approach the surface in step 1 above. It will modify the their properties and thereby affect the catalytic performance of the surface.

For an initial study of this effect, we consider a model system consisting of a diatomic AB molecule placed parallel to the field of Equation (24) with an A–B interatomic distance equal to R. It should be noted at the outset that the effect of a given electrostatic field on a diatomic molecule is minimal compared to the effect on a larger molecule containing delocalized orbitals. Thus, our model will provide a minimal estimate of the electric field effect. We will assume that there is one valence electron per atom and that the nuclear charges equal $+e$ each.

In the absence of the electrostatic field due to the surface, the total energy is written as

$$E_{\text{tot}}(R) = 2\epsilon_1(R) + E_{\text{rep}}(R) \tag{25}$$

where ϵ_1 is the lowest orbital energy, and E_{rep} represents everything else. This expression is equivalent to the one used with the non-SCC DFTB method of Seifert and coworkers.[29,30] The orbital energy is calculated by solving

$$\hat{F}_0 \psi_1 = \epsilon_1 \psi_1 \tag{26}$$

in which $\hat{F}_0$ is the field-free single-particle operator. Here, ψ_1 is approximated as a linear combination of two Gaussians, each centered at one of the two atoms,

$$\psi_1(\vec{r}) \simeq c_{\text{A}} \chi_{\text{A}}(\vec{r}) + c_{\text{B}} \chi_{\text{B}}(\vec{r}) \tag{27}$$

$$\chi_{\text{A}}(\vec{r}) = \left(\frac{2\alpha}{\pi}\right)^{3/4} e^{-\alpha|\vec{r} - \vec{R}_{\text{A}}|^2}$$
$$\chi_{\text{B}}(\vec{r}) = \left(\frac{2\beta}{\pi}\right)^{3/4} e^{-\beta|\vec{r} - \vec{R}_{\text{B}}|^2} \tag{28}$$

with $\vec{R}_{\text{A}}$ and $\vec{R}_{\text{B}}$ being the atomic positions. The matrix elements for the field-free single-particle operator are parameterized as

$$\langle \chi_A | \hat{F}_0 | \chi_A \rangle = \epsilon_A$$

$$\langle \chi_B | \hat{F}_0 | \chi_B \rangle = \epsilon_B$$

$$\langle \chi_A | \hat{F}_0 | \chi_B \rangle = t(R) = t_0 e^{-\gamma R} \tag{29}$$

while the overlap integrals are evaluated analytically. Finally, $E_{rep}(R)$ is taken to have the form

$$E_{rep}(R) = E_0 e^{-kR} \tag{30}$$

where, for a pre-specified k, E_0 is subsequently determined so that the lowest total energy in the absence of an electrostatic field is found for a given bond length.

The effects of the electrostatic field are calculated analytically. An upper limit for the field strength can be estimated as follows. In atomic units, a typical charge transfer between surfaces due to a difference in shape may be up to ± 0.5 $|e|$ per cell, whereas a typical surface cell may have a size of 10×10. Thus, we may set q_i in Equation (24) as roughly up to ± 0.005 and thereby consider field strengths up to $4\pi(\pm 0.005)$ or about ± 0.05.

Our results for the four systems whose parameter values are given in **Table 1** are shown in **Figure 15**. These values are similar to those found for hydrogen atoms and the hydrogen molecule. In order to simplify the presentation, both the total energy and the orbital energies were scaled and shifted so that the smallest and largest values are equal to -1 and $+1$, respectively. That is to say, with z_{max} and z_{min} being the largest and smallest values of the quantity z, respectively, we define

Table 1. Parameter values and some key quantities in the four sets of calculations for a diatomic molecule in the presence of an electrostatic field.

Parameter	1	2	3	4
α	0.2	0.2	0.2	0.2
β	0.1	0.1	0.1	0.1
ϵ_A	−0.4	−0.5	−0.4	−0.2
ϵ_B	−0.2	−0.1	−0.2	−0.4
t_0	−2.5	−2.5	−1.5	−2.5
γ	0.6	0.6	0.6	0.6
R_0	2.0	2.0	2.0	2.0
k	5.0	5.0	5.0	5.0
$E_{tot,min}$	−1.21588	−1.29367	−0.94896	−1.19003
$E_{tot,max}$	−1.15265	−1.19774	−0.84439	−1.17870
$\epsilon_{i,min}$	−0.66637	−0.68716	−0.49449	−0.68042
$\epsilon_{i,max}$	1.57327	1.56839	0.53169	1.62071

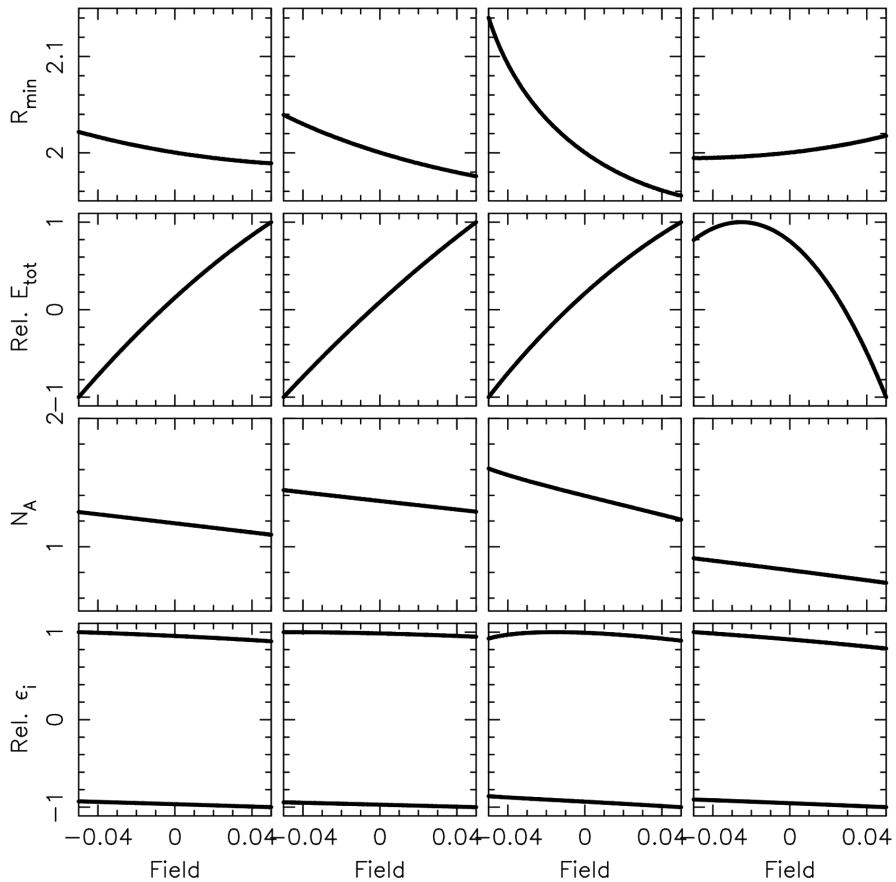

Figure 15. Molecular properties as a function of field strength, E, for the four sets of parameters given in Table 1. The first column corresponds to parameter set 1, the second column to parameter set 2, etc. The top row shows the optimized bond length, the second row the relative total energy, the third row the Mulliken gross population on atom A, and the last row the relative energies of the occupied and unoccupied orbitals.

$$z_{\text{rel}} = \left[2z - (z_{\max} + z_{\min})\right] / (z_{\max} - z_{\min}) \quad (31)$$

The values of $z_{\max}$ and $z_{\min}$ are given in Table 1.

Our results in Figure 11 show how key properties of the molecule depend on the electrostatic field. These properties include the structure (here, the bond length), total and orbital energies, and the electronic charge distribution, as quantified through the Mulliken gross population on one of the two atoms. Of course, it is not surprising that the molecular properties will change as a function of electrostatic field. But it is noteworthy that the changes over the range of fields considered here are substantial. For example, the equilibrium bond length changes between roughly 1% and above 5%, whereas for all systems of Figure 15, the Mulliken population changes up to above 10%. Moreover, such fields will often be present in heterogeneous catalysis simply due to charges associated with the set of surfaces of the catalyst. This implies that different samples of the same catalyst but with different shapes may have significantly different catalytic properties for a given chemical reaction, an issue that has hardly been considered in the past. At the moment of writing, we are extending the model just outlined to address the potential importance of shape-dependent electrostatic fields on a catalytically activated reaction occurring at a polar surface.

6. Summary and Conclusions

Whereas there exists a large number of studies regarding the bulk properties of crystalline materials, as well as the properties of individual surfaces, the interplay between these surfaces as determined by the bulk has hardly been studied at all. A step toward an understanding of this interplay was made by Tasker almost 40 years ago, when he demonstrated that the electric field generated by certain sequences of parallel layers of charged atoms in the surface regions would lead to an instability of the bulk structure and, consequently, such polar surfaces could not exist without major structural relaxation. In the present paper, we have reviewed and further developed our initial extension of this idea to systems of varying shape that contain multiple surfaces. Charge transfer between the different surfaces can provide an alternative mechanism for stabilization. Together with overall charge neutrality, the bulk stabilization condition either partially or completely determines the charge flow that can occur. This condition, which depends upon the surfaces involved, then leads to a dependence upon the shape of the material. It follows that the same individual surface may possess different properties when it occurs in samples that differ in their shape. In other words, there is an interplay between all the surfaces of a given sample through the bulk part of the system.

In the case of an individual surface, its properties are typically studied using a slab geometry. In order to get a feeling for the effect on the bulk structure of an individual charged surface, we carried out DFT calculations on a slab of polar ZnO. For this system, the surface charge compensates the dipolar electric field due to the ionic bilayer structure. It was found that the force associated with the computed charge density of about $0.3e$ per surface unit cell creates an estimated typical atomic displacement of 0.03 Å.

In order to determine the effect on bulk properties due to the interplay between individual surfaces that may be charged in order to satisfy the generalized Tasker condition, we turned from the slab geometry to a set of parallelogram (in 2D) samples, all of which have the same individual surfaces but different shapes. The particular property considered was the dipole moment per atom—essentially the polarization—which has a direct contribution from the charged surfaces. For a parallelogram, unlike other cases, the generalized Tasker conditions on the surface charges plus the overall charge neutrality requirement yield a unique value for the dipole moment per atom. Based on model calculations, we demonstrate that, in general, this value does indeed depend on the specific shape of the parallelogram. As it turns out, the generalized Tasker conditions are shown to have a profound impact on the dipole moment per atom through surface contributions.

In addition to bulk properties, local surface properties will also depend on the interplay between (charged) surfaces that is required to achieve stability. For the possible magnitude of this effect, the case of heterogeneous catalysis was considered. A model was constructed to simulate the initial interaction as a molecule approaches a catalytic surface. We examined the effect of realistic electrostatic fields due to surface charges on key properties of the molecule. Using a diatomic molecule, which represents the case of minimal interaction, a substantial effect on the internuclear distance and atomic charge was found. This indicates a potentially large effect on the performance of a catalyst due to its shape, a subject that is ripe for future investigation.

Even though ZnO has been used in the wurtzite structure to illustrate the concepts of our study, we emphasize that our theory is applicable to many other systems. This includes not only the thoroughly studied perovskites (see, e.g., the work by Eglitis et al.[31–33]) but also quite different types of systems like ionic organic crystals and intermetallic crystalline compounds as well as other crystalline systems. On the other hand, for molecular crystals, charge transfers may be suppressed whereby our results will be irrelevant for those systems.

Acknowledgements

This work was supported by the German Research Council (DFG) through project SP 439/37-1. Moreover, one of the authors (M.S.) is very grateful to the International Center for Materials Research, University of California, Santa Barbara, for generous hospitality. Moreover, the authors thank Mohammad Molayem for many useful discussions.

Conflict of Interest

The authors declare no conflict of interest.

Keywords

bulk properties, crystals, dipole moment, heterogeneous catalysis, polarization, shape, surfaces

Received: August 1, 2018
Revised: September 5, 2018
Published online: September 30, 2018

[1] M. Springborg, M. Zhou, M. Molayem, B. Kirtman, *J. Phys. Chem. C* **2018**, *122*, 11926.
[2] P. W. Tasker, *J. Phys. C* **1979**, *12*, 4977.
[3] B. Meyer, D. Vanderbilt, *Phys. Rev. B* **2001**, *63*, 205426.
[4] B. Meyer, D. Marx, *Phys. Rev. B* **2003**, *67*, 035403.
[5] G. Kresse, J. Hafner, *Phys. Rev. B* **1993**, *47*, 558.
[6] G. Kresse, J. Hafner, *Phys. Rev. B* **1994**, *49*, 14251.
[7] G. Kresse, J. Furthmüller, *Phys. Rev. B* **1996**, *54*, 11169.
[8] G. Kresse, J. Furthmüller, *Com. Mat. Sci.* **1996**, *6*, 15.
[9] J. P. Perdew, J. A. Chevary, S. H. Vosko, K. A. Jackson, M. R. Pederson, D. J. Singh, C. Fiolhais, *Phys. Rev. B* **1992**, *46*, 6671.
[10] J. P. Perdew, K. Burke, M. Ernzerhof, *Phys. Rev. Lett.* **1996**, *77*, 3865.
[11] Y. Liu, W. Xu, Y. Shan, H. Xu, *J. Phys. Chem. C* **2017**, *121*, 15711.
[12] H. Sawada, R. Wang, A. W. Sleight, *J. Solid State Chem.* **1996**, *122*, 148.
[13] R. F. W. Bader, *Atoms in Molecules: A Quantum Theory*, Oxford University Press, New York **1990**.
[14] K. Momma, F. Izumi, *J. Appl. Crystallogr.* **2011**, *44*, 1272.
[15] T. Hanada, in *Oxide and Nitride Semiconductors: Processing, Properties, and Applications*, (Eds: T. Yao, S.-K. Hong), Springer, Heidelberg, Germany **2009**.
[16] C. Noguera, *J. Phys. Condens. Matter* **2000**, *12*, R367.
[17] J. Goniakowski, F. Finocchi, C. Noguera, *Rep. Prog. Phys.* **2008**, *71*, 016501.
[18] A. Wander, F. Schedin, P. Steadman, A. Norris, R. McGrath, T. S. Turner, G. Thornton, N. M. Harrison, *Phys. Rev. Lett.* **2001**, *86*, 3811.
[19] D. Mora-Fonz, T. Lazauskas, M. R. Farrow, C. R. A. Catlow, S. M. Woodley, A. A. Sokol, *Chem. Mater.* **2017**, *29*, 5306.
[20] M. Setvin, M. Reticcioli, F. Poelzleitner, J. Hulva, M. Schmid, L. A. Boatner, C. Franchini, U. Diebold, *Science*, **2018**, *359*, 572.
[21] M. Molayem, M. Springborg, B. Kirtman, *Phys. Chem. Chem. Phys.* **2017**, *19*, 24724.
[22] With the notation of our previous work [1], for $s = 0$ both systems have $\vec{a} = (5, 0)$, $\vec{b} = (0, 3)$, $\vec{u}_1 = (1, 1)$, $\vec{u}_2 = (3.5, 2.5)$, $d_{11} = d_{12} = d_{22} = 4$. For $s = 1$, the only change is $\vec{u}_2 = (2.0, 2.5)$. For the covalent system, we have $\epsilon_1 = -6$, $\epsilon_2 = -8$, $t_{0,11} = 8$, $t_{0,12} = 24$, $t_{0,11} = 6$, whereas for the ionic system we have $\epsilon_1 = -2$, $\epsilon_2 = -8$, $t_{0,11} = 2$, $t_{0,12} = 9$, $t_{0,11} = 4$.
[23] D. Vanderbilt, R. D. King-Smith, *Phys. Rev. B* **1993**, *48*, 4442.
[24] R. Resta, *Rev. Mod. Phys.* **1994**, *66*, 899.
[25] B. Kirtman, F. L. Gu, D. M. Bishop, *J. Chem. Phys.* **2000**, *113*, 1294.
[26] K. N. Kudin, R. Car, R. Resta, *J. Chem. Phys.* **2007**, *127*, 194902.
[27] M. Springborg, B. Kirtman, *Chem. Phys. Lett.* **2008**, *454*, 105.
[28] N. A. Spaldin, *J. Solid State Chem.* **2012**, *195*, 2.
[29] D. Porezag, T. Frauenheim, T. Khler, G. Seifert, R. Kaschner, *Phys. Rev. B* **1995**, *51*, 12947.
[30] G. Seifert, D. Porezag, T. Frauenheim, *Int. J. Quant. Chem.* **1996**, *58*, 185.
[31] R. I. Eglitis, D. Vanderbilt, *Phys. Rev. B* **2007**, *76*, 155439.
[32] R. I. Eglitis, M. Rohlfing, *J. Phys. Condens. Matter* **2010**, *22*, 415901.
[33] R. I. Eglitis, *Appl. Surf. Sci.* **2015**, *358*, 556.

10. Summary

Theoretical simulations can be applied not only to explain some specific chemical reaction phenomena and mechanism from the level of electrons, atoms and molecules (illustrated in part 6), but also carried out to provide a correct direction for practical research and do a preliminary evaluation with mathematical models and abstractions of systems (illustrated in parts 7 and 8).

1. In part 6, theoretical simulation is performed to explain the C–H functionalization mechanism of carbene and catalyzed by a dirhodium complex using the Gaussian 09 software. We have studied the catalytic properties of a dirhodium complex, Rh_2(*S*-TCPCH_3)$_4$ containing *S*-ligands, for the C–H functionalization of 2-methylpentane when reacting with a donor/acceptor carbene.

   I. The dirhodium carbenoid is easier formed after the donor/acceptor carbene (*p*-Br-C_6H_4)CN=N(COOCH_3) initially has entered the chiral crown of Rh_2(*S*-TCPCH_3)$_4$ followed by an N_2 elimination reaction. Subsequently, the 2-methylpentane approaches the crown of the catalyst along the direction towards the methoxy group. The insertion reaction of the carbene carbon atom into the tertiary C–H bond involves an energy barrier of 12.21 kcal mol^{-1}. The tertiary site is best suited for the C–H functionalization compared with the secondary and primary sites. The whole energy barrier of the C–H functionalization at the tertiary site is 2.24, 11.99, 10.22, and 14.07 kcal mol^{-1} lower than those at the two secondary and the two primary sites, respectively.

   II. By analyzing the structures, NBO charges, and Hirshfeld surfaces, the site-selectivity of the catalyst could be ascribed to intermolecular hydrogen bonding, steric hindrance, and weak interactions. For the tertiary C–H bond functionalization the larger number of weak hydrogen bonds gives a better compensation of the steric hindrance than what is the case for the primary and secondary C–H bond functionalization.

III. For the chiral dirhodium catalyst Rh_2(*S*-TCPCH$_3$)$_4$ with *S*-ligands, the enantioselective C–H functionalization at the tertiary site of 2-methylpentane resulted mainly in the *R*-configuration product for the reaction of the donor/acceptor carbene (*p*-Br-C$_6$H$_4$)-CN=N(COOCH$_3$). Since the *R*- and *S*-configuration products involve similar hydrogen bonding the difference in the yield is mainly due to steric hindrance, because of differences in the deformation of the chiral crown of the catalyst. Therefore, when 2-methylpentane reacts with (*p*-Br-C$_6$H$_4$)CN=N(COOCH$_3$) for the chiral dirhodium catalyst Rh_2(*S*-TCPCH$_3$)$_4$, the energy barrier for the formation of the *R*-configuration product is 3.00 kcal mol^{-1} lower than that of the *S*-configuration product.

IV. We also considered a simplified, achiral dirhodium formate catalyst Rh_2–(O$_2$CH)$_4$. Here, the mechanism for the tertiary C–H functionalization is similar to that catalyzed by Rh_2(*S*-TCPCH$_3$)$_4$. However, due to the lack of the *S*-configuration phthalimido ligands for this catalyst, the formation of the R-P has to overcome an energy barrier that is 6.14 kcal mol^{-1} higher than that found for the Rh_2(*S*-TCPCH$_3$)$_4$ catalyst. Hence, the chiral arrangement of the ligands of the dirhodium catalyst plays an important role in the excellent site-selectivity. The chiral ligands can provide intermolecular bonding, steric hindrance, and weak interactions with the reactants.

As just summarized, we have arrived at a detailed understanding of the mechanisms for the high site- and enantio-selectivity when the reactions are catalyzed by a chiral dirhodium complex. It demonstrates that the dirhodium carbenoids, derived from the reactions of the dirhodium(II) catalysts (*S*-configuration ligands) with the donor/acceptor diazo compounds, preferably leads to a C–H functionalization at the tertiary sites resulting in an *R*-configuration product. The excellent site- and enantioselectivity for some C–H bond functionalization could be rationalized through energy barriers, intermolecular hydrogen bonding, steric hindrance, and weak interactions.

Even though we have studied a specific reaction in great detail we are convinced that our conclusions are generally valid also for other catalytic reactions involving chiral complexes and for which limited space is available for the catalytic reaction.

2. In part 7, the interplay between the surface and bulk properties of macroscopic crystalline materials is studied with an emphasis on polar surfaces. To that end, we generalized an analysis, originally proposed by Tasker [45], for the identification of stable polar surfaces. Thereby, we could show that it is always possible to stabilize a given surface through a charge redistribution involving the entire set of surfaces. A surface that should not be stable when considered individually may very well be observed experimentally after it has been stabilized by a such charge redistribution. Moreover, in two different experiments focusing on the same surface, but for samples of different shapes, one may observe different charge distributions on that surface. As the charge density of the surface is modified, even spatially local properties like catalytic activity can be influenced.

   A special, relevant property associated with the charge distribution is the bulk dipole moment per atom. It was shown how the values for this property can be calculated subject to the generalized Tasker constraints. From the results of calculations for very large systems, based on a sufficiently simple model, we were able to show that applying these constraints leads to a change in the dipole moment per atom or per unit in the thermodynamic limit. For some shapes, the resulting value of the dipole moment per atom is not uniquely determined through the generalized Tasker condition. However, in the case of any real system, it will have a specific value determined by detailed energetic considerations that lie beyond the scope of this work. Essentially, any physically reasonable value can be obtained in contrast with the assumption often made that for samples of the same material the possible values differ by at most a lattice vector [67].

   Our analysis allows for further understanding of theoretical studies on the polar surfaces of, for instance, ZnO. When the system is modeled in such studies using

an infinite, periodic slab, there are only two surfaces, and only the component of the electric field $\vec{E}$ perpendicular to these surfaces may be nonvanishing. This leads to two conditions related to the charge redistribution (i.e., vanishing $\vec{E}$ as well as charge neutrality), whereby the changes in the charges on the two surfaces are uniquely determined according to our procedure. This coincides with the results of Meyer and Marx [49], for example. Whether this is realized through surface states or through a lower symmetry on the surface is a question we do not try to address in the present work. On the other hand, our study suggests that consideration of other shapes (particularly containing more surfaces) would provide many more possibilities to realize this same surface.

Our results can also be used to throw some further light on the recent study on the (001) surface of $KTaO_3$ [51]. The authors observed that after the surface is created it undergoes an insulator-to-metal transition, which we interpret as being a first consequence of stabilizing the surface through a charge redistribution. When the surface is subsequently exposed to water vapor, a further stabilization occurs which we consider is likely accompanied by a further charge redistribution. A detailed analysis of this qualitative picture, however, lies outside the scope of the present work.

3. The focus was slightly different in part 8. Whereas, there exists a large number of studies regarding separately the bulk properties of crystalline materials as well as the properties of individual surfaces, the interplay between these surfaces as determined by the bulk has hardly been studied at all. A step toward an understanding of this interplay was made by Tasker almost 40 years ago, when he demonstrated that the electric field generated by certain sequences of parallel layers of charged atoms in the surface regions would lead to an instability of the bulk structure and, consequently, such polar surfaces could not exist without major structural relaxation. In this work, we have reviewed and further developed our initial extension of this idea to systems of varying shape that contain multiple surfaces. Charge transfer between the different surfaces can provide an alternative

mechanism for stabilization.

I. Together with the condition of overall charge neutrality, the bulk stabilization condition either partially or completely determines the charge flow that can occur. These conditions, which depend upon all the surfaces involved, then lead to a dependence of the surface charges on the shape of the material. It follows that the same individual surface may possess different properties when it occurs in samples that differ in their shape. In other words, there is an interplay between all the surfaces of a given sample through the bulk part of the system.

II. In the case of an individual surface, its properties are typically studied using a slab geometry. In order to get a feeling for the effect on the bulk structure of an individual charged surface, we carried out DFT calculations on a slab of polar ZnO. For this system, the surface charge compensates the dipolar electric field due to the ionic bilayer structure. It was found that the force associated with the computed charge density of about 0.3 $|e|$ per surface unit cell creates an estimated typical atomic displacement of 0.03 Å. Even though we considered ZnO in the wurtzite structure to illustrate the concepts of our study, we emphasize that our theory is applicable to many other systems. This includes not only the thoroughly studied perovskites (see, e.g., the work by Eglitis et al. [64-66]) but also quite different types of systems like ionic organic crystals and intermetallic crystalline compounds as well as other crystalline systems. On the other hand, for molecular crystals, charge transfers may be suppressed whereby our results will be irrelevant for those systems.

III. In order to determine the effects on bulk properties from the interplay between individual surfaces that may be charged in order to satisfy the generalized Tasker condition, we turned from the slab geometry to a set of parallelogram (in 2D) samples, all of which have different shapes. The particular property considered was the dipole moment per atom—essentially the polarization—which has a direct contribution from the charged surfaces. For a

parallelogram, unlike other cases, the generalized Tasker conditions on the surface charges plus the overall charge neutrality requirement yield a unique value for the dipole moment per atom. Based on model calculations, we demonstrate that, in general, this value does indeed depend on the specific shape of the parallelogram. As it turns out, the generalized Tasker conditions are shown to have a profound impact on the dipole moment per atom through surface contributions.

IV. In addition to bulk properties, local surface properties will also depend on the interplay between (charged) surfaces that is required to achieve stability. For the possible magnitude of this effect, the case of heterogeneous catalysis was considered. A model was constructed to simulate the initial interaction as a molecule approaches a catalytic surface. We examined the effects of realistic electrostatic fields due to surface charges on key properties of the molecule. Using a diatomic molecule, which represents the case of minimal interaction, a substantial effect on the internuclear distance and atomic charge was found. This indicates a potentially large effect on the performance of a catalyst due to its shape, a subject that is ripe for future investigation.

V. In the case of a chemical interaction in the presence of a heterogeneous catalyst, the smaller molecule will slowly approach a specific surface of some catalyst sample that has some shape. In this process, the molecule will feel the presence of the surface through the electrostatic potential that the charge distribution as a consequence of the generalized Tasker condition. The molecule may respond to this, both by changing structure and by a redistribution of the electrons within the molecule. Thus, a molecule approaching the surface will feel a potential that depends on the overall shape of the sample and, moreover, will interact with different frontier orbitals of the two surfaces. Both effects can affect the catalytic properties of the surfaces.

With the continuous improvement of calculational methods and the rapid growth in computer technology, it will become possible to simulate increasingly complex

systems with highly reliable theoretical models and methods, and the theoretical calculations will be more and more important in scientific research. Of course, if the practical application will be performed in reality, the experimental research is the last step. But based on the good correlation between theoretical models and experimental results, the theoretical simulation can be used as a preliminary evaluation and a way of obtaining a correct direction for the experimental researches.

Complete List of Publications

1. **M. J. Zhou*** and M. Springborg, Theoretical study of the mechanism behind the site- and enantio-selectivity of C–H functionalization catalysed by chiral dirhodium catalyst. *Phys. Chem. Chem. Phys.*, 22:9561-9572, **2020**.

2. **M. J. Zhou***, M. Springborg and B. Kirtman, Theoretical Treatment for Properties of Surfaces and Their Interplay with Bulk Properties of Crystals. *Adv. Theory Simul.*, 2:1800117, **2019**.

3. M. Springborg*, **M. J. Zhou**, M. Molayem and B. Kirtman, Surfaces, Shapes, and Bulk Properties of Crystals. *J. Phys. Chem. C*, 122:11926−11932, **2018**.

4. L. Zheng, **M. J. Zhou (Co-first author)**, Z. Huang, Y. Chen, J. Gao, Z. Ma, J. Chen and X. F. Tang*, Self-protection mechanism of hexagonal WO_3-based DeNOx catalysts against Alkali poisoning. *Environ. Sci. Technol.*, 50(21): 11951-11956, **2016**.

5. **M. J. Zhou**, T. L. Yang and L. Dang*, Theoretical studies on palladium-mediated enantioselective C–H iodination, *J. Org. Chem.*, 81:1006–1020, **2016**.

6. **M. J. Zhou**, Y. Li and L. Dang*, Theoretical studies on the mechanism of the michael addition reaction catalyzed by a thiourea-cinchona-amine: triple activation, *Asian J. Org. Chem.*, 4:904 –911, **2015**.

7. J. Chen, Y. Chen, **M. J. Zhou**, Z. Huang, J. Gao, Z. Ma, J. Chen and X. F. Tang*, Enhanced performance of Ceria-based NO_x reduction catalysts by optimal support effect. *Environ. Sci. Technol.*, 51:473−478, **2017**.

8. Y. Chen, Z. Huang, **M. J. Zhou**, Z. Ma, J. Chen and X. F. Tang*, Single silver adatoms on nanostructured manganese oxide surfaces: boosting oxygen activation for benzene abatement. *Environ. Sci. Technol.*, 51:2304−2311, **2017**.

9. W. Qu, Y. Chen, Z. Huang, J. Gao, **M. J. Zhou**, J. Chen, C. Li, Z. Ma, J. Chen and

X. F. Tang*, Active tetrahedral Iron sites of γ-Fe_2O_3 catalyzing NO reduction by NH_3. *Environ. Sci. Technol. Lett.*, 4(6):246-250, **2017**.

10. Y. Chen, Z. Dong, Z. Huang, **M. J. Zhou**, J. Gao, J. Chen, C. Li, Z. Ma, J. Chen and X. F. Tang*, Tuning electronic states of catalytic sites enhances SCR activity of hexagonal WO_3 by Mo framework substitution. *Catal. Sci. Technol.*, 7:2467-2473, **2017**.

11. Y. Chen, Z. Huang, J. Gao, **M. J. Zhou**, J. Chen, C. Li, Z. Ma, J. Chen and X. F. Tang*, Sodium rivals silver as single-atom active centers for catalyzing abatement of formaldehyde. *Environ. Sci. Technol.*, 51(12):7084-7090, **2017**.

12. Y. Chen, G. Tian, **M. J. Zhou**, Z. Huang, C. Lu, P. Hu, J. Gao, Z. Zhang* and X. F. Tang*, Catalytic control of typical particulate matters and volatile organic compounds emissions from simulated biomass burning. *Environ. Sci. Technol.*, 50:5825−5831, **2016**.

13. Y. Chen, Z. Huang, **M. J. Zhou**, P. Hu, C. Du, L. Kong, J. Chen and X. F. Tang*, The active sites of supported silver particle catalysts in formaldehyde oxidation. *Chem. Commun.*, 52:9996−9999, **2016**,.

14. M. S. Javed, X. Han, C. Hu, **M. J. Zhou**, Z. Huang, X. Tang and X. Gu*, Tracking pseudocapacitive contribution to superior energy storage of MnS nanoparticles grown on carbon textile. *ACS Appl. Mater. Interfaces*, 8:24621−24628, **2016**.

15. **M. J. Zhou**, C. H. Tian, X. H. Chen, S.N. Wang, J. F. Liu, H. Q. Hu and C. Zhang*, The inclusion insight of $–CH_3$ and $–CH_2OH$ modified β-cyclodextrins with one trans-resveratrol molecule: A theoretical study, *J. Theor. Comput. Chem.*, 11:1057-1073, **2012**.